Embodied Modular Neural Control of Walking in Stick Insects

From Biological Models to Evolutionary Robotics

Arndt von Twickel

Embodied Modular Neural Control of Walking in Stick Insects

From Biological Models to Evolutionary Robotics

Embodied Modular Neural Control of Walking in Stick Insects

From Biological Models to Evolutionary Robotics

Inaugural-Dissertation

zur

Erlangung des Doktorgrades

der Mathematisch-Naturwissenschaftlichen Fakultät

der Universität zu Köln

vorgelegt von

Arndt von Twickel

aus Berlin

Köln

März 2012

Berichterstatter:
Prof. Dr. rer. nat. Ansgar Büschges
Dr. rer. nat. Silvia Gruhn
Prof. Dr. rer. nat. Frank Pasemann

Tag der mündlichen Prüfung:
06.04.2011

Für Teresa und Helene

Abstract

Walking requires the flexible co-ordination of many degrees of freedom. Biomechanical and nervous systems have to interact with the environment to fulfill this challenging task. Due to the complexity of interactions, important questions, especially regarding the neural control of walking, remain unanswered. Biological models are promising tools to integrate available data and to generate testable hypotheses, but they face the problem of a huge parameter space. Therefore, this thesis combines (neuro-)biological models of stick insect walking with the complementary approach of evolutionary robotics.

On the one hand, extremely simple single-leg controllers are developed by artificial evolution that exploit properties of the body and the environment. General principles of sensori-motor couplings are discovered and the importance of hysteresis in neural walking control is demonstrated. On the other hand, neuro-biological models of single-leg stepping control in stick insects are thoroughly tested under multiple perturbing conditions in stick insect as well as in robotic models. Their robustness and behavioral adaptability is demonstrated, suggesting that they are suitable to work as modules of hexapod controllers. Subsequently, the impact of muscles on a set of neural control structures and behavior in robotic as well as in stick insect models is investigated using a muscle model derived from the stick insect extensor muscle. Employing evolutionary parameter optimization of neural controllers it is shown that muscle properties reduce the requirement for neural intra-joint feedback and that behaviors become more robust under perturbing conditions. Furthermore, it is demonstrated that diverse and simple neural mechanisms may be used to compensate for the slowness of muscles observed in stick insects. Finally, a modular approach to hexapod controller development is taken, integrating the evolved and neuro-biologically inspired single-leg controller structures with additional sensori-motor couplings. Coupling structures are either derived from behavioral based biological data or by artificial evolution. Robust hexapod walking is demonstrated for robotic and stick insect models with and without muscle properties.

The results show that the integrative approach presented in this thesis allows to develop robust control mechanisms for walking machines and to provide testable hypotheses about the neural basis of inter-leg coupling mechanisms.

Parts of this thesis have been published (s. page 161 for a list): von Twickel and Pasemann (2007); von Twickel et al. (2011, 2012); von Twickel and Pasemann (2005, 2006); von Twickel et al. (2008a,b, 2011); Hülse et al. (2007); von Twickel et al. (2006); Zahedi et al. (2008); von Twickel (2004).

Zusammenfassung

Laufen erfordert die flexible Koordination zahlreicher Freiheitsgrade. Biomechanische Systeme und Nervensysteme müssen mit der Umgebung interagieren, um diese anspruchsvolle Aufgabe zu erfüllen. Aufgrund der Komplexität der Interaktionen bleiben wichtige Fragen unbeantwortet, insbesondere bezüglich der neuronalen Kontrolle des Laufens. Biologische Modelle sind vielversprechende Werkzeuge, um verfügbare Daten zu integrieren und überprüfbare Hypothesen zu generieren. Jedoch haben sie das Problem eines riesigen Parameterraumes. Daher kombiniert diese Arbeit neurobiologische Modelle des Laufens der Stabheuschrecke mit dem komplementären Ansatz der evolutionären Robotik.

Einerseits werden mit Hilfe künstlicher Evolution sehr einfache Einbeinkontroller entwickelt, die Eigenschaften des Körpers und der Umgebung ausnutzen. Allgemeine Prinzipien der sensomotorischen Kopplung werden herausgearbeitet und die Bedeutung von Hystereseeffekten bei neuronaler Laufkontrolle wird demonstriert. Andererseits werden neurobiologische Modelle von Einzelbein-Laufkontrollern bei Stabheuschrecken sowie bei Robotermodellen unter verschiedenartigen Störbedingungen gründlich getestet. Ihre Robustheit und Verhaltensanpassungsfähigkeit wird demonstriert, was ihre Eignung als Module von Sechsbeinkontrollern nahelegt. Anschließend wird die Auswirkung von Muskeln auf einen Satz neuronaler Kontrollerstrukturen und auf das Verhalten, sowohl in der Robotik als auch bei Stabheuschreckenmodellen, erforscht. Dies geschieht mit Hilfe eines Muskelmodells, das vom *Extensor tibia* Muskel der Stabheuschrecke abgeleitet wurde. Unter Verwendung von evolutionärer Parameteroptimierung von neuronalen Kontrollern wird gezeigt, dass Muskeleigenschaften die Anforderungen für eine neuronale Intra-Gelenk-Rückkopplung reduzieren und dass das Verhalten unter Störbedingungen robuster wird. Weiterhin wird dargelegt, dass diverse einfache neuronale Mechanismen genutzt werden können, um die Tiefpassfiltereigenschaften der Muskeln, die bei Stabheuschrecken beobachtet werden, zu kompensieren. Schließlich wird ein modularer Ansatz zur Entwicklung von Sechsbeinkontrollern genutzt, der evolvierte und neurobiologisch inspirierte Einzelbeinkontrollerstrukturen um weitere sensomotorische Kopplungen ergänzt. Kopplungsstrukturen werden entweder von verhaltensbasierten biologischen Daten oder mit Hilfe von künstlicher Evolution abgeleitet. Robustes Sechsbeinlaufen wird für Robotermodelle und Stabheuschreckenmodelle mit und ohne Muskeleigenschaften demonstriert.

Die Ergebnisse zeigen, dass der integrative Ansatz, der in dieser Arbeit dargelegt wird, die Entwicklung robuster Kontrollmechanismen für Laufmaschinen und die Generierung überprüfbarer Hypothesen zur neuronalen Basis von Beinkopplungsmechanismen erlaubt.

Contents

Part I.

Background and Approaches

1. Introduction

> "The results [...] suggest a different metaphor: the nervous system is one of a group of players engaged in jazz improvization, and the final result emerges from the continued give and take between them. [...] As a consequence, one cannot assign credit for adaptive behavior to any one piece of this coupled system."
>
> *(Chiel and Beer (1997))*

How does the brain work? How is robust behavior generated? Both questions are intimately connected with one another: The notion that nervous systems control motor behaviors (cp. Fig. 1.1A) such as posture, locomotion and manipulation has been replaced by a more complex view. According to the view of embodiment and situatedness (cp. Fig. 1.1B, Beer (2009); Nishikawa et al. (2007)) the nervous system may only influence the operation of the body's actuators against its skeletal system, possibly modifying its influence by sensory information. Motor behaviors are then sequences of effort (force) and flow (movement) combinations between body and environment. On molecular, morphological and (neural) control levels biological motor systems are highly modular, distributed and hierarchically organized (Büschges, 2005; Dassow and Munro, 1999; d'Avella and Tresch, 2002; Flash and Hochner, 2005; He and Deem, 2010; McGowan et al., 2010; Orlovsky et al., 1999; Redies and Puelles, 2001; Schmitz et al., 2001). Ultimately motor behaviors emerge from a multitude of interactions (or feedback loops) between multiple modules (Chiel et al., 2009; Hatsopoulos, 1996; Maturana and Varela, 1992; Pfeifer and Bongard, 2006). To understand the system's performance, a reductionist approach is thus not sufficient. This irreducibility necessitates a whole systems approach, integrating knowledge of brain, body and environment. Such an integrative approach poses non-trivial challenges: Experimentally recording more than a very limited subset of the system's components activities under artificial – not to speak of natural – conditions is extremely difficult (Ritzmann and Büschges, 2007). Furthermore a formal analysis is complicated by the numerous non-linear feedback-loops within the motor system.

Locomotion Locomotion is a behavior which is very well suited for an integrative approach: First of all it is a challenging behavior to investigate in basic research and has important areas of application, namely robotics (Siciliano and Khatib, 2008) and prosthetics (Herr and Kornbluh, 2004). For animals, locomotion primarily serves the orientation fitness and, therefore, to approach resources and avoid sources of stress (Jander, 1975). Terrestrial animals have to move across three dimensional and often complex structured surfaces (Franklin, 1985; Grillner, 1981). In order to fulfill this task,

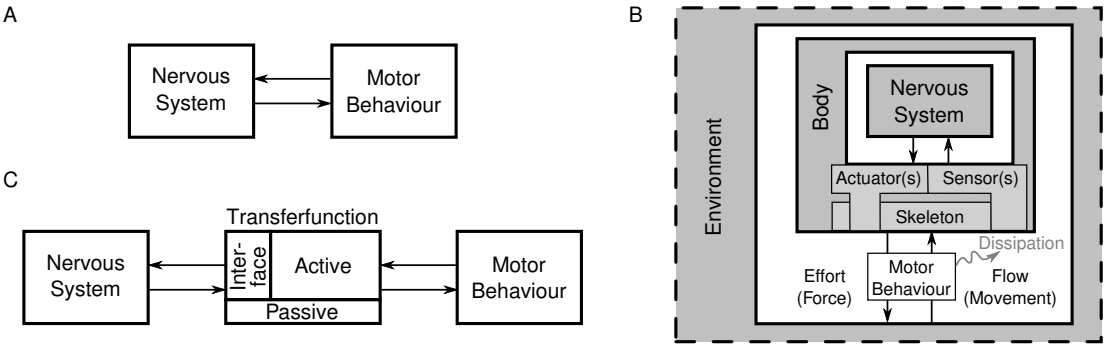

Figure 1.1.: **A** Nervous system centered view of motor behavior. **B** Motor behaviors are the result of an (mechanical) energy exchange between an organism (or robot) and its environment. The energy exchange is defined by the two conjugate variables flow (movement) and effort (force, torque). Body and environment on the one hand and nervous system and body on the other hand are mutually coupled and the interactions between them determine the motor behaviors. The body may sense motor behaviors via sensors and influence them via its actuators ("low level control"). Actuators act either via a rigid skeleton or via a soft skeleton which is again (partly) configured by the actuators. The nervous system cannot directly determine motor behaviors but rather influences (ideally extends the capabilities of) the body to modify the motor behavior ("high level control"). Depending on the situation body and environment constrain or facilitate the task of the nervous system. Figure modified from Chiel and Beer (1997). **C** Pragmatic view of motor control for comparability of nervous systems in simulated and robotic models vs. biological organisms: All properties of body and environment are represented by a transfer function which provides an interface for the nervous system that may influence the active part but not the passive part. It outputs the motor behavior and feeds back sensory information. Cp. chapter 2 for a detailed discussion

the control of locomotion in animals and robots has to be extremely flexible and adaptive, in addition to the "basic" task of co-ordinating many degrees of freedom (DOFs).

Furthermore, locomotion is a behavior that is well accessible to the experimenter (Alexander, 2002), which is especially important to correlate neural and behavioral data (Orlovsky et al., 1999). A huge number of studies on neural as well as on behavioral locomotion control exists for many species. Over the last decades substantial progress has been made in research on walking machine control (Bekey, 2005) and neuro-biological control mechanisms of walking in animals (Büschges et al., 2008; Orlovsky et al., 1999). Current knowledge leads to the hypothesis that the organization of locomotion control systems is a key to understand the flexibility and adaptivity observed in animals. As depicted in Fig. 1.2 for the stick insect, locomotor systems have a modular and hierarchical organization, on the neural as well as on the mechanical level (Orlovsky et al., 1999). Nevertheless only two animal species exist for which the neural control of single-leg stepping was extensively investigated: the cat (Büschges, 2005; Ekeberg and Pearson, 2005) and the stick insect (Büschges, 2005; Ekeberg et al., 2004). In both species the operational principles underlying single-leg stepping control show important similarities, including the major importance of sensory signals for the transition between different walking phases (Pearson et al., 2006). In comparison with the cat, knowledge about the organization of the neural control system in stick insects is advanced (Büschges et al.,

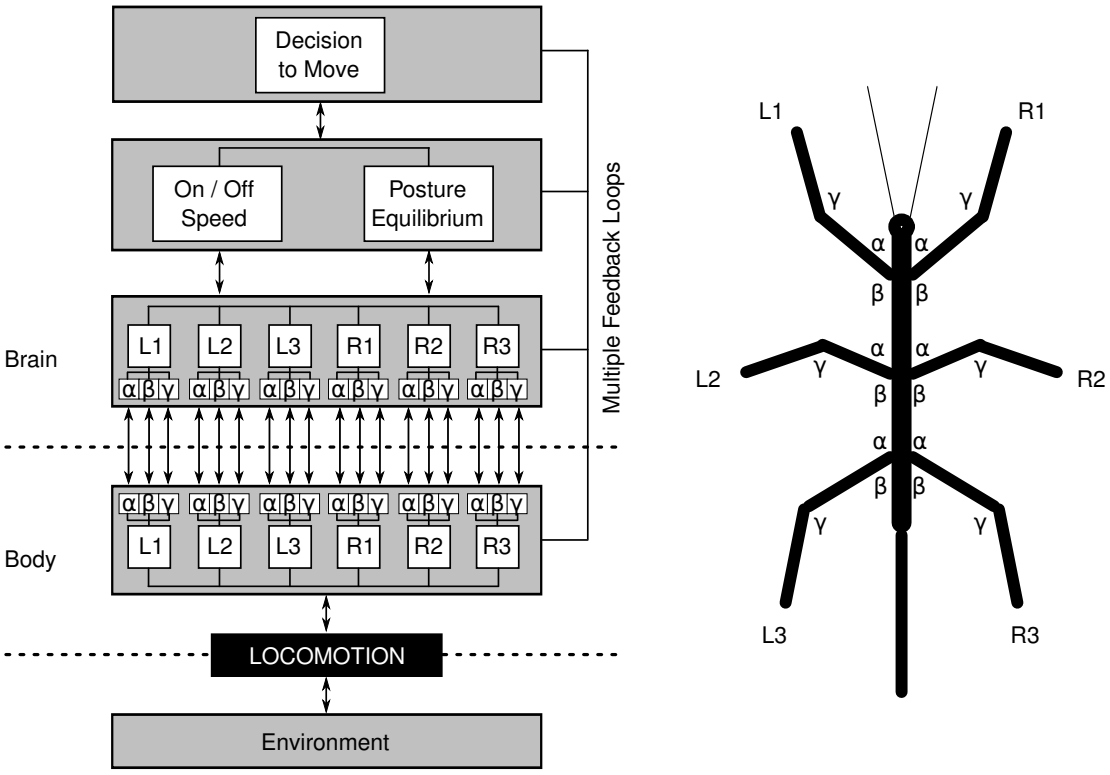

Figure 1.2.: Locomotor systems, such as walking stick insects, have a modular and hierarchical organization on neural and mechanical levels. A large number of feedback loops connects mechanical and neural modules. Here the stick insect is depicted as consisting of six leg modules (L1–L3, R1–R3) which again consist of three joint modules each (α–γ). Partly adapted from Orlovsky et al. (1999)

2008). Therefore, the stick insect was chosen here as the biological target organism.

Simulations Despite of this enormous progress in locomotion control research, knowledge about the interaction of sensori-motor loops in walking control (on the neural level) remains limited due to the system's complexity combined with limited experimental techniques and a lack of formal tools (see above). This becomes increasingly obvious when going from intra-joint to intra-leg to inter-leg coordination of movement. Already in 1836 the brothers Wilhelm and Eduard Weber demonstrated the power of combining detailed biological data and numerical simulations by visualizing human walking sequences (Weber and Weber, 1836)[1]. This was even before experimental methods were available to visualize human walking in this detail. Muybridge and Marey presented their famous photographies of walking sequences in humans and other animals in the 1870s (see e.g. Muybridge, 1967). Today, numerical simulations and robotic models have become invaluable tools in motor control research (Azevedo et al., 2007; Pearson et al.,

[1]Furthermore, the Weber brothers stated that it would be possible to derive general control principles of human walking from simulation (Weber and Weber, 1836)

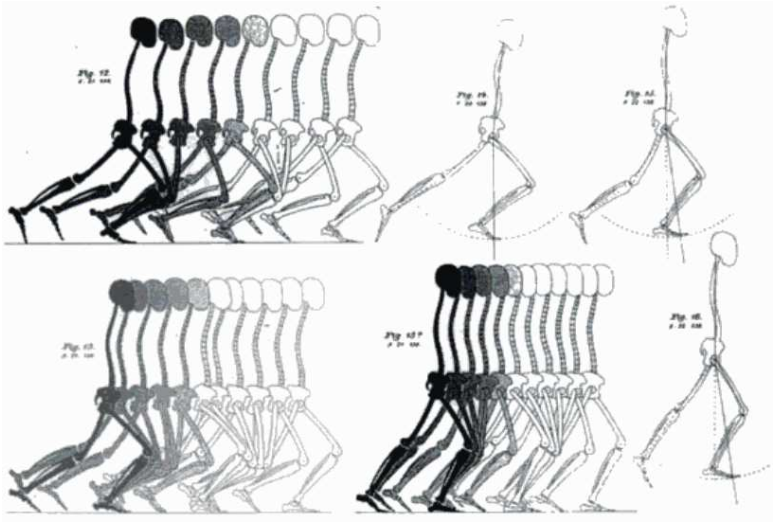

Figure 1.3.: One of the first simulations and visualizations of human walking by the two brothers Wilhelm and Eduard Weber. Table XV from Weber and Weber (1836)

2006; Scrivens et al., 2008; Webb, 2009). Models of biological locomotion control exist of e.g. stick insects (single legs: Cruse 1980; Schumm and Cruse 2006, and hexapods: Beer et al. 1997; Cruse et al. 2007), cockroaches (Beer et al., 1997; Pearson and Iles, 1973) and cats (Frigon and Rossignol, 2006; Maufroy et al., 2008; Pearson et al., 2006; Yakovenko et al., 2004, usually restricted to two legs), lampreys (Grillner, 2006) and salamanders (Ijspeert et al., 2007). Simulation studies allow to: 1. Test if the collected data is sufficient to generate the behavior under study. 2. Systematically "play" with parameters and alternative control mechanisms to generate new hypotheses about mechanisms of sensori-motor couplings. This will guide subsequent experimental research. 3. Derive new control techniques for walking machines.

Evolutionary Robotics, Animats and Robots In contrast to "wet" experiments, simulations allow to access all parameters during an experiment (or simulation run). But even seemingly simple walking simulators have a huge parameter space, considering neural, mechanical and environmental subsystems. Tuning parameters by hand, possibly according to available biological data, is time consuming. Furthermore, it introduces a subjective bias in form of the experimenter. In this context a promising approach to efficiently explore parameter space and to reduce the experimenters bias[2] is the artificial life approach to evolutionary robotics (Beer, 2009; Bongard, 2011; Nolfi and Floreano, 2000; von Twickel and Pasemann, 2007). Often extremely simplified artificial agents, termed animats, are employed to investigate general control problems like locomotion (Beer, 1990; Dean, 1998; Meyer, 1995; Webb, 2009). Artificial evolution studies, ranging

[2]Preconceptions may of course only be reduced but not completely eliminated, because in one form or another the experimenter selectively puts knowledge into the simulation (cp. Wischmann, 2008, for a detailed discussion).

from very abstract (cp. e.g. Beer, 2003) to biological grounded ones (cp. e.g. Izquierdo and Lockery, 2010) have provided testable hypotheses to biology. Furthermore, they have shown how complex behavioral tasks may be solved by rather simple neural networks when taking into account properties of body and environment. To verify that simulation results are not due to simulation artifacts, a transfer of the results to an actual robot were suggested:

> "[...] the experiments with an actual robot ensure that an essence of reality is maintained and that no critical disabling problems have been ignored"
>
> *(Brooks, 1989, p. 1)*

Thus, many of the above mentioned bio-inspired controllers were developed to be deployed on a physical walking machine (e.g. Beer et al., 1997; Ijspeert et al., 2007; Maufroy et al., 2008), using the biorobotics approach (Beer et al., 1998; Webb, 2002).

Functional and Morphological Modeling Approaches to Stick insect Locomotion Control Two basic approaches are used to derive walking controllers from biological data according to Cruse et al. (2007), the "functional" and the "morphological" approach:

The "functional", or behavior-based, approach builds up controllers with the primary goal to match behavioral data, not focusing on direct correlations with the neural and bio-mechanical substrate of the stick insect. The latter approach builds up on long history of research (cp. e.g. Bässler, 1983; Buddenbrock, 1921; Wendler, 1966) and has been pursued by Cruse and coworkers over the last two decades resulting in multiple iterations of the WALKNET controller (see e.g. Cruse et al., 2004, 2007; Dürr, 2001; Kindermann, 2002; Schumm and Cruse, 2006). WALKNET describes, to an extent unmatched by other approaches, the behavioral repertoire of the six-legged stick insect. Especially the inter-leg coordination rules derived from behavioral data ("Cruse rules", see Cruse (1990)) have been very influential. These rules were quantified in different behavioral contexts (Dürr, 2005) and intensively tested in simulations and on robots (e.g. Calvitti and Beer, 2000; Dürr et al., 2004). As a principle problem of the functional approach the correlation of model controller structure with biological controller structure is difficult. From a theoretical point of view (Negrello et al., 2008) one and the same functionality may be produced by an arbitrary number of control structures and therefore WALKNET is only one of many possible controller structures able to produce the stick insect behavior.

The "morphological", or neuro-biologically based approach, as e.g. taken in Ekeberg et al. (2004) for the single-leg of a stick insect, incrementally builds up a controller from available neuro-biological data and information about the bio-mechanical system. Subsequently it compares its behavior with that of the natural counterpart. This approach naturally allows to correlate biological and model controller structure. Additionally, recent data on neural inter-leg coordination from walking stick insects (Borgmann et al., 2007, 2009; Ludwar et al., 2005) is available. It does neither directly support nor reject the Cruse rules.

Thus, a combination of both, functional and morphological, approaches is employed here to advance the understanding of neural inter-leg coupling. In this context, the single

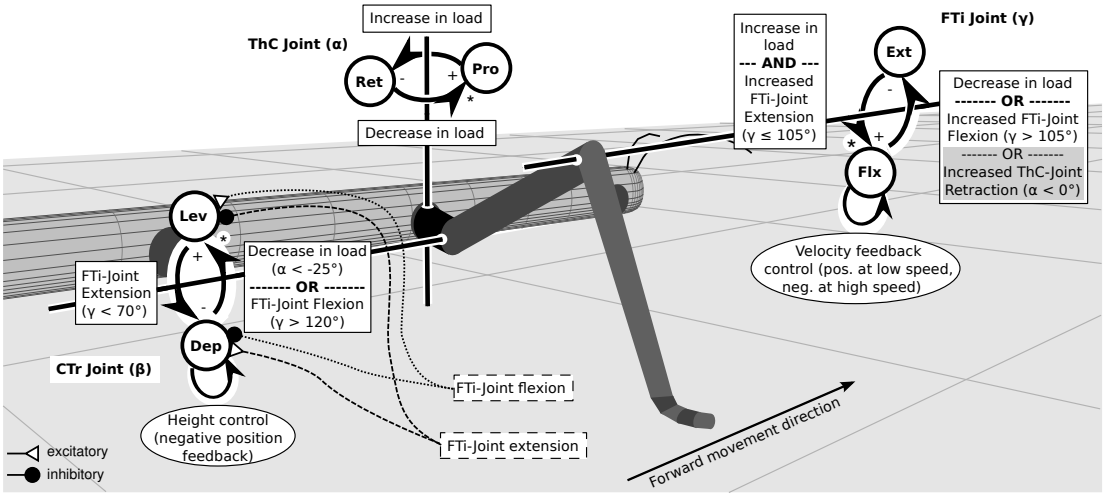

Figure 1.4.: Summary of rules given in Ekeberg et al. (2004) for each of the three main joints (joint axes are shown as solid black lines) of forward walking middle-legs: 1. State transition (timing) rules in joint controllers (boxes with solid outline), 2. Two types of magnitude control rules exist a. rules applying to one joint state (ellipse with solid outline) and b. rules that always apply (boxes with dashed outline). In brackets sensor signals used are given. Multiple conditions are connected via Boolean AND and OR. In case of conflicting state transition rules those marked with a * have priority. Optional conditions are shown with a gray background. Abbreviations: Protraction (Pro), Retraction (Ret), Levation (Lev), Depression (Dep), Flexion (Flx) and Extension (Ext). The name of each joint angle is given in Greek letters in brackets after the joint name

leg stick insect controller model based on neural data ("Ekeberg controller", see Ekeberg et al., 2004) is promising to serve as a link between behavioral based hexapod controllers ("functional" approach) and neuro-biological findings of single leg control mechanisms and inter-leg coupling influences ("morphological" approach).

Neuro-Biologically Derived Single-Leg Controller The Ekeberg controller model (see Fig. 1.4) is based on the following hypotheses: 1. Each of the three main leg joints Thorax-Coxa (ThC), Coxa-Trochanter (CTr) and Femur-Tibia (FTi) possesses its own autonomous control module, generating alternating activity in the antagonistic motor neuron pools via a bistable element (Bässler and Büschges, 1998). 2. Central connections are not sufficient to generate stable phase to phase inter-joint coupling, rather sensory signals can influence the generation of motor activity in two ways: a. by directly inducing transitions in the bistable elements ("timing influence") and b. by modifying the magnitude of the motor outputs ("magnitude influence") (Bässler and Büschges, 1998).

As an example the CTr joint controller will be explained hereafter, for the remaining two joints ThC and FTi please see Fig. 1.4. An in depth explanation, including event sequence diagrams not shown here, and detailed references are given in Ekeberg et al. (2004). The CTr joint controller may be in either of two states (levation or depression) and sensory signals determine which of the states is active ("timing influence"). If on the

one hand the femoral chordotonal organ (fCO) signal FTi-joint (γ) extension below 70°, depressor state is activated. If on the other hand fCOs signal γ flexion above 120°or if TC-joint position (α) sensors signal advanced retraction below -25°or leg load sensors signal decreased load, levation state is activated. In case of conflicting state transitions the one from depression to levation is given priority (not explicitly mentioned in the original publication, personal communication with authors). During depression phase sensory signals have an additional magnitude influence on the motor outputs, resulting in functional body height control: 1. CTr-joint position (β) is under negative feedback control and 2. FTi-joint position (γ) has an influence on CTr-joint motor activities such that body height changes due to FTi movement are reduced.

This neuro-biologically based model of single-leg control was successful in analyzing the (neural) mechanisms that result in the generation of a step cycle. However, some issues could not be resolved. E.g. the high movement velocities found in real stick insects during the step cycle could not be reproduced. This was attributed to the simplified muscle model employed (Ekeberg et al., 2004). Mechanisms of magnitude control, such as the control of walking velocity, or the controller's suitability as part of a hexapod controller were explicitly not addressed.

Objectives and Outline of This Thesis As laid out above, already a large body of literature exists on the interplay of neural control, body and environment in the generation of walking behaviors, in biology as well as in robotics. This thesis specifically focuses on the integration of (neuro-)biologically inspired models of stick insect locomotion and the artificial life approach to evolutionary robotics – it has four main objectives:

- To investigate general principles of sensori-motor couplings in single-leg stepping by employing the artificial life approach to evolutionary robotics.
- To investigate the mechanisms of magnitude control in the neuro-biologically inspired single-leg controller presented by Ekeberg et al. (2004) (see above) in the context of the controller's suitability to work as a module of a hexapod controller.
- To investigate the influence of a model of the stick insect extensor muscle (Blümel et al., 2011b; Guschlbauer et al., 2007) on the neural control of stepping.
- To establish a framework in which morphological and functional approaches to stick insect locomotion modeling and the complementary artificial life approach to evolutionary robotics may be merged and compared (cp. Fig. 1.5) and to demonstrate the framework's performance using the example of hexapod walking.

In chapter 2 the constraints and opportunities imposed by body and environment on (neural-)control and motor behavior, in biology as well as in robotics, are discussed in detail. This is a basic requirement to establish comparability and transferability of neuro-controllers between (simulated) stick insects and robots.

Chapter 3 and 4 introduce the basic simulation tools and techniques and establishes standardized interfaces for a controller transfer between simulated robotic and

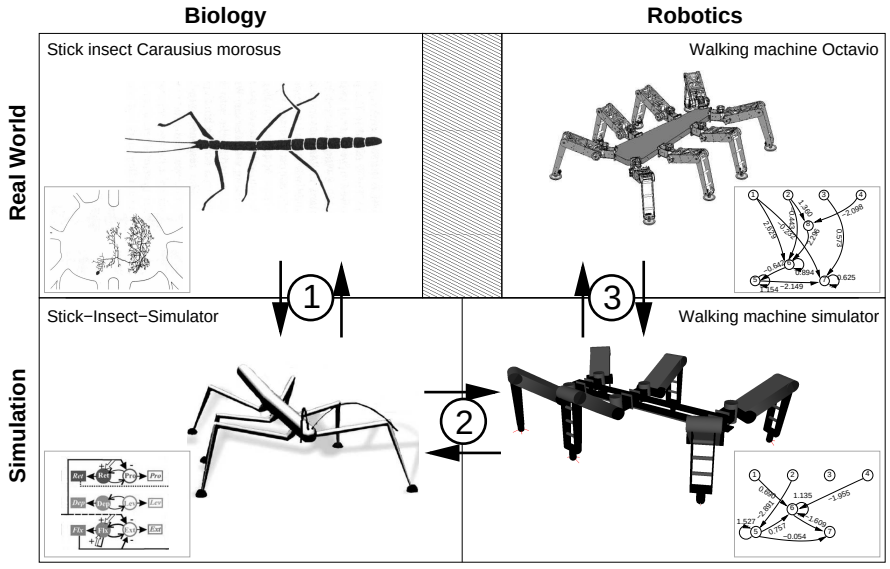

Figure 1.5.: A direct exchange of neural walking controllers between stick insect and robot is difficult because of their different constraints. To alleviate this effect, controller transfer and comparison was done in 3 steps via two simulations with standardized control interfaces

stick insect models: in chapter 3 the neural network model employed for all controllers throughout this thesis is presented, examples of the modular implementation of neuro-biologically inspired models are given and finally artificial evolution is explained as a tool to develop and optimize neural network controllers. Chapter 4 gives details of the physical simulator, the implementation of the biological and robotic models as well as of the environmental scenarios and, last but not least, the implementation of the stick insect extensor muscle model as a modular neural network.

In chapter 5 extremely simple evolved single-leg neuro-controllers, which mainly rely on reflex-oscillators formed by sensori-motor couplings are presented. Their robust behavior under changing environmental conditions is demonstrated. The controllers are analyzed to derive elementary mechanisms of sensor-driven walking control and the results are discussed in detail in the context of biology.

Chapter 6 gives the results of a simulation study of the neuro-biologically inspired single-leg stick insect controller initially presented by Ekeberg et al. (2004). It analyzes the controllers performance under perturbing conditions, either driving a stick insect or a robotic model, in comparison to available biological data and shows possible mechanisms of velocity control. Finally, using support force measurements, the single-leg controller's suitability as a module of a hexapod controller is discussed.

In chapter 7 the constraints and opportunities imposed by a stick insect extensor muscle model (Blümel et al., 2011b; Guschlbauer et al., 2007) on neural control and single-leg stepping behavior in robotic and stick insect models are investigated. On the one hand, it is shown that the application of pairs of the muscle model to all joints may simplify neural control, specifically by reducing the need for neural intra-joint feedback,

and make stepping behaviors more robust. On the other hand, multiple hypotheses on neural control mechanism that compensate for the strong low-pass characteristics of the muscle's activation function are tested.

Chapter 8 demonstrates the performance of the framework that was established in the previous chapters by presenting evolved as well as bio-inspired hexapod controllers. For the first time it is demonstrated, that the neuro-biologically inspired single-leg stick insect controller, initially presented by Ekeberg et al. (2004), may be successfully deployed for hexapod walking. This is done by integrating it with the "Cruse" coupling rules derived from behavioral experiments (Cruse, 1990). Furthermore the roles of leg specialization and local vs. global co-ordination are shown.

Finally in chapter 9 a general conclusion is presented and an outlook on future research in the context of this thesis is given.

2. Constraints of Walking Control in Biology and Robotics

> "We have now to consider the parts which are useful to animals for movement in place (locomotion); first, why each part is such as it is and to what end they possess them; and second, the differences between these parts both in one and the same creature, and again by comparison of the parts of creatures of different species with one another. First then let us lay down how many questions we have to consider. "
>
> *(Aristotle: On the Gait of Animals, written 350 B.C.E, cited after Aristotle (2007))*

In order to achieve comparability of (neural) control systems in biological systems and in technical systems, as required by an integrated biorobotics approach, the input-output behavior of the body-environment subsystems should in the ideal case be statically and dynamically equal. Since this is difficult to put into practice it is crucial to recognize the functional constraints and opportunities (Chiel and Beer, 1997) imposed by the body and the environment on the control system (cp. Fig. 1.1C). As the smallest common motor control modules in biology and robotics, articulated joints with only one degree of freedom (DOF) already show all features of a motor system as depicted in Fig. 1.1B. Hereafter examples of constraints and opportunities, contrasting biology and robotics, are discussed in the context of 1DOF articulated joints.

2.1. Passive Properties

The passive mechanical system has self-stabilizing effects, reducing necessary control efforts and providing stabilization with zero time delay (Blickhan et al., 2007; Kubow and Full, 1999; Sponberg and Full, 2008). These effects are called "preflexes" (Loeb et al., 1999) or "self-stability"(Blickhan et al., 2007).

Joint Geometry A single DOF rotatory joint will constrain movements to rotations around a common axis. The geometry of the joint, i.e. its axis orientation may have significant effects on the motor behavior and its control complexity. E.g. stick insects possess a slanted rotation axis in the Thorax-Coxa joint (Cruse and Bartling, 1995) that simplifies stance control by automatically performing a loading and unloading behavior during a single retraction of the joint, not requiring the control of other joints. This principle has been transferred to walking machines, e.g. the hexapod MAX (Pfeiffer,

2007). Similar principles have been found in cockroaches and transferred to robots (Quinn et al., 2003). Soft bodied animals (see Benny's contribution) and robots (Trivedi et al., 2008) may use similar control simplifications by configuring appropriate joints. Rotatory movements around a joint axis are usually further constrained by stops at either end that may have stabilizing effects and reduce control efforts, e.g. in passive (McGeer, 1990b) and active walkers (Pratt and Pratt, 1999) ("knee locking") and in flapping-wing micro air vehicles (Wood, 2007).

Elasticity and Damping The visco-elastic properties of musco-skeletal systems in animals (Ghatak et al., 2009) have a large influence on movement control, depending on the scale of the system: In small limbs like cockroaches, crabs and stick insects they produce sufficient forces relative to determine gravity independent resting posture in the absence of neural activations (Hooper et al., 2009; Yox et al., 1982) and to reject perturbations (Jindrich and Full, 2002). As another example passive force allow a single muscle to control a joint, as e.g. in the stick insect tarsus (Radnikow and Bässler, 1991). Series elastic elements transmitting force from the actuators to the skeleton extend the functional range of the actuators: They provide an overload protection for the actuators as well as a means to store mechanical energy (Roberts and Azizi, 2010), increase power output and increase energy efficiency (Biewener, 2003; Lichtwark and Barclay, 2010). The relative importance of energy efficiency vs. stability is discussed in the context of limb size, suggesting a higher importance for elastic energy storage during cyclic locomotion in larger animals (Dudek and Full, 2006). On the other hand in small animals like locust and mantis shrimp elastic energy storage in tendons and skeletal structures is exploited for jumping behaviors (Burrows, 2010; Heitler, 1974; Zack et al., 2009) and similar mechanism have been implemented into robots (Kovac et al., 2010). Elastic energy storage in larger limbs does play a less important role (Bobbert, 2001). Passive damping seems to be also scale dependent, increasing with decreasing limb size (Garcia et al., 2000). E.g. in cockroaches it is hypothesized that legs have substantial damping properties that reject perturbations and simplify control (Dudek and Full, 2006). E.g. in Zakotnik et al. (2006) it was demonstrated in an insect simulation how passive joint damping allows for a (unloaded) feed-forward joint position control as previously observed in cockroaches (Watson and Ritzmann, 1998). In larger limbs passive joint damping was found to have a much less important or even negligible role, as e.g. in studies of human posture control (Peterka, 2002) and hopping (Rapoport et al., 2003).

Passive Properties in Robotics In robotics passive joint properties are used to e.g. suppress vibrations of feet during swing phase of bipedal walking (Seyfarth et al., 2009) or to absorb perturbations in small hexapod robots (Koditschek et al., 2004; Sangbae Kim and Cutkosky, 2004). In larger robots (Raibert et al., 2008) the strategy of "proximal actuation and distal compliance and energy dissipation", as found in goats (Lee et al., 2008), is used to soften interactions with irregular environments. An extreme example of the exploitation of passive (joint) properties are passive walkers that produce walking behaviors without any control and by only using gravitational energy (McGeer,

1990a). Gravitational energy may be replaced by low-power actuators and simple control schemes, resulting in minimal energy walking devices on level ground (Collins et al., 2005). One passive property that is exploited in such systems is the resonance frequency resulting from the systems natural frequency and its damping. Controllers may entrain (or tune) to the mechanical resonance frequency via feedback structures (Futakata and Iwasaki, 2008; Hatsopoulos, 1996; Iwasaki and Zheng, 2006; Taga, 1995). In contrast robots using traditional control schemes like joint angle control are assumed to be much less energy efficient, e.g. with scaling effects removed the Honda humanoid Asimo (Hirose and Ogawa, 2007) is estimated to use at least 10 times the energy of a human (Collins et al., 2005). Williams and DeWeerth (2007) found a greater resonance tuning range for less damped systems, suggesting a scale dependency of resonance tuning.

Scaling As already indicated above scale dependency of passive properties imposes severe constraints on motor behaviors and its (neural) control (Biewener, 2005; Ritzmann et al., 2004), some argue that limb size has a larger effect on the (neural) control strategy than the organisms evolutionary history, giving the following example (Hooper et al., 2009): In small animals the influence of gravitational forces due to limb inertia is small compared to elastic and frictional joint forces whereas in larger animals the opposite is true. Therefore in larger animals, and robots like passive walkers, ballistic limb movements are possible and motor neuron activity is only required during acceleration and deceleration phases. This effect of scaling on passive forces is especially important to keep in mind when building robotic models to investigate motor control in animals: E.g. robotic models of small insects like stick insects and cockroaches are often, due to technical and financial reasons, scaled up by factors of 1000 or larger (Dillmann et al., 2007; Pfeiffer, 2007; Quinn et al., 2003; Spenneberg and Kirchner, 2007). To some extent the application of a non-dimensional analysis using criteria of geometric and dynamic similarities (Alexander, 1989) may improve comparability despite differences in scale.

2.2. Active Properties

Despite the opportunities offered by passive mechanical properties in motor systems they do not suffice to explain many motor behaviors in animals and to equip robots with desired capabilities, e.g. active forces in human postural control were found to be 10 times larger than passive forces (Peterka, 2002), variable-damping knee prostheses were found to offer advantages over mechanically passive designs (Johansson et al., 2005) and behavioral capabilities of passive walkers are too limited as to be of practical use (Pratt and Pratt, 1999; Vanderborght, 2011). What is added to the robustness and versatility of motor systems by active components? What can be controlled by active systems and how? As depicted in Fig. 1.1B motor behaviors at a joint may be described by a power exchange between body and environment (plus heat dissipation) and are determined by the two conjugate variables flow (movement) and effort (force). Neither body nor environment may determine both variables at the same time (Hogan, 1985; Pons, 2005) and this is the basis of the notion of situatedness. Therefore an active motor system may

control either the flow (position, velocity, ...), the effort (force, force change, ...) or a relation between the two. The latter takes into account the dynamic interaction between body and environment and is therefore essential in motor control (Hogan, 1985). Such relations are either admittances (ratio of flow to effort) or impedances (ratio of effort to flow). Particular impedances are e.g. stiffness (specific ratio of force to deviation from an equilibrium position) or damping (e.g. specific ratio of force to velocity) (Levine, 1996). How is impedance control realized in biological and robotic systems and how is it constrained?

Actuators Force producing elements or actuators in the context of motor behavior are transducers which transform energy from one form of energy to mechanical energy or the other way around (Pons, 2005). In biology muscles use chemical input energy whereas robotic actuators mostly, but not exclusively, use electric energy as input. Actuators impose strong constraints on motor control because of their non-linear static and dynamic properties under passive and active conditions. Biological actuators do constrain motor behavior (Brezina and Weiss, 2000) but are shown to simplify the control demands on the neural control system (Buehrmann and Paolo, 2006; Hof, 2003) and make motor behaviors more robust (Gerritsen et al., 1998). Actuators are affected by external load showing a dynamic damping, in muscles this is the expressed by the force-velocity relationship (Hill, 1938). Low-pass filter properties due to the load dependence may even be enhanced by the actuators activation dynamics: E.g. in the extensor tibiae muscle of the stick insect middle leg contraction time constants are extremely slow in a range from 200-700ms and asymmetric to the relaxation time constants in the range from 20-150ms (Hooper et al., 2007). The relaxation time constants in arthropods may be further reduced by an inhibitory input. In an antagonistic configuration the low-pass properties may lead to co-contractions without co-activations (Zakotnik et al., 2006). On the other hand extremely fast muscles with weaker low-pass properties have been found in animals, in sound-production of insects up to 550Hz and in weight bearing locomotion up to 110Hz (Wu et al., 2010). Together the low pass filter properties result in a limited bandwidth, i.e. limited maximum oscillation frequency, and reduced frequency for optimal power output (Neptune and Kautz, 2001) of the actuators. At the same time they smoothen switched and noisy control input signals as e.g. the summation of single spikes in biological systems (Hooper et al., 2007). More generally muscles may act as filters expressing only specific patterns from their inputs (Morris et al., 2000). Additionally to the stabilizing non-linear velocity damping (Haeufle et al., 2010) biological muscle have a non-linear force-length dependence (Rassier et al., 1999) which on the one hand limits maximum force production in certain length ranges but on the other hand stabilizes the muscles working range during oscillatory movements. Depending on the behavioral context and their activation muscles may act as motors, brakes, springs and struts (Dickinson et al., 2000): Whereas the roles as motors and struts (cp. also soft-bodied animals, Benny) are rather obvious the roles as adaptive brakes and as springs are less intuitive: Active muscles have the property of producing greater forces during lengthening than during shortening. Hereby they absorb mechanical energy which is

either directly dissipated as heat or stored in elastic structures of muscle and tendon and may be recovered in a context dependent time interval (Lindstedt et al., 2001). Active control of damping, despite the loss of energy, is a very important feature of motor systems (Blickhan et al., 2007; Dudek and Full, 2006; Wakeling et al., 2003).

In traditional engineering actuators with a high impedance, i.e. achieving maximal power output at high speeds, like electromagnetic DC-motors are employed and non-linearities are often undesired and (partly) compensated for by integrated controllers (Siciliano and Khatib, 2008). "Emerging actuator technologies" (Pons, 2005) which have properties more similar to biological systems like a low impedance (Pratt, 2002) and desired non-linearities have become important research targets with the increase in bio-mimetic and especially humanoid robots. Two examples will be given hereafter: Hydraulic and pneumatic actuators have a high power to weight ratio and may display static properties like the force-length relation similar to muscles but dynamic properties (e.g. force-velocity curve) differ substantially (Klute et al., 2002). By adding serial and parallel structures biological properties may be approximated much better but disadvantages such as a noisy operation and the required hydraulic pump remain (Herr and Kornbluh, 2004; Klute et al., 2002). Multiple robots employ this technology (Raibert et al., 2008; Vanderborght, 2011) but autonomous operation is restricted to larger machines, e.g. being equipped with a combustion engine to power the pump (Raibert et al., 2008). Artificial muscles that are polymer-based like biological muscles have features most similar to the natural counterpart (details covering the different types may be found in Bar-Cohen, 2004; Herr and Kornbluh, 2004; Pons, 2005): They may have a low impedance like natural muscles, they can absorb (reusable) energy, they can exceed the power of muscles and they may be manufactured in dimensions similar to natural muscles. As a disadvantage they are diffusion limited making scaled up versions technically difficult. So far they have only been employed in experimental robotic prototypes.

Force Transmission Actuator forces have to be transmitted to the skeleton to influence motor behaviors. Usually force transmission involves impedance matching between actuator and plant, i.e. body and environment, via varying transmission ratios (Bennet-Clark, 1995; Farahat and Herr, 2010; Hogan, 1985; Pons, 2005; Pratt, 2002). In biology this is predominantly done via series elastic tendons that attach at the skeleton with specific lever arms but additional serial and parallel tissue linkages suggest that muscles cannot be viewed as independent actuators (Maas and Sandercock, 2010). A contributing factor to impedance matching in some biological muscles is their function as an automatically varying gear (Azizi et al., 2008). Furthermore force transmission by tendons allows variations in actuator placement relative to the joint, e.g. to place actuators more proximal to the body. In robots using electromagnetic DC-motors gearboxes with high transmission ratios are usually required to achieve impedance matching (Campolo, 2010; Pons, 2005). Compared to the biological counterpart these technical transmission devices may have, depending on the gear type, quality and transmission ratio, several disadvantages such as lower efficiency, high stiffness, high-reflected inertia, poor backdrivability and backlash. Partly these effects are compensated for by active control

(Albu-Schäffer et al., 2007; Mei et al., 2004; Nef and Lum, 2009). It is argued that for robots to mimic their biological counterparts performance they require low impedance actuators (Pratt, 2002) and if possible with controllable impedance (Herr and Kornbluh, 2004). Furthermore an optimized joint stiffness has favorable effects on energy consumption (Scheint et al., 2008). Many bio-inspired robots employ force transmission strategies similar to biology, e.g. tendon-like structures or other series-elastic elements (Nakanishi et al., 2007; Pratt and Krupp, 2004; Seyfarth et al., 2009; Suzuki and Ichikawa, 2004).

Actuator Configuration and Impedance Control Actuator configuration of single joints vary depending on the organism/robot and its functionality: From zero (passive) to a high number of actuators (over-actuated) with diverse properties are found. Traditionally and most common in robotics is one reversible (double-acting) actuator per joint (Siciliano and Khatib, 2008). In contrast animals employ muscles which may only develop force in one direction (single-acting) and achieve reversible actuation via an antagonistic arrangement of actuators. In contrast to a single reversible actuator antagonistic schemes allow co-contraction of actuators and therefore feed-forward stiffness control with zero time delay (Loeb et al., 1999) independent of position and generally for an increased joint stiffness (Lee et al., 2006). Stiffness control is e.g. important to allow for a similar locomotion on different surfaces (Farley et al., 1998). Further advantages of co-contractions include an increase of the joints dynamic range (Zakotnik et al., 2006), a facilitation of rapid torque rise (Yeadon et al., 2010), increased bandwidth (Verdaasdonk et al., 2007), increased robustness to perturbations (Gribble and Ostry, 1999) and increased movement accuracy (Gribble et al., 2003; Missenard et al., 2008). Co-contraction has the disadvantage of increased energy consumption (Winter, 2009), therefore it is argued that it should be avoided (Cruse, 2002), but others (Koditschek et al., 2004) argue that energy management with respect to perturbations may be as important as with respect to energy minimization. Even more than a pair of antagonistic muscles at a joint might have functional advantages, e.g. two extensors at the coxa-femur joint of cockroaches were found to serve different roles during the same movement cycle, namely that of motor and brake (Ahn and Full, 2002).

In robotics stiffness control is traditionally achieved via proportional feedback control of reversible actuators (Espenschied et al., 1996). A major disadvantages usually is the low bandwidth due to controller delays, mechanical time constants of the actuators and backlash effects of the gears, leading, amongst others, to delayed reactions to unexpected disturbances. These disadvantages may be partly overcome by high-frequency controllers in combination with precise (and costly) sensors and actuators (Albu-Schäffer et al., 2007). Together with new actuator technologies (Klute et al., 2002; Pons, 2005) antagonistic joint actuation schemes in robotics recently received increased attention (Grebenstein and van der Smagt, 2008; Martinez-Villalpando and Herr, 2009; Siciliano and Khatib, 2008; Vanderborght, 2011). These schemes only work well with back-drivable actuators (Siciliano and Khatib, 2008) and require a nonlinear (quadratic) transmission stiffness to allow for an independent control of stiffness and equilibrium position (Bicchi and Tonietti, 2002; English and Russell, 1999; Thorson et al., 2007). Due

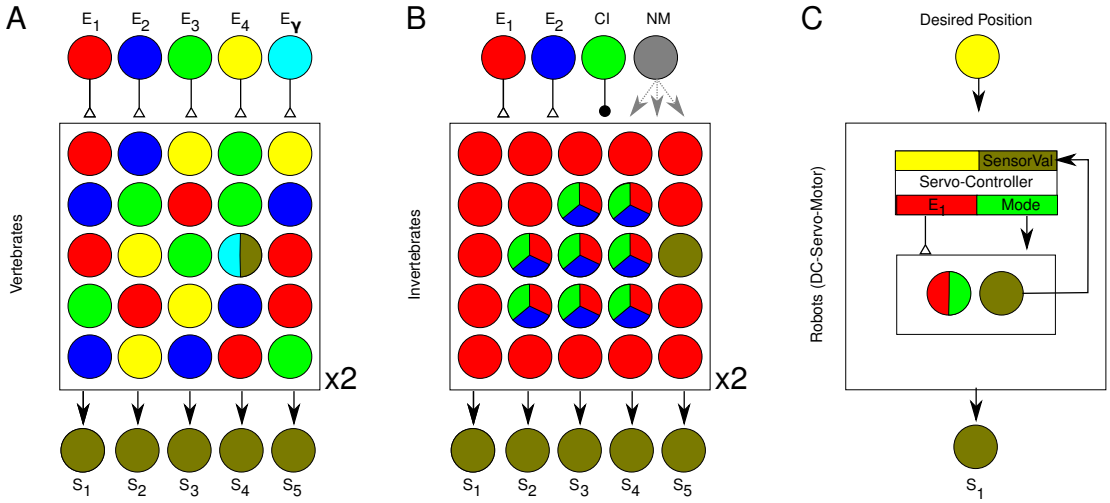

Figure 2.1.: Schematic comparison of joint control interfaces in **A** vertebrates, **B** invertebrates and **C** robots with electromagnetic DC-motors with integrated servo controllers. Motor modes may be either forward, backward, relaxed or brake. Actuators are depicted by a square containing (multiple) modules (e.g. muscle fibers). Actual number of motor inputs and sensor outputs in biological system are often much higher than displayed. Note that the biological interfaces have to be at least duplicated (x2) since usually at least two antagonistic actuators act on one joint. Abbreviations: E excitatory motor input, CI common inhibitor motor input, NM neuro modulatory motor input, S Sensor. **a** and **b** adapted from Rathmayer (2001)

to reversibility of robotics actuators alternative actuator arrangements are employed, e.g. separating actuators that control position and stiffness (English and Russell, 1999; Ham et al., 2007; Siciliano and Khatib, 2008) or separating fine-positioning and fast and strong actuators (Klug et al., 2005). These alternative actuator arrangements may be advantageous with respect to energy consumption (Laffranchi et al., 2009; Vanderborght et al., 2009).

2.3. Control Interface

(Neural) motor control systems are constrained by the control interface to biomechanics parts of the motor systems: 1. By how different actuators and features thereof may be independently controlled. 2. By which sensory information is available. The first question should be: How is the interface of the controller defined? E.g. in robotics a very commonly used actuator module is a servo-motor. A servo motor includes an angle sensor and possible further sensors but often only has one input channel, the desired position, and no output channel. Internally a controller generates motor commands from the externally supplied desired position and the internal sensor input. So the controller interface could be the desired position input or as the internal sensor outputs and motor commands.

Control interfaces of articulated joints in biology and robotics especially differ in the sheer number of in- and output channels (Ritzmann et al., 2000): In extreme cases

articulated joints in robots only possess one motor input channel and no sensor output channels as described above. In contrast in biology the number of sensor output and motor input channels per joint is usually high resulting in redundant sensor information. In many cases the specific role of each sensor output and motor input remains unclear as is e.g. the case for the joint angle sense in hands of humans (Johnson, 2004).

The high number of channels in biological motor control systems is illustrated by human tibialis anterior muscle, as one of multiple muscles driving the foot ankle joint, which was approximated to have 200 (excitatory) motor units (Xiong et al., 2008). In the same joint muscular- and tendon-sensors code for forces and position as well as their derivatives (Duysens et al., 2000; Kavounoudias et al., 2001). In the Femur-Tibia joint of the stick insect the extensor tibiae muscle is innervated by only three motor neurons, two excitatory and one inhibitory one (Bässler, 1993), and its antagonist flexor tibiae muscle by at least 14 (Bässler, 1993) and up to 27 (Goldammer et al., 2007) excitatory motor neurons and 2 inhibitory motor neurons (Debrodt and Bässler, 1990). These numbers do not take into account extra actuator control channels that are provided by neuromodulation in arthropods (Belanger, 2005; Hooper et al., 2007; Mentel et al., 2008). Multiple sensor outputs exists for the same joint coding for the flow and its derivatives, i.e. position, velocity and acceleration and combinations thereof, as well as for the effort and its derivative (Bässler, 1993), i.e. forces and in some units specifically their on- or offsets (Zill et al., 2004). Biological sensors are generally very specialized (Blitz and Nusbaum, 2007). Derivatives of flow and effort are often "calculated" mechanically. Frequently sensors measuring the effects of a joints motor behavior are placed more proximal than the joint itself which can be seen as an adaptation to limited transmission speeds from sensors to control modules. Transmission speeds are generally not an issue in robotic systems.

In robotics on the other hand the sensory (and motor) equipment is generally much more restricted and much less redundant. Mostly at least one (angular) position sensor is used as part of a servo-motor unit, often an additional force (or torque) sensor or temperature sensors to signal overheating actuators. Often commercially available sensor modules are used which are not specifically designed for the task. Derivatives of the basic sensory qualities are usually derived computationally, mostly in a central control unit, sometimes locally as part of a sensor unit. E.g. one of the most advanced walking machines to date, the quadruped BigDog, has 50 sensors for 16 active and 4 passive DOFs, including not only joint proprioceptors but also internal state and exteroceptive sensors (Raibert et al., 2008). On average this is just two and a half sensors per DOF.

Secondly the type of control inputs differ: In robotics reversible motor inputs are common, i.e. with a single input signal the joint may be commanded to move in either direction or to produce positive or negative torques (Siciliano and Khatib, 2008). In biology motor inputs are single-acting but partly inhibitory control inputs exist in addition to excitatory ones.

The large differences might be attenuated with the advance of emerging actuator and sensor technologies. E.g. polymer based artificial muscles are diffusion limited like natural muscles (Bar-Cohen, 2004). Therefore future developments might include a high number of parallel arranged artificial muscles per joint with a corresponding high

number of input channels.

2.4. Conclusion

Concentrating on 1DOF articulated joints the importance of a whole systems view of motor systems has been demonstrated. Constraints and opportunities of passive and active motor control and control interfaces have been demonstrated giving contrasting examples in biology and robotics. The examples could only provide a glimpse of the systems complexity and perspectives thereon (Turvey and Fonseca, 2009), i.e. many properties such as fatigue effects, redundancy, segmentation, inter-joint interactions via multiple reflexes, whole body movements and others have been left out. Nevertheless they underline the importance of taking into account the constraints and opportunities provided by the motor systems, especially when comparing biological and robotic systems, as done in the remainder of this thesis.

Last but not least motor behaviors and their control are not only studied from the perspective of functionality (how is behavior generated?) but also from the perspective how and why they have evolved (Clayton and Hen, 2005; Dumont and Robertson, 1986; Katz and Harris-Warrick, 1999; Kavanau, 1990; Newcomb and Katz, 2009; Rose, 2004; Tierney, 1996). This view may give additional insight into the nature of constraints and opportunities in motor systems.

3. Artificial Neural Networks as Walking Controllers

> "[...] it involves the reciprocation or vibration of the limb. Confining ourselves to one leg, we can see that this swings back and fore like a pendulum, implying that there is a nervous arrangement, such that the completed movement forward sets on the commencing movement backward, and conversely."
>
> *(Alexander Bain: The senses and the intellect, cited after Bain (1855), p. 263)*

Purely mechanical driven walkers like passive walkers (McGeer, 1990a; Wisse, 2004), mechanical moving toys or art robots such as the "strandbeast" (Jansen and Niemeijer, 2007) already show impressively robust locomotion behaviors, yet their behavioral repertoire is limited when compared to animals. Therefore, technical and biological walkers usually possess control systems. These control systems are operational closed but because they are structurally coupled with the (artificial) organism's body they may extend its behavioral capabilities (cp. Fig. 3.1 and Maturana and Varela, 1992). Whereas animals usually employ neural control systems, simulated and robotic walkers may use a multitude of different control systems (see e.g. Levine, 1996; Siciliano and Khatib, 2008, for an overview). These range from purely technical systems, like finite-state machines, to artificial neural control systems, which mimic certain properties of the biological counterpart. Throughout this thesis exclusively simple artificial neural networks were employed. This had several reasons: First of all artificial neural networks focus on the connectivity structure rather than on complex properties of single elements (Haykin, 1999). Artificial neural networks are well suited for evolutionary algorithms (cp. Nolfi and Floreano, 2000, for details), as used in this thesis. Powerful computational tools to develop and analyze the artificial neural networks were available (Ghazi-Zahedi, 2008; Hülse et al., 2004).

This chapter gives an overview of the neural network's constituting elements and its connectivity structure and modular architecture. Furthermore, examples of how neural networks and neural modules were derived from neuro-biological and behavioral data are given that serve as a basis for the simulation experiments presented in part II. Subsequently, the method of artificial evolution is introduced, which allows to optimize either the parameters of a given neural network structure or to develop novel network structures. Finally approaches to analyze such networks are shortly explained.

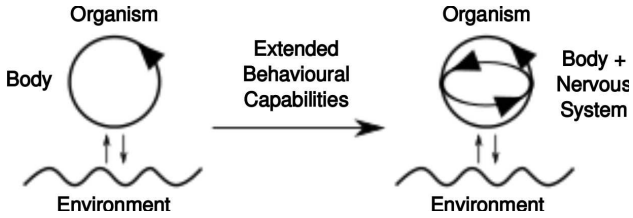

Figure 3.1.: Nervous systems allow to extend the behavioral capabilities of an (artificial) organism. Adapted from Maturana and Varela (1992)

3.1. Recurrent Neural Networks

3.1.1. Neuron Model

As depicted in Fig. 3.2, all neurons of the neuro-controllers were of the simple additive type with either the standard sigmoidal transfer function:

$$1 \qquad \frac{}{x} \qquad \mathbb{R} \tag{3.1}$$

or the sigmoidal transfer function

$$2 \qquad \frac{x \quad x}{x \quad x} \qquad \frac{}{2x} \qquad \mathbb{R} \tag{3.2}$$

Both transfer functions are interchangeable by using the following formula (see Pasemann, 2002, for details):

$$\frac{\frac{x}{2}}{} \qquad \mathbb{R} \tag{3.3}$$

Furthermore, both transfer functions show an almost linear behavior around zero input and both are strictly monotone and differentiable, which is important for e.g. the application of optimization algorithms.

Sensor neurons were an exception because they used the unbounded identity function as transfer function. The discrete time dynamics of a recurrent neural network with neurons was given by

$$k \qquad k \quad \sum_{i=1}^{m} \quad ki \quad i \tag{3.4}$$

where $_k$ is the output of neuron k, $_k$ denotes a bias term, $_{ki}$ is the synapse from i to k and is either or . Note that the discrete time dynamics incurred a fixed sequence of updates which here was an update of all neuron activations (the weighted sum of all inputs plus the bias) followed by an update of all neuron outputs. In turn this meant for neural pathways that each additional synapse entailed a time delay of one time step. Network update was done either with or with , depending

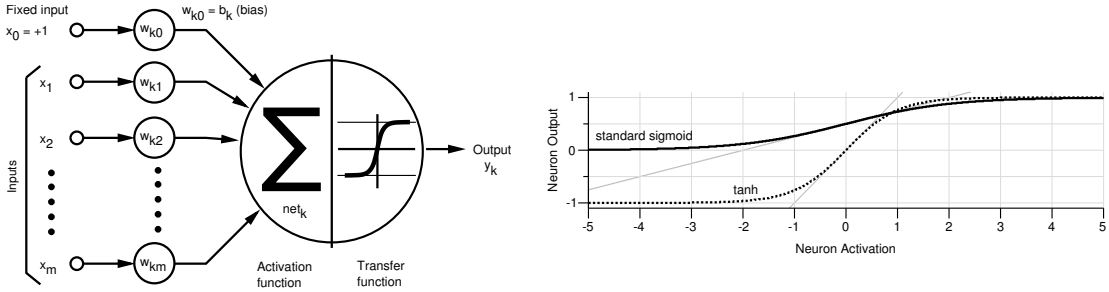

Figure 3.2.: Schema of the time discrete neuron model with a sigmoidal transfer function

on the simulation platform (cp. chapter 4 for details).

Which of the two presented transfer functions is used is, to a large extend, up to the experimenter. On the one hand, the function has an output range of] [and this might e.g. be conceptually simpler to use for the motor neurons of wheel driven robots where a negative output could correspond to backward drive, a positive output to forward drive and an output of zero to a stop. For further possible advantages of the function, such as hardware implementation details, cp. Hild (2008). On the other hand, the standard sigmoid is conceptually simpler to compare with biologically neurons, because its outputs are in the range of] [and, therefore, never negative. As a result, the output of a neuron with a standard sigmoid may be simply suppressed by a large negative input, whereas for the a more complex neural structure is necessary to achieve the same. Alternatively, outputs of the function may simply be reinterpreted as ranging from minimum to maximum firing rate, irrespective of their sign, or the other way around for the standard sigmoid. Here, was used for the simple robotic simulator AMOS (cp. section 4.2.1), because the hardware target platform supported it. On the other platforms the standard sigmoid was used due to its better comparability with biology (see above).

The standard additive time discrete neuron with a sigmoid transfer function is far from a realistic, or biophysical, model of biological neurons (cp. Feng, 2004; Haykin, 1999; Izhikevich, 2007, for details), but they share some interesting properties: the bounds of the nonlinear transfer functions can be interpreted as an analog of the bounded firing rate of biological neurons and the activation function can be interpreted as the summation of synaptic input at the dendrites and soma level in biological neurons. Additionally, the simple neuron model was employed here because of its computationally efficiency, its rich dynamics when coupled with other simple neurons (see below), and its good analyzability.

The Integrated Structure Evolution Environment (ISEE) software package (Ghazi-Zahedi, 2008) was used to simulate neural networks (NN). It allowed to perform online structure and parameter manipulation, plotting and logging to relate structure and parameter changes to changes in behavior.

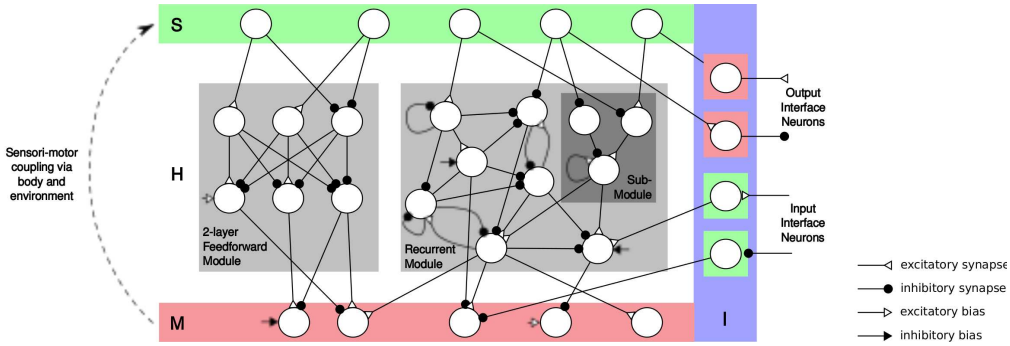

Figure 3.3.: Schematics of a modular neural network consisting of an input or sensory (S) layer, a hidden (H) layer, an output or motor (M) layer, several modules and an in- and output interface (I) layer. As examples a 2-layer feed-forward module and a recurrent module with a sub-module are shown. The in- and output interface neurons connect to external neurons and, therefore, the network may be employed as a module of an even larger network. Neurons are depicted as circles. They each may have a positive or negative bias and incoming and outgoing synapses connect them with other neurons

3.1.2. Modular Recurrent and Feed-Forward Networks

Multiple simple neural units may be coupled to form a neural network (cp. Fig. 3.3). Usually such a network possesses an input layer with sensor neurons, a hidden layer with hidden neurons and an output layer with motor neurons. If all neurons are strictly ordered in layers and connections only occur uni-directional from input layer to output via the hidden layers, the network has a feed-forward architecture. If loops are found within a neural network it is called recurrent. But note that even feed-forward networks may have feedback loops, i.e. sensori-motor couplings through body and environment. Neurons may be grouped into modules, whereby a module is e.g. defined with respect to connectivity or function. Neural modules may possess dedicated interfaced through which they interact with other neurons and neural modules.

Already small recurrent networks of this type may generate complex dynamics (Pasemann, 2002), e.g. two-neuron networks may show fixed-point, periodic, quasi-periodic and chaotic behaviors. No restrictions were imposed on the structure of the network, therefore arbitrary recurrent connections and an arbitrary number of inter-neurons were allowed. The neuro-controllers were developed either by hand-design or by artificial evolution (see below).

3.1.3. Simulator Net Coupling

The network output have to be coupled to the bodies motor system, i.e. DC-motors or muscles, and the network inputs to the bodies sensor system, e.g. joint angle and foot contact sensors (cp. Fig. 3.4). To map the output space of the bodies sensors to the input space of the sensor neurons and the output space of the motor neurons to the input space of the motor or muscles, a linear mapping function was applied. Also note that network frequency and sensor and motor update frequencies could differ, e.g. in the stick insect simulator only every fourth step of the sensor and motor update data was

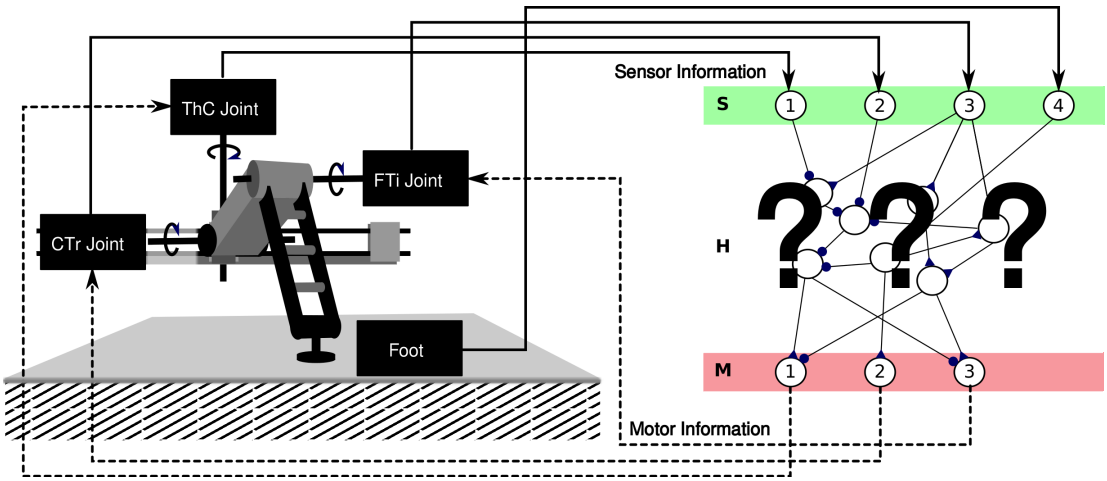

Figure 3.4.: Schematics depicting the coupling between the sensor and motor neurons of the neural network on the one side and sensors and motors of the body on the other side. The sensori-motor equipment, and therefore the number of in- and outputs of the neural network controller, depended on the simulator platform and the experiment, please see chapter 4 for details. To develop network structures that result in an efficient overall behavior of neural network and body when interacting with the environment is a major goal of this thesis

exchanged with the neural network. For details of the mapping intervals and update frequencies for the different platforms, please see chapter 4.

3.2. Deriving Neural Networks from Neuro-Biological Data

Based on Ekeberg et al. (2004) the rule based controller (see Fig. 1.4) was implemented as a modular neural network, using the standard sigmoid as transfer function. The network update frequency was fixed to 100Hz. Required neuro-modules are described in detail hereafter together with the implementation process that resulted in the final neuro-controllers.

3.2.1. Neuro-Modules as Functional Units

Boolean AND and OR Approximators Neural approximations of Boolean AND and OR functions were required to map the rule dependencies for state transitions derived from neuro-biological data. As can e.g. be seen in Fig.1.4 the transition from Extensor to Flexor state in the FTi joint required two conditions (increase in load and FTi joint extension) to be true at the same time, i.e. they were AND connected. The simplest neural implementation consisted of one neuron with two inputs. The underlying mechanism was the same as that of the threshold module variant 1 (see above), except that the threshold was applied to the sum of the two inputs. Varying the ratio of the bias to the input weights shifted the separation plane. Varying the absolute weights and the bias modified the sharpness of separation. Those two parameter sets that were used in

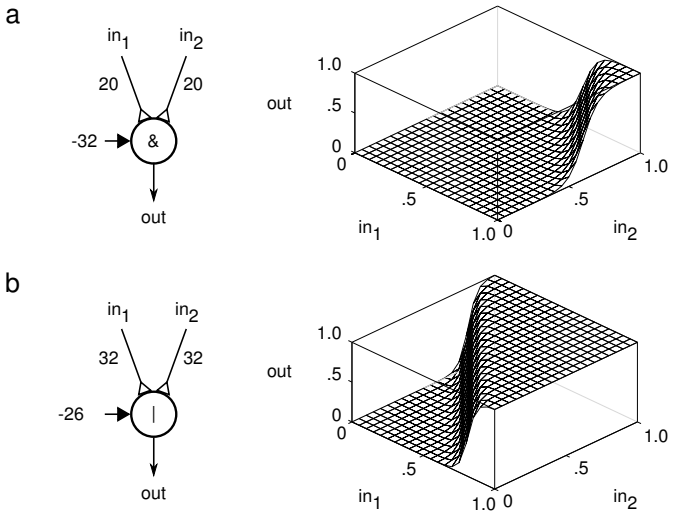

Figure 3.5.: Neuro-modules approximating Boolean AND (**a**) and OR (**b**) functions. See text for details

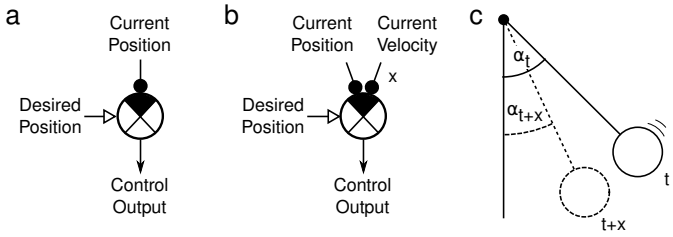

Figure 3.6.: **a** Standard single neuron servo-mechanism. **b** Servo-mechanism additionally using velocity input to act on predicted future position and therefore increasing stability and/or allowing larger loop amplification factors. **c** Pendulum model of the reflex loop adapted from McMahon (1984). See text for details

this paper and that resulted in AND and OR behavior are given in Fig. 3.5. Note that synaptic input weights of both modules were not equal - this was due to the synaptic weight and bias value range limitations of the robot platform.

Position and Velocity Servo Module (Comparator) In the original model a servo-mechanism was found in the CTr joint as height controller and in the FTi joint as velocity controller. Throughout this work servo-mechanisms (see Fig. 3.6) were also employed for all forward walking controllers in the ThC joint and to fixate the ThC joint during the sidewards walking experiments. A simple servo-controller could be realized with a single neuron acting as a comparator comparing a reference (angular) position α as input and the desired position as bias. By scaling input weight and bias and/or the output weight the loop amplification could be adjusted. Due to time-delays and noise on sensors and actuators higher amplification factors led to instabilities. Instead of PID-controllers the angular velocity of angle α could be used as an additional input to the comparator for

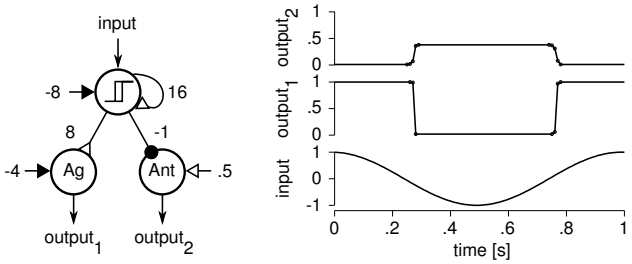

Figure 3.7.: Neuro-module to alternatingly activate antagonistic motor-neurons and to adjust relative activation strength

enlarging stable loop amplification ranges (McMahon, 1984). Velocity could stabilize the reflex loop by predicting future positions at time :

$$\alpha \qquad \alpha \tag{3.5}$$

The prediction time interval should be scaled to account for the total time-delay due to sensors, actuators and neural processing.

Antagonist Activation Module As already mentioned above ("Bistable Module") antagonistic motor-neurons should be activated in an alternating way. Bistable elements were perfectly suited as premotor neurons projecting to both antagonist motor-neurons with opposite signs Cruse (2002). By tuning the strength of the synapses and the bias terms the relative activation of the antagonist motor-neurons could be adjusted (see Fig. 3.7).

Bistable Module Bistable elements were needed as modules for the neural equivalent of the biological controller serving two functions: 1. as threshold elements detecting if sensor values fulfill given conditions, i.e. joint angle °, and 2. as premotor elements ensuring alternating activation of antagonist motor neurons. In this case a simple approach was taken by using only one neuron. There are two variants (see Fig. 3.8):

1. The simplest solution was to take one neuron with a large input weight resulting in a fast saturation of the sigmoidal transfer function relative to a change in input size. Increasing input weight made the effective threshold function more steep. The bias value was used to adjust the desired threshold (decreasing bias shifts the threshold to larger input values and vice versa). There were two drawbacks to this solution: 1. The approximation quality of the step function is positively correlated with the size of the input weights and bias values, but depending on the platform the neural network is running on their maximum absolute values are limited. E.g. on the 16bit microprocessor driving Octavio the maximum weight range was limited to [[(6bit including the sign) to maximize fractional digit precision (which was a trade off with the absolute weight range and in this case

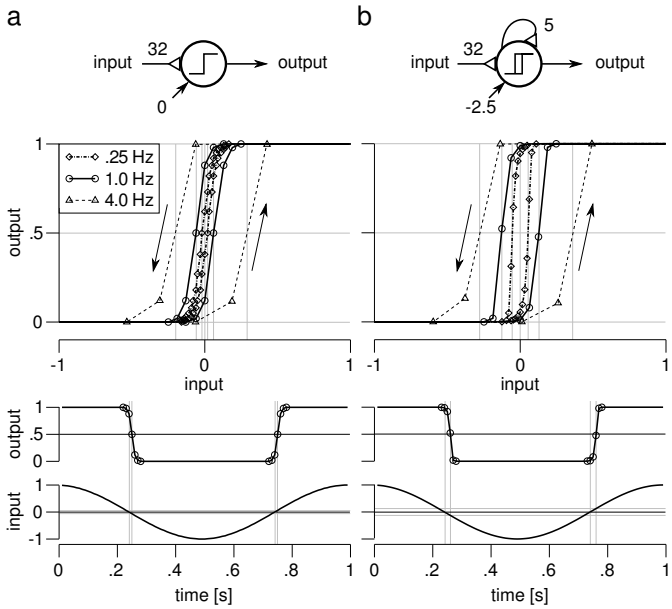

Figure 3.8.: Two variants of a single neuron bistable module. **a** without and **b** with positive self-coupling. The xy plots (neuron output vs. input) show the hysteresis effect dependence on input signal frequency for three exemplary chosen frequencies as well as on the self coupling weight (compare a and b). The time-plots show input threshold to output switch time delay dependency on self coupling weight. Individual data points are only shown for transitions. Not shown: Variant b is less noise sensitive

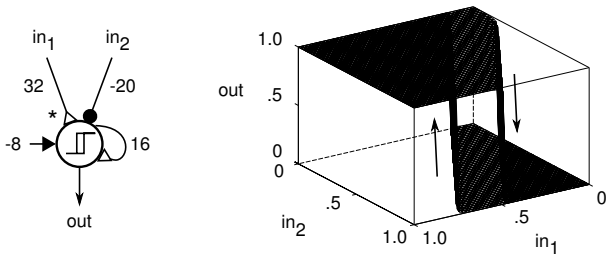

Figure 3.9.: Neuro-module serving as a switch with separate inputs for on (input 1) and off (input 2) switching. By using asymmetric input weights (unequal absolute input weights) one of the inputs can be given a higher priority. In the example shown input 1 (marked with a *) has priority over input 2 because it can switch on out independent of the state of input 2. Input 2 on the other hand can only switch off out if input 1 is smaller $\approx 0\,5$. Note that each data point in the 3D plot was retrieved after 100 iterations to minimize transient effects

would be 10bit, i.e.) and computing speed. 2. It was very sensitive to noisy input values around the desired threshold.

2. Extending the above solution by a positive self-coupling of the neuron required smaller input weights, effectively increased the steepness of the threshold function and reduced noise sensitivity because it acted as a simple low-pass filter. If self-coupling weights surpassed the critical value (which was 4.0 for the standard sigmoid), the neuron showed hysteresis, further reducing noise sensitivity. Increasing self-coupling weight resulted in a wider hysteresis and stronger low pass filter behavior. Depending on the frequency of the input signal a hysteresis effect was observed with sub-critical self-couplings due to the time-discrete dynamics of the neuro-module. A disadvantage of the extended solution was that the time-delay before switching occurred increased with increasing self-coupling weights.

The extended hysteresis version was chosen (parameters as given in Fig. 3.8b) as threshold element for sensor values as well as bistable premotor module ensuring antagonistic activation of the motor neurons. This was mainly due to its superior tolerance to noisy sensor values as seen in most robotics systems (see e.g. von Twickel and Pasemann, 2007). When calculating threshold parameters (bias values, cp. Table 3.1) the "delay" effect of the self-coupling had to be taken into account.

Switch Module with Separate and Prioritized On and Off Triggers Bistable elements (see above) as premotor elements ensured alternating activation of antagonist motor neurons. In the biological model two separate modules were used (at least in the CTr and FTi joints) for on and off switching of the respective bistable element. Depending on the parameters chosen and the sensory input, the two modules could have contradictory outputs, e.g. one commanding to switch from levation to depression and the other vice versa. In this case the inputs were prioritized (see Fig. 3.9). The original implementation (Ekeberg et al., 2004) achieved the same with if-else-expressions, where the if case had highest priority.

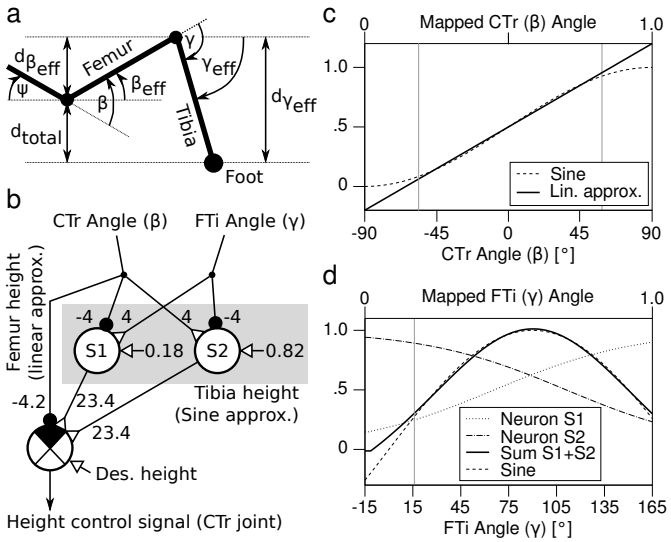

Figure 3.10.: **a** Body height depends on CTr ( ) and FTi (γ) joint angles as well as on the CTr joint angle offset (, which was 0 for the robot and varies for the different legs of the stick insect). **b** Proposed neuro-module to control the body height of the walking machine using the sum of the height influences of both joints as reference input and the desired height as control input to a comparator. Its output was used to control CTr motor neurons (parameters are given for the robotic model with 0). **c** CTr height influence was linearly approximated (shown here for 0), **d** FTi height influence with a two neuron sine approximator (shown here for $_{eff}$ 0)

Two-Joint Height Control Module As summarized in Ekeberg et al. (2004) (see also Fig. 1.4) two sensory influences affect the *magnitude* of the CTr motor neuron output but not directly the *timing*:

1. Intra-joint CTr negative position feedback is assumed to be a major component of height control in standing and walking animals (Cruse et al., 1993).

2. Inter-joint FTi CTr influences exist that affect the Levator to Depressor activation ratio such that it is increased upon increased flexion and decreased upon increased extension (Bucher et al., 2003).

As depicted in Fig. 3.10, these magnitude influences were abstracted and combined in a height control servo module (cp. position servo above) for the CTr joint. We assumed that the coronal plane was parallel to the ground and that the leg segments Trochanterofemur (Femur) and Tibia had constant lengths. Then the height of the body above the ground was determined by the angular position of the two joints CTr (β plus offset which is 0 for the robot) and FTi (γ) in combination with the segment lengths of Trochanterofemur ($_m$) and Tibia ($_{i\ i}$):

$$_{eff} \qquad _{eff} \tag{3.6}$$

$$\beta \qquad _m \qquad \gamma \quad \beta \qquad _i \tag{3.7}$$

The height influence of the CTr joint was linearly approximated whereas the height influence of the FTi joint was given by a simple sine approximator; both were sufficiently accurate within the "normal" movement ranges (for comparison see Cruse and Bartling, 1995). CTr and FTi height influences were summed in a comparator neuron as controlled variable and subtracted from the desired height reference input. This resulted in a proportional height control servo. By multiplying all inputs to the comparator by the same factor and/or by multiplying the output synapse strength by a factor, the gain of the servo could be adjusted. Note that the ThC joint angle α and the axis offset had an influence if the axis offset was non-zero as in the stick insect model. This influence was not taken into account here, and no neuro-biological evidence for such an influence exists. In contrast, the WALKNET implementation of a CTr height controller (Dürr et al., 2004) uses all three leg joint angles.

Parameters of the height control module in Fig. 3.10 were initially tuned for the robotic model and needed to be modified for the stick insect model because of different factors: The ratio of trochantero-femur length to tibia length in the stick insect (FL: 1.073, ML: 1.065, HL: 1.042) differ from the robotic model (1.065) (see Table D.1) but to such a small extent that this factor was neglected. Leg plane rotations by and as well as a β range and mapping offset of 30°(see Table 4.5) compared to the robotic model resulted in an effective β offset. Neglecting the influence of in combination with the ThC joint angle α the offset is β_m . Multiplying this offset with the synaptic weights (s. Fig. 3.10) from the CTr (β) angle sensor to the comparator and the sine approximator neurons S1 and S2 resulted in additive bias correction terms for the respective neurons.

3.2.2. Bio-Inspired Single-Leg Controller

Assembling the above described neuro-modules to map the rules shown in Fig. 1.4 to a neural network and setting threshold parameters converted from those given in Ekeberg et al. (2004), we obtained the middle leg forward walking controller depicted in Fig. 3.11: For all joints (proximal to distal from left to right) from top to bottom proprioceptive intra- or inter-joint sensory signals were processed by threshold elements, combined with other sensor signals via Boolean elements and fed to bistable modules that functioned as premotor elements. Per joint one bistable premotor element antagonistically activated two motor neurons. In the CTr joint a parallel pathway from sensor to motor neurons existed that functioned as a height control module.

Neural threshold parameters were determined to meet two conflicting requirements: Noise tolerance and fast switching. A broader hysteresis, i.e., a larger self-connection , results in better noise tolerance but delays switching, and vice versa. Parameters $_i$ and (cp. Fig. 3.8) provided an optimal trade-off for both criteria within the synaptic weight limits of the network (see section 3.1.1). The desired threshold was given as sensor neuron output value ( ) which was mapped from the original sensor range (see Table. 4.3). The bias value was then determined as

$_i$ (3.8)

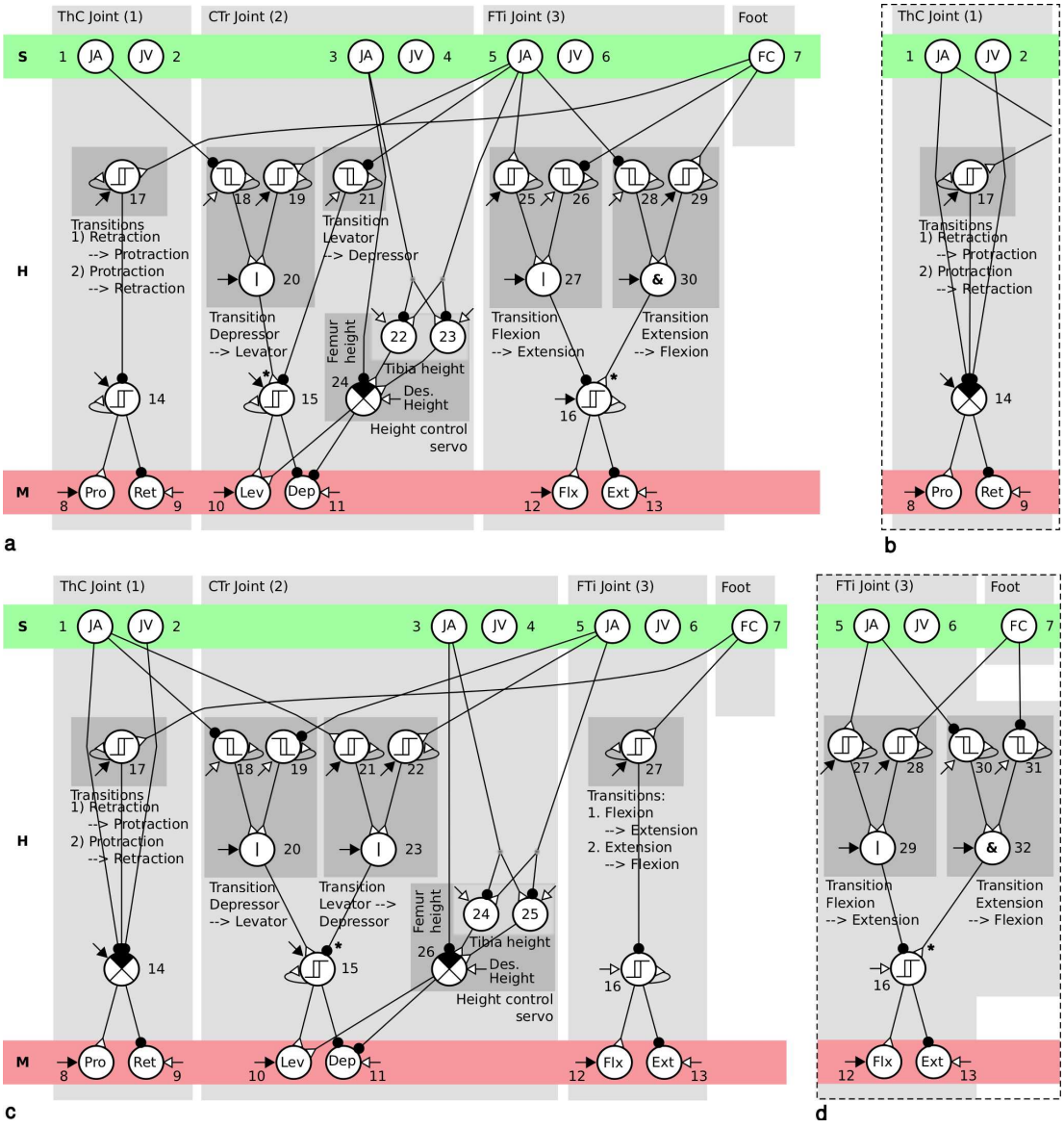

Figure 3.11.: **a** Complete Controller transferred from Ekeberg et al. (2004) without modifications. Controller structure is applicable for middle- and front-legs. Abbreviations: Sensor or Input layer (S), Hidden layer (H), Motor or Output layer (M), Joint Angle (JA), Joint Velocity (JV) and Foot Contact (FC). Motor Neuron abbreviations are given in Fig. 1.4. Neurons are numbered for easier reference from text. For a detailed description of the modules employed see section 3.2.1. **b** Alternative ThC joint control module extended by a neural servo to stabilize the joints working range. Restricted (sidewards) walking is achieved by setting the connection strength to zero and by instead supplying the ThC neural servo with a fixed reference input via the bias of neuron 14 (not shown). **c** Hind-leg controller transferred from Ekeberg et al. (2004) with the same modified ThC joint control module as in middle- and front-leg controllers. CTr and FTi joint control modules have a different structure and partly different synapse signs. **d** Alternatively a FTi control module with the same structure as in middle- and front-legs but two inverted synapse signs is used in the hind-leg

Table 3.1.: Transition rule switch parameters (joint angles) converted into neural parameters of sensor neuron (SN) and threshold neuron (TN). Parameters are given for front-leg (FL), middle-leg (ML) and hind-leg (HL) as well as for forward walking (FW) and sidewards walking (S). For conversion formula see equation 3.9 and text. Entries marked with * were corrected from Ekeberg et al. (2004)

Joint	Transition		Signal	Leg	Dir	Op	Thres [°]	Thres [SN Out]	SN–TN	TN–TN	Bias adj.	TN Bias
FTi	Flx	Ext	γ angle	ML	FW,S		105.0	0.667	32	5	3.2	-20.63
				FL	FW		95.0	0.611	32	5	3.2	-18.86
				HL	FW	-	-	-	-	-	-	-
	Ext	Flx	γ angle	ML	FW,S		105.0	0.667	-32	5	3.2	22.03
				FL	FW		95.0	0.611	-32	5	3.2	20.26
				HL	FW	-	-	-	-	-	-	-
CTr	Dep	Lev	α angle	ML	FW		-25.0	0.361	-32	5	3.2	12.26
				ML	S	-	-	-	-	-	-	-
				FL	FW		*10.0	0.556	-32	5	3.2	18.48
				HL	FW		-45.0	0.250	-32	5	3.2	8.70
			γ angle	ML	FW		120.0	0.750	32	5	3.2	-23.30
				ML	S		105.0	0.667	32	5	3.2	-20.63
				FL	FW		98.5	0.631	32	5	3.2	-19.48
				HL	FW		*55.0	0.389	-32	5	3.2	13.148
	Lev	Dep	α angle	ML,FL	FW,S	-	-	-	-	-	-	-
				HL	FW		5.0	0.528	32	5	3.2	-16.19
			γ angle	ML,FL	FW,S		70.0	0.472	-32	5	3.2	15,81
				HL	FW		*90.0	0.583	32	5	3.2	-17.96

Additionally, the nonlinear threshold module behavior had to be taken into account, e.g. hysteresis effects introduced a shift of the switch threshold, depending on input signal frequency (cp. Fig. 3.8). A bias adjust factor ( ) was experimentally determined as the difference of the bias calculated above and the bias at which the threshold unit output crossed 0.5 in the desired direction (cp. vertical lines in Fig. 3.8) at a step cycle frequency of 0.75 Hz. This frequency was assumed to be the "standard" step frequency. An extended bias value calculation resulted:

$$_{i} \tag{3.9}$$

For example using $_{i}$ and the correction factor would be approximately . Resulting neural parameters are given in Table 3.1 for angle thresholds. Foot contact threshold was set to half of the maximal activation of the foot contact sensor. Parameters are given for all leg types (front-, middle- and hind-legs).

Parameters not prescribed by the neural rules nor explicitly given in the module descriptions are here called "free" parameters. They were tuned by hand (with the exception of the body support force simulations, see section 6.2.4) while observing the resulting behavior. As subjective criteria stable and fast walking on flat ground were used. "Free" parameters were the premotor and height control to motor neuron synaptic weights, the motor neuron bias values and the reference inputs to the CTr height controller and the ThC servo controller.

3.2.3. Extended Bio-Inspired Single-Leg Controller

See Fig. 3.12 for an extended version of the bio-inspired controller from Figs. 3.11a+c. The same controller structure is used for front-, middle- and hind-legs and only parameters are individually modified for each leg. The sensor interface was extended by joint angle acceleration (3, 8, 14) and joint torque and torque derivative (4-5,9-10,15-16) sensor neurons. The motor interface was extended by a tarsus attachment motor neuron (27, cp. Fig. 4.8).

Furthermore, modules were added or extended, i.e. ThC and FTi joints were equipped with switchable positive and negative velocity servos, which were suppressible (44,76) during swing (Bartling and Schmitz, 2000; Schmitz et al., 1995; Schneider et al., 2006). Their set-point was switchable between flexion and extension velocities (74,75), respectively pro- and retraction velocities (42,43). The CTr height control influence was made suppressible (93,62) during swing. Grayed out neurons 91, 92 and 94 supplied balancing inputs to the motor neurons, that became necessary to cancel bias offsets of the velocity servos during their suppression. To allow stable biphasic flexion-extension movements during stance, a flexion suppression mechanism was introduced (95) that was activated after a switch from flexion to extension during stance and inactivated upon stance to swing transition. To support a switchable inactive state, position control servos were added for ThC and FTi joints. To account for a deployment on the robotic model without muscle model, range limiters in ThC and FTi joints (49-50,81-82) were added to supply stabilizing passive forces towards the joint angle limits. Finally, a positive and

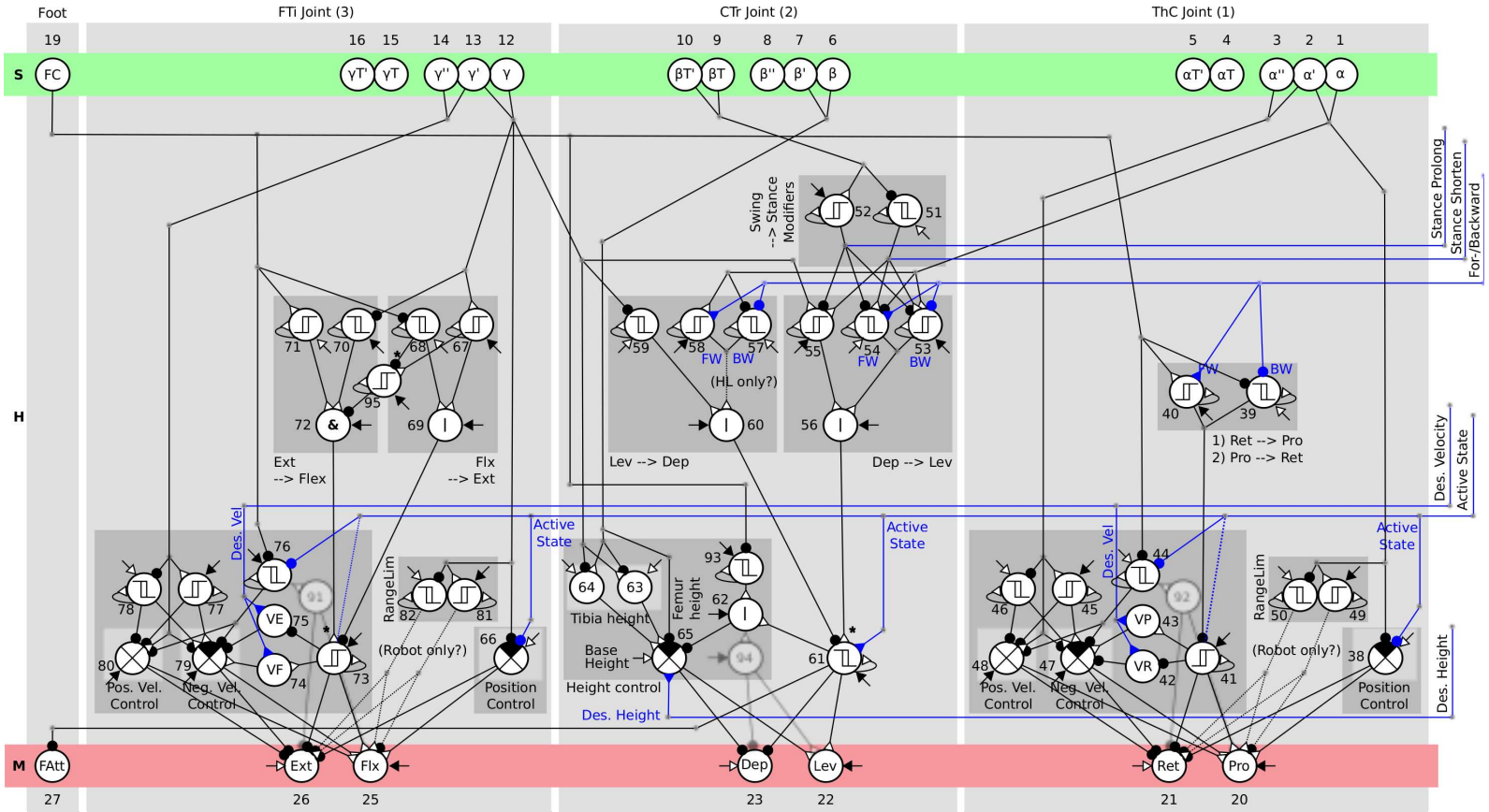

Figure 3.12.: An extended version of the neuro-biologically inspired controller from Figs. 3.11a+c. For details see text

negative CTr torque threshold module was introduced to support ongoing stance or trigger stance-swing transitions (51,52) (Akay et al. (2001, 2004, 2007), also cp. (Schilling et al., 2007)).

The leg external interface was configured to include all sensor neurons as output neurons and multiple extra interface neurons as leg inputs. These included: inter-leg coupling inputs to shorten or prolong the stance phase by shifting the PEP (Cruse, 1990), an active state switch, a walking direction switch, a desired walking velocity and a desired body height.

3.2.4. Bio-Inspired Hexapod Leg-Coupling Modules

Since neural data on inter-leg coupling mechanisms in stick insects is still sparse (Borgmann et al. (2007, 2009); Ludwar et al. (2005), but see Daun-Gruhn (2010) for model hypothesis), the well tested "Cruse-Rules" (see Cruse, 1990, for a summary), which were derived from behavioral studies, were neurally implemented to serve as coupling influences for the neuro-biologically inspired single-leg controllers presented above. In Fig. 3.13 the findings of Cruse (1990) are summarized and the neural implementation and their performances presented:

- Rule 1 is a rostrally[1] directed influence which inhibits the start of swing in the rostral leg if the caudal[2] leg is in swing and for a time period of 100ms after touchdown. If the swing phase is prolonged also the negative coupling influence is prolonged. This coupling influence is exclusively active ipsi-laterally. Neurally this is realized as follows: foot contact information from the caudal leg is send to the rostral leg where it is post processed by a combination of a threshold element and a differentiation, leading to the desired coupling influence signal.

- Rule 2 is also rostrally directed and additionally active in the contra-lateral direction. This influence excites the start of the swing phase in the rostral leg shortly after touchdown of the caudal leg. The neural implementation is analog to Rule 1.

- Rule 3 is caudally directed, but also acts between contra-lateral front- and hind-legs. It excites the start of swing in the caudal leg with increasing strength while

[1] towards the head
[2] towards the tail

Figure 3.13. ***(facing page)*****: a–c** From left to right: The behavioral effects of the first three stick insect inter-leg coupling rules derived from behavioral data ("Cruse-Rules", see Cruse (1990) for details), a summary of the leg pairs they apply to, the neural implementations that were used here and their respective performance are shown. Anterior-posterior foot movements during stance phase are given as a solid black line, during swing phase as a dashed line. A gray background denotes when the negative coupling influence is active. Note that only the relevant neural structures are shown and that the coupling influences are derived in the receiving leg based on sensory information from the sender leg. In the performance plots, a gray background denotes stance phase. See text for details

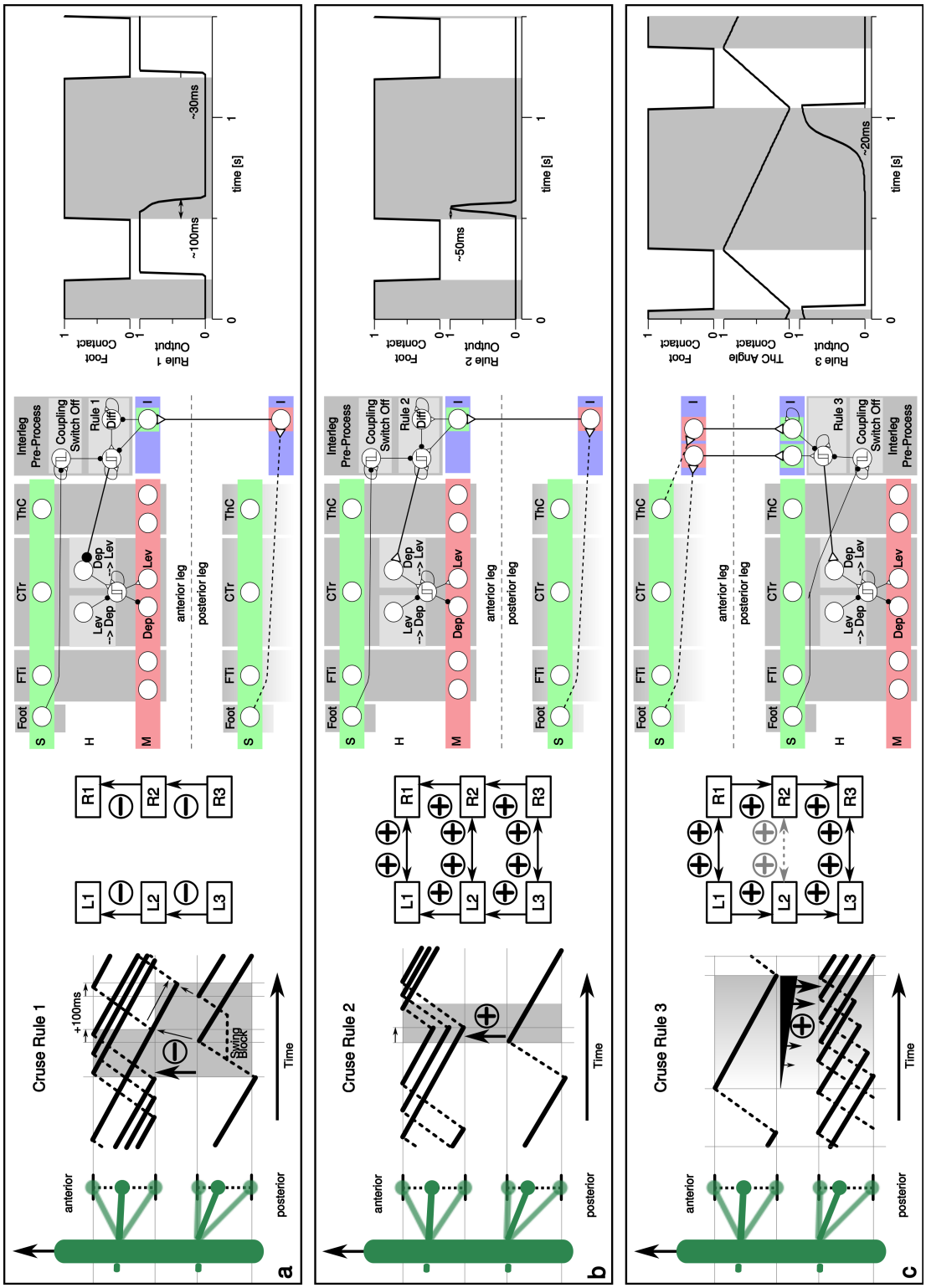
Cruse Rule 1
Cruse Rule 2
Cruse Rule 3
anterior
posterior
Time
+100ms
Swing Block
L1
L2
L3
R1
R2
R3
Interleg Pre-Process
Coupling Switch Off
Rule 1
Rule 2
Rule 3
Diff
Dep --> Lev
Lev --> Dep
Foot
FTi
CTr
ThC
S
H
M
I
anterior leg
posterior leg
Rule 1 Output
Foot Contact
~100ms
~30ms
Rule 2 Output
~50ms
Rule 3 Output
TThC Angle Contact
~20ms
time [s]
a
b
c

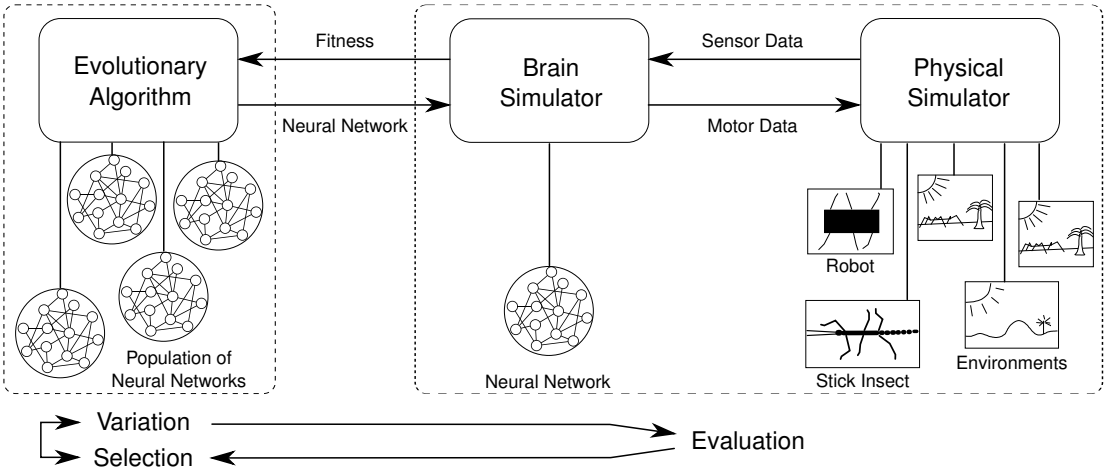

Figure 3.14.: Artificial evolution as an evaluation–selection–variation loop

the rostral leg is retracting. The neural implementation simply exploits the scaled and shifted sigmoidal transfer function together with a suppression of the influence during swing.

3.3. Artificial Evolution as a Tool to Generate and Optimize Neural Controllers

Artificial evolution was employed as a tool to develop neural control structures for the locomotion of simulated robotic or stick insect walkers with single legs as well as with six legs. An overview of the evolutionary process is given in Fig. 3.14 and is shortly described hereafter: Neural networks generated by the evolutionary algorithm were successively send to the brain simulator. The brain simulator processed one net at a time and communicated with the physical simulator to exchange sensor and motor data. The simulator processed a certain number of steps (this depended on the simulator, see chapter 4 for details) without communicating with the brain simulator. Then communication took place and the net was updated according to the sensory data received from the simulator and the internal state of the net. Subsequently a new motor output was generated which in turn was send to the simulator. This net-update-simulation-loop was continued for a specified number of cycles and if desired, the loop itself was run through several times, each time with a different environment. In the course of the simulation a fitness value was calculated constantly. After the simulator/net-update process had completed the specified number of cycles, the final fitness value was send back to the evolutionary algorithm. It continued to send nets to the brain simulator for evaluation until all nets of one generation were evaluated. The evolutionary algorithm then selected a certain number of nets (selection process) according to their fitness values generated during evaluation. The selected nets were reproduced and the "offspring" underwent a variation process. A new generation was then ready to be evaluated. This

variation-evaluation-selection loop Hülse et al. (2004) was run through repeatedly until the evolutionary process was stopped by the user. During evolution the user had the possibility to change several parameters to influence the variation-evaluation-selection loop, e.g. population size, weighting of fitness terms, number of evaluation cycles, mutation probabilities, the type of evolution (structural/parameter evolution), etc.

3.3.1. Evolutionary algorithm

The ENS^3-algorithm was used as the evolutionary strategy (Hülse et al., 2004): ENS^3 is an implementation of a variation-evaluation-selection loop operating on a population of neuro-modules. The algorithm works on a population which is divided into parents and offspring. Several operators were put to work on the neuro-modules:

- The *evaluation* operator which consists of a fitness function that measures the performance of each neuro-module. The desired number of neurons and connections can be negatively added to the fitness function by means of a cost function to keep the size of the evolved networks within limits.

- The *selection* operator is of stochastic nature. It determines the number of offspring for each neuro-module by means of a rank process, based on the results of the evaluation operator, and by means of a Poisson distribution. Each neuro-module with a number of offspring greater than zero is passed on to the next generation. User definable parameters determine the mean size of the new population as well as the selection pressure (e.g. elitism can be forced).

- The *reproduction* operator creates a certain number of copies (offspring) of each individual neuro- module, whereby the number of copies is determined by the selection operator.

- The *variation* (or *mutation*) operator realizes both a combinatorial and a real-valued variation in a stochastic manner. On one hand the combinatorial variation accounts for insertions and deletions of hidden neurons and connections which are determined by per-neuron and per-connection probabilities (random variable [ ]). On the other hand the real-valued variation is responsible for the variation of the weight and bias terms. The probability of variation is determined by another random variable [ ], its magnitude by a Gaussian distributed random variable.

The algorithm has no formal stop criterion – it is rather assumed that the user determines the "right" time to end the evolutionary process by monitoring relevant parameters.

3.3.2. General Techniques Used During Evolution

Numerous parameters had to be set before/during evolution. On the one hand, there exists no standard common procedure but on the other hand, the setting of parameters was not performed arbitrarily. Rather, some general strategies exist which could serve as a guideline. Some of the strategies employed during this work are summarized here:

- The weightings of different terms of the fitness functions were adapted to the state of evolution: E.g. during the evolution of locomotion controllers first a high reward was given for smooth and slow oscillatory movements and only a low or no reward for forward movement. Then, as some individuals arose in the evolutionary process that made smooth forward movements an increasingly higher reward was given for the forward movement while at the same time the weighting of the oscillatory term was decreased.

- It was tried to keep the evolved networks small to avoid a large parameter space because the larger the parameter space the less likely new/better solutions were found by the evolutionary algorithm. Additionally it was easier to analyze smaller nets later on. The small size was achieved by first allowing arbitrary growth of the neuronal structure to just introduce costs for neurons and synapses when the behavior met the demands defined prior to the experiment.

- If a functional principle was discovered in a net (e.g. a special connection structure) the neuro-module was manually edited according to the principle discovered, deleting neurons and connections not required, and then re-subjected to parameter evolution.

- Environments were (randomly) changed in the physical simulation in every generation to obtain maximal robust controllers. To even carry this idea further a defined set of environmental scenarios (cp. section 4.3) could be successively put in place during each generation to make sure the nets had at least an average performance in each of these environments.

- The evolution was started several times with varied seed nets, to obtain different start-points in the parameter space.

- Mutation probabilities and amplitudes were adapted to the state of evolution, e.g. evolution was started with high mutation probabilities and amplitudes, which corresponded to large leaps on the weight-space-landscape, and these high amplitudes and probabilities were decreased as soon as functional controllers arose (fine-tuning by successively smaller steps on the weight-space-landscape).

- Structure evolution was followed by parameter evolution: Once a network performed sufficiently good, its structure was fixed and the parameters were optimized.

Single Leg Evolution

During the evolution of single legs, some of the following assumptions were made, depending on the experiment:

- Slow and large amplitude oscillatory movements are a prerequisite for the development of robust walking.

- Minimized swing-stance ratios increase stability, especially for later use in hexapod controllers (cp. section 3.3.3 below).
- Foot sliding should be minimized for maximum efficiency and stability.
- Body heights in a certain range should be reached to ensure that controllers are able to support the body weight.
- Strong lateral movements (cp. single-leg rail experimental setup in section 4.1.1) are inefficient and might cause instabilities upon deployment in hexapod controllers.

These assumptions were implemented either in the respective fitness function or as terminate try signals (see below).

3.3.3. Modular Evolution of Hexapod Controllers

The goal of using artificial evolution as a tool during the course of this work was to find alternative control structures to those known from robotics and biology or to extend or combine known control structures. For single-legs it is relatively simple to evolve neural controller, even from scratch, and to analyze the resulting controllers. The search-space for single-legs is comparatively small, due to the small number of sensor and motor neurons and the limited kinematics of a single 3DOF leg. For more complex behaviors and the coordinated control of multiple legs the search space was massively increased. Therefore, multiple approaches were followed to reduce the search space without reducing the possible solutions so far that only trivial solutions would result Rempis et al. (2008):

Assumptions were made about the controller architecture in stick insects and this was in turn assumed to be of a general advantage for locomotion control architectures:

- Every leg possesses its own control module.
- Controller for front-, middle- and hind-legs differ but contra-lateral leg controllers are symmetric.
- The connectivity between legs is smaller than inside of a leg controller.
- Several sensory influence important for inter-leg coupling are known from behavioral experiments in biology such as foot contact and load information or ThC angle as a measure for retraction (cp. Cruse, 1990).

Therefore, the evolution software ISEE was extended to support arbitrary modular neural controllers with inter-module coupling structures and enforceable symmetry constraints (cp. Fig. 3.15). For inter-module couplings interface neurons were introduced to which inter-module connectivity was restricted. Single-leg modules could either be seeded with empty networks or e.g. with known structures from biology (cp. neurobiologically inspired controllers above). Evaluations always took place for complete controllers and the same fitness was applied to all modules.

Furthermore, assumptions were made about the desired behavior:

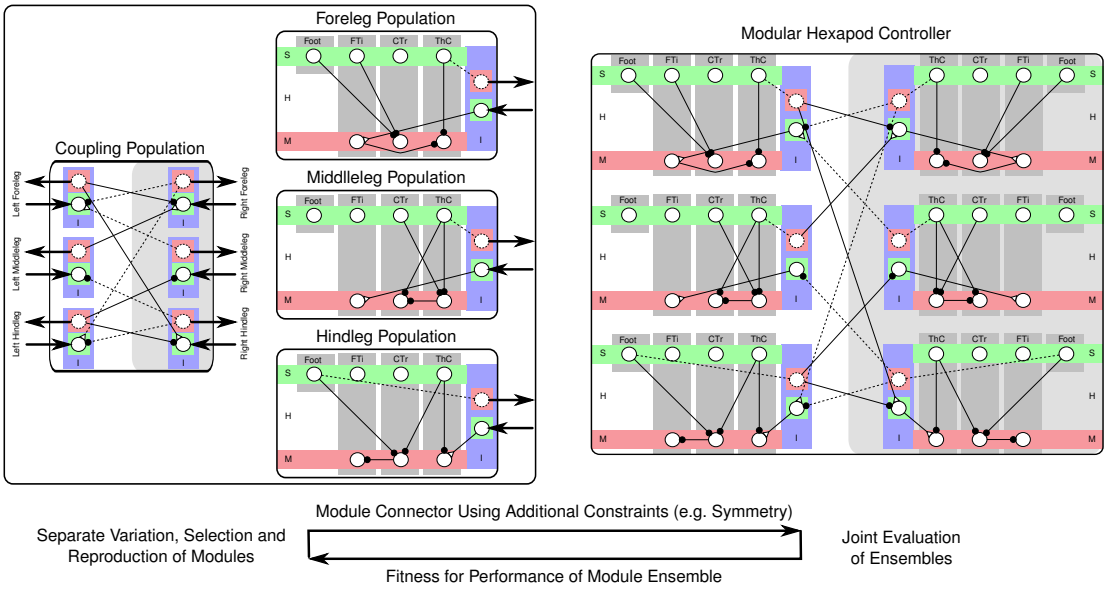

Figure 3.15.: Modular evolution concept: Single leg modules and coupling modules are selected, reproduced and varied separately but only module ensembles, i.e. complete hexapod controller, are evaluated and the resulting fitness is assigned to all modules. Depending on module network size the fitness value used for selection may be varied afterwards. To minimize the search space additional constraints may be imposed, as e.g. the lateral symmetry depicted

- During walking joints have a limited working range.
- Force/Torques above a certain threshold are detrimental.
- Rhythmic movement inside a certain frequency and amplitude range have to occur to achieve efficient locomotion.
- Controllers should be robust to be able to cope with varying environments or increased noise levels without dramatic performance results.
- For multi-legged walking certain footfall patterns lead to instability, e.g. if multiple neighboring legs enter swing phase at the same time.
- Segments other than the feet (tarsi) or lower legs (tibiae) should not have contact with the environment to ensure exclusive body support by the legs. As an exception it is known from stick insects that they may use their abdomen to support the body (Bässler, 1983).

These assumptions were either implemented as terminate-try signals, which could stop evaluations or in the fitness function. Additionally it was assumed that the initial conditions (posture, torques) are crucial to achieve a stable walking rhythm. Therefore, initially mechanical support could be given for the body and terminate try signals and fitness terms were disabled during a "warm-up" evaluation phase. A combination of

multiple of these strategies allowed to successfully develop more complex controllers, e.g. for hexapods (cp. chapter 8).

3.3.4. Evaluation of Performance

Terminate Try Signals

Thresholds could be applied to sensory signals or a combination of multiple sensory signals to terminate ongoing evaluations. If a behavior was so faulty, that it did not promise to improve, further evaluation was considered unnecessary. Cp. the above paragraphs for a justification. Terminate try signals were, depending on the simulation experiment, triggered as follows:

- Joint angles that exceeded an angular range observed during stick insect walking (Cruse and Bartling, 1995) by more than 10°.
- Segments other than feet (tarsi) and lower legs (tibiae) that touched the environment.
- A minimum walking distance was not reached in a specified time.
- A foot was not lifted for a certain amount of time, usually the time of a typical step cycle plus a tolerance period.
- A certain body height was surpassed, indicating e.g. undesired jumping movements.
- An unrealistically high fitness, indicating simulation errors like unnatural explosive movements.
- An average amount of foot sliding, defined as the sum of all feet movements in the horizontal plane during stance.

These terminate try signals were either implemented as part of the physical simulator or as part of the fitness function and could be disabled during "warm-up" phases. Thresholds could be modified during experiments to e.g. become more strict with increasing fitness. Employing these signals was found to be very efficient and even necessary for successful evolution of hexapod controllers: on the one hand, they reduced the overall number or evaluations steps and therefore allowed more evaluations in the same amount of time. On the other hand, they were extremely efficient in removing undesired behavioral features.

Fitness Functions

The fitness was first calculated for each try individually as the sum over all single step fitness values. Hereby the total number of steps could differ if terminate try conditions were used (s.a.). If multiple tries were evaluated the total fitness for was subsequently calculated.

Single-Leg Experiments The total fitness for time steps was calculated by taking into account multiple terms:

$$i \qquad \sum_{i=} \qquad \begin{matrix} \alpha \\ \beta \\ \gamma \end{matrix} \tag{3.10}$$

The individual fitness terms had the following meaning:

- The *wayTerm* simply was the total forward displacement.
- The *bodySupportTerm* could take values between 0 (no support by the leg, i.e. full body support by the rail) and 1 (full support by the leg). The term was derived from a force sensor in the single-leg rail setup (cp. section 4.1.1). The relative influence of the term could be changed by parameter as follows: If was set to 1 the height term was fully weighted, i.e. if there was full support of body weight the way term was multiplied with 0 (or more with decrease of weight support), if was set to 0 the height term was effectively disabled and the way term was always multiplied with 1.
- The *footContactTerm* could take values between 0 (no contact) and 1 (maximal contact. Forward displacement was therefore only rewarded during foot contact.
- The *swingStanceTerm* was derived by division of two counters for swing duration and stance duration. As a condition for stance a combination of a foot contact threshold and a load threshold were taken, otherwise swing was assumed.
- The *footSlidingTerm* was used to counteract behavior where the foot was not really lifted during walking and to counteract artificial behaviors resulting from the footContactTerm (see above): sometimes agents evolve that performed explosive pushes, let the foot slide on the ground and took all the resulting fitness. Foot sliding was defined as the sum of foot movements in the horizontal plane when the foot was close to the ground. In case of perturbation scenarios where foot friction was minimized, this term was disabled.
- The *frequencyAmplitudeTerm* was used to overcome the bootstrap problem. This term rewards frequencies and amplitudes in predefined regions which each have wide plateaus to not favor any specific frequencies and/or amplitudes.
- The *lateralMovementTerm* punished lateral body movements above a certain threshold.

The individual fitness terms could be scaled or disabled during experiments by modifying parameters α .

Hexapod Experiments The total fitness for time steps was calculated by taking into account multiple terms:

$$i \qquad \sum_{i=} \qquad \alpha \tag{3.11}$$

Note that several fitness terms from the single-leg fitness function are now implicitly included in the global stability criterion: e.g. if the body is not supported by the legs or lateral force become to high, the walker stumbles or falls down. These instabilities result in a decreased fitness and might even trigger the terminate try mechanism. The new binary (0,1) term *footContactConstraintsTerm* is the product of a *contralateralFootContactConstraintTerm* and an *ipsilateralFootContactConstraintTerm*. The former becomes 0 if at any time two contra-lateral legs are not in contact with the ground simultaneously and is 1 otherwise whereas the latter is calculated analogous for ipsi-lateral leg pairs.

Multi-Try Evaluation Fitness values of n single tries were calculated from the individual try fitness values as follows:

$$\overline{\qquad\qquad} \qquad i \qquad i=1 \tag{3.12}$$

Multiplication was used opposed to addition because all tries had to perform well in order to achieve a good fitness instead of one exceptionally well performing try that could balance bad performing tries. I.e. robust generalized behaviors and not specialized behaviors were desired.

3.3.5. Analysis

After several evolution runs had been conducted the performances of the best nets of all evolution runs were compared with each other and, if available, with some reference controllers. The overall best performing nets or nets having a particular interesting structure were afterwards subjected to further analysis. As a first step in the analysis of the structure-function-relations of a controller, its behavior was described qualitatively as well as quantitatively (cp. section 3.3.4 above). A tool showing the activities of the neurons and the strengths and signs of the synapses during the robot-environment interaction (simulation) in form of an animated neural net gave first visual clues. Using the tool in single step mode together with its plotting capabilities (all neuron outputs could be plotted) allowed further inspection. Also, the activities of all neurons could be arbitrarily set (stimulation/lesion experiments) during the simulation to examine the influence of certain connections and sensor inputs. Finally, the neuro-modules were analyzed as dynamical systems to identify loops, hysteresis effects, CPGs etc. (Pasemann, 2002).

4. Embodiment in Dynamic Simulations of Stick Insects and Robots

> "[I]n proportion as a body is more capable than others of doing many things at once, or being acted on in many ways at once, so its mind is more capable than others of perceiving many things at once. [...] And from these [truths] we know the excellence of one mind over the others."
>
> *(Benedict de Spinoza: Ethics, IIP13S, first published posthumously in 1677, cited after de Spinoza (1994))*

Without a body no behavior may take place and the properties of a specific body have a major influence on possible behaviors and their control through the nervous system (Chiel and Beer, 1997; Hatsopoulos et al., 1995; Pfeifer and Bongard, 2006, also cp. chapter 2). Therefore, a body is needed to investigate locomotion control. Depending on the objectives, this may either be a biological organism, a robot, a simulation of one of the former two or even an abstract animat (Beer, 1990; Dean, 1998; Meyer, 1995; Webb, 2009). Throughout this thesis, experiments have exclusively been performed in simulations because of: 1. their accessibility, i.e. the ease to change and to access all simulation parameters, necessary for a thorough analysis and for generating novel hypotheses by "playing around", 2. their speed, which is essential for performing a high number of evaluations as required by evolutionary robotics, 3. their power to describe available data from biology and robotics in a unified way, 4. their suitability to test the explanatory power of existing hypotheses (cp. e.g. Ekeberg et al., 2004) and to visualize them, and finally 5. their low cost, when compared to real robots.

Overall three walker models were simulated (cp. Fig. 4.1): One stick insect model and two robotic models, whereby the first closely modeled a complex walking machine (Octavio) and the second only loosely corresponded to a more simple walking machine (AMOS-WD06). The rationale for employing multiple simulations was that the more detailed, or data-driven, models allowed to build a bridge to transfer and compare controllers between biology and robotics, whereas the simple, more theory-driven, model allowed to explore more general ideas without spending too much time on implementation details (Beer and Williams, 2009). Due to standardized interfaces between neural controllers and simulations, specific controllers could be transferred between and tested across all simulations, as long as their sensori-motor equipment used by the controller matched. The two more complex simulations (stick insect and Octavio) were equipped with more sensors, e.g. load, velocity and acceleration sensors, and could be driven via three different motor interfaces, ranging from simple servo control to more complex antagonistic control with and without muscle models. All simulated walkers could be

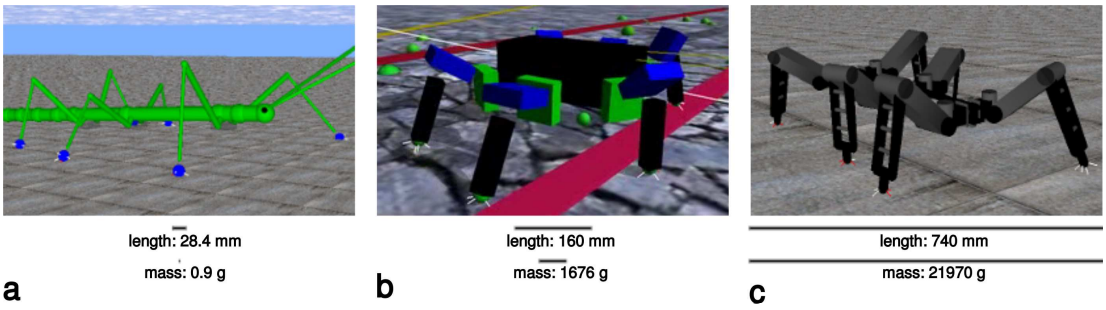

Figure 4.1.: One simulation of a biological organism (**a** Stick Insect) and two simulations of walking machines (**b** Amos WD06 and **c** Octavio) were employed in the experiments described in this thesis. The bars below the images give an impression of the relative body lengths (FL to HL coxae) and body masses. Note for the stick insect mass that the smallest point that may be printed here corresponds to a mass that is still $\approx$ 00 times larger than that of a stick insect. The absolute lengths and masses are additionally given below the respective bars

tested in different environments and under multiple perturbing conditions.

Hereafter the physical simulator used for all three simulations is described, together with the implementation of sensor- and motor-systems, including muscle models. Subsequently specific details of the three simulators are given and finally the environments and perturbing scenarios used for performance evaluation are presented.

4.1. Physical Simulator

A physical simulator in the context of this thesis mainly had to fulfill four criteria: 1. it had to be fast to allow a large number of evaluations, 2. it had to be stable to allow unattended operation, 3. it had to be sufficiently precise to a) allow transferability of controllers from robot simulations to robots with at least qualitatively comparable behaviors or b) the biological simulation had to show a good behavioral performance match with the target organism, and 4. it had to have compatible interfaces with the hardware to allow an easy transfer of controllers between simulator and hardware.

Based on these criteria, physical simulations of the walking machines Octavio and AMOS-WD06 and of the stick insect *Carausius Morosus* were built on top of the OpenDynamicsEngine (ODE Smith, 2009) based simulator called Yet Another Robot Simulator (YARS, Zahedi et al., 2008). The ODE library is a game physics engine geared towards speed, a prerequisite for performing a large number of evaluations as required by the evolutionary robotics approach. Successful transfers of complex controllers from simulations to real robots, as well as behavioral matches between stick insect simulation and real stick insect were used as the criterion of sufficient precision. Previous studies with the same simulation environment but different robotic platforms (Fischer et al., 2004; Markelic and Zahedi, 2007; Wischmann et al., 2005) have shown that the transferability criterion was met with a simulator where morphology, motors and sensors were only roughly approximated but where available parameters were carefully tuned and noise levels on sensors and motors slightly exaggerated.

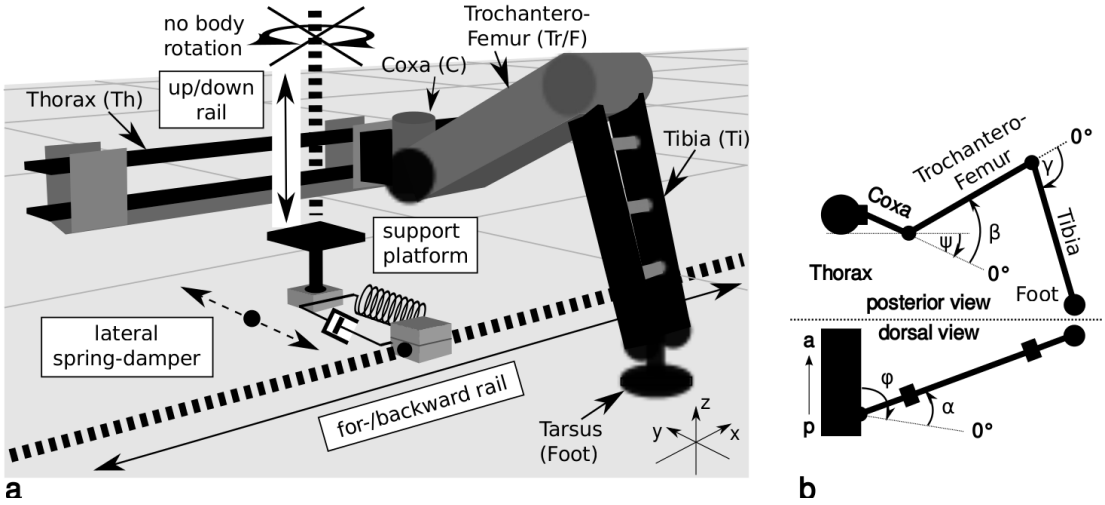

Figure 4.2.: **a** Single leg simulator setup with a three degrees of freedom (DOF) rail setup. For- and backward movements were only slightly damped, optional sidewards movements were restricted by a stiff spring-damper system and up- and downward movement was damped, unrestricted in upwards direction and limited in downwards direction by a support platform. No rotational movements were allowed. Additionally segment names of the walking machine are given. For joint names see Fig. 1.4. **b** Schematic figure of joint angle conventions (zero point and sign) and joint axes ("leg plane") offsets and (which are both zero for the robotic models). For details see Cruse and Bartling (1995). Abbreviations: anterior (a) and posterior (p)

All relevant sensor and motor properties, muscles, skeleton, joints, contact surfaces, friction properties and moments of inertia were implemented in YARS and each simulation, including walking machine and environment, was given in Extensible Markup Language (XML). The XML file could be automatically reloaded and, therefore, allowed to easily change parameters or modify the simulator structure during experiments. E.g. multiple randomized perturbation scenarios could be used, increasing their difficulty during an experiment. YARS connected to the ISEE package (cp. previous chapter 3), which simulated the neural network (NN), via User Datagram Protocol (UDP) communication. The physical simulation update frequencies varied between and (see description of specific simulations below) and every second or fourth step (again depending on the specific simulation) the NN update was triggered, sending sensor values and receiving new motor activations. A 3D-Visualization and parameter plotters allowed to closely monitor the simulation experiments. Additionally all parameters could be logged for a subsequent analysis.

4.1.1. Single Leg Simulator Setup

Following the modular approach, single leg walking experiments were supported for all three simulations: the torso of the single legged walking machine was mounted on a rail system. It allowed for for- and backward movements, which were damped to stop movements during stance in a reasonable time interval, and slightly damped up-

and downward movements with a ventral hard stop, simulating the remaining legs. Optionally, it had a lateral spring-damper system to simulate lateral force influences of other legs (see Fig. 4.2). This allowed for small lateral movements similar to hexapod walking in stick insects (cp. Kindermann (2002)). As an exception, the spring-damper system was replaced by a simple damper in sidewards walking simulations. Up-down and sidewards rails optionally included force sensors to measure forces exerted by the leg.

The joint setup was similar to the one described in Ekeberg et al. (2004): Each leg had three active hinge joints, namely Thorax-Coxa (ThC), Coxa-Trochanter (CTr) and Femur-Tibia (FTi). CTr and FTi joint axes were parallel to each other but in the robotic models, and different from the biological model, the ThC joint axis was parallel to the dorso-ventral axis and orthogonal to the other two joint axes. Contrary to this and the biological model in Ekeberg et al. (2004), real stick insects have a ball and socket ThC joint. This may be viewed as a functional hinge joint where the axis of rotation changes during walking (Cruse and Bartling, 1995). The lack of slanted rotation axes of the ThC joint potentially had implications for the control complexity and a significant effect on the ground reaction forces during stance.

4.1.2. Sensory System

Two classes of sensor were used: on the one hand, sensors were employed that mimicked real sensors of the robots or biological organism and these were used as inputs to the neural network controller, additionally to evaluation and analysis purposes. All simulated walkers possessed angle sensors for the three main leg joints and foot contact sensors which were realized as very low range distance sensors. Depending on the simulator and experiment, additional sensors were used, including angular velocity, angular acceleration, joint torque and its derivative of all main leg joints. Angular velocity and torque values were directly supplied by the physics engine, angular acceleration and torque derivative had to be manually derived from the previous two: Derivatives at time step were approximated by the finite difference method and division by the number of difference time steps , resulting in a difference quotient:

——————— (4.1)

Hereby a number of difference time steps of either two or three was chosen, depending on the simulator and sensor signal. Due to the discrete nature of the physics engine and its rather low precision the manually derived sensor signals showed undesired oscillations and therefore have to be post-processed to obtain signals comparable to those supplied by real robotic and biological walkers. For post-processing either moving average filters with filter size

$$\frac{\overset{1}{i=}}{i} \tag{4.2}$$

whereby was usually chosen to be four time steps. Alternatively infinite impulse

response (IIR), i.e. recursive, filters with factor

$$1 \tag{4.3}$$

were applied, whereby was usually chosen between 0.07 and 0.15. Note that the application of the above filters incurred a time delay of the respective sensor signal. Since the physics engine was updated two to four times more often than the neural network this effect was reduced. Overall time delays between one and three time steps relative to the neural network resulted.

On the other hand, sensors were employed that were solely used for evaluation and analysis purposes. All simulators were equipped with body coordinate (xyz) sensors to track body position and velocity. This was e.g. utilized in the fitness function during evolution to reward fast walkers. Optionally coordinate sensors (xyz) for each foot were employed, giving absolute and relative (to torso) positions. They were e.g. used to visualize foot trajectories. During single-leg experiments force sensors in the rail structure could be used to register the 3 force components that corresponded to the forces that a leg exerts on the ground.

To enforce the development of robust controllers, gaussian noise of 1-2% (or more in perturbing experiments, cp. section 4.3 further below) was added to all neural network sensor inputs.

4.1.3. Motor System

Whereas biological walkers employ multiple antagonistically acting muscles to produce motor behaviors (for stick insects see e.g. Bässler (1983)), in robotic walkers the most abundant actuation employs single acting rotatory electrical direct current (DC) motors together with a position servo controller (Siciliano and Khatib, 2008). To ease transferability and comparability of controllers between robotics and biology, both actuation mechanisms were implemented together with different control interfaces. Fig. 4.3 gives an overview of all actuation and motor control implementations used. The two intermediate implementations (Fig. 4.3 b+c) approximated antagonistic control without requiring computationally costly controllers. To exploit the full motor dynamics the following general approach was chosen: The neural network gave antagonistic motor activations via two motor neurons (MNs). These were mapped on the four states (forward, backward, brake, relax) of the motor H-Bridge[1] and the pulse width (PW) of the pulse width modulation (PWM)[2] control signal. The mapping was performed as follows (cp. also Fig. 4.3 e):

1. Low activations ( ) in both antagonistic MNs resulted in a *relaxed* motor (consuming no energy, producing no active torque).

[1] H-Bridges are electronic circuits with four operational modes allowing 1. to disconnect both motor terminals resulting in a free run or relaxed mode with minimal friction and no active torque, 2a+b. voltage to be applied in either direction to reverse motor polarity, 3. to shorten the motor terminals resulting in brake mode and effectively increasing rotational friction.

[2] PWM control allows to supply intermediate amounts of power by varying the ratio of discretely switching on and off the power supply.

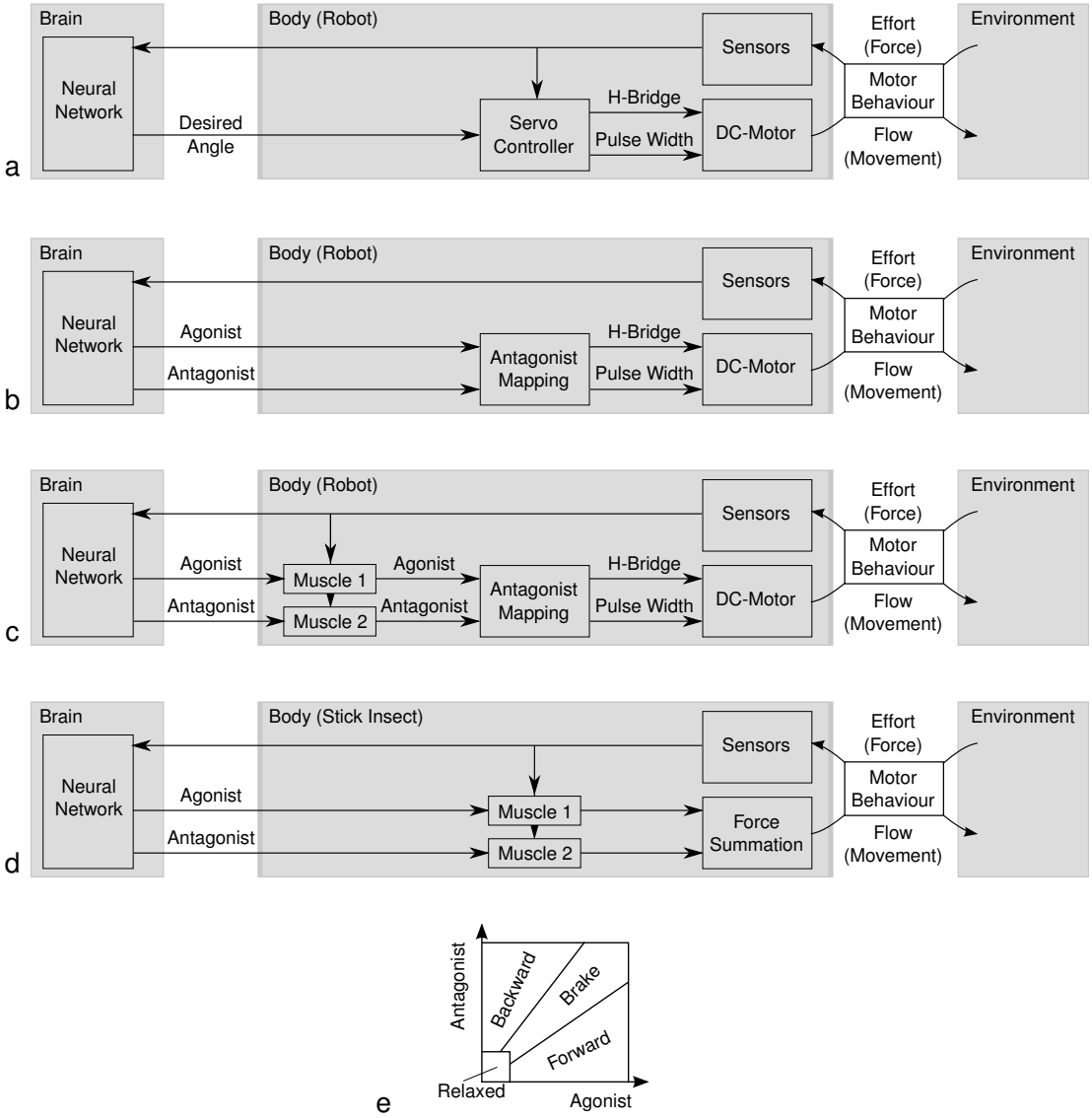

Figure 4.3.: Different types of motor control implemented include: **a** A position servo control where the neural network controller commanded a desired position. The servo controller tried to reach or maintain the desired position by applying torque via the DC-motor in relation to the difference of desired and actual position. Optionally derivative and integrative terms were taken into account. **b** A virtual antagonistic control, where the low level properties of DC-motors could be directly exploited by the neural network, e.g. by using the brake or free-run modes of the DC-motor. Antagonistic input mapping is schematically explained in **e**, for details see text. **c** Two muscle models, each implementing torque-angle, torque-velocity, torque-activation and passive torque-angle characteristics similar to biological muscles, were employed as a layer in between the neural network and the virtual antagonistic control (see text for details). **d** A biological model of a pair of antagonistically acting muscles. The sum of their force outputs was directly applied to the joint. As in **c**, the muscles had direct access to sensory information

2. A strong absolute ratio in favor of one MN

---

resulted in a *forward* (positive ratio) respectively *backward* (negative ratio) movement. The larger the absolute difference ( ) the higher the power output of the motor (resulting in higher torques and/or velocities, depending on the environment).

3. Otherwise approximately equal MN activations resulted in the motor *brake* mode and therefore increased effective joint friction without consuming energy. The effective brake strength was set proportional to the sum of motor neuron activations ( ).

The motor activation and environmental conditions (external torques) determined the joint movement. This was registered by sensors and fed back into the neural network, together with other sensory information. Note that the virtual antagonistic control interface offered a larger motor control space (cp. Patel, 2008, for examples). Furthermore, a position servo could still be realized inside of the neural network, additionally to a possible parallel direct control of the motors.

Gaussian noise of 2% (or more in perturbing experiments, cp. section 4.3 further below) was added to all motor neuron outputs to increase the robustness of developed controllers.

4.1.4. Muscle Model

In biological organisms motor neuron activity is often insufficient to predict the motor response (Brezina and Weiss, 2000; Hooper and Weaver, 2000). Therefore, in order to understand the performance of the neural control system, one needs to consider muscles and to differentiate between neural and muscular control contributions. Furthermore, muscle like properties promise to offer simplifications to the neural control system, which might be exploited in walking machine control (cp. chapter 2). Here muscle models based on data from the stick insect were applied to stick insect and robot simulations.

Ekeberg et al. (2004) employed muscle models with linear force-length and force-velocity characteristics, based on sparse data from Storrer (1976) and noted:

> "[...] the simulation based on these data was not able to generate fast muscle contraction velocities that would have been necessary to generate appropriately fast swing movements [...] This is because the linear force–velocity relationship used here underestimates the muscle force at high contraction velocities. Future studies will address the trajectories during swing and stance and the force regulation to maintain body posture. At that stage, a more accurate model of the non-linear nature of the muscles will have to be taken into account [...]"
>
> *(Ekeberg et al., 2004, p. 297-298)*

Here a more accurate Hill-type muscle model is employed, based on a model by Blümel et al. (2011a,b) and on more recent and detailed data of the extensor tibia muscle in the stick insect (Guschlbauer, 2009; Guschlbauer et al., 2007; Hooper et al., 2007).

To conform with the general requirement of the simulators used in the context of this thesis, namely low computational costs with sufficient accuracy, and to allow for an easy transfer to robot hardware, the Hill-type muscle model of Blümel et al. (2011b) was "translated" into a neural network with equivalent input-output characteristics. Hereby lever arm properties at the joint were taken into account. Therefore, muscle activation, joint angle and angular velocity were used as inputs and a single output corresponded to the resulting joint torque. A modular neural network was hand-designed to reproduce the input-output characteristics of the Hill model, consisting of the following three modules (cp. Fig. 4.4):

- Two positively self-coupled neurons in series effectively formed a second order infinite impulse response (IIR) low-pass filter (Hild, 2008), that, with appropriate parameters, replicated the *muscle activation function* (Guschlbauer et al., 2007; Hooper et al., 2007). Cp. Fig. 4.4 b for the filters response to a square wave input.

- The sigmoidal transfer function of a single neuron was exploited, together with appropriate input- and output-scaling via weights and a shift via the bias, to replicate the *passive torque-angle properties* of the muscle. Cp. Fig. 4.4 c for the modules characteristics.

- A feed-forward neural network structure was hand-designed to approximate the *torque-angle, torque-velocity and torque-activation characteristics* of the muscle model. Its parameters were optimized by standard backpropagation of error[3] using the Java Neural Network Simulator (JavaNNS, Fischer et al., 2002). The training and test set sizes were 3366 each (6 activation levels x 11 angles x 51 velocities). The final network displayed a quadratic error for the test set of
  . Cp. Fig. 4.4 d for the module's input-output characteristics for four discrete muscle activations.

To adapt the extensor tibia muscle model to the other muscle characteristics and to investigate the roles of the different muscle model components in- and outputs of the neural modules could be shifted and scaled. If e.g. the input velocity was set to a constant value of zero, the force-velocity influence was disabled. In a similar manner all sub-components could be disabled or their characteristics changed.

In contrast to the above mentioned muscle characteristics, the series elasticity component was not considered here. On the one hand, this was due to the computational cost and possible resulting instabilities during simulation (Pearson et al., 2006). On the other hand, the influence of the series elasticity on walking behavior is assumed to be relatively small when compared to the other muscle model components because it is stiff, i.e. has a short length, when compared to the active muscle force (Guschlbauer et al.,

[3]Standard backpropagation of error is a widely used method to train neural networks with a feed-forward architecture, see e.g. Haykin (1999) for details.

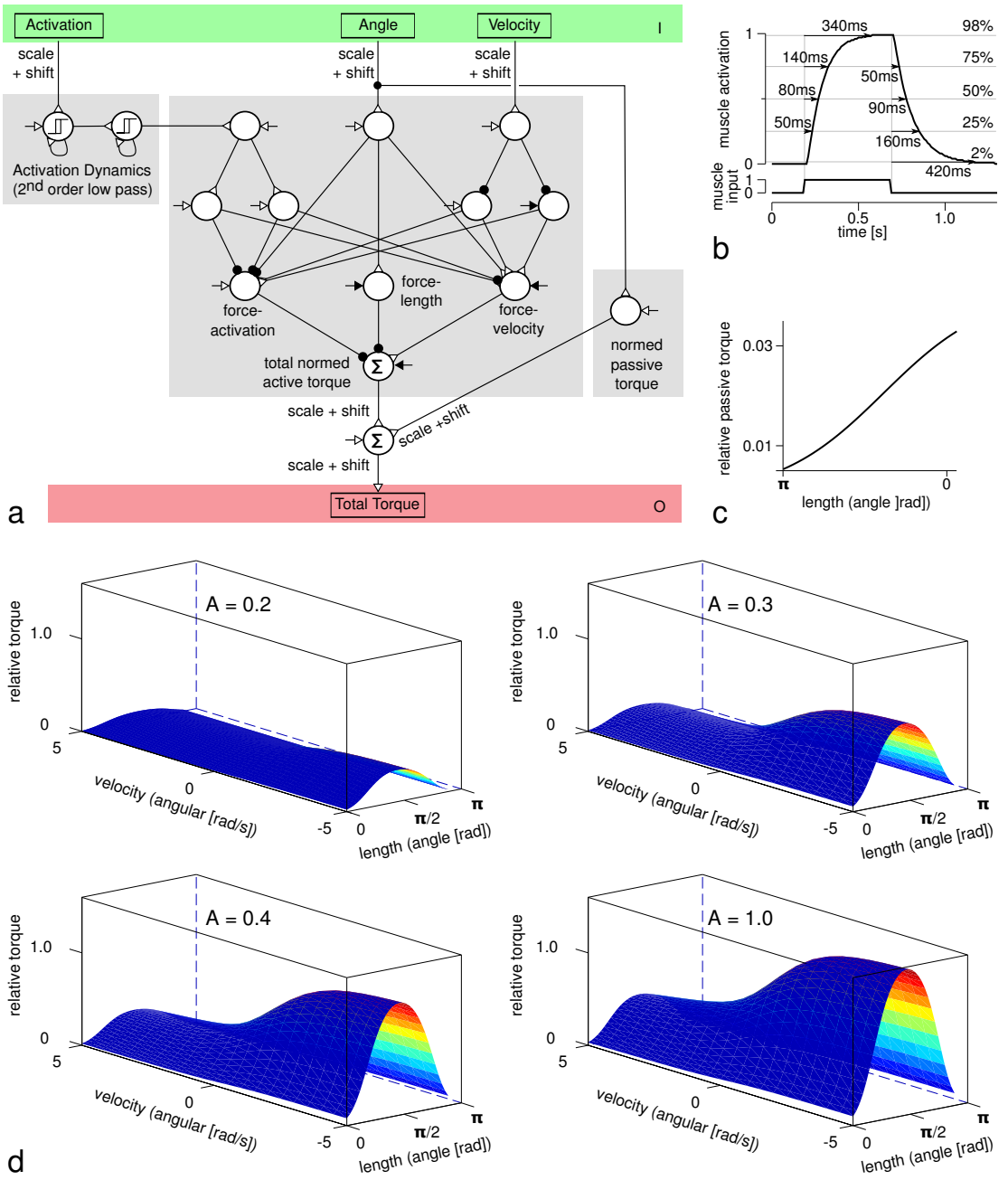

Figure 4.4.: **a** Structure of the modular neural network that approximated the input-output functionality of the extensor tibia muscle of the stick insect (as found in e.g. Blümel et al., 2011b; Guschlbauer et al., 2007) together with the lever arm properties at the femur-tibia joint. Despite the three inputs (I) and one output (O) the network consisted of three modules, approximating the activation function, the passive torque-angle and the combined activation-angle-velocity-torque characteristics. By adjusting the in- and output synaptic weights and bias values of these modules, characteristics could be individually shifted and scaled. **b-d** Input-output characteristics of the three modules: **b** activation dynamics, **c** passive force and **d** combined activation-angle-velocity-torque (shown for four discrete activation levels A). Note that muscle output torques were given relative to maximum muscle torques in the positive velocity range, i.e. relative muscle torques may exceed 1.0 (maximal relative torques in the negative range reach $\approx$)

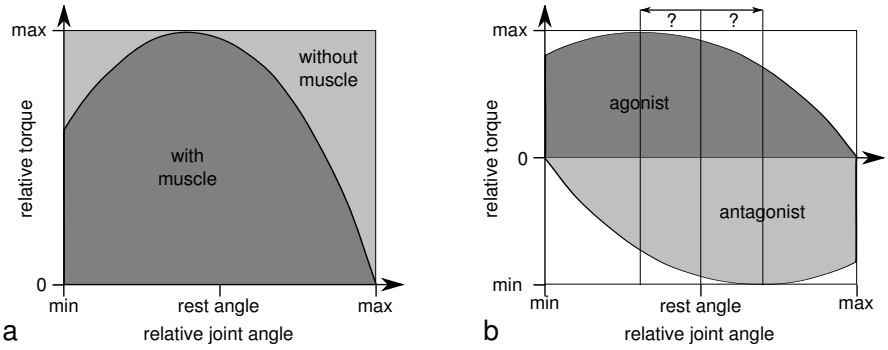

Figure 4.5.: **a** Schematic comparison of maximal joint torques produced by the DC-motor with and without muscle model depending on joint angle. Effectively the muscle model may only reduce the maximal torque output of the DC-motor. **b** Schematics of possible joint angle offsets of antagonist muscles regarding their force-length (torque-angle) relationships. The question marks indicate offsets that need to be determined

2007). Generally, the role of series elasticity in walking is smaller in smaller animals (cp. chapter 1) and smaller in slower walkers (Cruse et al., 2007).

Concerning the application to robotics, the use of the muscle model presented above together with a DC-motor raised several problems, whereby one was found to be fundamental: torque-angle and torque-velocity characteristics limited the maximum motor torque outside of the angle and velocity optima, as schematically depicted in Fig. 4.5 a. Furthermore, in the stick insect extensor muscle, for negative velocities the torque may reach times the maximum torque at zero velocity. If this property shall be captured by the DC-motor it has to be scaled up accordingly to allow normal maximum torque production at zero velocity. Since increased motor torques incur other trade-offs, such as an increased mass, this is often not desired. In the context of this thesis the first problem was simply accepted and for the second problem the maximum torque was set to that at zero velocity. This cut off all higher torques at negative velocities but still allowed higher torques for negative velocities at sub-maximal muscle activations or at length ranges outside of the force-length maximum. Further minor problems concern the inherent torque-activation and torque-velocity characteristics of the DC-motor. When using the muscle model, these have simply been disabled in simulation because for a transfer to hardware they could be merged with the respective muscle characteristics.

Apart from the extensor tibia muscle of the middle leg, detailed, yet more limited, data is only available for its antagonist, the flexor tibia muscle (Guschlbauer, 2009): It is much stronger than the extensor but has a slightly lower maximum velocity (cp. table D.1). Multiple open questions remained:

- How do maximum effective joint torques and joint angular velocities scale for the other muscles of the same leg and of other legs? It is e.g. known that the hind-leg femur-tibia joint mainly performs extension movements during stance phase – are the relative maximum joint torques and joint angular velocities reversed for this joint in the hind-leg?

Table 4.1.: Relative maximum joint torques that may be produced by the respective muscle (models). Joint torque contributions of antagonists are asymmetric and stronger for the stance muscles (rows colored in light-gray). Values other than those for the ML FTi joint are based on assumptions. Since HL FTi mostly performs extension movements during stance it is not clear if the antagonists relative strengths should be reversed (colored in dark-gray)

Max. Rel. Torque				
		FL	ML	HL
ThC	Pro	0.4	0.4	0.4
	Ret	1.0	1.0	1.0
CTr	Lev	0.4	0.4	0.4
	Dep	1.0	1.0	1.0
FTi	Flx	1.0	1.0	1.0 (0.4)
	Ext	0.4	0.4	0.4 (1.0)

Max. Rel. Angular Velocity				
		FL	ML	HL
ThC	Pro	1.0	1.0	1.0
	Ret	0.7	0.7	0.7
CTr	Lev	1.0	1.0	1.0
	Dep	0.7	0.7	0.7
FTi	Flx	0.7	0.7	0.7 (1.0)
	Ext	1.0	1.0	1.0 (0.7)

- How do effective passive muscle torques scale for the other muscles?
- How are the active and passive force-length characteristics of antagonistic muscles shifted relative to one another (cp. schematics of Fig. 4.5 b).
- How do multiple inhibitory and excitatory motor neurons interact in the activation of antagonistic muscles?
- How do slow and fast muscles fibers interact during locomotion?
- Which role do neuro-modulators play during locomotion in any joint (cp. chapter 1, Belanger, 2005; Hooper et al., 2007; Mentel et al., 2008)?

Due to the many open questions the following assumptions were made: All antagonistic muscle pairs had identical properties as the flexor-extensor pair of the middle-leg. Stance phase muscles, i.e. retractors, depressors and flexors, were always chosen to have a maximum effective joint torque 2.5 times that of the swing phase muscles and a maximum effective joint angular velocity 0.7 times that of the swing phase muscles (cp. table 4.1). An exception was the hind leg femur-tibia joint where both possibilities were tested.

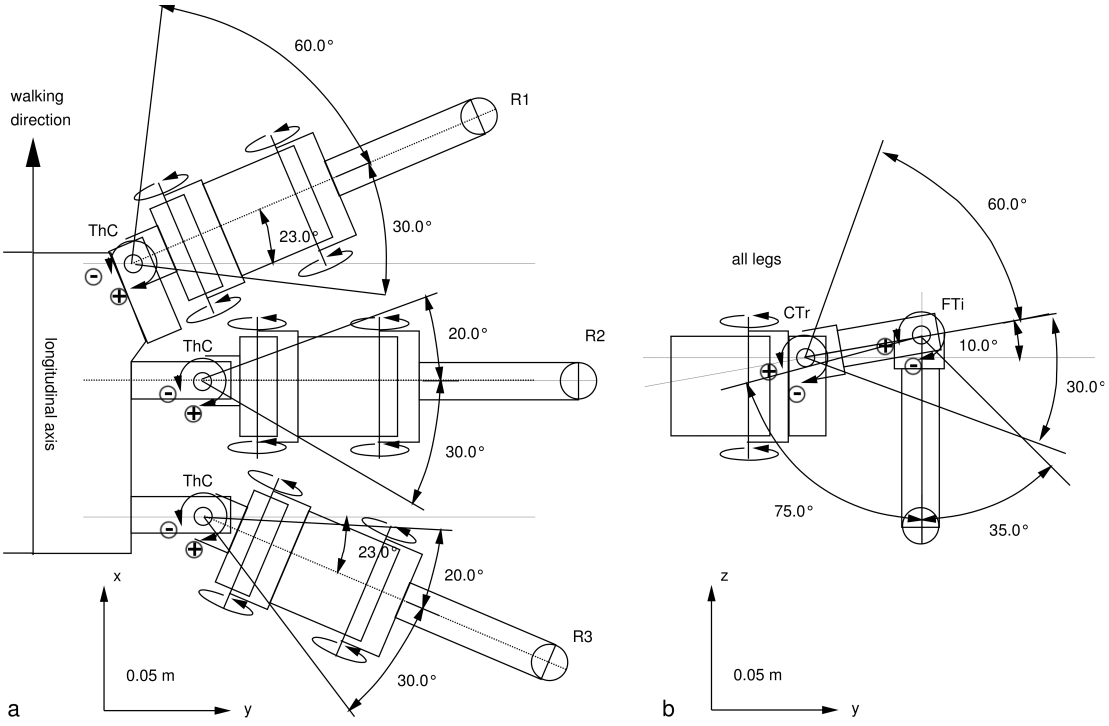

Figure 4.6.: Dimensions, joint working ranges and mappings of all legs of the robot AMOS-WD06 in **a** dorsal and **b** posterior view. ThC joint ranges are in the horizontal plane, relative to the longitudinal body axis and increasing with retraction. CTr joint ranges are relative to the horizontal plane, increasing with levation. FTi joint ranges are relative to the plane that includes CTr and FTi joint axes, increasing with extension. Masses were as follows: thorax 0.8kg, coxa 0.065kg, trochanter and femur 0.065 kg and tibia and tarsus 0.016kg. All joints were powered by servo motors of one type (max. force = 0.3 , max. velocity = 1.2)

4.2. Simulation of Biological and Robotic Walkers

The three simulated walkers depicted in Fig. 4.1 were employed in the simulation experiments presented in this thesis. They did not only differ in their sensori-motor equipment, but e.g. also in their joint arrangement and even more in their relative scaling as schematically depicted for body length and mass by the length of the bars in Fig. 4.1 below the simulator images. In the following, an overview and comparison of the specific implementations of the three simulators is given.

4.2.1. Simple Walking Machine AMOS-WD06

The morphology of this simple simulated robot (see Fig. 4.6) was constrained by the physical properties of a rather simple physical walking machine: Only two types of sensors were employed (three angle position sensors and one foot contact sensor per leg). The robot was constructed by assuming that different legs (fore-, middle- and hind-leg) have to fulfill different tasks and therefore need to have a distinct morphology.

Limited by the constraints of the physical walking machine (e.g. dimensions of the motors), the only morphological differences were the attachment points on the body and the initial orientations at the body as well as the angle ranges of the joints: The fore-legs had a working range in front of the shoulder joint, the middle-legs around the shoulder joint and the hind-legs behind the shoulder joint. These working ranges and the joint arrangement (from proximal to distal: forward-backward, upward-downward and outward-inward) were similar to those of the stick insect (Cruse and Bartling, 1995). It has to be noted however that the ThC joint was modeled as a hinge joint with its axis parallel to the dorso-ventral axis and not as a ball and socket joint as it is realized in the stick insect. Other details of the model, e.g. the type of motors (only one servo motor per joint, no co contraction) and the length and masses of the segments differed from those of the stick insect (see Fig. 4.6).

To allow for neural networks with as transfer function (cp. chapter 3) to control the robot, motor and sensor signals had to be mapped onto the interval [ ]: They were mapped in such a way that the minimum angle possible corresponded to a value of and the maximum angle to . For the contact sensor this was different: A value of zero indicated "no contact" and a value of "maximal contact", because it was realized by means of a very short ranged (0.8 [ ], 125 [°] opening angle) infrared distance sensor. Force sensors were not used in contrast to the two more complex simulators. Mapping conventions, i.e. which sign corresponded to which movement direction, and working ranges of the joints are indicated in Fig. 4.6. To account for later use on the hardware robot, artificial noise of 2% (gaussian distribution) was added to all sensor- and motor-signals. Since all simulated legs contained three motors and four sensors, all single leg controllers had four input- and three output-neurons.

In contrast to the more complex robotic model (cp. section below), the rail setup did not allow sidewards movements. Additionally it differed in the update frequency: this simulator was updated with 100Hz and each fourth step sensor and motor data was exchanged with the neural net, resulting in a neural network update frequency of 25Hz.

4.2.2. Modular Walking Machine Octavio

Details of the robot hardware are given in von Twickel et al. (2006, 2012)[4]. Additionally, in table D.1 detailed technical data of robot and stick insect are given side by side, together with scaling ratios: E.g. the total body mass was times that of the stick insect, which is in the same order of magnitude as the cube of ratio of front- to hind-leg coxa distance (, the robot does not have an abdomen like the stick insect, therefore comparing total body length is not helpful), the ratio of maximum stance phase joint torques ( ) and ratio of tibiae lengths ( ). This roughly matches the geometric similarity criterion and equal Froude numbers as a prerequisite for dynamic similarity (Alexander, 1989), e.g. when using maximum walking velocities from restricted single leg stick insect preparations for comparison (Gabriel et al., 2003).

A summary of the sensor and motor equipment of the simulated robot is given in

[4]see also http://www.ikw.uos.de/ neurokybernetik (last visited: 02/28/2011)

Table 4.2.: Sensor and Motor Equipment of the walking machine Octavio. Sensors marked with * were not used as controller inputs but only for analysis

Segment/Joint	Sensors	Motors
Body	(x,y,z) coordinate sensor*	
	Lateral Torque to rail*	
	Dorso-Ventral Torque to rail*	
Joints (3x)	Angle	DC motor
	Angular Velocity	(Antagonist-
	Torque*	ically
	Torque Change*	controlled)
Foot	Contact	

Table 4.3.: Mapping of sensor values to sensor neuron outputs in the walking machine Octavio

Sensor	in min	in max	out min	out max
γ (angle)	-15°	165°	0.0	1.0
β (angle)	-90°	90°	0.0	1.0
α (angle)	-90°	90°	0.0	1.0
FC (foot contact)	no contact	contact	0.0	1.6
α β γ (velocity)	-300°/s	300°/s	0.0	1.0
Joint Torques	-10N	10N	0.0	1.0
(Joint Torque)'	-200N/s	200N/s	0.0	1.0

Table 4.2. Other sensors were exclusively used for analysis and as inputs for fitness functions during evolutionary parameter optimization (see below). Sensor-outputs were mapped onto sensor neuron (SN) inputs as specified in Table 4.3. For motor neurons no mapping was needed. To account for a use on the hardware robot, artificial noise of 1% (gaussian distribution) was added to all sensor- and 2% to all motor-signals used as inputs to, respectively outputs from, the neural controller. All noise levels are given relative to the respective mapping ranges.

This robotic model allowed sidewards movements of the single-leg rail setup which could be either solely damped for sidewards stepping experiments or equipped with a spring-damper system for forward stepping experiments. This latter setup was used to simulate lateral force influences of other legs (see Fig. 4.2). This allowed for small lateral movements similar to hexapod walking in stick insects (cp. Kindermann (2002)). Up-down and sidewards rails included force sensors to measure forces exerted by the leg.

Applying the strategy of increasing sensor- and motor-noise levels to obtain controllers that could easily be transferred to the hardware platform was not sufficient, i.e. controller parameters had to be substantially modified during transfer to reproduce a similar behavior in hardware (Patel, 2008; von Twickel et al., 2012; Zahedi et al., 2008). Itera-

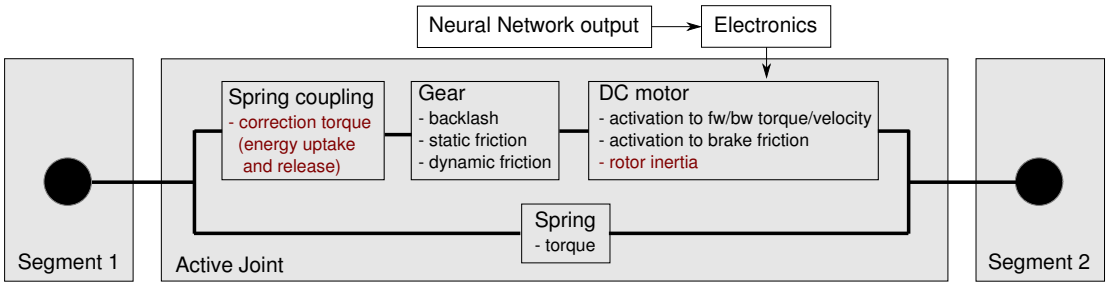

Figure 4.7.: Complex joint setup in the Octavio simulation. Note that the pre-stressed spring is only present in the second joint (CTr). Joint properties shown in red are not simulated due to stability and/or speed reasons

tive testing revealed that the active joint models (cp. Fig. 4.7), had to be additionally improved. Using single joint pendulum test setups, passive and active joint properties like passive and active damping, spring properties, backlash and activation to torque and velocity characteristics were investigated and the results incorporated into the active joint model. Subsequently parameters were optimized. Further model properties like spring coupling and rotational inertia were discarded due to improve simulation stability. Instabilities arose due to a combination of the discrete time simulation, the desired high simulation speed and the multiple interacting joints in the hexapod robot.

Employing this more sophisticated simulator during controller development showed an improved transferability of controllers, i.e. only few parameters had to be tuned during the transfer from simulator to hardware. At the same time neither speed (10-70x real-time on a Pentium M 1.7Ghz Notebook) nor stability had to be sacrificed. For an example of a controller transfer see Patel (2008); von Twickel et al. (2012).

This simulator was updated with 200Hz and every other simulation step sensori-motor data was exchanged with the neural network controller, resulting in a neural network update frequency of 100Hz. Accounting for a later transfer to hardware, the optional muscle models were updated synchronously with the neural network, i.e. only with 100Hz.

4.2.3. Stick Insect *Carausius Morosus*

Detailed data of the simulated stick insect is given in table D.1, where it is directly compared with that of the robot Octavio (cp. also section 4.2.2 above). In the following, differences to the Octavio simulator, not given in the technical data overview, are presented.

If the stick insect model was driven without the optional muscle model, a 2-mode motor activation (forward and backward) was used, compared to the 4-mode motor activation mirroring the DC-motor properties as used by the Octavio robot simulator (cp. Fig. 4.3 e). The resulting joint torque was simply the sum of the antagonistic activations. Like the robotic model, symmetric maximum velocities and torques were

Table 4.4.: Leg plane rotation offset angles in the stick insect simulation

Angle / Leg	Fore-leg	Middle-leg	Hind-leg
	34	37°	29°
	84	92°	114°

Table 4.5.: Mapping of sensor values to sensor neuron outputs in the stick insect model. Values are only shown if the differ from the robotic model Octavio

Sensor	in min	in max	out min	out max
β (angle)	-60°	120°	0.0	1.0
α β γ(velocity)	-900°/s	900°/s	0.0	1.0
Joint Torques	-0.2mN	0.2mN	0.0	1.0
(Joint Torque)'	-4N/s	4N/s	0.0	1.0

assumed for agonists and antagonists and both were set to the corresponding maximum of both measured in the stick insect. By employing the optional muscle models, this symmetry could be broken. To compensate for a potentially missing stabilization by a muscle model, joint damping was introduced analogous to the robot damping. Parameters were chosen to stabilize the movement, i.e. to suppress unwanted oscillations, and to be as low as possible. Static joint damping was set to 0.001 and quadratic dynamic joint damping to $0.001\frac{m\ m}{}$).

As indicated in Fig. 4.2 b and explained in detail in Cruse and Bartling (1995) the leg-plane (plane containing all leg segments due to parallel CTr and FTi joints) was rotated by angles and resulting in a non-orthogonal ThC joint axis with a different orientation towards the thorax for fore-, middle- and hind-legs. Values taken from Cruse and Bartling (1995) are summarized in Table 4.4.

Due to modified joint axes orientations and resulting joint angle offsets, when compared to the robotic models, sensor ranges and mappings had to be changed for the CTr joint. Due to actuator scaling differences, joint velocity and joint torque ranges and mappings had to be modified as well. Values are supplied in Table 4.5.

The center of mass of stick insects is approximately located between or even behind the hind leg coxae (cp. table D.1). This potentially leads to stability problems in hexapod walking. Real stick insects solve this problem by a tarsus attachment mechanism. This system consists of, on the one hand, the retractor unguis muscle which, upon activation, flexes the tarsal claw Radnikow and Bässler (1991) and, on the other hand, adhesive pads on the ventral side of the tarsi, which work by contact maximization due to their micro-mechanics and a fluid secretion mechanism (Gorb et al., 2002; Scholz et al., 2008). Especially due to the fine-tuned tarsal secretion, adhesion works well on slippery as well as on rough surfaces (Dirks et al., 2010; Drechsler and Federle, 2006) and is very economic from a metabolic point of view (Dirks and Federle, 2011). This tarsal adhesion mechanism was functionally replicated here by a serial combination of a slider joint at

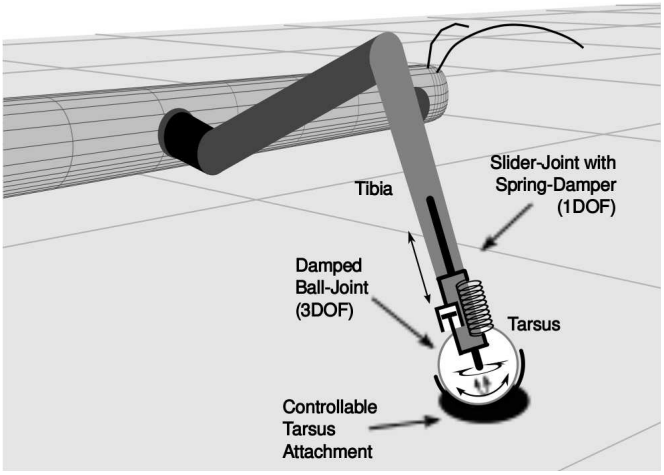

Figure 4.8.: Schematics of the implementation of the attachable tarsus of the simulated stick insect: The tarsus was attached to the tibia via a slider joint with spring damper properties. The tarsus could, upon contact and motor neuron activation, be attached to the environment with a 3DOF damped ball joint. Detachment occurred upon motor neuron deactivation or a surpassed force threshold

the tarsus and a ball and socket joint which could be attached to the environment. The slider joint had a spring constant of 0.0001 and a damping constant of 0.01 . The ball joint had a damping constant of 0.01 for all 3DOFs.

In the real stick insect it is known that the retractor unguis of the foreleg is activated and deactivated together with the flexor tibia. This is ascribed to two mechanisms (Bässler and Büschges, 1998): an excitation by load signaled via campaniform sensillae and an inhibition by a protracted leg position, signaled via ThC proprioceptors. The question is if this mechanism is the same for middle- and hind-legs, because there biphasic flexion-extension movements occur during stance. Due to the simplified mechanics employed in simulation retractor unguis was simply activated together with the depressor muscle which allowed attachment throughout stance phase but timely detachment for a smooth stance-swing transition. In further studies the modular approach should be followed to activate and deactivate the retractor unguis depending on sensory signals. Foot attachment took place if a physical contact existed in simulation and the corresponding attachment motor neuron (corresponding to the retractor unguis motor neuron in stick insects) was active above threshold. Detachment took place if the motor neuron was below threshold or a force threshold was reached. The latter was not relevant for the simulations performed here, because the attachment was very strong compared to the forces occurring during the simulation experiments. This mechanism is similar to the one presented in Schilling et al. (2007). Additional to the tarsus attachment mechanism, stick insects may stabilize their posture by using their flexible abdomen as a "carrying wheel". Therefore the stick insect simulator allowed contacts of abdomen

Table 4.6.: Physical unit rescaling factors that were applied to the stick insect simulator to obtain a stable simulation

Unit	Scale Factor
length	^{2}
mass	
force	
torque	
velocity	^{2}
acceleration	

and environment, i.e. no terminate try signal was used in this case (cp. section 3.3.4).

Due to the extremely small masses of the stick insect together with relative high torques, simulations were initially very unstable. Stable simulations were achieved by two measures: on the one hand, all units were consistently rescaled (cp. table 4.6) to exploit the double precision numerical range of the physics engine[5] (Smith, 2009) and, on the other hand, the simulation update frequency was doubled compared to the Octavio simulation. This meant that the simulator was updated with 400Hz and every fourth step sensori-motor data was exchanged with the neural network controller, resulting in a 100Hz controller update frequency. The optional muscle models were also updated with 400Hz, differing from the Octavio simulation.

4.3. Simulation of Environments and Perturbing Conditions

Neural networks were developed and evaluated under flat terrain (E1) and multiple other environmental conditions as depicted in Fig. 4.9. Four types of perturbing conditions were used in the context of this work: 1. The ground was fragmented into blocks that varied in height relative to body suspension height (E2–E3). 2. External forces were applied to the torso simulating up- and downhill walking (E4) as well as sidewards kicks (E8). 3. Foot contact (E5) and joint friction (E6) were increased. 4. Noise levels on motors and/or sensors were varied (E7). All environment parameters, such as average step height or distance, could be randomized during evaluations and evolution. Details are given alongside with the experimental data.

[5] Rescaling was allowed because size dependent factors, such as e.g. aerodynamics resistance, were not present in the simulation.

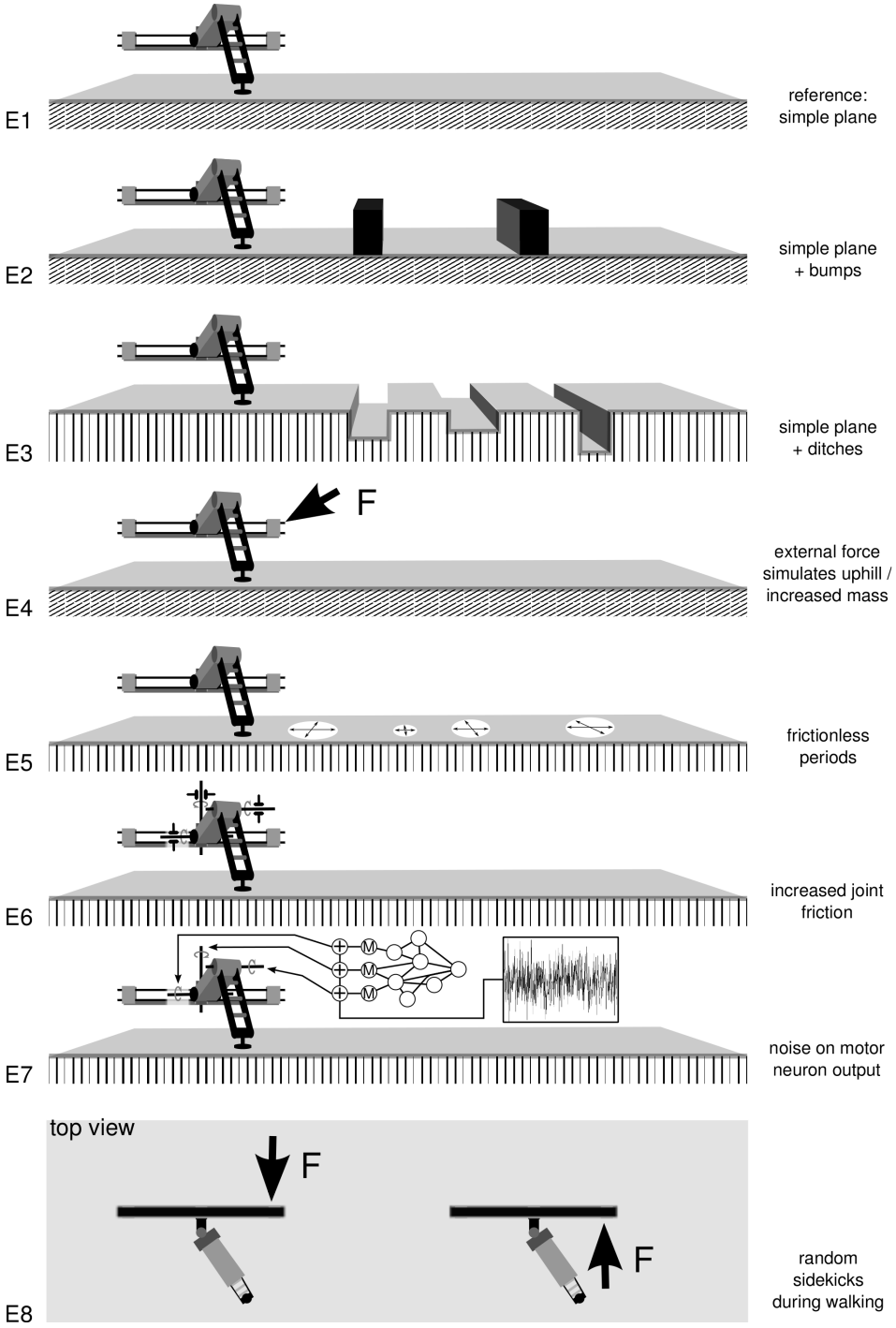

Figure 4.9.: Example environments and perturbing conditions **E1**–**E8** used during evaluation of the behavioral performance of robot and stick insect simulations driven by neural networks

Part II.

Simulation Experiments

5. Evolved Single-Leg Neuro-Controllers

As a prerequisite for developing neural control for walking machines that are able to autonomously navigate through rough terrain, artificial structure evolution is used to generate various single leg controllers. The structure and dynamical properties of the evolved (recurrent) neural networks are then analyzed to identify elementary mechanisms of sensor-driven walking behavior. Based on the biological understanding that legged locomotion implies a highly decentralized and modular control, neuro-modules for single, morphological distinct legs of a hexapod walking machine were developed by using a physical simulation. Each of the legs has three degrees of freedom. The presented results demonstrate how extremely small reflex-oscillators, which inherently rely on the sensori-motor loop and e.g. hysteresis effects, generate effective locomotion. Varying the fitness function by randomly changing the environmental conditions during evolution, neural control mechanisms are identified which allow for robust and adaptive locomotion. Relations to biological findings are discussed.

5.1. Approach

The prime intention of the experiments described in the following was to find examples of neural mechanisms which allow physical, biologically-inspired machines to show characteristics of biological locomotion. Using artificial evolution it turns out that there are many different mechanisms realizable with larger as well as smaller networks, and only a few of them, those which were completely analyzable, are presented here. This includes that it was not tried to identify the "globally optimal" solution for the task, believing that there is no convincing argument for benchmarking single leg control. Thus, a statistical evaluation over a large number of evolution runs, as for instance done in (Psujek et al., 2006), was not considered here. Instead, it was intended to compile a catalog of possible robust control mechanisms, the performance of which should be judged when in cooperative action for driving a multi-legged walking machine.

Inspired by work reported for instance in (Ekeberg et al., 2004), locomotion controllers were developed and evaluated for single three Degree Of Freedom (DOF) legs of the physical walking machine AMOS-WD06 (cp. section 4.2.1) to later develop controllers for the whole walking machine by coupling the single leg controllers (cp. chapter 8). This approach has already been employed before (Beer and Gallagher, 1992; Brooks, 1989; Jacob et al., 2005; Schmitz et al., 2001). Here various tools and techniques have been applied, including physical simulation (cp. section 4.2.1), structure evolution of (recurrent) neural networks (cp. section 3.3), and analysis of the resulting neuro-dynamics.

During structure evolution both the number of inter-neurons and synapses was varied, only the number of input- (4) and output-neurons (3), corresponding to the available

sensors and motors, was kept constant. Selection of controllers was with respect to walking distance in a given time (cp. section 3.3.4), and robustness in the sense that equal performance should be achieved under different environmental conditions (obstacles, holes, etc., cp. Fig. 4.9 E1-E3 for examples). Controllers were evaluated in seven different environmental scenarios with the fitness obtained in each environment being added to the total fitness. Therefore, the total fitness value was a good measure for the general performance of the controller. Poor or especially high fitness values for single environmental scenarios were good indications for specialized control. Uncontrolled vertical movement of the body was not observed during evolution, therefore body height was not directly included in the fitness function. Attention was paid to control the size of the evolved networks by means of cost terms, punishing large networks and high connectivities. Most of the effective neuro-controllers turned out to be quite small and larger ones did not perform better.

After several evolution runs (each about 250 generations) the performances of the best networks were compared with each other and, if available, with some reference controllers. Reference controllers were either constructed Central Pattern Generator (CPG) controllers (see Fig. 5.2 b) or a network being an equivalent of the neuro-biologically based finite state model found in (Ekeberg et al., 2004) (see Fig. 5.2 a). The overall best performing networks (generalists in the sense that they showed robust behavior under changing environmental conditions) or those having a particular interesting structure (e.g. specialists in overcoming high obstacles) were subjected to further analysis afterwards. The analysis included behavioral as well as neural aspects, e.g. lesion- and stimulation-methods. Analysis of the controllers showed that sensory inputs and dynamical effects, like hysteresis, play a major role for walking pattern generation and for a robust behavior under changing environmental conditions. In particular most of the controllers worked without a CPG and instead made use of the physical properties of the body and the environment via the sensori-motor loop (Beer and Gallagher, 1992; Brooks, 1991; Chiel and Beer, 1997).

5.2. Mechanisms of Forward Walking

A multitude of single leg controllers performing equally well in propelling the body forward were developed. In the following the different motor patterns generated by prototypical fore-, middle- and hind-leg-controllers are shortly described to point to divergent requirements in terms of motor control for the different leg types. Subsequently two reference controllers and two rather complex controllers developed in the artificial evolution experiments are introduced. Finally two extremely small (in terms of neurons and synapses) example controllers are presented and analyzed in detail to demonstrate the mechanisms discovered.

A fore-leg movement on even terrain generated by a typical fore-leg controller can be described as follows (compare Fig. 5.1 a): At the Anterior Extreme Position AEP the fore-leg controller has just completed its swing phase and made foot contact with the ground. The CTr joint (see Fig. 4.6 for joint terminology) has already started moving

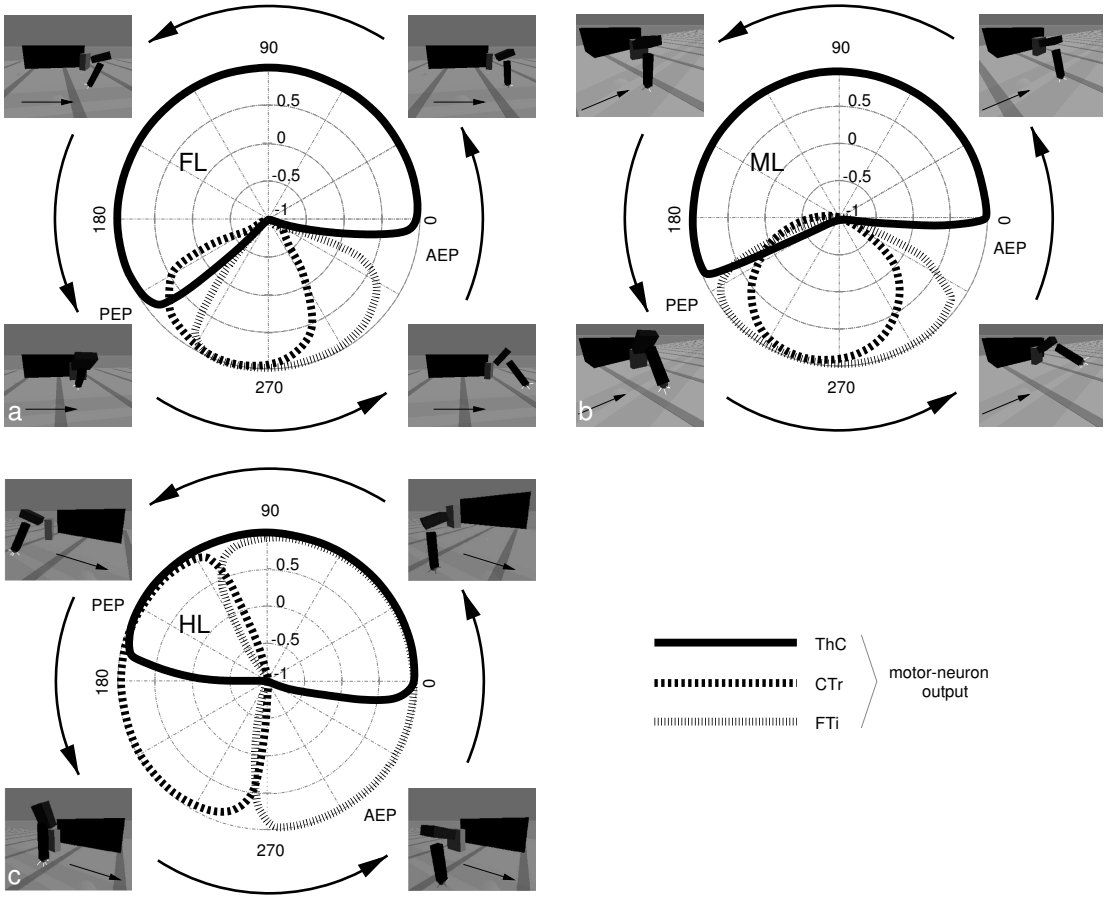

Figure 5.1.: Differences in motor-neuron output between prototypical forward walking (a) Fore- (FL), (b) Middle- (ML) and (c) Hind-legs (HL). Motor-neuron output (,) is plotted against the phase of a swing-stance step cycle (0° is defined as the time of first maximum in ThC motor neuron output after transition from minimum output, angles are thus within the cycle and not joint angles). FL and ML motor-neuron outputs are similar, because they both perform a pulling movement to propel the body forwards. The HL instead employs a pushing movement. For mapping conventions cp. section 4.2.1. Posterior Extreme Position (PEP), Anterior Extreme Position (AEP)

downwards (negative motor output) to support the body whereas the FTi and the ThC joint only now start moving inwards (negative motor output) respectively backwards (positive motor output) and exert force on the ground to pull the body forwards. After the leg has accelerated and almost reached the Posterior Extreme Position PEP the CTr joint is activated to move the leg up when it has reached the PEP. Once the leg is in the air, the ThC and FTi joints are moved forwards respectively outwards. The CTr joint is then activated to move downwards so that the foot reaches the ground at AEP. At this point the cycle starts anew. The phase relations between the three joints of the middle-leg are almost identical to those of the fore-leg (compare Fig. 5.1 b). The middle-leg exerts its force to the ground more parallel to the body than the fore-leg which rather pulls the body forward with its foot being in front of the body. On the other hand the hind-leg movement differs significantly from those of the fore- and middle-leg because it moves the body forward rather by pushing than by pulling it (compare Fig. 5.1 c). During the stance phase the CTr joint moves downward (negative motor output) and the FTi joint outwards (positive motor output). The ThC joint supports this backward movement but starts with the retraction (positive motor output) only when the other two joints already started exerting a backwards directed force. Consistent with this observation the hind-leg controllers differed stronger from the fore- and middle-leg controllers than those two in between.

Apart from the differences between the controllers of fore-, middle- and hind-legs, similarities could be noted, e.g. the motor neurons of all controllers approximately acted as toggle switches, either being activated maximal positive or maximal negative. Since the motor output only represents the target value (reference angle value for the servo motor), the actual movements differed, due to the inertia of the body, the friction of the ground, etc., significantly from the motor output rather resembling a sine or zig zag curve (see Figs 5.3 – 5.6). In addition to some parameter optimized reference controllers (see Fig. 5.2 a+b) a large quantity of controllers with diverse structures for fore-, middle- and hind-legs was developed by artificial evolution. Some of the controllers were rather complex (see Fig. 5.2 c+d) and since their performance was not superior to that of much smaller controllers, only small controllers were subjected to a detailed analysis. Results for the analysis of two small controllers is presented hereafter.

Two key mechanisms in nets without inherent neural oscillators were found responsible for the oscillatory motor output during walking. The first mechanism involves hysteresis through neural elements which is demonstrated on one of the simplest controllers that was found in the course of the evolution experiments. This fore-leg controller is depicted in Fig. 5.3 and it consists of one sensory input from the ThC angle sensor, one self connection (larger than one) and all motor neurons connected in series with one connection being inhibitory. That makes a total of four neurons (including the sensor neuron) and four synapses being involved in the control of the leg. The performance of this controller is comparable to that of more complex controllers (see e.g. Fig. 5.2). Important is the fact that no neural oscillator can be found in this structure only leaving the possibility of an oscillation via the environmental loop (1-6-7-5-1). The motor signal analysis showed that some kind of bistable element exists in the controller. One possible realization is a neuron with a self connection that displays a hysteresis effect. For a hys-

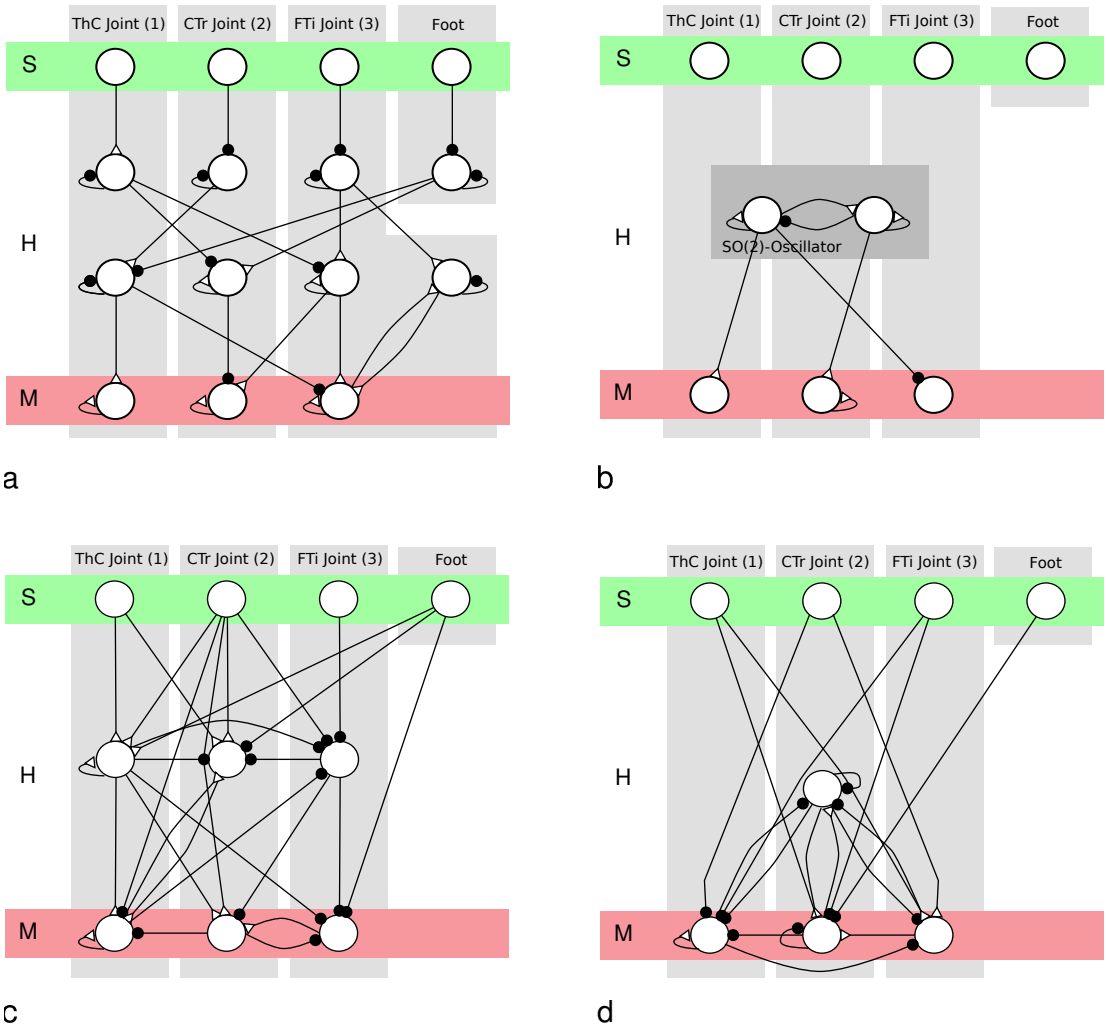

Figure 5.2.: (a)+(b) Two parameter optimized reference controllers: (a) A simple neural interpretation of the finite state mechanism found in (Ekeberg et al., 2004), optimized for a hind-leg. (b) SO(2)-oscillator (Pasemann et al., 2003) as CPG with evolutionary optimized parameters and connections to the motor neurons of a fore-leg. (c)+(d) Two examples of structurally evolved (c) hind- and (d) middle-leg controllers that were not considered for further analysis because of their complexity. They were not able to produce stable walking without sensory inputs. Neither their nor the performance of the reference controllers was superior to the small controllers presented in this chapter. Open triangles denote excitatory synapses, small filled circles inhibitory synapses

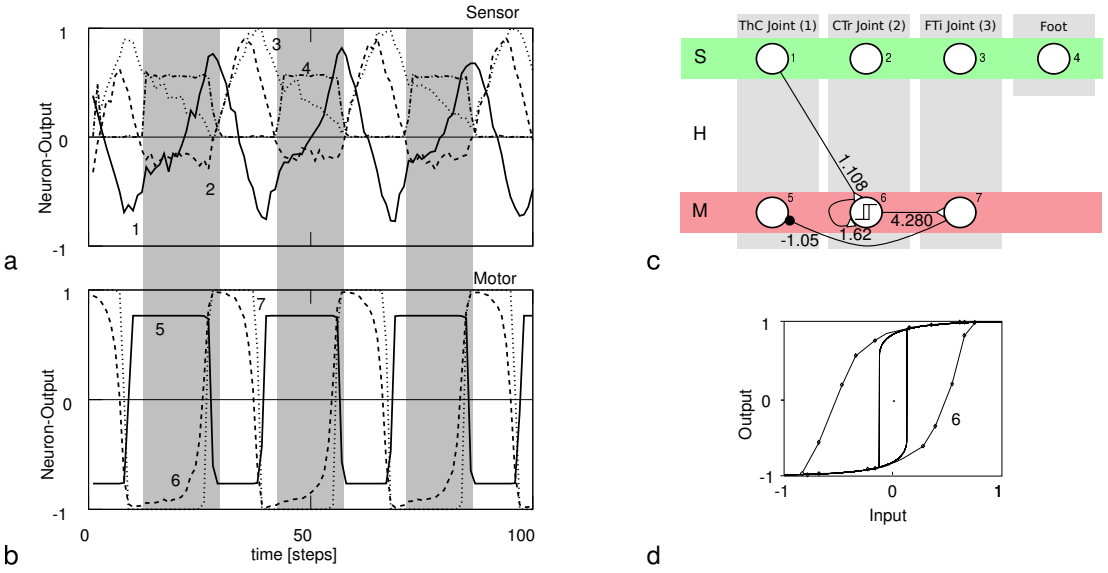

Figure 5.3.: Single Leg controller (fore-leg) with a neural hysteresis element (self-connection larger than one) and a feedback loop via the environment: (a+b) neuron-outputs during walking on even terrain. The black bars below sub-figure a denote stance phase. (c) Structure of the network. Note that only one sensor gives input to the net. The dashed line denotes feedback via the body and the environment. (d) Hysteresis as obtained in bifurcation studies for a single neuron with self-connection (iterations 000, inner curve) and hysteresis under locomotion (transient condition, outer curve) of neuron six. Shown is the output of the neuron against its input

teresis effect to take place the self-connection has to be larger than plus one (Pasemann, 1993). Such single neuron hysteresis elements are found in many of the leg controllers, irrespective of their function as fore-, middle- or hind-leg controllers. Its possible role in locomotion control is as follows: In this particular net (see Fig. 5.3) the central neural element is neuron six which receives the only sensory input, has a self connection greater one and therefore is a hysteresis element. It is also the first element in the chain of all motor neurons. The other motor neurons have the same phase or a phase shifted by ° compared to neuron six.[1] Neuron seven is in phase with neuron six, neuron five in para-phase. This suggests to take a closer look at the role of the hysteresis element. Therefore the output of neuron six was plotted against its input (see Fig. 5.3 d), once for input sequences during normal locomotion and once for a sine-function with a high number of iteration steps as the input. The first thing that may be noted is that the hysteresis element may account for the observation of a bistable element. This is due to the fact that basically two stable fixed points exist in the hysteresis domain either pulling the output of the neuron towards or depending on the history of the system. As can be seen in Fig. 5.3 d an important difference exists between the hysteresis curve obtained during a bifurcation study and the one under experimental conditions. This is caused by the former hysteresis acting as an attractor which is never

[1] Of course they are additionally shifted by either one or two time-steps.

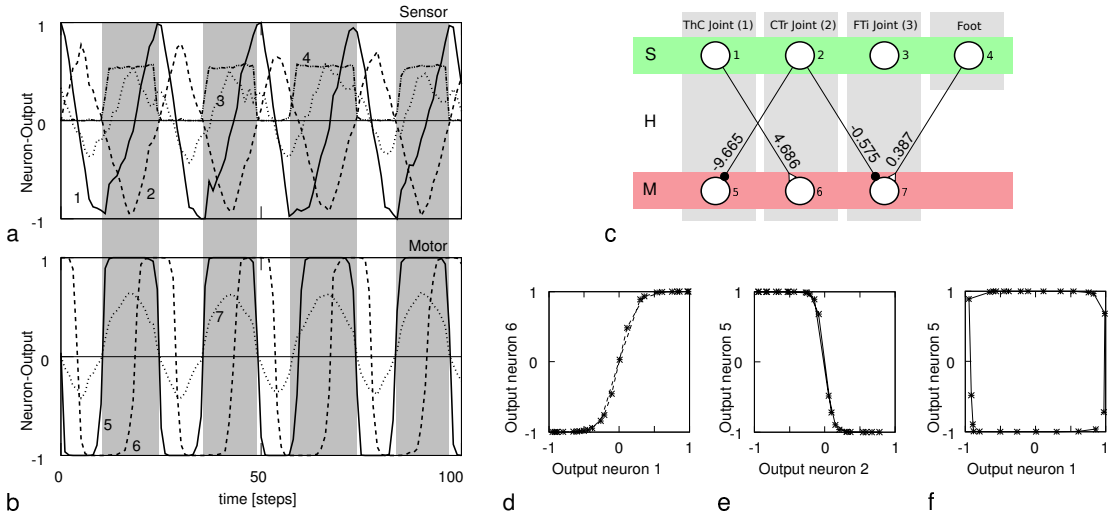

Figure 5.4.: Single Leg controller (hind-leg) without any neural feedback and two environmental feedback loops: (a+b) neuron outputs during walking on even terrain. The black bars below sub-figure a denote stance phase. (c) Structure of the network. The dashed lines denote feedback via the body and the environment. (d, e + f) Oscillations occur without neural feedback. The effect results from the time-delay of the motor-sensor interaction, from the nonlinear transfer-function of the neurons and from the large magnitude synapses

reached under real conditions because the input values change too fast. One can therefore regard the frequency of the input signal as an additional parameter determining the transient behavior of the system. If e.g. the walking movement is slower (faster), the switch from the negative to the positive stable fixed point and vice versa is completed earlier (later) relative to the phase of the input signal. All motor neurons act as bistable elements, neurons seven and five even stronger than neuron six. This can be explained by the strong connection ( ) from neuron six to neuron seven which amplifies the signal from neuron six therefore pushing it faster to the maximum/minimum of the nonlinear transfer-function . Note that, unlike in most of the biological systems, the ThC-joint backwards movement starts at the end of the swing phase (see Fig. 5.3 a), shortly before the foot touches the ground. See the "Discussion" section for a comment on this.

The second mechanism found in the evolved single leg controllers also involves oscillations induced by the sensori-motor loop but without any neural feedback being involved. A single leg controller, in this case a hind-leg controller, in which no neural feedback occurs is depicted in Fig. 5.4 c. Although only four synapses exist, mapping three of the four sensors, including the foot contact sensor, to the three motor neurons, this simple feed-forward structure makes up the functional controller. In a simplified view two loops exist: The first passes through the environment twice (1-6-2-5-1), the second only once (7-4-7). In reality both loops are coupled through the environment, e.g. the foot contact is not only dependent on the FTi-motor, but also on the CTr-motor and the environment. The motor outputs of the net (see Fig. 5.4 b) suggest that bistable

elements exist in the controller and therefore not only in controllers with neural hysteresis elements but also for controllers without any self connections, as for example shown in Fig. 5.4. Here, a combination of the motor-environment-sensor interaction, strong weights and the nonlinear sigmoid transfer function have been found to generate the underlying mechanisms. In Fig. 5.4 d–f the loop 5-1-6-2-5 is looked at in detail. Subplots *d+e* show (inverse-) -like curves which are steeper than the normal because of the strong connections ($_1$ and $_2$). These steep -like curves push the majority of the inputs to values close to plus and minus one, respectively. This explains the bistability, but not the slow oscillations. To understand the induced slow oscillations depicted in subplot *f*, the properties of the motor-environment-sensor loop have to be considered. In a simplified point of view, the loop through the environment contains a time delay element which, together with the steep -like transfer signal, accounts for the slow oscillations observed.

It has to be noted that the two mechanisms described above were not unique to the controllers belonging to one of the leg types and no predominant expression of one of the mechanisms (sensori-motor loop with or without neural feedback) in controllers for one of the leg types was observed.

5.3. Mechanisms of Adaptivity

In the previous section changing environmental conditions have been neglected in the study of single leg controllers, although all of the controllers were developed under randomized environmental conditions (obstacles and irregular footholds, see above). To clarify if and how the controllers adapt to a changing environment, their performance in environments with obstacles and gaps has been studied. Note that pure specialists were not considered here, meaning that all analyzed controllers are robust in the sense that they are able to navigate in all seven environmental scenarios studied (see above). Nevertheless they can be specialists in the sense of having a particular good performance in a subset of the scenarios. First of all, it was found that the controllers containing a sensori-motor loop somehow react on the environment, e.g. on steps or gaps. The controllers e.g. prolong their swing phase when encountering an obstacle or increase their frequency when the leg looses ground contact. To further investigate if any "meaningful" reactions occurred in the environment interaction the controllers were subjected to a detailed analysis. Two examples, one for an obstacle and another for a gap situation, are given below.

In Fig. 5.5, it is shown (for a middle-leg) how the dynamic interaction with the environment can enable a controller to overcome an obstacle. Note that similar obstacles were part of the environments during evolution and therefore an implicit part of the fitness function. Nevertheless the obstacle height is novel because all obstacles presented during evolution were less high than the one shown here. First, the behavior under normal conditions (no obstacles in the way) is explained to subsequently depict the changes that occur during an obstacle contact. Under normal conditions, the walking pattern is generated by the 5-1-6-2-5 loop which passes the environment twice and has

two hysteresis elements: During the stance phase motor neuron five is activated ( ) and with a dead time (and a nonlinear transformation), caused by the properties of the motor and the environment, the activation is transferred into an actual backward movement. This backward movement is in turn registered by the angle sensor one, which then activates (positive weight) motor neuron six. The dead time caused by the environment and the hysteresis element ensures that the CTr joint is only moved upwards at the end of the stance phase. This movement in turn is registered by angle sensor two and results in a negative activation of motor neuron five (negative weight) causing the joint to move forward. Additionally, motor neuron seven is activated (negative weight). It is important to note that a dead time causes the FTi only to be moved outwards with a delay relative to the forward and upward movements of the ThC and CTr joints. The result is that the foot is not lifted high enough to overcome the obstacle discussed below. Finally, the forward movement negatively activates neuron six, resulting in a downward movement, in turn causing a positive activation of neuron five and the cycle starts anew.

During contact with an obstacle, the leg hits the obstacle in late swing phase when the CTr joint is about to move down and the FTi joint is not bend far outwards yet. Then the foot cannot overcome the obstacle but rather is positioned right in front of the obstacle. In the following stance phase the body is pushed forward but the movement is restricted because of the obstacle being in the way (ThC joint does not reach its hindmost position). The hysteresis of neuron six ensures that the CTr and FTi joints are activated with the normal amplitude. Switching back to swing phase the foot hits the obstacle again and the hysteresis of neuron five keeps up the forward movement (positive feedback). Following from this the ThC and the CTr joint are active longer than usual. But since the dead time of the switch from negative (downward) to positive (upward) motor activation of the FTi joint is roughly constant, its positive activation now overlaps with that of the two other joints (see arrows in Fig. 5.5 a+b for actual movement and motor activation). In total this overlap causes the foot to be lifted higher and in a further backwards ThC position than under normal conditions and the leg successfully overcomes the obstacle. One has to note that the reaction is phase dependent, i.e. the foot is only lifted up and the swing phase prolonged if the leg hits an obstacle during early swing phase, otherwise it terminates the swing phase as under normal conditions without lifting the leg any higher than usual. This is because in late swing phase the ThC joint has moved forward far enough to result in a negative output of its angle sensor and therefore it causes the CTr joint to move downwards.

In the case displayed in Fig. 5.6, the dynamic environment interaction causes the controller (hind-leg) to reposition the leg to find support for foot contact. Neuron six takes a central role in this behavior: Under normal conditions its activation is determined by a combination of the ThC motor neuron, the ThC sensor neuron and the foot contact sensor outputs and by its own excitatory self-connection (hysteresis element). The ThC joint can influence neuron six via its motor- and sensor-neurons in both a negative and a positive way whereas the foot contact sensor can either have a negative influence (negative weight) or no influence at all. Note that the synapse from the foot contact sensor weighs stronger than both synapses from the ThC joint together. That means if

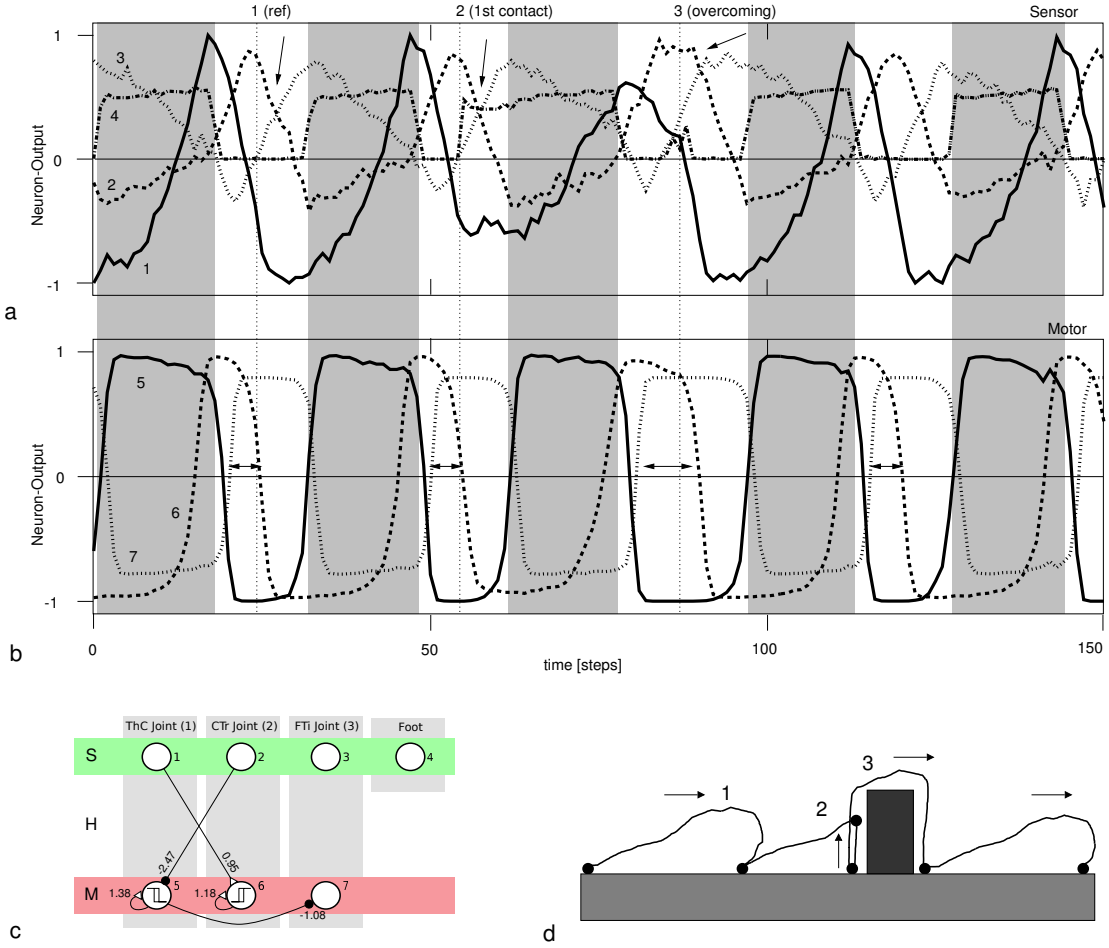

Figure 5.5.: A dynamic environment interaction enables a foreleg-controller to raise its leg higher then usual when encountering a step. One sequence where a step is overcome is shown here: (a+b) Time-plot of Sensor- and Motor-neurons. The arrows point to the overlap in motor neuron output of neurons 6 and 7 in sub-figure b and the resulting overlap in actual movement of the CTr and FTi joints in sub-figure a when overcoming the obstacle (point 3 in time) compared to situations where it is not (point 1+2 in time). This overlap results in the leg being lifted up higher than during normal swing phase. The black bars below sub-figure a denote stance phase. (c) Foreleg-controller. (d) Schematic drawing of the leg-step interaction. The arrows indicate locomotion direction and the numbers correspond to the points in time depicted in a+b. For details see text

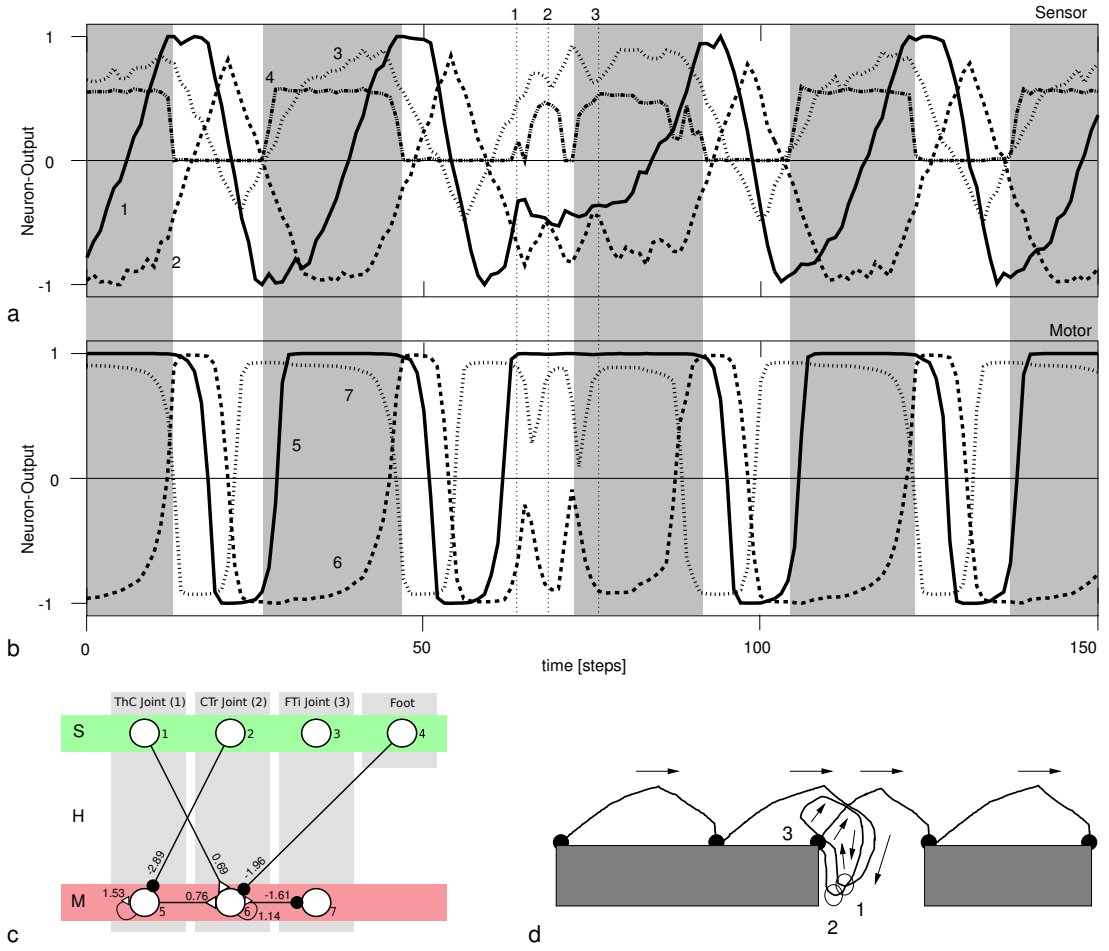

Figure 5.6.: A dynamic environment interaction enables this hind-leg-controller to find supportive ground when encountering a gap. One sequence where a gap is crossed is shown here: (a+b) Time-plot of Sensor- and motor neurons. The black bars below sub-figure a denote stance phase. (c) Hind-leg-controller. (d) Schematic drawing of the leg-gap interaction. The numbers correspond to the points in time in a + b. For details see text

there is no foot contact the movement of the CTr joint roughly follows that of the ThC joint (with a time delay). If there is no foot contact at all the CTr joint lifts the foot of the ground too early during the stance phase. This is counteracted by the foot contact which negatively activates neuron six and subsequently keeps the joint down. Only when the foot contact is lost, the joint may move upwards. If no foot contact is made in the beginning of the stance phase, the leg quickly enters the swing phase, again resulting in a higher frequency swing-stance cycle. If the foot makes a contact with the ground while it is being pulled back (note that the CTr and FTi joints act synergetically by moving together either downward and outward or upward and inward) positive feedback puts it back on the ground. This can result in a searching-like movement (see points 1, 2 and 3 in time, Fig. 5.6 a,b+d). Once sufficient ground contact is made the swing phase is finished.

Network Size Versus Redundancy Many of the evolved controllers were very small and often had very few sensory inputs. Because their performance was comparable to more complex controllers, the question arose what particular advantage could result from a higher complexity. One experiment was done to test the hypothesis that a higher complexity and more sensory inputs make the controllers more robust and less prone to failures due to sensor outages. In Fig. 5.7, the movement of the joints is shown for two different controllers under locomotion conditions. During the experiment all sensors giving input to the net were stimulated one after another and fixed to predefined values to see if the locomotory movements would stop. The top four plots show the movements resulting from a more complex controller like that described in Fig. 5.2a. It can be seen that the controller tolerates sensor values to be fixed over a wide range (note that a negative input via the foot-sensor does not occur under simulation conditions) without terminating locomotory movements. In contrast, the stimulation of the only sensory input to the net from Fig. 5.3 results in an immediate breakdown of oscillatory movement. Altogether, this underlines the hypothesis of advantages through redundancy.

5.4. Transfer of Results and Approach to a Robot With an Antagonist Motor Interface

Fig. 5.8 demonstrates that the approach presented in this chapter could also be applied to the more complex robotic model Octavio (cp. section 4.2.2), using e.g. antagonistic motor interfaces (cp. section 4.1.3). When transferring results from the experiments presented above, bistable elements as premotor elements were found to be essential to ensure antagonistic activation of the motor-neurons of one joint (cp. Fig. 3.7). For some controllers additional intra-joint feedback was necessary during the controller transfer to compensate for the missing servo-controller. The resulting leg controllers could also be simply be transferred to hardware with only minor parameter tuning, preserving qualitatively the same behavior (cp. Chakraborty, 2007; Patel, 2008, for more examples and details).

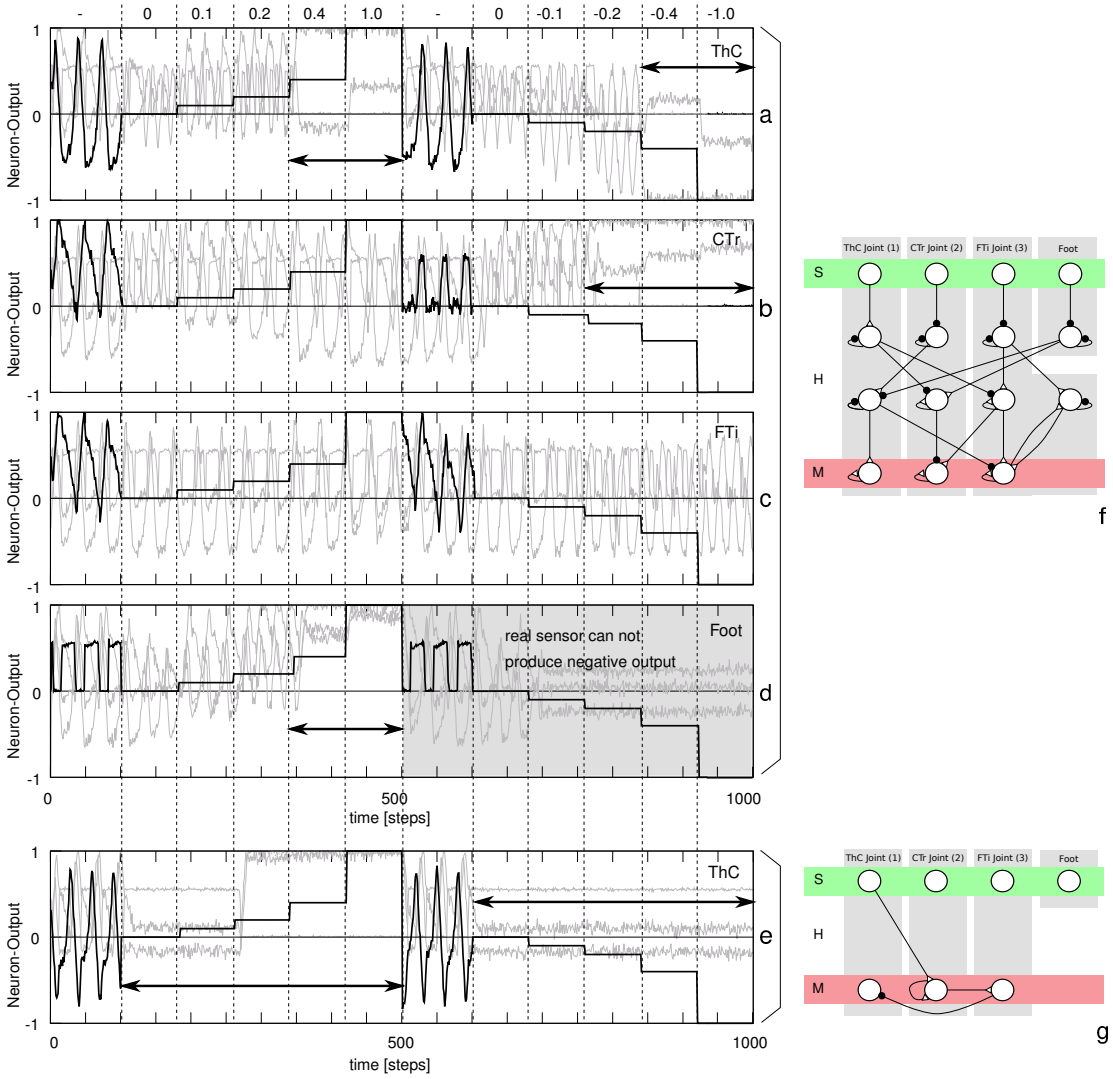

Figure 5.7.: Stimulation experiment: Control networks with several sensory inputs may have a higher tolerance regarding the failure of a sensor when compared to a network with less inputs. In this case a very simple network (**g, e**) with one sensory input is compared to a more complex one (**f,a–d**). Per trial one sensor (name given in right top of respective time plot) was subsequently fixed to discrete output values (see very top of the figure for values). The stimulated sensor is depicted in black whereas the other sensors are shown in gray. The comparison was done under locomotion conditions. The horizontal black arrows in the time plots indicate the phases without oscillatory activity in the net

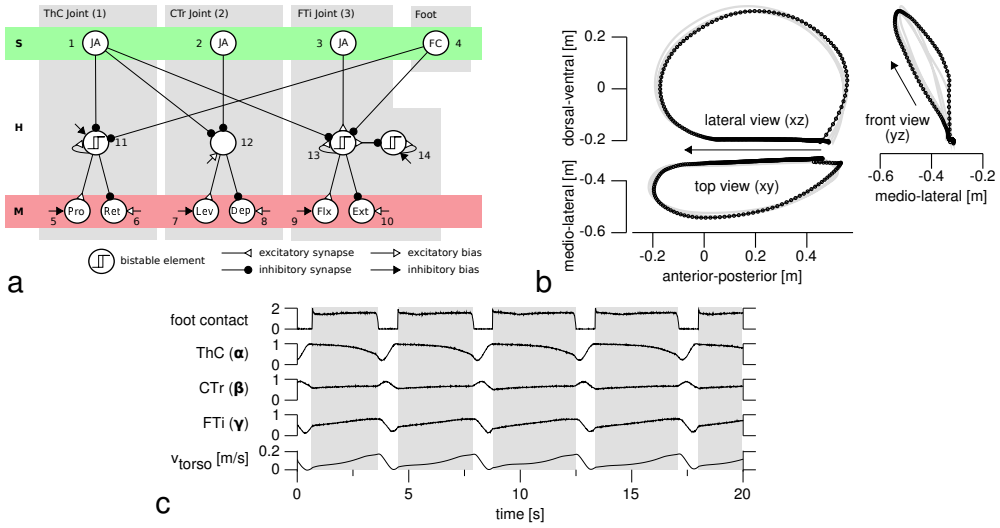

Figure 5.8.: Example of a reflex driven single leg neuro-controller for the more complex robotic model Octavio with antagonistic motor control and its performance.

5.5. Discussion

Though in recent years the information available on the neural control of walking has increased rapidly, important parts in the "puzzle" concerning the structure and mechanisms of neural walking controllers still remain unclear (Orlovsky et al., 1999). Research on the stomatogastric system for example has shown the complexity of a neuro-biological system (see e.g. Heinzel et al. (1993)) that, in comparison to the control of walking, is considered to be "simple". For this reason several researchers have recently begun to take a synthetic approach (Dean, 1998) by means of simulations, mainly to test hypotheses from biology (Dean et al., 1999). Additional to the test of hypotheses the approach taken here considers simulation as a tool to find new hypotheses and therefore alternative perspectives to a problem: Artificial evolution was not only used to perform a parameter optimization on a given structure, e.g. on a biological inspired controller, but mainly to develop controller structures from scratch. The only prior knowledge given was the morphology of the simulated robot including its sensors and motors, the type of neural elements allowed for the controller, the initial sensor- and motor neurons corresponding to the sensors and motors of the robot and the optimization goal ("move forward as fast as you can"). Nevertheless one has to note that the context was wider than in many other studies because of the randomized environment. The evolved structures are distinct to biological systems in that control structures are not optimized for a whole bunch of tasks but only for one specific task (Dumont and Robertson, 1986). The analysis of evolved structures therefore allows to find out about the very principles of a well defined control problem. Further on, artificial evolution does not narrow the possible outcome, because it does not build upon structures originating in evolutionary history and possibly developed for totally different tasks. Finally, artificial evolution inherently

makes use of the sensori-motor loop therefore taking into account the properties of the body and the environment.

Controllers were developed for three legs, each with a distinct morphology which was caused by different operating ranges of the ThC joint relative to the longitudinal body axis. Consistent with the results of (Ekeberg et al., 2004) the differences between the movements of the hind-leg and the two other legs (middle- and fore-leg) were much more pronounced than that between the middle- and the fore-leg. This is due to the hind-leg performing a "pushing" movement, albeit the other two legs rather perform a "pulling" movement. Consequently the controllers for the hind-leg on the one side and for the fore- and middle-leg on the other side are not compatible. One suggestion is that this different functionality can be achieved by simply changing the signs of specific connections in the controllers. This will be investigated in a forthcoming publication.

Concerning the movement trajectories of the simulated legs, a difference could be found when compared to biology: The controller depicted in Fig. 5.3 caused the leg to start retraction at the end of swing phase, shortly before touchdown. To the authors knowledge this has not been observed in biological systems, e.g. in stick insects the legs always exert a forward directed force during touchdown (Cruse and Bartling, 1995). Hence here the function may either be to reduce the breaking force during touchdown or simply to decrease the operating range of the ThC joint during stance to ° ° (compare Fig. 5.3 a) which is close to the one observed in freely walking stick insects (° °, Cruse and Bartling (1995)).

The diversity of evolved controller structures, both in terms of number of inter-neurons and number and topology of synapses, ranged from structures that were too complex to be analyzed to extremely small and simple structures. Note that there was an evolutionary pressure (cost term in the fitness function) that favored smaller controllers. But the speed term was by far the most important term in the fitness function. Therefore only small nets were favored that performed equally well as larger ones. Common to all controllers was the existence of a sensori-motor loop passing through the environment. Interestingly, none of the evolved larger structures (see e.g. Fig. 5.2) showed a superior performance (in terms of the task considered) when compared to the best performing smaller structures. Some of the smallest controllers (see e.g. Fig. 5.3) were also some of the best performing controllers.

Two mechanisms have been found to be important in the evolved locomotion controllers: 1. The exploitation of body and environment properties, like the physical inertia of the body, by including sensori-motor loops, and 2. the non-linearity of the neural elements, generating in particular hysteresis effects. These mechanisms caused the slow oscillations necessary for smooth walking. Furthermore, they caused the motor outputs to act roughly like bistable elements, either being fully activated to move to one side or to the other. This effect is also termed "relaxation oscillator" or "bistable system" and agrees with the literature on stick insect motor activation, i.e. the stance-swing transition (Bässler and Büschges, 1998).

The hysteresis effect was caused by a neural element having an overcritical positive ( ) self-connection (see e.g. Fig. 5.3 and Pasemann (1993)). In biology hysteresis is observed in sensory neurons (Zill and Jepson-Innes, 1988), central neurons (Kononenko

and Dudek, 2006), motor neurons (Lee and Heckman, 1998) and basically all visco-elastic systems, e.g. in muscles (Kostyukov, 1998). In biological neurons hysteresis is explained by a combination of the kinetics and dendritic distribution of ion channels (Lee and Heckman, 1998) and usually occurs in combination with bistability (Toth et al., 1998). In some cases hysteresis is considered as a problem to the nervous system that has to be compensated for (Hatsopoulos et al., 1995), in others as a useful mechanism that e.g. supports the switch between different behaviors (Toth et al., 1998) or that compensates for undesired muscle properties (Zill and Jepson-Innes, 1988). In the neural controllers presented here, hysteresis serves to produce robust bistable systems that show a short term memory effect, noise reduction and a time delayed switching. Therefore the hysteresis supports an efficient switching between two movement directions and effectively adds to the "time delay" arising from the sensori-motor loop (see below).

The contribution of the sensori-motor loop was as follows: Strong weights in connection with the bounded function caused bistability by leading to a very steep overall "transfer function". A time delay in the loop through the environment due to the physical inertia of the body, for example the delay between motor command and actual movement, caused the slow oscillations. Theoretical considerations support the importance of the sensori-motor loop, the nonlinear neural elements and the time delay and suggest that the total feedback loop has to be positive to allow bistability to occur (Cruse, 2002; Prochazka et al., 1997).

In all of the presented controllers a sensori-motor loop was needed to drive the oscillation, therefore representing *Reflex-Oscillators*. None of the evolved networks contained a *Central Pattern Generator (CPG)*. Our results are therefore consistent with those of (Beer and Gallagher, 1992): They showed that the structure of single leg locomotion controllers developed by artificial evolution depends on the availability and reliability of sensory feedback during evolution. When reliable sensory information was available (like it was always the case in this study), reflex-oscillators were developed, otherwise either CPG's or a mixture of both. At least two explanations are conceivable: 1. A reflex oscillator represents the superior solution to the problem. 2. The boundary conditions (evolution parameters, fitness function etc.) either favored the development of reflex oscillators or they interfered with the formation of a CPG. It is argued, that CPGs producing the quasi-rhythmic walking patterns "are not only unnecessary but could even cause the behavior to deteriorate in unpredictable situations" (Cruse, 2002, p. 278).

Surprisingly the comparison of the reflex controllers with some constructed, parameter optimized, CPG controllers (not discussed in this paper, but see Fig. 5.2 b for an example) demonstrated an approximately equally good performance when averaged over different environmental scenarios. CPG solutions showed a "brute force" approach where walking movements were only driven with constant velocity, independent of the environment (as per definition of the CPG). In contrast, the reflex oscillators displayed adaptivity under changing environmental conditions (see below). Assuming that both are equally well suited for solving the task, the reflex controller would have had the advantage of less connections and less internal neurons, as was shown by (Beer and Gallagher, 1992). In that case the cost function would have favored the reflex controllers. But in some runs there was no cost function restricting the size and the connectivity

of the neuro-controllers and still no neural oscillators emerged. Therefore under the given simulated physical boundary conditions the reflex controllers might have the advantages of a simpler structure, resulting in a better evolvability, and of adaptivity in certain environmental situations.

For several biological systems it has been established that a CPG can, without any sensory input, generate the rhythm responsible for locomotion (e.g. in lampreys, see Grillner et al. (1998)) or for the stomatogastric system of crustacea (Selverston et al., 1999). In other animals, such as the stick insect, CPGs have been found but their overall contribution to locomotion is still unclear (Büschges, 2005). It is believed that very fast running animals rather rely on CPGs, with sensory inputs acting only modulatory, whereas animals, that walk slowly and possibly on rough terrain, to a stronger extent rely on sensory inputs to generate the locomotion motor pattern (Delcomyn, 1999). For very fast movements the sensory feedback in biological organisms is too slow (Cruse, 2002) and therefore CPGs become necessary. In this case neural compensation of "mismatches" between environment and motor commands is not sufficient and has to be augmented by intrinsic properties of the musco-skeletal system (Jindrich and Full, 2002). This problem does not hold for artificial systems, such as the one employed here, where signal transmission is generally fast enough.

"How do the neural mechanisms of the demonstrated controllers compare with those known in the stick insect?" "What is the reason that we do not find three central rhythm generating networks controlling the three main leg joints?" In answering these questions we argue that 1. The role of the joint CPGs could so far not be demonstrated under real (in contrast to the so-called fictive) walking conditions (Büschges et al., 1995) leaving the questions unanswered of how big their contribution is to overall pattern generation. 2. A possible role of the CPGs is to prevent co-contraction of the antagonistic muscles by means of alternation of activity (Büschges et al., 1995). In our simulation the use of a single motor per joint excludes the possibility of co-contraction and the bistability of the motor neurons supports a sharp transition from one movement direction to the other. Each of our motor neurons can therefore be seen as a module controlling one joint. These "modules" do not have the intrinsic capability to oscillate, rather three of them are coordinated by sensory information (see e.g. Fig. 5.4), resulting in a functional single leg controller. This organization, where sensory input determines the timing of behavioral transitions, was also found in stick insects (Büschges, 2005).

Other simulations, e.g. with oscillators that incorporate sensory inputs, should be helpful to determine the advantage or disadvantage of certain combinations of CPG and reflex (-oscillator) influences. The additional evaluation of the controllers in terms of energy efficiency would be beneficial in revealing the biological relevant advantages and disadvantages, possibly underlining the advantages of reflex control.

Further examples also demonstrated benefits from explicitly taking into account the dynamic interaction with the environment. Very simple evolved leg controllers showed a "meaningful" reaction to the environment: 1. If a leg hits an obstacle in early swing phase the foot was lifted higher up, enabling the leg to climb over the obstacle, which would be impossible during a normal swing phase (see Fig. 5.5). 2. If the foot did not make contact with the ground at the end of the swing phase then it was lifted up and

down faster than during normal swing and stance cycles until a ground contact was made, and the normal swing phase was finished (see Fig. 5.6). These two behaviors are similar to the "searching movements" and the "elevator reflex" described for locusts in (Pearson and Franklin, 1984). It is however not stated here that the behaviors observed during the simulation are identical to those in animals. They are only intended to show examples of how "simple" the underlying neural mechanisms of such a behavior can be.

Starting with the development of single leg controllers the question is, how they can cooperate to generate locomotion of a multi-legged machine, because then every leg somehow affects every other leg: 1. mechanically and possibly 2. neurally. Therefore a co-development might be necessary to develop a functional controller for multileg walking control. Currently single leg controllers, similar to the ones presented in this paper, are used to evaluate different coupling mechanisms for driving a simulated hexapod robot under rough terrain conditions. First results indicate that the modular approach is able to endow the physical walking machine with the desired adaptive behavior. Although a modular concept to construct a locomotion controller was successfully employed by other research groups before (see e.g. Ferrell (1995), Schmitz et al. (2001) and Quinn et al. (2003)), they did not focus on structure evolution of neuro-controllers.

The simulation experiments demonstrated also that if the physical properties of the body and the environment are taken into account then controllers for complex tasks, in this case walking of a 3DOF leg, can itself be quite simple and realized by a small network. On the other hand these simple controllers cannot be understood without knowledge about the body, the environment and the task, since their main function (oscillation) does not occur without an environmental interaction. It seems promising to continue and expand the artificial evolution experiments to systematically analyze the possibilities of multifunctionality in single leg controllers (e.g. forward-, backward- and curve-walking), of inter-leg coupling and coupling with other, non-locomotory sensory/motor systems. The final goal of this endeavor is to generate sensor-driven behaviors of walking machines acting autonomously in rough terrain.

6. Bio-Inspired Single-Leg Neuro-Controllers

This chapter presents modular recurrent neural network controllers for single legs of a bio-mimetic six-legged robot equipped with standard DC motors. Following arguments of Ekeberg et al. (2004), completely decentralized and sensori-driven neuro-controllers were derived from neuro-biological data of stick-insects. Parameters of the controllers were either hand-tuned or optimized by an evolutionary algorithm. Employing identical controller structures, qualitatively similar behaviors were achieved for robot and for stick insect simulations. For a wide range of perturbing conditions, as for instance changing ground height or up- and downhill walking, swing as well as stance control were shown to be robust. Behavioral adaptations, like varying locomotion speeds, could be achieved by changes in neural parameters as well as by a mechanical coupling to the environment. To a large extent the simulated walking behavior matched biological data. For example this was the case for body support force profiles and swing trajectories under varying ground heights. The results suggest that the single leg controllers are suitable as modules for hexapod controllers, and they might therefore bridge morphological and behavioral based approaches to stick insect locomotion control.

6.1. Approach

To discuss sensori-motor control mechanisms in a more general setting here, the Ekeberg controllers for front-, middle- and hind-legs were implemented as modular neural networks (cp. section 3.2). This simplifies their comparison with a variety of other neuro-controllers, their usage as initial modules in modular artificial evolution (see e.g. Hülse et al., 2007; von Twickel and Pasemann, 2007) and their deployment on physical robots. The translated single leg controllers were tested on a physical simulation of the modular walking machine Octavio (cp. section 4.2.2) and validated on a simulated stick insect (cp. section 4.2.3). Both models were equipped with an antagonistic motor interface (cp. section 4.1.3) but not with muscle models. Tests were performed under different perturbations, especially considering multiple environmental conditions (cp. section 4.3). Some aspects of the controllers performance, like velocity control by parameter variation and swing trajectory dependence on initial swing conditions, were analyzed in detail.

Evolutionary Parameter Optimization In some simulation experiments parameters of front-, middle- and hind-leg controllers were separately optimized with an evolutionary algorithm (cp. section 3.3). Here, resulting controllers were compared with respect to

their ability to support the body weight during stance phase of forward walking. This was assumed to be indispensable for realizing hexapod walking behavior. Therefore a fitness function with two multiplicative terms was used (cp. section 3.3.4): the wayTerm and the bodySupportTerm. Individuals with good body support properties and fast walking received a good fitness whereas individuals which specialized for on or the other task received a worse fitness. Additionally terminate try signals (cp. section 3.3.4) for all joint angles were used and, therefore, desired joint angular ranges (but not explicit trajectories!) prescribed.

All structure evolution parameters were disabled, allowing only synapse strength and bias strength changes during evolution. Evolution was seeded with the front-, middle- and hind-leg controllers described in the results section. Parameters of the height control module were fixed because of its fragile parameter set. In the "restricted" case only motor and premotor neuron bias values as well as synapses to motor neurons were allowed to change. In the "unrestricted" case all input and output synapses of the height control module were allowed to change, as well as all other parameters of the networks. Maximum evaluation time was set to 2000 steps (corresponding to 20 s), population size to 100 and evolution was run for 1000 generations. For each leg type evolution was repeated 5 times, and the best performing network of the last generation of each evolution was taken as a basis for analysis.

6.2. Robotic Model

6.2.1. Middle-Leg Walking

Restricted (Sidewards) Middle-Leg Walking

In biological experiments the term "restricted preparation" denotes a fixated ThC joint resulting in solely CTr and FTi joints moving the leg in a vertical plane. This was the only experiment where sufficient neural data was available to fully describe a functional walking controller and therefore we performed a corresponding simulation first. In the simulation conducted here the ThC joint was not mechanically fixated but rather neurally by means of a stiff neural servo controller with constant reference input. The restricted middle-leg controller shown in Fig. 3.11b is a modified version of the controller shown in Fig. 3.11a that, additionally to the neural ThC servo, has all sensori-motor influences between ThC and other joints removed. Neural network parameters were translated from the Ekeberg controller as described above and remaining parameters, especially synapse strengths between the bistable elements and the motor neurons, were tuned by hand. Simulation results for parameters given in appendix E are depicted in Fig. 6.1a (foot trajectory) and Fig. 6.3a (time plot of important simulation parameters like sensor and motor activations). Peak sidewards torso velocity during a step was

$m\ x$.

A simple swing-stance cycle is depicted in Fig. 6.2: During swing phase the FTi joint was in extensor state and the CTr joint in levator state. A progressed extension of the FTi joint caused the CTr joint to switch from levation to depression state at the swing

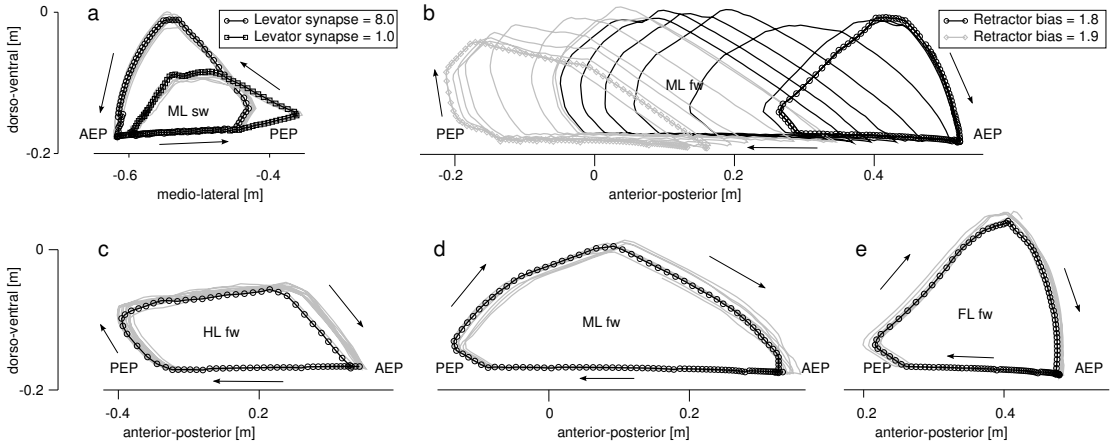

Figure 6.1.: Foot trajectories of stepping (in brackets figures with the respective controller structure are given, see appendix E for neural parameters): **a** restricted (sidewards) in middle-leg (Fig. 3.11b), **b** forward in middle-leg (Fig. 3.11a), **c** forward in hind-leg (Fig. 3.11c), **d** forward in middle-leg (Fig. 3.11b) and **e** forward in front-leg (Fig. 3.11b). Medio-lateral distances are relative to the midline of the torso, anterior-posterior distances relative to the coxa position of the respective leg. Each trajectory shows a 10 s run, and for exactly one step cycle individual data points for every simulation time step are shown as black markers on a black line, the rest in gray. This is slightly different in sub-figure **b** where one 10 s trajectory is shown as a black line and the other as a gray line to allow distinction between both in overlapping regions. For both trajectories the last step cycle of the 10 s periods has individual markers for each time step. Arrows indicate the direction of foot movement and anterior and posterior extreme positions (AEP and PEP) are labeled. In each of **a** and **b** two trajectories are plotted to show the influence of changing a single parameter (indicated in inset legend): Changing the strength of the levator synapse in the restricted middle-leg controller resulted in changing trajectory height (**a**). Changing the retractor bias in the unrestricted and unmodified middle-leg controller resulted in the trajectory either drifting anterior or posterior. For details see text

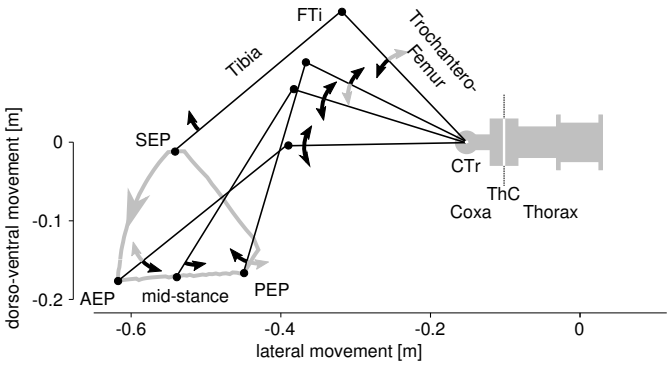

Figure 6.2.: Anterior view of a restricted middle-leg swing-stance cycle. Joint movement directions are indicated as black arrows at the next distal segment, and, if a transition took place, the old movement direction is additionally given in gray. Note that during stance the CTr height controller was active, therefore both CTr movement directions occurred. For details see text

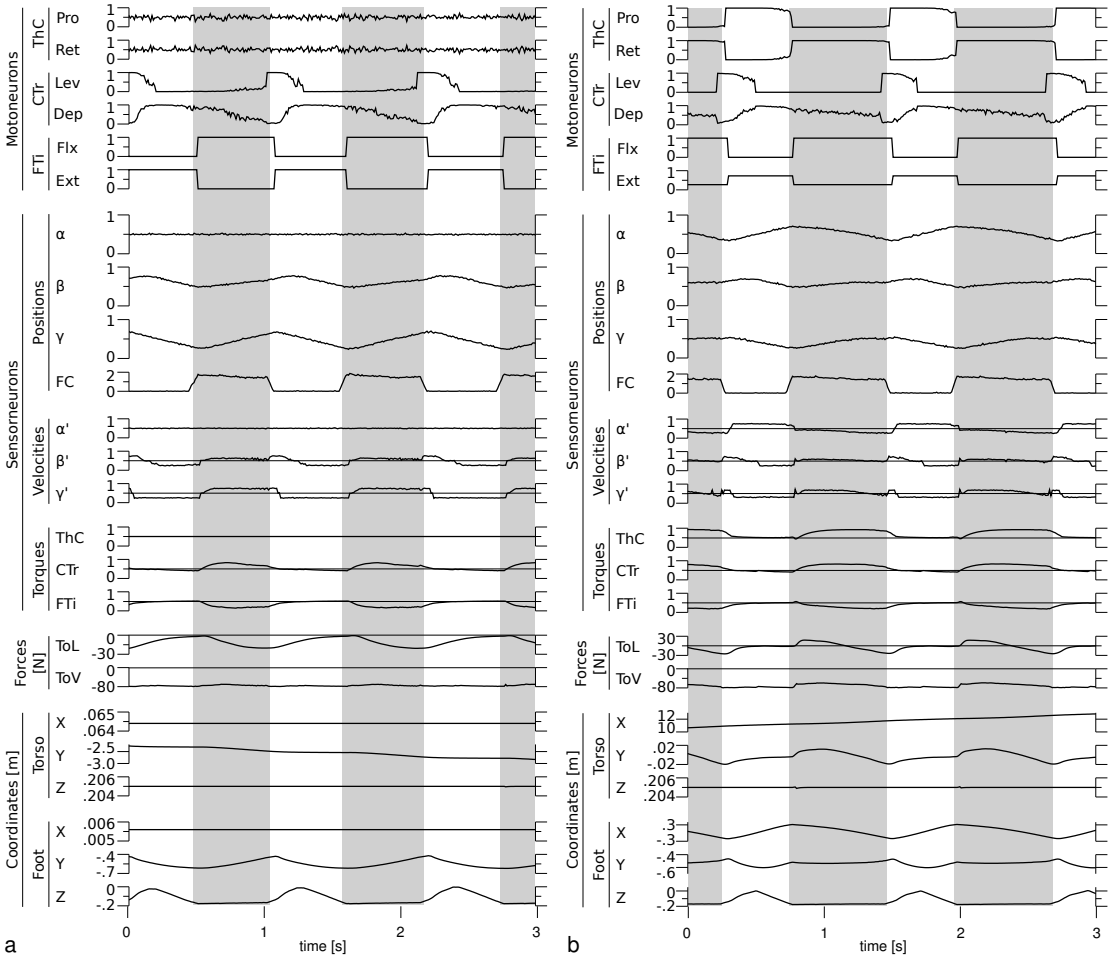

Figure 6.3.: Various data of **a** restricted (sidewards) and **b** forward walking in a single middle-leg. Grey areas indicate stance phase. Velocities, torques and forces are shown together with a base line indicating zero velocity, torque or force. For abbreviations see Fig. 1.4 and 3.11 and additionally: Foot Contact (FC), Torso Lateral (ToL), Torso Vertical (ToV)

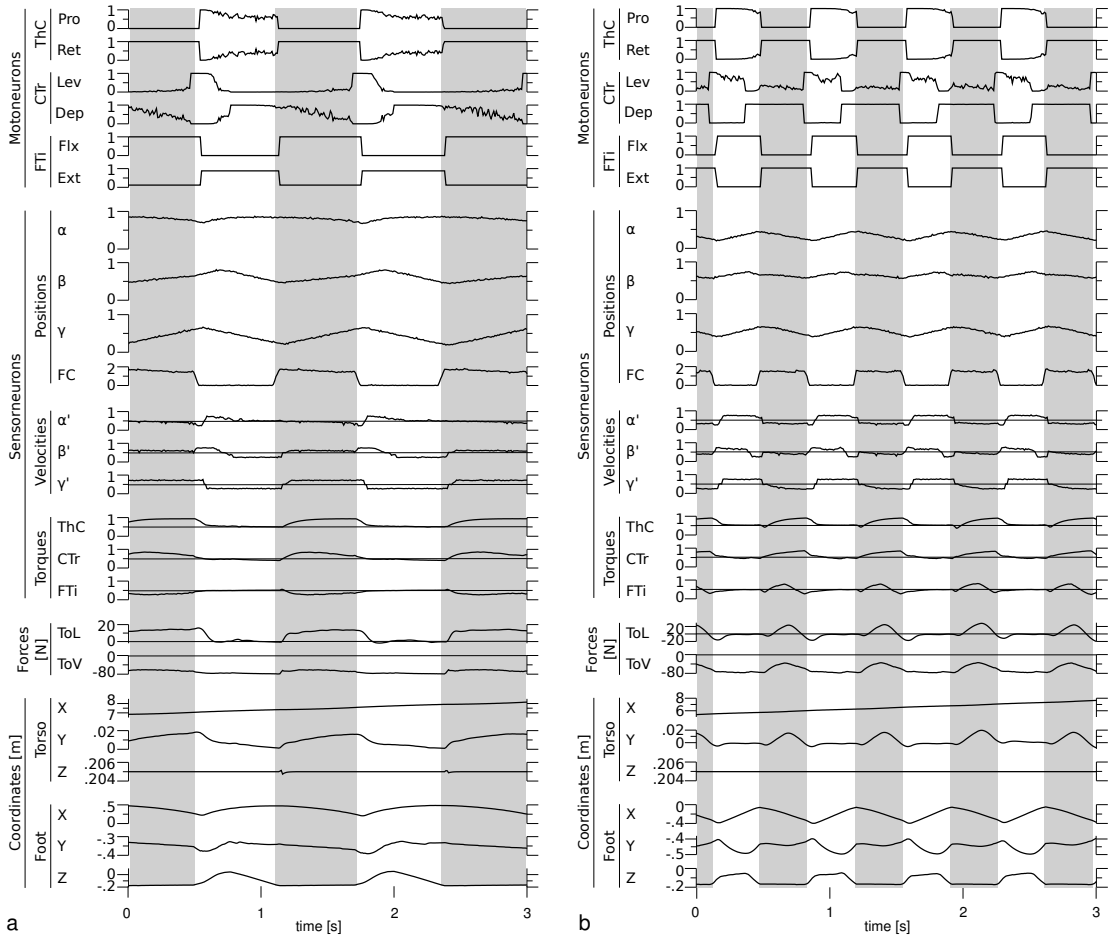

Figure 6.4.: Various data of forward walking in single **a** front- and **b** hind-legs. For abbreviations and further explanations see Fig. 6.3 and text

extreme position (SEP). Subsequent ground contact at AEP resulted in the FTi joint to change extension to flexion state, resulting in the stance phase where FTi was in flexion and CTr in depression state. During stance phase the CTr joint displayed its height control mechanism. Progressed flexion in FTi caused FTi and CTr to change states at the PEP resulting in the swing phase, and the swing-stance cycle started over again. Overall, restricted middle-leg controller translation to a neural network and test on the simulated robot worked well. One has to keep in mind that by changing synapse strengths to the motor neurons behavior could be easily modified. Additional to the example given above (trajectory height) e.g. a slow down of stepping could be achieved via a decrease in flexor synapse strength.

Kinematics of restricted stepping was similar to that found in von Uckermann and Büschges (2009) and Fischer et al. (2001) but differed in details. In von Uckermann and Büschges (2009) 1. the absolute movement of the CTr joint is more limited and 2. the CTr joint angle shows two depression maxima during stance phase. Two adaptations allowed to reproduce results of the biological experiments: 1. Tuning the neural parameters, especially levator synapse and bias values, the initially flat trajectory could be reproduced (see Fig. 6.1a) and 2. raising the body height in the simulator setup, such that it matched that of the experiment in von Uckermann and Büschges (2009) (trochantero-femur parallel to ground and tibia at an right angle to the ground allow for ground contact), the two depression peaks during stance could be reproduced because CTr then had to depress during end of stance to continue ground contact (data not shown).

Forward Middle-Leg Walking

Without the restriction of fixating the ThC joint, the leg was expected to be able to walk forward by employing all three DOFs. The controller structure shown in Fig. 3.11a corresponds to the original Ekeberg controller and parameters were calculated as explained above. As an exception, premotor- to motor neuron synapse strengths were tuned by hand (cp. section 3.2.2). Using this approach, no robust parameter set could be found that resulted in stable trajectories in the desired range. As shown in Fig. 6.1b for the parameter set given in appendix E it was difficult to stabilize the working range of the ThC joint – slight parameter changes resulted in ThC trajectories either drifting anterior or posterior. In anterior and posterior positions finally stable trajectories would result but not in the desired working range for middle-legs. By performing very precise parameter tuning, trajectories in the desired range could be achieved for a short time but upon minor external disturbances they again drifted away.

Extension of Middle-Leg Forward Controller The controller in Fig. 3.11 a was extended by a neural servo controller of the ThC joint to stabilize its working range, and the resulting controller structure is shown in Fig. 3.11 b. Parameters not determined by the rules given above were tuned by hand to achieve stable forward walking. Simulation results for the parameter set given in appendix E are depicted in Fig. 6.1d (foot trajectory) and Fig. 6.3b (time plot of important simulation parameters). Peak forward

torso velocity during a step was $_{m\ x}$. Again tuning parameters resulted in modified behaviors, e.g. decreasing retractor and/or flexor synapse strength resulted in slower walking (see section 6.2.1 for details), ThC comparator bias could shift AEP and PEP, and all parameter influences given for the restricted middle-leg controller also held for this one.

Alternative extensions to the original ThC joint controller module of the middle leg, all based on intra-joint sensori-motor feedback, have been tested, e.g. position dependent agonist and antagonist output limitation, corresponding to simple linear muscle models. These solutions, although not shown here, also worked fine in stabilizing the ThC working range.

Kinematics of forward stepping was found to be similar to the stick insect (cp. e.g. Fig. 3 in Cruse and Bartling 1995) with one exception: Fig. 6.3b shows that with the parameters chosen the FTi joint was in flexion state throughout the stance cycle. A biphasic flexion-extension movement during stance, as frequently seen in the stick insect (Cruse and Bartling, 1995), could be achieved by modifying parameters for two threshold units (data not shown): First, the threshold for FTi flexion leading to a transition from depression to levation (neuron 19) needed to be set so low that it was practically disabled and the ThC retraction threshold (neuron 18) led to the transition to levation. Second, the threshold for FTi flexion leading to a transition from flexion to extension (neuron 25) needed to be set so high that extension was triggered by flexion movements normally achieved during mid stance and not only later by the loss of foot contact (neuron 26). Since smooth movements only resulted if the flexion-extension transition took place while ThC(α)-joint angle was $^{\circ}$ resulting controllers showed to be very sensitive to changes in environmental conditions. Adding a neural ThC angle influence on flexion-extension transitions allowed robust stepping under different environmental conditions, together with the biphasic FTi movement during stance.

Velocity Control

In Fig. 6.5 details of the velocity control are given: Locomotor speed (due to the single leg simulations it was measured as average velocity during stance) could be varied between 0.26m/s and 0.75m/s by exclusively changing retractor and flexor bias parameters. 11 sets of both parameters were manually chosen to cover the range between the slow and fast locomotor speeds (for parameter sets with corresponding velocities see appendix E). Up to a locomotor speed of velocity increase was mainly achieved by a decrease in step cycle duration. While swing phase duration was approximately constant across all velocities a decrease in stance duration was responsible for the decrease in total step duration. The increase in stance velocity in turn was caused by an increase in flexion and retraction velocity (data not shown). With the parameters chosen the flexion velocity increase had a larger influence than the retractor velocity increase resulting in the side effect of a slightly decreased step length: Since levation was triggered above a flexion threshold (neuron 19) increased flexion velocity led to a slightly earlier levation during stance. For velocity increases above an increase in support length (distance body travels during contact phase, Halbertsma (1983)) was observed while

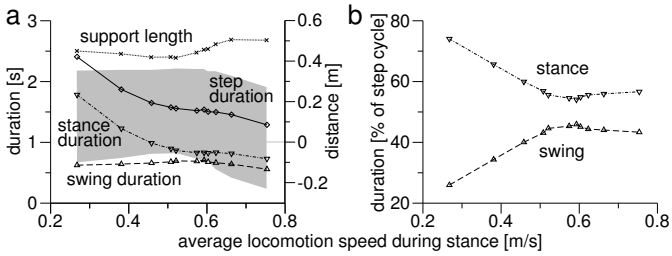

Figure 6.5.: Relative changes in the duration of swing and stance phases of the step cycle as well as changes in the support length at different speeds of forward locomotion in the middle leg. Locomotion speed was controlled by changing retractor and flexor motor neuron (neurons 9 and 12, see Fig. 3.11) bias values. Data is displayed for 11 bias parameter sets (given in appendix E), each averaged across 5 steps. In **a** absolute step cycle, swing and stance durations and the support length, together with anterior-posterior tarsus range relative to the coxa during stance (gray area), are given whereas in **b** swing and stance phase duration relative to the total step cycle duration is given. Locomotor speed was calculated by averaging torso velocity during stance phases. See text for details

both stance and swing phase duration slightly decreased. For the parameter sets chosen stance velocity increase was predominantly due to an increase in retraction velocity. In this situation the switch from depressor to levator activity was first triggered by the retraction signal (neuron 18) and not the flexion signal (neuron 19). This resulted in an extended, i.e. more retracted, step. Therefore, the FTi angle at PEP was not as flexed as during slower movements, and the angular range to reach the extension inducing depression was smaller. This led to shorter swing phases. The bistability of the ThC comparator input ( ), together with the extended retraction, led to a larger error signal in the ThC servo (neuron 14) during early swing and therefore to a higher protraction velocity.

Test of Controllers Under Different Perturbing Conditions

Leg controllers were tested with regard to their robustness under perturbing conditions. In Fig. 6.6 results are shown for the middle-leg, using the same neural structure (Fig. 3.11b) and neural parameter set (appendix E) as above. The controller proved to be robust against substantial changes in all tested conditions:

Ground Height Variations In Fig. 6.6a ground height was varied, alternating every 0.8m between low steps and high steps. Heights were randomly chosen in the ranges [ ] and [ ] below torso support height. Ground height variations were tolerated without disrupting the walking behavior. During stance phase the foot was more medial for low steps and more distal for high steps (s. Fig. 6.6f). During some steps the swing trajectory appeared to be especially flat, during others especially high. Therefore swing data of the same simulation but for an extended number of swings (40) was plotted in different formats in Fig. 6.7: First of all in the overlaid swing trajectories (Fig. 6.7a) a correlation of low and anterior PEPs on the one hand and high and posterior PEPs on the other hand was noted. In contrast, x and z components of AEPs were

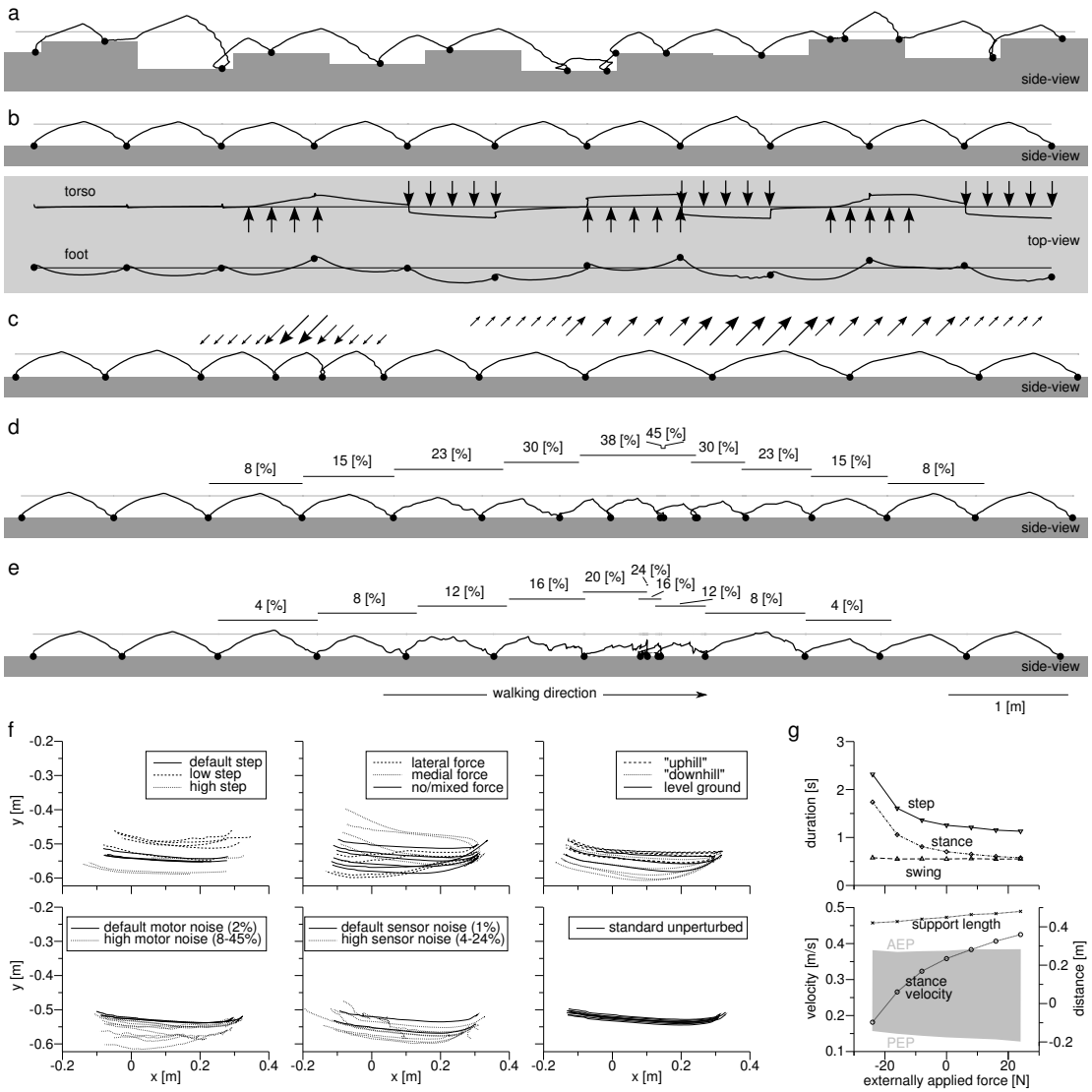

Figure 6.6.: Middle-leg walking forward under different perturbing conditions. Foot trajectories in world coordinates are shown as a black line, foot contact with ground as black dots and ground as gray area. Viewpoints are indicated in figure. **a** Ground height changes with fixed body suspension height (straight gray line). Total time period was ≈20 s. **b** Sidewards forces of 80 N were applied to torso whenever arrows are shown with direction of the arrows (note that torso was fixed to a lateral spring-damper system so it had an equilibrium position shown by thin line, see Materials and Methods section for details). Periods of force application were randomly chosen between 0.9 and 1.1 s. Total time period was ≈15 s. **c** Forces with magnitudes 8, 16 and 24 N were applied at an angle of 45°from anterior-dorsal and posterior-ventral to simulate up- and downhill walking. Arrows show when forces were active, in which direction and with which strength. Periods of force application were randomly chosen between 0.9 and 1.1 s for all forces. Total time period was ≈14 s. **d** Gaussian noise on motor neuron output. Magnitudes of noise application are indicated in the figure. Periods of noise application were randomly chosen between 1.4 and 1.6 s. Total time period was ≈19 s. **e** Gaussian noise on sensor neuron input. Magnitudes of noise application are indicated in the figure. Periods of noise application were randomly chosen between 1.4 and 1.6 s. Total time period was ≈20 s. **f** For all perturbing conditions above (a–f) and the reference flat ground condition the dorsal view of the foot stance trajectories relative to the middle-leg coxa is given. For details see text. **g** For the simulated up- and downhill perturbing condition (c) average stance velocity and other important step cycle parameters (s.a. Fig. 6.5) are given for the external force levels listed above (each data point was averaged from 7 consecutive steps)

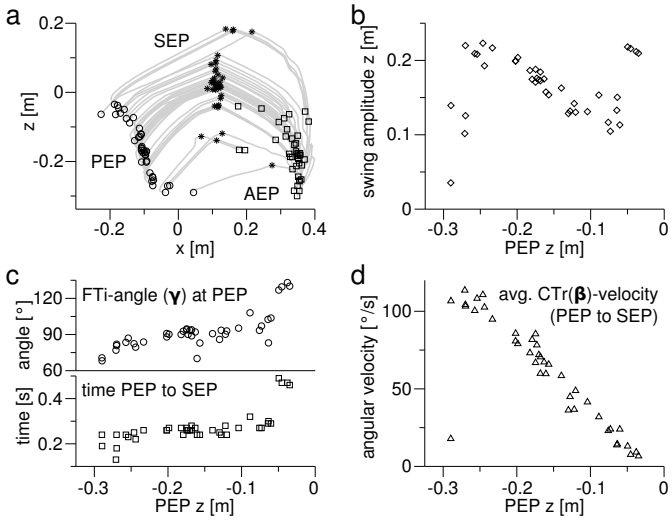

Figure 6.7.: Detailed swing trajectory data from 40 consecutive steps, taken in an environment with varying ground to torso suspension height (see Fig. 6.6a): **a** Lateral view of swing trajectories (gray) with markers for posterior-, swing- and anterior-extreme positions (PEP, SEP and AEP). **b** Swing height ( ) vs. PEP height. **c** FTi angle (γ) at PEP and PEP to SEP duration vs. PEP height. **d** Average CTr ( ) angular velocity in PEP–SEP interval vs. PEP height. Note that 4 swings from low and 4 swings from high ground deviated from the general pattern. See text for details

less correlated because the x component was, especially for low AEPs, less variable. Therefore, also the anterior-posterior swing length was positively correlated with the PEP height, i.e. high PEPs resulted in longer swings than lower PEPs. With some exceptions (see below) PEP–SEP slopes continuously decreased with increasing PEP height resulting in a negative correlation of dorsal-ventral swing amplitude ( ) and PEP height, i.e. swing amplitude decreased with increasing PEP height (Fig. 6.7b).

As mentioned above, two types of deviations occurred from the average swing behavior: For very high PEPs dorsal-ventral swing amplitudes could be much larger than for slightly lower PEPs, and for very low PEPs dorsal-ventral swing amplitudes could be much lower than for slightly higher PEPs. Dorsal-ventral swing amplitude depended on mainly two components: tarsus levation time and levation velocity. Levation time was dependent on the state of the CTr and FTi premotor neurons which were in turn dependent on the antagonistically acting state transition modules. Levation velocity was mainly dependent on the CTr height control module. In the "normal" cases, where the negative swing height to correlation held, levation time moderately increased with PEP height (0.24s with of -0.29m and 0.29s with of -0.06m, see Fig. 6.7c). As shown in the same sub-figure, this levation time increase was due to the FTi angle at PEP because the further the FTi joint was flexed, the longer it took for it to reach the extension threshold during swing triggering depression (neuron 21 in Fig. 3.11). Therefore, a higher levation velocity for lower PEPs had to compensate for the shorter levation times and additionally had to cause the differences in swing height

amplitude. In Fig. 6.7d a strongly decreasing average CTr angular velocity between PEP and SEP is shown for increasing PEP heights supporting this hypothesis. For one extreme outlier the very low average angular velocity of CTr (° at -0.29m) was responsible for the low swing height. It was caused by a swing phase where the CTr joint was not switched to swing phase but rather its height controller was initiating a levation in response to FTi flexion. This led to ground contact loss and in turn to a switch from flexion to extension in the FTi joint and a switch from retraction to protraction in the TC joint. The extension quickly triggered a depression via the height controller. For the remaining outliers the time from PEP to SEP and therefore the FTi-angle at PEP was identified as the cause: For very low PEPs FTi was less flexed in three cases (depression-levation switch caused by TC angle retraction threshold) leading to a shorter extension period and therefore a faster switch from levation to depression. For very high PEPs FTi was flexed stronger in four cases leading to a longer extension and therefore to a longer levation time.

Lateral "Kicks" In Fig. 6.6b lateral forces with a magnitude (80N) larger than a third of the robots weight (, corresponding to the weight that one leg had to support in tripod gait) were applied alternatingly from both sides with pauses in between. Due to the lateral spring-damper suspension system perturbation forces would lead to movements during force on- and offset. During stance lateral torso movements were compensated by the leg joints (especially the FTI joint) and not by a sliding foot. Forces did not disrupt the walking behavior and only had a minor influence on swing trajectories despite the obvious lateral shifts during lateral force application. In Fig. 6.6f it is shown that during stance phase lateral directed forces decreased the torso-foot distance whereas medial directed forces increased it. Larger perturbation forces (data not shown) could lead to instability in the sense that beyond FTi extension the foot was dragged across the ground, or that beyond FTi flexion the foot was tilted inwards.

Simulated Up- and Downhill Walking In Fig. 6.6c up- and downhill walking was simulated by an application of varying forces at angles of ° from either anterior-dorsal ("uphill") or posterior-ventral ("downhill"). Forces corresponded to approx. 4%, 8% and 12% of body weight and, if assuming other assisting legs as during tripod or wave gait in a hexapod, the per leg forces were proportionally higher (3–5 times, i.e. 12%–36% in tripod and 20%–60% in wave gait). Under these perturbing conditions the leg controller showed robust walking behavior and, together with the bio-mechanical system, a velocity adaptation. In Fig. 6.6g data of separate simulation runs for each external force level are shown: "uphill" locomotion speed was reduced and "downhill" locomotion speed increased. The velocity adaptation was mainly due to a step duration variation, which was in turn due to a stance duration variation, and to a small extent due to support length variations. Note that forces were applied independently of stance or swing phase and therefore the variation in global swing amplitude did not correspond to the step length relative to the torso (s. Fig. 6.6f).

Noise on Sensor and Motor Neurons In Fig. 6.6d and e noise of varying levels was applied to all motor neuron outputs (d) respectively all sensor-neuron inputs (e) at the same time. On the one hand noise levels on motor neuron outputs could be increased to without disrupting basic stepping. With increasing noise levels swing trajectories became smaller in height and length as well as slightly more jittery and showed increasing lateral deviations (cp. Fig. 6.6f). Beyond noise level no regular walking behavior could be observed any more. On the other hand noise levels on sensor-neuron inputs could only be increased to before becoming disruptive. Both increased sensor and motor noise additionally shifted the foot position during stance further distal (s. Fig. 6.6f).

6.2.2. Test of Controllers in Front- and Hind-Legs

In Ekeberg et al. (2004) the middle-leg controller structure was also tested on front- and hind-legs. For the front-leg only parameters of the original middle leg controller had to be changed because kinematics does change little compared to the middle-legs: ThC joints of front-legs are on average more protracted during stepping. Here the parameters given in Ekeberg et al. (2004) were directly translated into neural parameters and applied to the original middle-leg controller structure shown in Fig. 3.11. The same problem of stabilizing the ThC working range appeared as initially in the middle-leg, so a neural ThC servo was included. This resulted in the same controller structure as finally used for the middle-leg (see Fig. 3.11 b). Employing this structure and tuning the "free" parameters resulted in stable forward walking in the desired working range. Simulation results for neural network parameters given in appendix E are shown in Fig. 6.1e (foot trajectory) and Fig. 6.4a (time plot of important simulation parameters). Peak forward torso velocity during a step was $_{m\ x}$. By changing parameters, front-leg walking kinematics could be changed in several ways. In addition to the behavioral flexibility listed for the middle-leg e.g. "anterior sidewards" stepping (i.e. forward walking largely without ThC joint contribution) could be achieved by either changing ThC comparator reference input or protractor and retractor synapse strength.

In contrast to the front-leg controller the structure of the middle-leg controller had to be modified in Ekeberg et al. (2004) in order to make it work as a hind-leg controller. The kinematics of the hind-leg differs significantly, especially the phase relation of the FTi joint relative to the other two joints, with the extensor being active during stance phase and the flexor during swing phase. Additionally to the modifications by Ekeberg et al. (2004) we had to introduce the neural ThC servo to stabilize the ThC working range, analogous to front- and middle-legs. The resulting structure is shown in Fig. 3.11 c. Parameter tuning by hand proved to be more difficult than for front- and middle-legs. Therefore a prioritizing switch module (see Fig. 3.9) was included in the CTr joint controller and resulted in robust walking behavior under standard conditions. Simulation results for the parameter set given in appendix E are shown in Fig. 6.1c (foot trajectory) and Fig. 6.4b (time plot of important simulation parameters). Peak forward torso velocity during a step was $_{m\ x}$. As in the other leg controllers behavior could be modified by changing neural parameters but due to the different kinematics

of the hind-leg (s.a.) differences in behavior control existed: For instance a combination of depressor and extensor synapse strength determined velocity during stance phase (and therefore step period), a combination of flexor and levator synapse strength determined swing velocity and duration (data not shown).

Under perturbing conditions, like changing ground height (data not shown, cp. section 6.2.1 for middle-legs), the performance of the hind-leg controller was not robust in all situations despite new parameter tuning. This was because the FTi joint was prone to flex too far, and subsequently the controller was "stuck" because the FTi joint would only switch to extension upon ground contact, but ground contact without extension was not possible any more. To obtain a more robust hind-leg controller two alternatives were tested (data not shown): 1. using a neural servo controller in the FTi joint analogous to the ThC joint, 2. using the FTi joint controller structure found in the front- and middle-legs (see Fig. 3.11 d and appendix E for controller parameters). Both solutions led to an increased stability in the FTi joint.

6.2.3. Test of Controllers on a Stick-Insect Simulation

As a proof of principle the front-, middle- and hind-leg controllers tested on the simulated robotic model were also tested on a simulated stick insect model. By only modifying "free" parameters (cp. section 6.1), qualitatively comparable stepping behavior could be produced. Neither the structure of the controller nor those parameters prescribed by neuro-biological data were modified. Detailed data and parameters are given in appendix E. Major differences that could be observed were, despite of the obvious differences due to scaling like locomotor speed, shorter step cycles and differently shaped foot trajectories.

6.2.4. Support Forces

Dorso-ventral Forces Are the single leg controllers shown above suitable as control modules in hexapod controllers? To answer this question their ability to support the body together with the mechanical system was investigated. Testing front-, middle- and hind-legs with the controllers given above and neural parameter sets given in appendix E showed that hind-legs and respective controllers could support body weight much more than middle-and front-legs, and that middle-legs would slightly outperform front-legs (see Fig. 6.8a, G0). This order was similar to the one found for stick insects walking on flat terrain by Cruse (1976) (see Fig. 6.8b). To verify that this finding was not due to hand-tuned parameters, parameter optimization was performed: The goal was to reach maximum walking speed with maximum body support force (details are given in section 6.1):

1. First, a restricted parameter set, consisting of motor neuron bias values, all synapse weights with motor neurons as targets, and all premotor neuron bias values, was optimized. Maximum support forces by front- and middle-legs increased with progressing parameter optimization, but leveled off in the same order as the hand

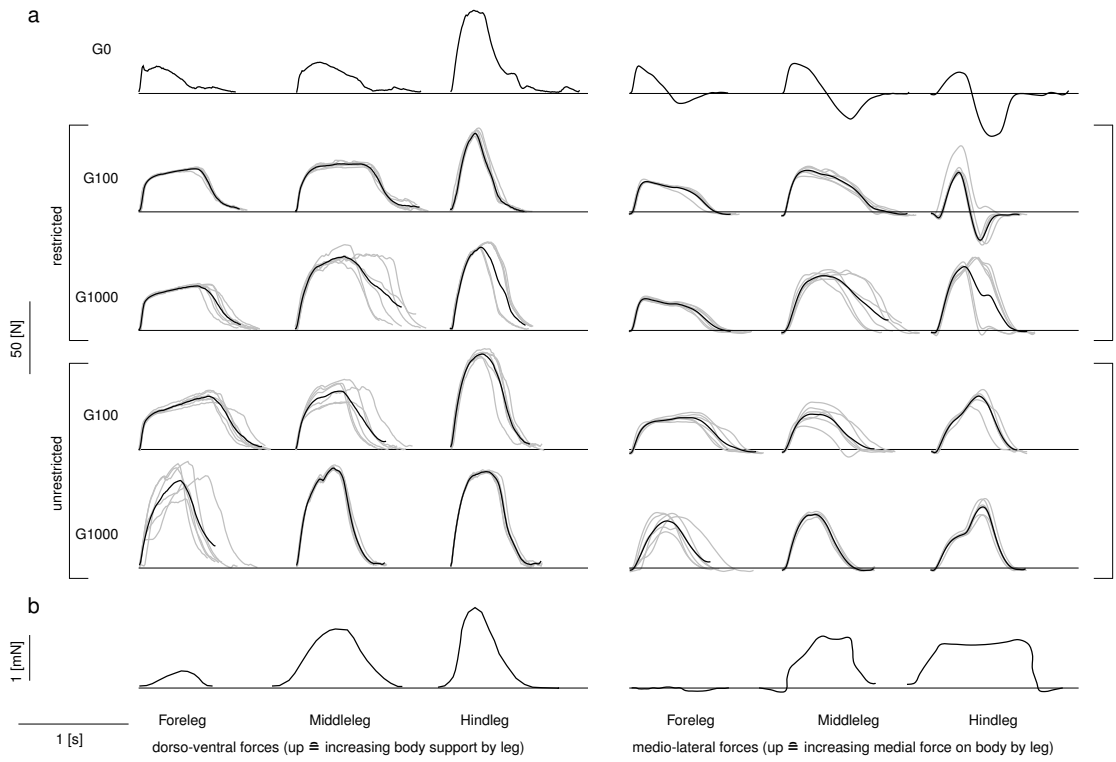

Figure 6.8.: Dorso-ventral and medio-lateral torso support forces (directions correspond to y- and z-axes in Fig. 4.2) by single legs: **a** in simulation (measured were forces between torso and rail suspension during forward walking) for hand tuned (G0) and parameter optimized controllers (G100 after 100 generations, G1000 after 1000 generations, restricted means optimization was only performed on a limited parameter set, cp. section 6.1) driving front-, middle- and hind-legs. For each situation 6 independent parameter optimizations were run and for each best controller forces of 5 consecutive step cycles were averaged (gray lines). Force profiles of all 6 controllers were again averaged to give the mean forces which are shown as black solid lines. See text for details. **b** in *in vivo* stick insect hexapod walking on a plane (ground reaction forces of the feet, data taken from Fig. 7 in Cruse 1976). Note that time between force profiles of different legs has no meaning in single leg experiments compared to the hexapod experiments by Cruse (1976)

tuned controller forces. Kinematics of optimized controllers (not shown) did not change much except that foot trajectories became more flat.

2. Second, almost all parameters (except internal parameters of the two-joint height control module) were made accessible to parameter optimization to check if extended parameter changes would allow front- and middle-leg controllers to develop similar support forces as the hind-leg controllers. As shown in Fig. 6.8 this is the case. Kinematics of optimized controllers (not shown) did change in such a way that not only the foot trajectories became more flat, but also the movement range of the FTi joint was decreased, and the mean tibia position became more vertical with respect to the ground.

Medio-lateral Forces Fig. 6.8 shows that controllers with initially hand tuned parameters sequentially displayed forces in medial and in lateral directions, unlike in the single legs in *in vivo* hexapod walking that almost exclusively displayed medial directed forces. Maximum forces were slightly larger in middle- and hind-legs but also front-legs showed non-negligible lateral forces, again different from the *in vivo* hexapod data. In both parameter optimization cases (restricted and unrestricted, see above for details) lateral forces vanished with progressing optimization, becoming more similar to the *in vivo* example. The front-leg medio-lateral forces, though smaller in magnitude than in middle- and hind-legs, persisted.

6.3. Stick Insect Model

Standard and extended (including ThC servo) controllers for front-, middle- and hind-legs tested on the robotic model above (cp. Fig. 3.11) were tested on the stick insect model. Modifications of "free" parameters (cp. section 3.2) were sufficient, i.e. parameters for the height control module (s. above) and premotor to motor couplings, to qualitatively reproduce the behavior found for the robotic model. Modified parameters are given in section 9.2. Data is shown in the same format as for the robotic model: Foot trajectories are given in Fig. 6.9 and time-plots in Figs. 6.10.and 6.11. Note that the tempts show a time range of only 2s compared to 3s for the robotic model. This is due to the higher frequency movements respectively shorter step durations. With the parameters given peak velocities $_{m\ x}$ during stance were found to be for restricted middle-leg stepping, for middle-leg forward stepping, for front-leg forward stepping and for hind-leg forward stepping. With the same parameters step cycle periods ranged from to , swing durations from to and stance durations from to . Analogous to the robotic model the standard controller, i.e. without a ThC servo, was not able to produce robust stepping in the middle leg (see Fig. 6.9b).

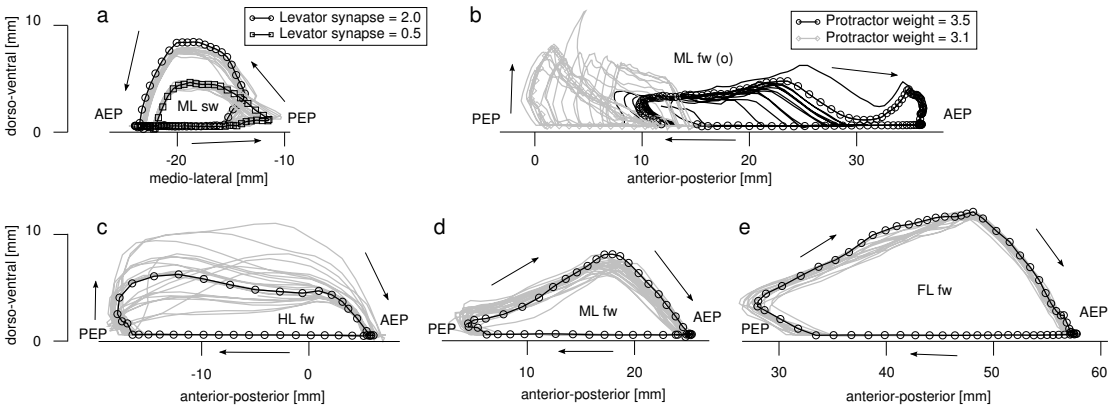

Figure 6.9.: Foot trajectories of stepping in the stick insect model (in brackets figures with the respective controller structure, see appendix E for neural parameters): **a** restricted (sidewards) in middle-leg (Fig. 3.11b), **b** forward in middle-leg (Fig. 3.11a), **c** forward in hind-leg (Fig. 3.11c), **d** forward in middle-leg (Fig. 3.11b) and **e** forward in front-leg (Fig. 3.11b). Medio-lateral distances are relative to the midline of the torso, anterior-posterior distances to the coxa position of the respective leg. Each trajectory shows a 10 s run and for exactly one step cycle individual data points for every simulation time step are shown as black markers on a black line, the rest in gray. This is slightly different in sub-figure **b** where one 10 s trajectory is shown as a black line and the other as a gray line to allow distinction between both in overlapping regions. For both trajectories the last step cycle of the 10 s periods has individual markers for each time step. Arrows indicate direction of foot movement and anterior (AEP) and posterior extreme positions are labeled. In each of **a** and **b** two trajectories are plotted to show the influence of changing a single parameter (indicated in inset legend): Changing the strength of the levator synapse (5 0) in the restricted middle-leg controller resulted in changing trajectory height (**a**). Changing the protractor weight ( ) in the unrestricted and unmodified middle-leg controller resulted in the trajectory either drifting anterior or posterior. For details see text

6.4. Discussion

6.4.1. Deriving Modular Neural Controllers

Feasibility of Modular Neural Network Implementation Ekeberg et al. (2004) showed in simulation how simple modules coupled in the sensori-motor loop may constitute a clearly structured controller (cp. Fig. 1.4) producing robust behavior. Thus, using the modular approach to neural networks (Hülse and Pasemann, 2006; Manoonpong et al., 2008; Pasemann, 1995; Pasemann et al., 2001), it was a feasible task to translate the finite state controller model into an equivalent neural network controller consisting of simple neuro-modules (see Fig. 3.11). Most of the network parameters were derived from parameters of the finite state controller by simple rules. Nevertheless some details had to be addressed: 1. In the original paper timing control was done by the finite state controller, magnitude control (e.g. CTr height control) integrated into muscle activation functions. Here, both features are integrated into a single neuro-controller using corresponding neuro-modules, thus leading to a more transparent structure. 2. No absolute torques and joint velocities, corresponding to specific muscle activations, were given, therefore muscle activations (here corresponding to premotor to motor synapse weights) had to be determined experimentally. 3. Multiple rules acting on a single joint could show contradictory outputs (and actually did so in behaviorally relevant situations, see results section), but the original publication does not state how these conflicts are resolved. Experiments showed that prioritizing the rules as indicated in section 1 and Fig. 1.4 was a successful strategy and the authors of Ekeberg et al. (2004) confirmed that they used the same strategy.

Benefits and Limitations Additionally to the advantages mentioned in the introduction (e.g. easy deployment on hardware and usage as modules in artificial evolution) the neural implementation had some limitations: 1. Without proper documentation of the modular structure, the functionality of the modules and the meaning of parameters (e.g. thresholds represented by dimensionless bias values) was not as clear as in the finite state controller. Therefore, a detailed description of the modules, including a clearly structured neural network layout and conversion tables for important parameters, was indispensable. 2. As usually done in recurrent networks without distinct layers, the neural network was updated in the order activations outputs with a frequency feasible for robot control. As a consequence significant time-delays could result. With the update frequency of 100Hz that was used throughout all experiments the maximum time delay was 40 ms with 4 synapses between sensor and motor neuron (cp. e.g. pathway in Fig. 3.11). To decrease this time-delay either the update rule had to be modified adding complexity to the system or the global update frequency had to be increased which was not desired on the robotic system Octavio. 3. Using single neurons as threshold approximators together with precision limits given by the hardware did not allow the same sharpness in transition as statements. Yet the neuro-threshold-modules employed in this context showed to have, in terms of behavior control, sufficiently sharp transitions and an increased benefit of noise robustness due to a hysteresis effect (s.

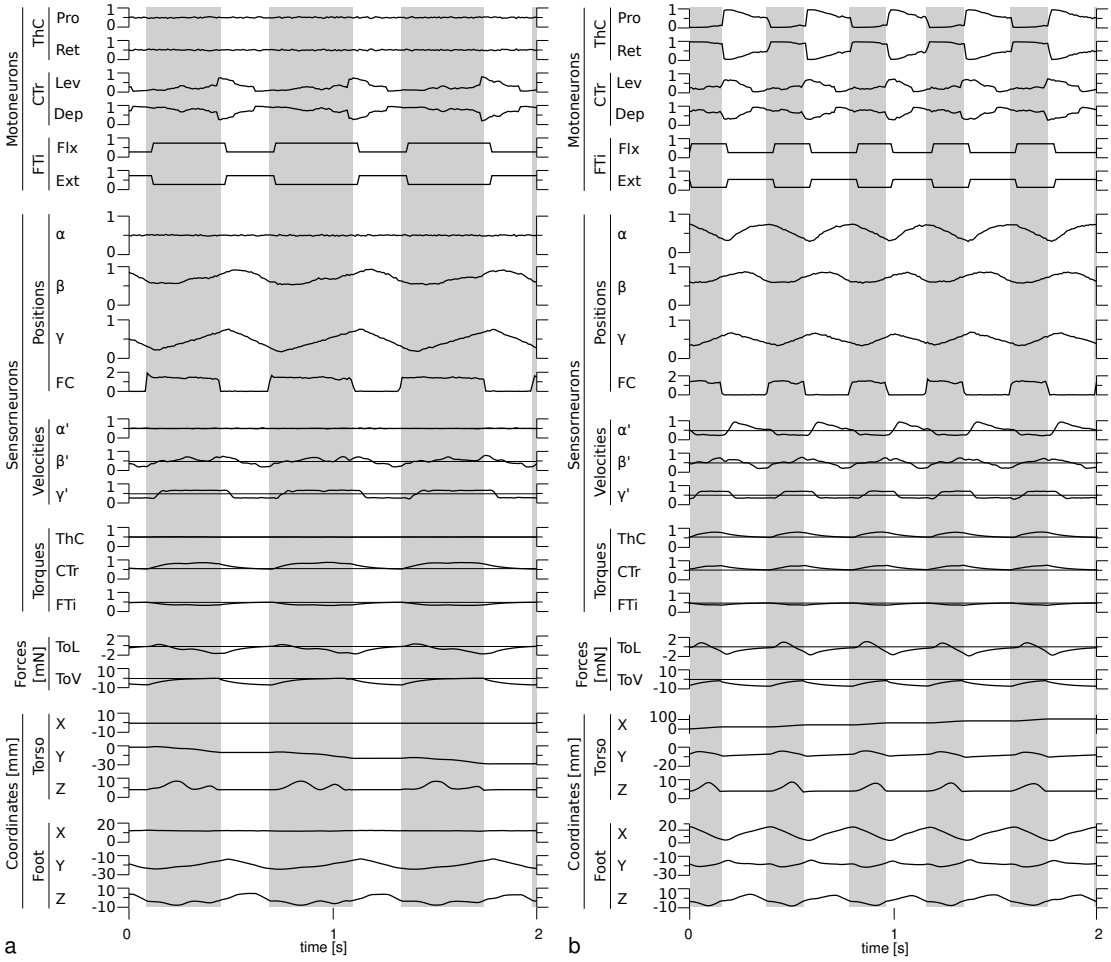

Figure 6.10.: Various data of **a** restricted (sidewards) and **b** forward walking in a single middle-leg of the stick insect model. Grey areas indicate stance phase. Velocities, torques and forces are shown together with a base line indicating zero velocity, torque or force. For abbreviations see Fig. 6.3

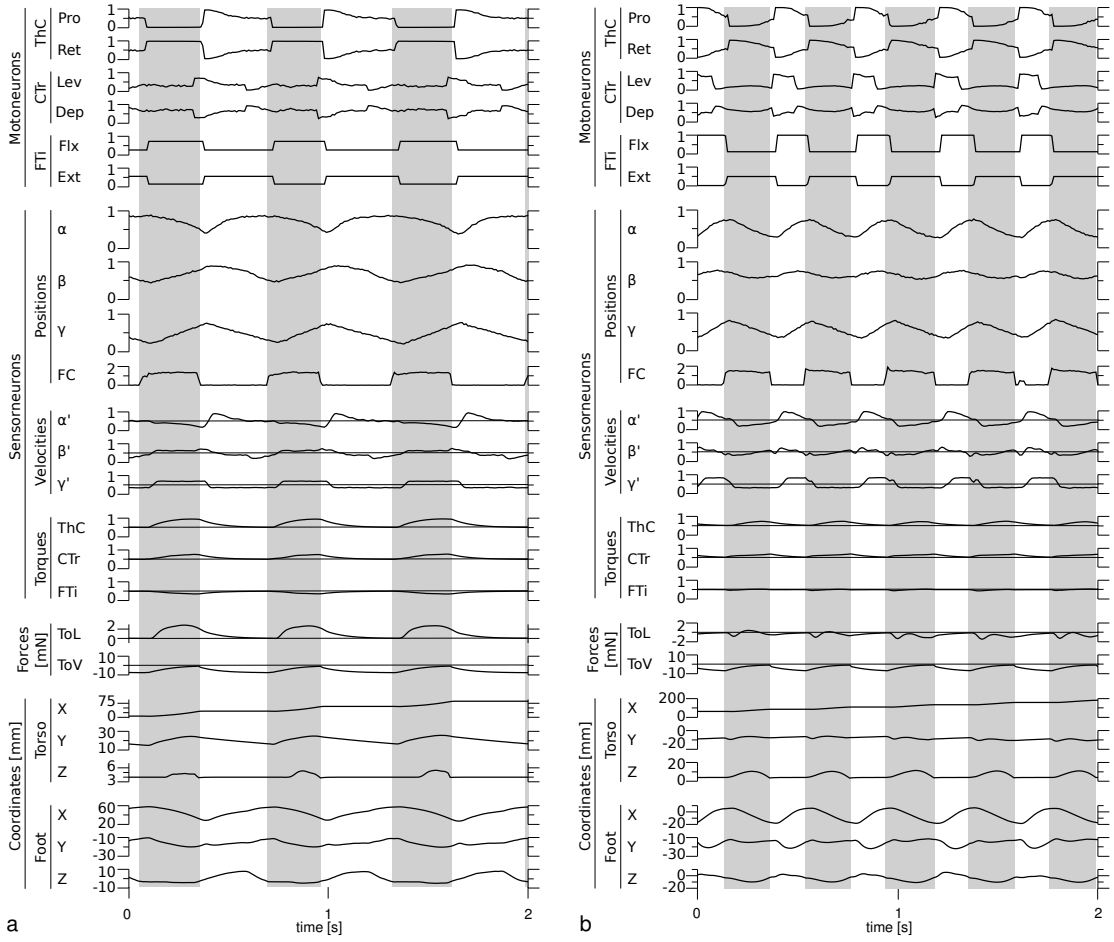

Figure 6.11.: Various data of forward walking in single **a** front- and **b** hind-legs of the stick insect model. For abbreviations and further explanations see Fig. 6.10 and text

Fig. 3.8).

6.4.2. Testing Controllers on a Robotic and a Stick Insect Model

Successful tests of modular single-leg neuro-controllers with identical structure on a simulated model of the physical robot Octavio as well as on a simulated stick insect model demonstrated the controllers robust performance despite large differences in scaling and biomechanics:

Differences in Mechanical Plant and Scaling In comparison with stick insects (or simulated models thereof) basic morphological features of the simulated walking machine Octavio, like number of legs, number of main leg joints, joint axes and main sensory qualities, were similar. One exception was the ThC joint axis which only had one DOF in the robot and was parallel to the dorsal-ventral body axis. In the stick insect it has two DOF but one main functional DOF and this axis has an offset to the dorsal-ventral body axis (Cruse and Bartling, 1995). It is argued that the medio-ventral to lateral-dorsal joint axis simplifies stance control: In the stick insect, by only performing a retraction movement, the leg is automatically loaded and unloaded during stance phase, not requiring the control of other joints.

Despite of differences in scale (cp. table D.1) geometric similarity and pre-conditions for dynamic similarity (Alexander, 1989) were roughly given (cp. section 4.2.2). Additionally increased stress, which is thought to cause larger animals to hold their legs straighter during walking (Biewener, 2005), was not a problem in the simulation of the scaled up robotic model used here. So this would have to be tested in the physical robot, taking into account differences between muscle-tendon and technical motor-gear-spring systems. Comparatively slow walking of stick insects, resulting in duty factors being much larger than in running animals, reduced the stress problem to some extent. Furthermore, limb size influence on unloaded limb motor control strategy as discussed in Hooper et al. (2009) did not qualitatively change the behavior of the scaled up model. This was attributed to the direction of the controller transfer: In small animals like stick insects persistent swing motor neuron activations are necessary to complete swing phase. But the same control strategy also worked for the robot Octavio where inertia was large compared to joint friction. The alternative control strategy of larger animals requires motor neuron activity only during acceleration and deceleration phases due to their ballistic limb movements. This would not be applicable to small animals where antagonist muscle passive forces and cuticular passive forces are larger than gravitational forces.

Motor vs. Muscle Systems Using virtual antagonists to drive one single motor-gear combination per joint in the robot (see section 4.2.2 and Fig. 4.3 for details) seemed overly complicated but had several advantages: It increased comparability with biological controllers, it was better prepared for migration to a machine with real antagonists and some control concepts were realized in a simpler way when using the antagonist motor interface. This was e.g. demonstrated for velocity control in the middle-leg (see

section 6.2.1). As a result of only having virtual antagonists real stiffness control by antagonist co-activation was not possible and muscle properties like force-length characteristics present in the stick insect (Guschlbauer et al., 2007) were missing in the real robot. Therefore a different walking behavior was expected when using the controller transferred directly from biology. For all controllers transferred, except the restricted middle-leg one, modifications were necessary in the ThC joint control (and for the hind-leg also in the FTi joint control) to achieve robust walking behavior, adding intra-joint position feedback leading to a stabilization of the joints working range. This may be thought of as a possible replacement for intra-muscular joint position feedback (or in other words position dependent actuation limiting feedback) due to the force-length characteristics. Ekeberg et al. (2004) used a simple linear muscle model and did not have to add this kind of intra-joint feedback in the ThC joint nor in the FTI joint for the hind-leg controller. As in the hind-leg FTi joint the environment could also – at least to some extend – contribute to joint working range stabilization by imposing constraints on joint movement. This could have been due to e.g. ground contact or gravitation. Rutter et al. (2007) compared the performance of controllers with a piecewise constant muscle model, a linear muscle model, and without a muscle model in the FTi joint. They found a more reliable ground contact detection when using any of the two muscle models. They attributed this to a reduced tibia extension at swing-stance transition improving performance of restricted and forward walking. In contrast, the swing-stance transitions were unproblematic in the model presented here. Probably this was due to using a ground contact sensor instead of a motor current ("load") sensor. An exception was the hind-leg controller where no intra-joint feedback in the FTi joint control module existed and this led to a fragile walking behavior (cp. section 6.2.2). Adding FTi intra-joint feedback stabilized the system. Lewinger et al. (2006) also found a drift of the ThC movement towards extreme joint positions without muscle models and suggested that the underlying plant must exhibit saturation in order to show robust behavior. A forthcoming publication will specifically address the question of how requirements change for neural controllers due to the presence or absence of muscles or muscle models.

Performance of Controllers

Kinematics As for the restricted middle-leg (cp. section 6.2.1), kinematics of forward stepping was found to be similar to that in the stick insect, especially considering the differences between front-, middle- and hind-legs (cp. e.g. Fig. 3 in Cruse and Bartling 1995 with Fig. 6.1 in this thesis). With one exception differences to observations in biology could be, as in the restricted preparation, explained by differences in parameter tuning and experimental setups: Robust biphasic FTi movements during stance (Cruse and Bartling, 1995) could only be achieved by structural changes in the neural controller (cp. section 6.2.1). A ThC influence on flexion-extension transition resulted in robust walking with biphasic FTi movements during stance but has not been found in the stick insect nervous system. As an alternative a two-phase positive/negative FTi intra-joint velocity feedback termed the "active reaction" (Bässler, 1988) is observed in stick insects and would lead to a stabilized flexion-extension transition during stance. Additionally

muscle properties might play a stabilizing role.

Cycle Periods Regarding minimum step cycle periods the robotic model came much closer to real stick insects when compared with Ekeberg et al. (2004). This was despite the scaling issues discussed above. Depending on parameters step cycle periods of 700ms to several seconds resulted (see Figs. 6.3 and 6.4) compared to 600ms to 2.5s for the stick insect (Fischer et al., 2001). In contrast, Ekeberg et al. (2004) found cycle periods between 6s and 10s. The much lower step frequencies in Ekeberg et al. (2004) were attributed to a slow swing movement caused by the linear muscle model. Unfortunately no exact simulation parameters were given to allow for a better comparison. The shorter cycle periods in the stick insect model presented here (400ms to several seconds, see Figs. 6.10 and 6.11) were, in addition to parameter tuning, due to the lack of force attenuation with length and velocity changes as caused by muscles in the real stick insect. Minimal swing durations were still longer in the robot (350-600 ms) and stick insect (170-340ms) simulations presented here than in the real stick insect (, Graham, 1985; Wendler, 1964). In the robotic model this was partly attributed to the slower actuators and in both models it was attributed to the swing control: Muscle properties limiting FTi extension were lacking and therefore led to prolonged swing phases (cp. discussion above).

Magnitude Control Differing from biological data (Bucher et al., 2003; Cruse et al., 1993; Hess and Büschges, 1997), the height control module was not only active during stance but also during swing phase. Since it did not have exclusive access to the CTr motor neurons reasonable walking behavior was generated nevertheless, including kinematics similar to stick insect data (see above). Additionally a gating mechanism may be introduced, disabling the height control module during swing or dynamically changing the height controls reference input via the CTr premotor neuron. Positive and negative velocity control during stance in the FTi joint (Bartling and Schmitz, 2000; Bässler, 1993) has not been taken into account, because it was not necessary for generating stable walking behavior and made the controller and resulting behavior more complicated to explain. In principle two additional modules are required to add the velocity feedback: 1. an additional comparator module with FTi velocity as input and its output projecting to FTi motor neurons, and 2. an additional threshold element with FTi velocity as input and the comparator as target. The comparator then has to be gated by the FTi premotor neuron, only activating it during flexion (stance) phase.

Changing Behavior by Changing Parameters As an example of behavior control by neural parameters velocity control in the middle-leg was investigated in greater detail. Two different mechanisms influencing walking speed were found (cp. section 6.2.1): The increase in velocity due to a decrease in stance phase duration with nearly constant swing duration and support length was also found in stick insects (Gabriel and Büschges, 2007; Graham, 1972; Graham and Cruse, 1981; Wendler, 1964). This is in contrast to the support length increase found for higher velocities in this study. In cats the same mechanism

was found (Goslow et al., 1973; Halbertsma, 1983), but contrary to the stick insect absolute stance duration could become lower than absolute swing duration. In addition, support length changes contributing to velocity changes were found (Halbertsma, 1983). As an underlying mechanism gain modulated sensory pathways and not purely central tonic influences are suggested in stick insects (Gabriel and Büschges, 2007) as well as in cats (Yakovenko et al., 2005). Functionally this mechanism agrees with the one presented here because stance phase motor neurons were completely deactivated during swing phase due to the bistable premotor elements. Therefore the bias parameters of the stance motor neurons effectively modulated the gain of the sensory influences during stance. With a slightly more complicated structure a parallel gain modulated pathway from sensors to motor neurons could be easily implemented.

The current model failed to control slow velocities below in a robust way because small differences in joint torque would decide between slow movements or no movements. Under noisy conditions or changing environments some kind of an extra velocity feedback mechanism, e.g. a mechanism similar to the active reaction found in stick insects (Bässler, 1993) and/or muscular properties (Guschlbauer et al., 2007), would be required.

For animals or walking machines velocity control cannot be restricted to single legs only, but rather multiple legs have to be coordinated. In stick insects neural coupling of leg velocities have only been found under some circumstances, e.g. in accelerating animals, and mechanical coupling between legs together with muscular properties are discussed as main factors (Gruhn et al., 2009). In Fig. 6.6c (simulated up- and downhill walking) it is shown that the current model could – without any neural parameter changes or central neural influences – adapt its velocity to changing environmental conditions, mainly due to stance phase duration changes. This is beneficial for an efficient mechanical coupling of multiple legs and leg controllers as modules of a hexapod controller.

Controller Robustness In section 6.2.1 the middle-leg controllers were demonstrated to be robust under multiple experimental perturbing conditions (Revzen et al., 2009; von Twickel and Pasemann, 2007) without matching the extreme flexibility exhibited by stick insects (see e.g. Blaesing and Cruse, 2004; Cruse et al., 2004). The latter would only have been possible if hypothetical extensions were made to the controller structure, e.g. to deal with specific reflexes, as is the case with functional modeling approaches (see below for a detailed discussion). Hereafter differences in behavior between the stick insect and robotic model, driven by the presented controllers, are discussed for the various perturbing conditions. On the single leg level one has to differentiate between disturbances occurring during swing and stance phases. In swing phase the leg is mechanically uncoupled from other legs. In stance phase the leg is mechanically coupled to the ground and all legs that are in stance phase at the same time (Bartling and Schmitz, 2000).

In a first simulation (see Fig. 6.6a) ground height was randomly varied relative to body suspension height without disrupting walking behavior. On the one hand this was

consistent with findings by Lewinger et al. (2006) who demonstrated their implementation of the Ekeberg controller to be robust against body height changes and against initial conditions. On the other hand the observed behavior was only partly consistent with behavioral data from the stick insect as shown for the swing phase dependence on take off position in Fig. 6.7. Simulation results were compared with data from Schumm and Cruse (2006) where swing trajectories were examined under varying PEP start positions: Small variations in anterior-posterior AEP positions and a negative correlation of dorsal-ventral swing amplitude and PEP height were consistent although swing height dependence on anterior-posterior and dorsal-ventral PEP positions could not be differentiated. A predominant swing height dependence on PEP height and not on anterior posterior PEP position made sense from the mechanistic point of view: Levation velocity (cp. Fig. 6.7d) mainly determined swing height and was dependent on the CTr height control module. The height control module produced larger levation activations for larger dorsal-ventral torso-tarsus distances but independent of the anterior posterior tarsus position. Nevertheless, a larger influence of FTi(γ)-angle at PEP on swing height for varying anterior-posterior PEPs has to be disproved experimentally. Its potential influence became obvious when investigating the "outliers" regarding swing height for extreme low and high PEPs in Figs. 6.6a and 6.7: Depending on the environmental conditions the FTi(γ)-angle at the beginning of swing could vary quite substantially leading to a variation in the duration of the initial swing phase (PEP–SEP). Two basic strategies could be applied to stabilize swing movements over a larger PEP height range and to achieve a closer match with biological data: First, FTi-movement could be stabilized via e.g. a velocity and/or position servo mechanism or a muscle model to result in less varying FTi-angles at the beginning of stance. Second, swing height could be controlled independently of FTi-angle at PEP via controlling e.g. the extension velocity during swing.

In a second simulation (see Fig. 6.6b) the regular walking pattern was not interrupted and swing trajectories were almost unaffected by lateral force applications ("kicks"). Exceptions were compliant lateral torso and tarsus movements during force application. Since no control module dealing explicitly with disturbances during stance (except the height controller) was contained in the leg controller, this result showed the implicit robustness of the bio-mechanical system together with the sensori-motor control, which does not explicitly control trajectories. More sophisticated reactions resisting or assisting perturbations and maintaining stability despite larger perturbation amplitudes would require extensions to the current controller, like e.g. negative and positive velocity feedback mechanisms found in stick insects (Bartling and Schmitz, 2000) and/or muscle like actuator properties. The observed lateral compliance seems favorable for coupling multiple legs in contrast to a very stiff controlled trajectory.

As shown in Fig. 6.6c robust walking behavior was maintained and locomotion velocity was adapted to different loading conditions, simulating "uphill" and "downhill" walking. This was mainly due to stance duration variations and to a minor extend due to a slightly increased support length (together with a posteriorly shifted PEP) during "downhill" walking. The decrease in velocity with increasing resistance forces was also found in single leg treadmill experiments in stick insects with different levels of belt friction

(of body weight) by Gabriel et al. (2003): Together with an increase in slow and fast motor neuron firing rates forces applied to the treadmill increased while peak velocities decreased with increasing levels of belt friction. In Cruse (1976) stick insects climbing up a vertical path (corresponding to 100% force of body weight against walking direction) AEP and PEP shifted rostrally, in addition to a general increase in stride amplitude. Both were discussed in the context of mechanical and muscular advantages in terms of upwards force production. Rostrally shifted PEPs during uphill walking are consistent with the results presented here as opposed to the AEPs and the support length increase which was observed in the simulation for "downhill" walking. In Foth and Graham (1983) static and velocity dependent loads were applied to the two sides of a split treadwheel separately with load amplitudes between 12.5% and 100% of body weight. In addition to the findings of Cruse (1976) it was found that forces up to of body weight per side (corresponding to 20% in wave gait and 40% in tripod gait) were compensated by raises in muscle forces. Above force of body weight, protraction duration was reduced to a minimum and became independent of step period, and retraction duration increased with increases in load. Dean (1991) applied different levels of static force (0.5–4 time body weight) assisting or resisting forward walking. In addition to the above mentioned studies he found swing duration increases for larger resisting loads. Furthermore he put forth the hypothesis that the retractor relaxation after strong stances is slower and therefore leads to slower and longer swing movements. When comparing the presented experiments with stick insect data it is important to consider that most experiments have been performed with multiple legs and at non-maximal locomotion speed. Here walking speed was close to maximum and only a single leg was active. For a more detailed comparison with biological data, our model should first be extended by muscular properties and/or load and velocity feedback control mechanisms, and then load adaptations under different velocities should be tested.

Robust stepping up to noise levels of on all motor neuron outputs or up to on all sensor-neuron inputs (cp. Figs. 6.6d and e) is qualitatively comparable to the experiments by Ekeberg et al. (2004): They showed that the original controller is robust (in the sense of qualitatively preserved behavior) against single random variations of threshold angles in a range of +/- ° and of muscle activation values of +/- . Kindermann (2002) obtained similar sensor noise tolerances (, depending on conditions) for a simulated hexapod but did not test motor noise tolerance. These noise tolerance tests can be seen as a rough sensitivity analysis. Motor- and bio-mechanical systems show to have a higher tolerance against noise than the neural system deriving the joint activation states from sensor inputs. We attribute this to the low pass filter characteristics of the mechanical system being much stronger than those of the joint state switching elements of the neural system. These are, in the neural implementation, realized as hysteresis elements. Including realistic muscle models, which have activation functions with strong low pass filter characteristics as in the stick insect (Hooper et al., 2007), should even increase the noise tolerance of the bio-mechanical system.

Body Support Forces For both vertical and medio-lateral body support forces (cp. section 6.2.4) it was found that force profiles could be altered by tuning "free" neural parameters, i.e. parameters not prescribed by the neural rules. By additionally tuning e.g. threshold parameters force profiles could be altered even more, also changing kinematics. This demonstrated the controllers flexibility to adapt to different body support requirements.

For vertical forces it was shown that force profiles of optimized controllers, with kinematics similar to the one found in biology, resulted in similar force profiles (Bartling and Schmitz, 2000; Cruse, 1976). Body support forces could be much higher for hind-legs than for middle- and front-legs. This is consistent with the requirement in the stick insect that hind-legs have to carry most of the body weight because their center of mass is located between them (Cruse, 1976). In Bartling and Schmitz (2000) vertical front-leg forces were found to be so weak that they could not be reliably used as a trigger signal. In contrast to the results shown here and in Cruse (1976) the same study found vertical forces of the middle-leg to be slightly larger than in hind-legs. In contrast to stick insects, front-legs of cockroaches have comparable vertical ground-reaction forces as middle- and hind-legs (Full et al., 1991). This in turn means that walking machines and animals with a different mass distribution might require different force profiles and possibly also different leg kinematics. Additionally the differences in joint axes setup when compared to the stick insect, especially slanted ThC joint axes in the ThC joint of the stick insect (Cruse and Bartling, 1995), might have a significant influence on the ground reaction forces during stance.

A lack of lateral directed body forces in parameter optimized controllers is again comparable to biological data, with the exception of the front-leg where lateral forces are negligible (Bartling and Schmitz, 2000; Cruse, 1976). In animals and robots it has been shown that medial directed forces from legs to the body are important to laterally stabilize posture and walking behavior (Dickinson et al., 2000; Komsuoglu et al., 2009).

In general different force profiles by the three leg types reflect their specialization, e.g. for pushing, pulling and generating brake forces (see e.g. Full et al., 1991; Graham, 1983). Further issues like force coordination between legs have to be investigated in the context of hexapod walking, e.g. the force coordination problem between legs (Lévy and Cruse, 2008).

Comparison with Existing Controllers First of all it has to be noted that the presented controllers share many structural and functional similarities with other walking controller models of stick insects, cats and humans. Similarities include the modular organization and the strong role of sensory feedback in timing (e.g. swing-stance and stance-swing transitions) and in magnitude control (e.g. negative feedback control of body height). These aspects have been discussed at length before (s. e.g. Büschges, 2005; Dürr et al., 2004; Ekeberg et al., 2004; Pearson et al., 2006). In the following, we will therefore focus our discussion on a different aspect. Two basic approaches appear to be used to derive walking controllers from biological data (Cruse et al., 2007): The "morphological" approach, as taken in Ekeberg et al. (2004) and in the study presented here,

incrementally builds up a controller from available neuro-biological data and information about the bio-mechanical system. Subsequently it compares its behavior with that of the natural counterpart. In contrast, the "functional" approach builds up controllers with the primary goal to match behavioral data, not focusing on direct correlations with the neural substrate of the stick insect.

The latter approach has been pursued by Cruse and coworkers over the last two decades resulting in multiple iterations of the WALKNET controller (see e.g. Cruse et al., 2004, 2007; Dürr, 2001; Kindermann, 2002; Schumm and Cruse, 2006). WALKNET constitutes a distributed controller which heavily depends on sensory feedback, whereby the (partly positive) feedback is mainly of proprioceptive nature. WALKNET describes, to an extent unmatched by other approaches, the behavioral repertoire of the six-legged stick insect. In addition to its advantages, three main problems of the current WALKNET implementation were identified: 1. As a principle problem of the functional approach the correlation of model controller structure with biological controller structure is difficult. From a theoretical point of view (Negrello et al., 2008) one and the same functionality may be produced by an arbitrary number of control structures and therefore WALKNET is only one of many possible controller structures able to produce the stick insect behavior. 2. WALKNET was developed in a kinematic simulation and therefore does not incorporate load information (but see Schilling et al. (2007) for such an extension) or detailed muscle properties. 3. In contrast to its mostly distributed structure it uses a leg global swing-stance selector net. By now no neuro-biological evidence has been presented that different neural controllers for stance and swing exist. All neuronal elements analyzed so far affect the motor output during both stance and swing phase (Büschges et al., 1994; von Uckermann and Büschges, 2009; Wolf and Büschges, 1995).

The "morphological" approach taken here addresses these three problems whereby the possibility of controller structure correlation is self-evident. Load information and muscle properties have already been implemented in the dynamic simulation presented here (see also section 6.2.4) and their influence on controller performance will be subject of a forthcoming publication. Concerning the "swing-stance selector net" a completely decentralized solution was employed: Only one structure existed for the control of both swing and stance and each joint locally decided about its movement phase. Each joint possessed a bistable premotor element with hysteresis properties that held the desired movement direction, e.g. levation or depression for the CTr joint. The desired direction could be overridden by parallel inputs to the motor neurons as was e.g. the case for the height controller in the CTr joint. Although this solution appears to be more elegant, it has yet to be demonstrated how more complex behaviors like different disturbance reflexes may work without a central selector network. We argue that the decision between swing and stance is an emergent property of the neuro-mechanical system, and locally this decision is deduced from multiple sensor- and neural-inputs.

When compared to the WALKNET controller the "morphological" controller presented here had some shortcomings: First of all discrepancies existed between the behavior produced by the single-leg controller on the one hand and that produced by the stick insect on the other hand (see discussion and results above). Then the neural data available

is not yet sufficient to build up a hexapod walking controller or controllers producing similarly complex behaviors as WALKNET. First steps have been taken on the neuro-biological side (Borgmann et al., 2009) and on the modeling side (Daun-Gruhn, 2010) towards a hexapod controller based on neuro-biological data. Further experiments will have to show if the current single leg controller structure is sufficient to act as a leg control module of a hexapod controller or if non-trivial extensions are necessary. Furthermore, the approach taken here employed different controller structures for front- and middle-legs on the one hand and hind-legs on the other hand. In contrast, WALKNET is able to produce the different behaviors by the same controller structure but using different parameter sets. The latter approach simplifies a modular implementation on robots but its neuro-biological relevance has yet to be shown. Theoretically even controllers with identical structures and parameters could achieve a similar functional diversity by just differing in biomechanics, sensory inputs or coupling influences.

In a complementary approach to the two basic biological modeling approaches the artificial life approach to evolutionary robotics is employed to derive minimal controllers, producing walking behaviors similar to that of the stick insects (see e.g. Linder, 2005; von Twickel and Pasemann, 2007). Comparing the controller structure presented here with the ones found in von Twickel and Pasemann (2007), containing e.g. only four synapses, the question arises of why a larger controller structure is needed at all. To one part this is due to the latter study working with single neuron servo interfaces, already including intra-joint sensory feedback and not requiring premotor neurons for antagonistic activations. To another part the advantage might be increased redundancy and therefore increased robustness against failures. Otherwise the advantage of a more complicated structure is not obvious and one will have to compare these different controller types in detail on single legs and as modules for hexapod controllers.

Bio-Inspired Single Leg Control A step-by-step method for deriving a neural network model from neuro-biological data via an intermediate finite state model was presented. Properties of single front-, middle- and hind-leg controllers were demonstrated including their robustness under multiple experimental perturbations, their flexibility in terms of body support forces, and feasible behavior modifications by parameter tuning. The modular structure of the controller allows for easy extendability, and its neural network implementation will simplify their transfer to walking machines. Taken together, the robustness and flexibility of the described controllers make them promising bootstrap modules for future evolutionary coupling experiments. Therefore this study is seen as a step towards the integration of behavioral and neural based approaches to locomotion control, and – on the other hand – as a first step towards the derivation of robust hexapod controllers for walking machines.

7. Implications of Muscle-Model Properties for the Neural Control of Single-Leg Stepping

The notions of morphological computation, embodiment and situatedness (Chiel and Beer, 1997; Paul, 2006; Pfeifer and Gómez, 2009, , cp. also chapter 1) imply two important hypotheses: on the one hand, nervous system may not be viewed independently from body and environment and, on the other hand, biological organisms and robots may profit from computations external to the nervous system, e.g. by a reduction of the required neural control complexity. In biological motor systems, muscles play a major role in movement generation and many studies have demonstrated their beneficial effects in robust behavior control. The widely used terms "preflex" (Loeb et al., 1999) and "self-stability" (Blickhan et al., 2007) illustrate that muscles may perform tasks similar to those traditionally ascribed to the nervous system, namely reflexes and stabilizing control mechanisms.

Whereas detailed experimental data is available for the performance of single isolated muscles in many species (cp. e.g., Guschlbauer et al., 2007, for the stick insect), data on the performance of single and multiple interacting muscles in natural movements, such as locomotion, and their interplay with the neural control system is more sparse, due to the complexity of the bio-mechanical systems and the required experimental approaches (Alexander, 1992; Anderson et al., 2006). Therefore, computer simulations, investigating the role of muscles in locomotion, have a long standing tradition, especially for humans (see e.g. Anderson et al., 2006; Audu and Davy, 1985; Chow and Jacobson, 1971; Taga, 1995; Zajac, 1993), but also for other species like cats (Ekeberg and Pearson, 2005; Yakovenko et al., 2004) and insects (Ekeberg et al., 2004; Jindrich and Full, 2002; Zakotnik et al., 2006).

In robotics and prosthetics the potential benefit of muscle properties in motor control has been recognized (Buehrmann and Paolo, 2006; Herr and Kornbluh, 2004; Siciliano and Khatib, 2008), especially in bio-robotics (Ritzmann et al., 2000). On the one hand, real biological tissue is seldom employed as robotic actuator (Dennis and Herr, 2005) and artificial muscles with characteristics of biological muscles are still not commercially available (also compare chapter 1). On the other hand, standard DC-motors are combined with alternative transmission devices (Iida et al., 2009; Marques et al., 2010; Schneider et al., 2006; Suzuki, 2007) or alternative control interfaces (Serhan et al., 2010; Seyfarth et al., 2007) to emulate properties of biological muscles.

In this chapter a muscle model derived from the stick insect extensor tibiae muscle (Blümel et al., 2011b; Guschlbauer et al., 2007, , cp. also chapter 4) was applied to the

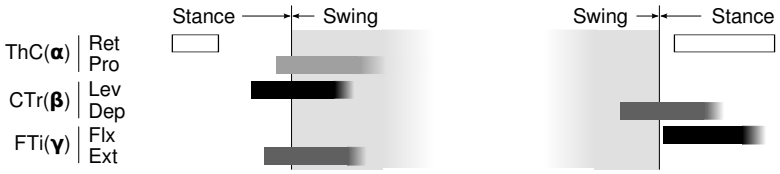

Figure 7.1.: Schematics of middle-leg muscle activations relative to swing-stance and stance-swing transitions during stick insect walking on a slippery surface. Swing-phase muscles, i.e. protractor and extensor, become active before the foot looses ground contact. Stance-phase muscles, i.e. retractor and flexor, become active only after ground contact is established. Adapted from Fig. 11 from Rosenbaum et al. (2010)

Octavio robot and stick insect simulations (cp. chapter 4) to answer the following question: How do constraints and opportunities change for the neural control of single-leg stepping if a muscle model layer, or a subset of its components, is employed antagonistically for all joints when compared to a pure antagonistic control without muscle model layer? In chapter 6 it was found that both robot and stick insect single leg controllers required additional intra-joint feedback to achieve robust stepping without muscle models. May this be replaced by muscle models? A previous study using a robotic model of a single stick insect leg, investigating the effects of a simple linear muscle model, by Rutter et al. (2007) suggests this. In contrast, in a prior simulation study by Ekeberg et al. (2004) a simple linear muscle model was found do be insufficient to replicate the short swing and stance durations found in real stick insects. Furthermore, in Hooper et al. (2007) it is suggested that stick insect muscles act as very slow filters with time constants between 200-700ms. How does this fit with the fact that stick insects are able to perform very short swing movements (100ms Graham, 1985; Wendler, 1964) with robust stance-swing and swing-stance transitions? Data presented by Rosenbaum et al. (2010) suggests a possible solution (cp. Fig. 7.1): muscles are activated and deactivated in advance to stance-swing transitions. But how are the muscle activations coordinated by central control mechanisms or sensory signals?

7.1. Approach

To answer the above questions, the parameters of a set of different neural controller structures (cp. Fig. 7.2) were tuned to control single-leg walking (cp. section 4.1.1) of robotic (cp. section 4.2.2), and stick insect walkers (cp. section 4.2.3) with and without an intermediate muscle model layer. Subsequently their performance was compared under flat terrain and different perturbing conditions (cp. Fig. 4.9 for an overview). As muscle model a neural network was tuned to replicate the input-output characteristics of the stick insect extensor tibia muscle and two differently scaled versions were used for each joint (cp. section 4.1.4 for details). To elucidate the role of the individual sub-components of the muscle model, namely its passive and active torque-angle characteristics, its torque-velocity characteristics, its torque activation characteristics and its activation function, any combination of muscle model components could be deactivated.

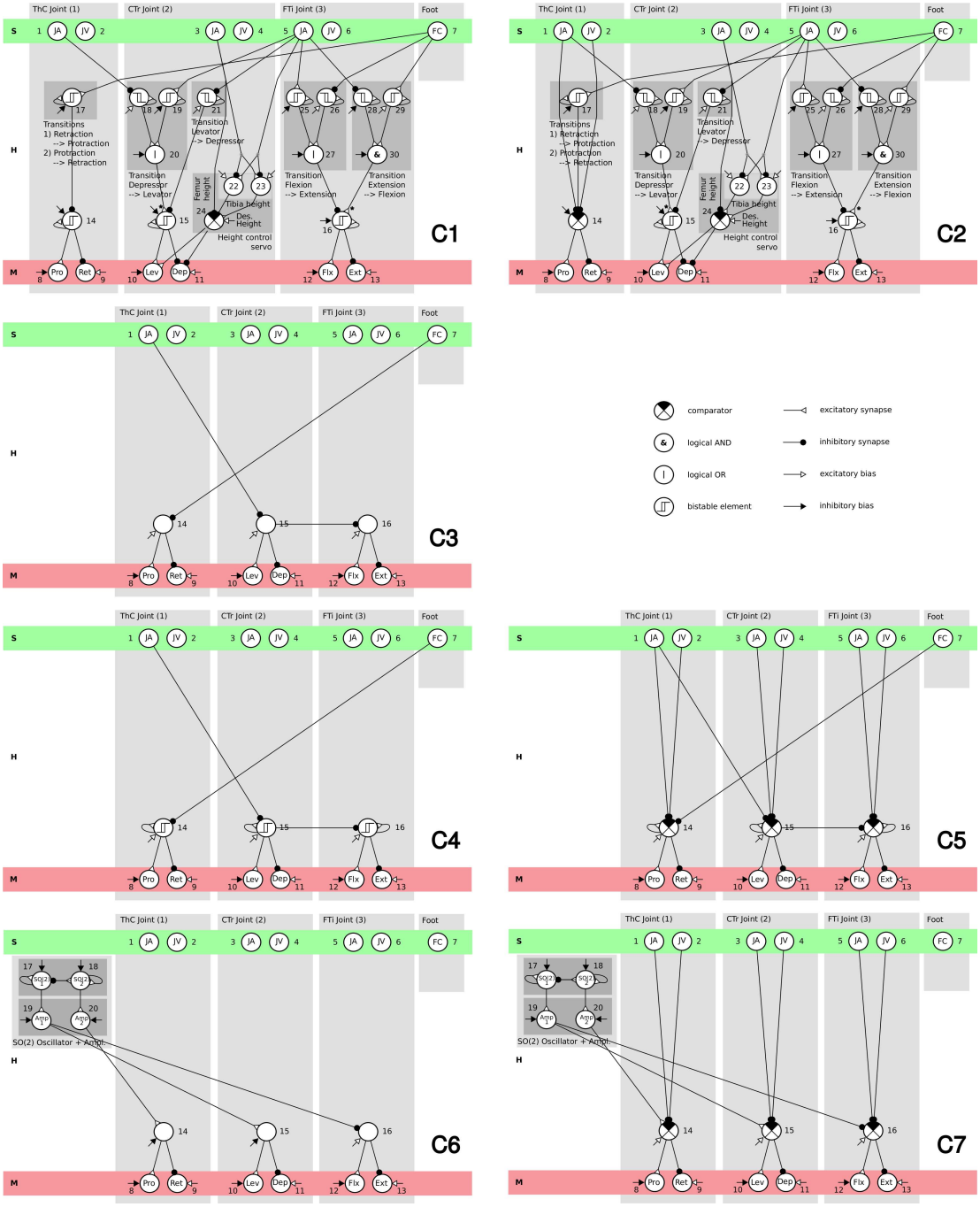

Figure 7.2.: Neural networks that were used to compare the behavioral performance of agents with and without muscle models. On the left side controllers are depicted that do not possess any explicit joint servo mechanism, whereas controllers on the right side are extended by neural joint servo controllers. The neuro-controllers comprise multiple hand-constructed controllers whereby controllers C1-2 were derived from biology (cp. von Twickel et al., 2011), C3-5 were derived from evolved neuro-controllers (cp. section 5, von Twickel and Pasemann (2007)) and controllers C6-7 employ simple 2-neuron oscillators (Pasemann et al., 2003)

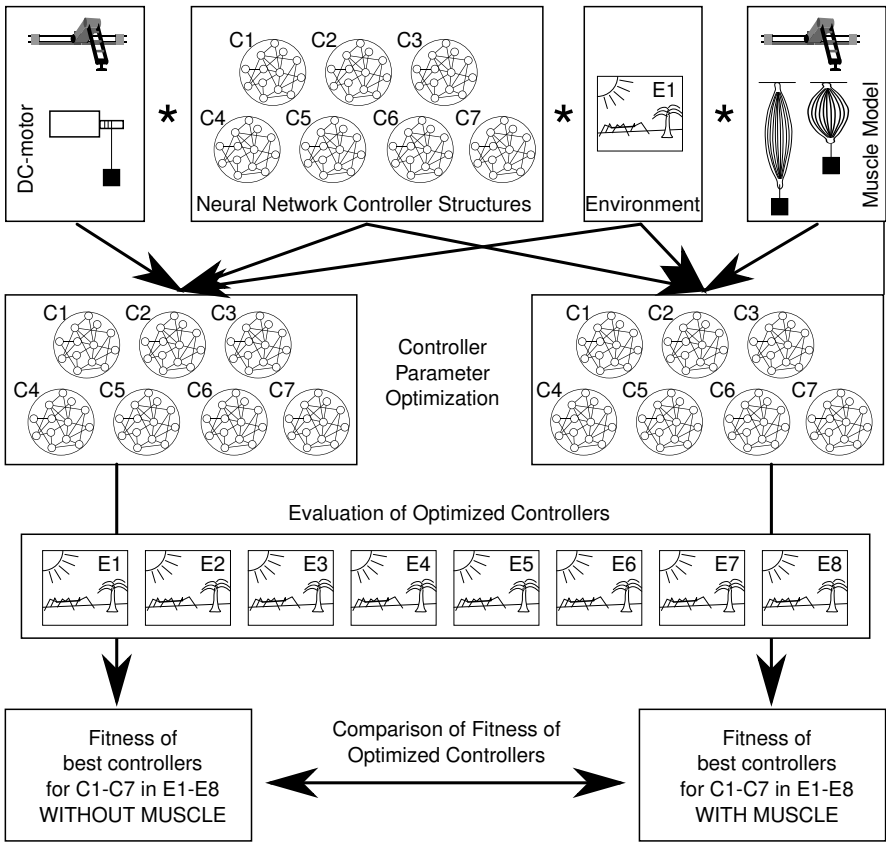

Figure 7.3.: Schematics of robustness comparison test for single leg walkers with and without muscle model. For each walker, with and without muscle model, seven distinct controller structures (C1-C7, cp. Fig. 7.2) are repeatedly optimized in a standard environment (E1). Afterwards the performances of the walkers with and without muscle model driven by the optimized controllers in eight different environmental and perturbation scenarios (E1–E8, cp. Fig. 4.9), including the standard environment, are compared

The controller test set (C1-C7) is depicted in Fig. 7.2: biologically inspired controllers (C1-C2, cp. chapter 6 and Ekeberg et al. (2004)), simple reflex-oscillators (C3-C5, cp. chapter 5 and Schumacher (2008)) and central oscillators without any sensory feedback (C6-C7, cp. chapter 5 and Benner (2008)) were used. Each of these controllers was tested with and without simple neural joint position servo-controllers, e.g. with and without explicit neural intra-joint sensory feedback. The reflex oscillator controller was additionally tested with and without self-couplings of the motor neurons which could potentially adjust time-delays and, therefore, inter-joint phase shifts (cp. chapter 5 for details).

On the one hand, neural controller parameters were tuned by hand to achieve a maximal performance with the given combination of simulator and muscle model under flat terrain conditions. To remove the subjective bias of hand tuning, the different controllers were also optimized by parameter evolution (cp. section 3.3) under standard

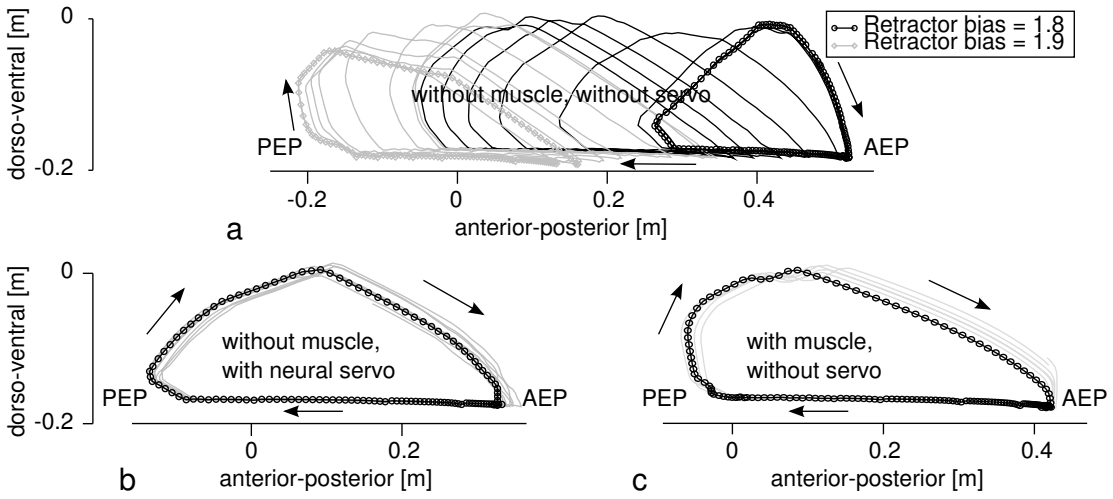

Figure 7.4.: Foot trajectories for different controller-body configurations: **a** Without a neural servo for the ThC joint the neuro-biologically inspired controller C1 is not able to maintain a stable walking trajectory when driving a single robotic leg without an intermediate muscle layer. To achieve a stable walking trajectory, either **b** additional ThC intra-joint feedback (here realized as a neural servo, C2, cp. chapter 6) or **c** an intermediate muscle layer is sufficient

environmental conditions (simple plane, cp. Fig. 4.9), once with muscle model and once without. The fitness function that was used is given in section 3.3.4. No synapses and/or neurons could be added or deleted. After 150 generations (population size 40), whereby each evaluation had a duration of 2000 time steps, the best individual of each evolution was tested under all 8 environmental conditions given in Fig. 4.9. This test was repeated for n=20 times and all single try fitness values were recorded. Afterwards mean values and standard deviations for all tests of specific individual-environment combinations were calculated to answer the question if a muscle model would make walking behaviors with given body-control combinations more robust. An overview of the method is given in Fig. 7.3.

Finally, for the stick insect model, the extended version of the biologically inspired controller (cp. Fig. 3.12) was parameter tuned. With and without using an intermediate muscle layer, or sub-components thereof, the goal was to match biologically realistic swing- and stance durations, as well as biologically realistic foot trajectories. If this was not possible by solely tuning parameters, extensions of the controller model were tested as well to hypothesize what kind of neural mechanisms could deal well with the constraints imposed by the muscle properties.

7.2. Robotic Model

7.2.1. Working Range Stabilization

In chapter 6 it was demonstrated that the neuro-biologically inspired controller C1 was not able to control robust forward stepping in a robotic model without muscle model.

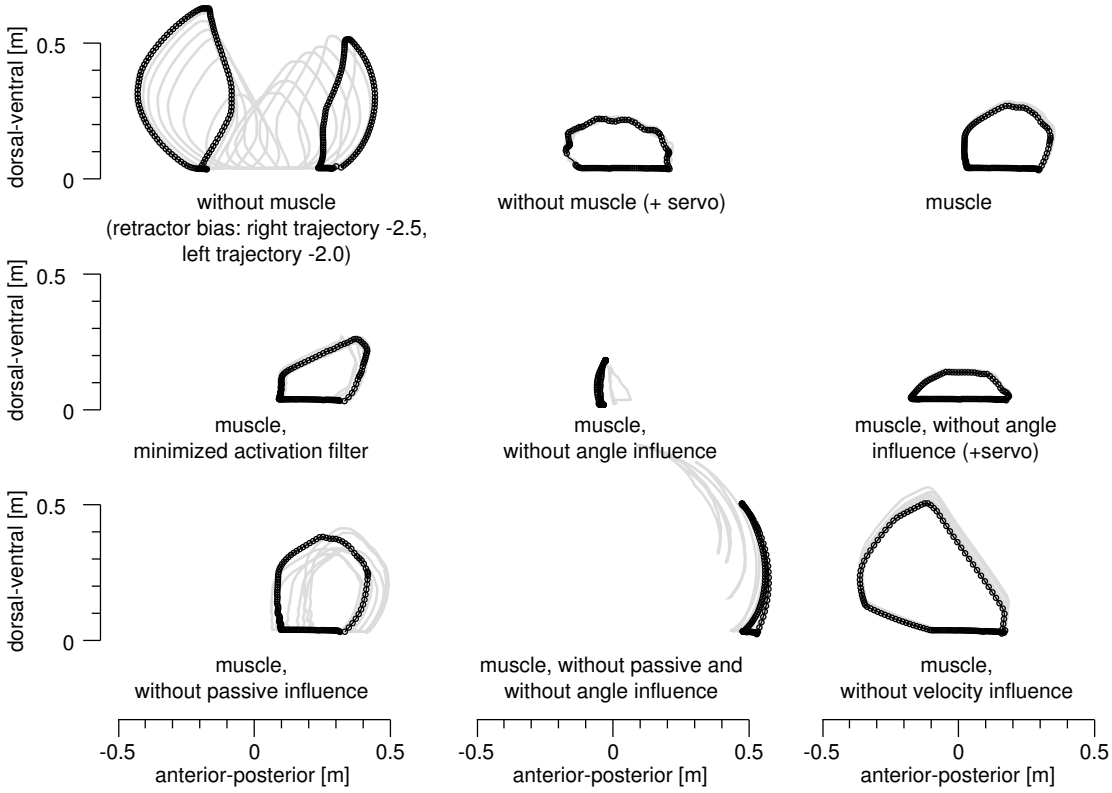

Figure 7.5.: The effect of using a muscle model, or different subsets of its components, on the forward walking foot trajectory controlled by a simple central oscillator (C6, C7) is depicted. As a crucial muscle model component the torque-angle characteristics was identified. Other muscle model components influence the trajectories stability and shape, but do not disrupt it. Foot trajectories for a 10s time period are displayed in gray and single step trajectories are given in black with additional markers for each time step

Only depending on subtle neural parameter changes, foot trajectories would diverge either to the anterior or posterior extreme positions of the ThC joint. Effectively either the anterior or posterior joint stops constrained this shift and stable anterior or posterior stepping resulted. To achieve stable walking trajectories without hitting the joint stops, additional ThC intra-joint feedback was required, resulting in controller C2. Here it is shown in comparison (Fig. 7.4) that stable forward walking may be achieved without any neural ThC intra-joint feedback, i.e. with the original controller C1, when an intermediate muscle model layer is employed. Therefore, the muscle model stabilizes the working range of the ThC joint despite a reduced controller complexity.

To investigate the effect of a working range stabilization via the muscle model in more detail, further experiments were carried out with a much simpler controller: a single central pattern generator (CPG) with a frequency of 0.8 Hz was used to drive all three joints without employing any sensory feedback, effectively resulting in a pure feed-forward controller. The controllers ability to robustly drive single robotic legs with and

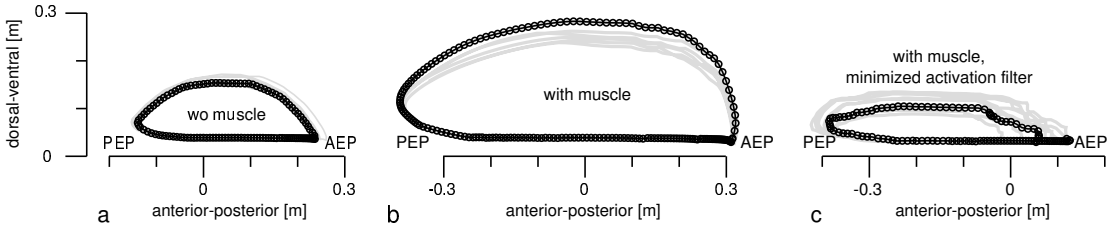

Figure 7.6.: The simplest controller tested (C3, reflex oscillator without any neural feedback, cp. chapter 5) can produce larger movement amplitudes and slower oscillations while driving **b** a simulated single robotic leg with muscle models when compared to **a** one without muscles or to **c** one with muscles but minimized low pass filters characteristics. Foot trajectories for a 10s time period are displayed in gray and single step trajectories are given in black with additional markers for each time step

without muscle models, or subsets thereof, was tested without (C6) and with additional intra-joint sensory feedback (C7). In Fig. 7.5 resulting foot trajectories are depicted: without a muscle model, foot trajectories diverge from the desired trajectory. In contrast to the neuro-biologically inspired controller (cp. Fig. 7.4), divergence takes place not only for the ThC joint but also for the CTr joint, resulting in very high swings and short stance phases as well as in either anterior or posterior stepping at the respective joint stops. As demonstrated in the same figure, additional neural servos or muscle model pairs for all joints allow a stable walking trajectory to be controlled by the simple oscillator. To determine which feature of the muscle model was responsible for the working range stabilization, subsets of the muscle model components were deactivated. Whereas the deactivation of the activation filter, the passive torque or the torque-velocity components had non-disruptive effects, a removal of the torque-angle component led to disturbed walking trajectories, which could be restored by the introduction of additional neural servo control for each joint. Removal of the passive torque component led to slightly more jittery and enlarged trajectories, removal of the activation filter to a slightly changed foot trajectory shape (but not total size) and a removal of the torque-velocity influence to enlarged foot trajectories.

7.2.2. Effect on Step Amplitude and Frequency

In the example above the step frequency was given by the neural oscillator. To determine the effect of the muscle model on the step frequency of a single leg, an extremely simple controller based on a reflex oscillator without any neural feedback was used (C3, cp. chapter 5). As depicted in Fig. 7.6, the controller produced larger movement amplitudes together with a muscle model and this was found to be due to the low pass filter characteristics of the muscles activation function. Without the low pass filter properties the movement amplitude was smaller and comparable to that without any muscle model. Step frequencies averaged across 10s were 0.85Hz without muscles, 0.87Hz with muscles but minimized activation filter and 0.56 Hz with complete muscles, i.e. the muscles with low pass filter properties decreased the step frequency and increased the step amplitude.

7.2.3. Robustness Against Neural Noise

In chapter 6 it was hypothesized that the noise robustness of the neuro-biologically inspired controller C2, using a neural ThC servo, could also be achieved or even surpassed when employing the same controller without a neural ThC servo on top of a simulated leg with muscle models. In the following, results with different muscle model configurations, that were tested under 2%, 48% and 64% gaussian noise on all motor neuron outputs, are presented. First results for the simplified restricted stepping case are presented because it was found (cp. chapter 6) that no extra intra-joint feedback was needed for stable stepping. It only employed the two DOFs of CTr and FTi joints. Subsequently the results for forward stepping, using all 3DOFs, are given.

Restricted (Sidewards) Stepping With only 2% gaussian noise on the motor neuron outputs, the restricted controller C2 with a neurally fixated ThC joint (cp. Fig. 3.11 b) produced stable stepping with any muscle model configuration, including the null muscle model. Without muscle model or with a minimized low pass filter activation property, trajectories became smaller, as found for the simple reflex controller above (cp. Fig. 7.6). With increasing noise levels (48% and 64%) the movement trajectories strongly decreased in amplitude for the null muscle model and for the muscle model with minimized low pass properties, up to the point where no effective lateral body movement results. All other muscle model configuration produced stable stepping with an amplitude comparable to the situation with only 2% noise. Therefore, the low pass filter properties of the muscle model's activation function seemed to play a prime role in increasing the noise robustness of the neuro-mechanical system.

The effect of the low pass filter properties of the activation function is underlined in Fig. 7.8 where the FTi motor neuron outputs of the controller network and the resulting FTi joint torques are compared for the cases with and without muscle model. At a noise level of 64% on all motor neuron outputs, the system with muscle model displayed much smaller noise levels on the joint torque output level. The noise reduction took place at the muscle level because the outputs of the antagonist muscle showed a low-noise output, resulting in a relatively smooth activation of the DC-motor (cp. Fig. 4.3 for a detailed description of the DC-motor activation mechanism). The motor basically switched between flexion (mode 1) during stance and extension (mode 2) during swing. Due to the remaining noise during swing the motor additionally switched into brake mode from time to time but not to a reversal of movement direction. This was different in the case without muscle model layer: during each swing and stance phase the motor could be switched to any of the four possible modes. Together with the very noisy motor activation, this lead to the jittery joint torques. Using the muscle model with a minimized low pass filter lead to comparable results as using no muscle model (data not shown).

Forward Stepping To verify that the muscle model's stabilizing effect under high motor neuron noise also holds for the interaction of all three leg joints, the experiment from above was repeated for standard forward stepping. The results are depicted in

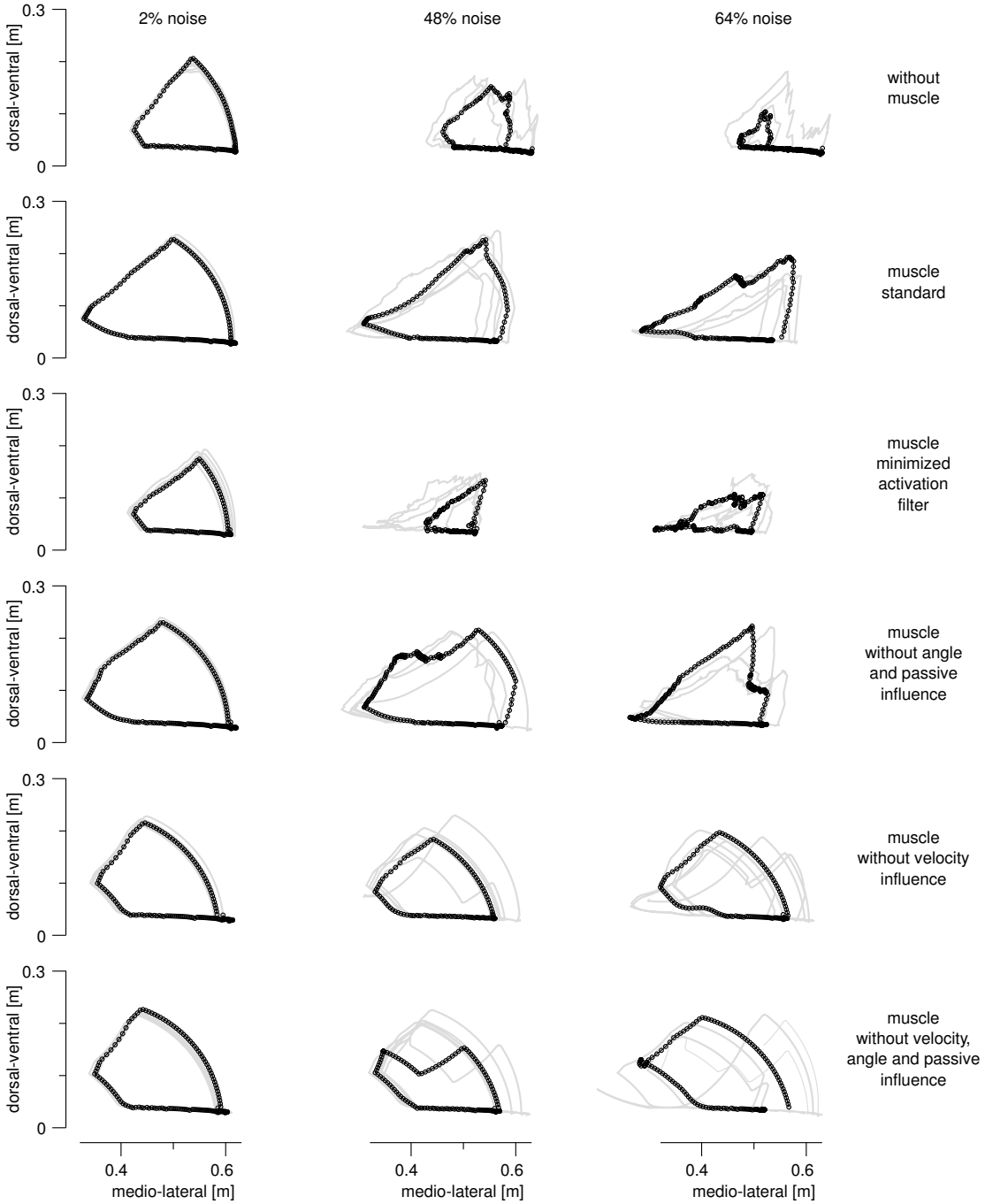

Figure 7.7.: Foot trajectories produced by the restricted neuro-biologically inspired controller (cp. Fig. 3.11 b) together with different muscle model configurations are shown under three motor neuron noise levels. The role of the low pass filter property of the muscle model's activation function in increasing the systems noise tolerance is demonstrated. Foot trajectories for a 10s time period are displayed in gray and single step trajectories are given in black with additional markers for each time step

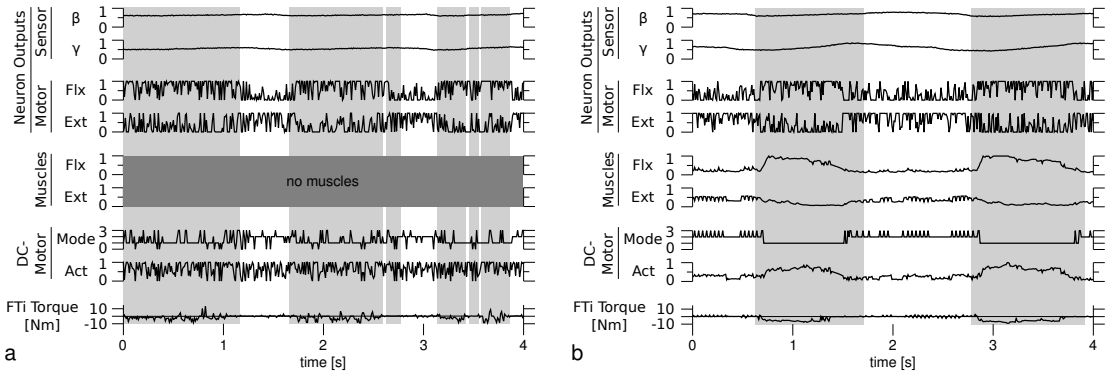

Figure 7.8.: Data on the neuro-motor-output transform is shown for motor neuron noise levels of 64% (gaussian noise), focusing on the FTi joint. Controller C2 was configured to control restricted sidewards stepping **a** without and **b** with muscle models. It is obvious that the muscle model significantly reduced noise levels during this transform and led to regular stepping compared to the irregular stepping without muscle model

Fig. 7.9: As for the sidewards stepping case, all configurations produced robust stepping movements for noise levels up to 64%, except those without muscle models or with minimized low pass filter properties. E.g. for a motor neuron noise level of 48% the standard muscle configuration led to a step period of 1.7s whereas the null muscle configuration led to a step period of 2.8s. At the same time the working rang stabilization discussed in detail in section 7.2.1 could be observed. The mechanism of noise reduction was identical to the one shown in Fig. 7.8 (data not shown). In contrast to the restricted stepping case the impact of increased noise on the different muscle model configurations becomes more pronounced: movement amplitudes are reduced and trajectories become more jittery. When the torque-velocity characteristics was disabled, movement trajectories were slightly larger. Furthermore, minimized low pass filter properties already led to smaller and more irregular movement trajectories with only 2% motor neuron noise.

7.2.4. Robustness Against Perturbations

To remove the possible bias of the experimenter when hand tuning parameters for the networks before comparison, a computational parameter optimization method was applied. The basic idea was to parameter optimize all controller structures from Fig. 7.2 (C1-C7) to walk as fast as possible, while minimizing foot sliding and the swing-stance ratio in a flat terrain environment without additional perturbations. Subsequently the best controller for each controller-muscle combination was evaluated in 7 perturbing conditions. Finally the performance between those trials with and without muscle models was compared. This method followed the evolutionary robotics approach, please see section 7.1 and Fig. 7.3 for details. In Fig. 7.10 results of this experiment are given for every controller-muscle-environment combination. Since the perturbing experiments were partly randomized the controllers fitness could fluctuate. Therefore, for each combination the evaluation was repeated 20 times and in the figure the averages and the

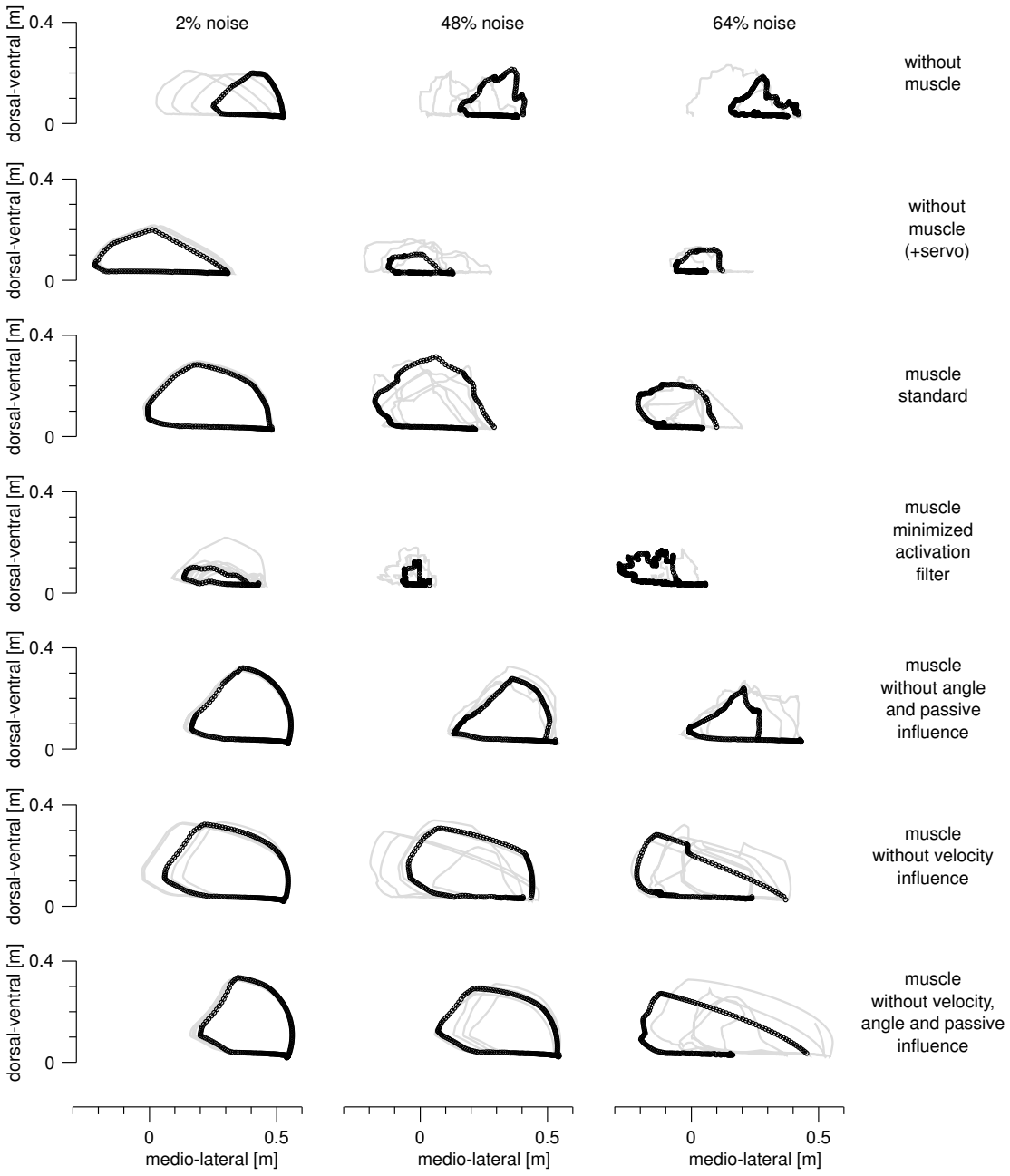

Figure 7.9.: Foot trajectories produced by the neuro-biologically inspired controller C1 and C2 (with and without neural ThC servo), together with different muscle model configurations, are shown under three motor neuron noise levels. The role of the low pass filter property of the muscle model's activation function in establishing stable walking trajectories and in increasing the systems noise robustness is demonstrated. Foot trajectories for a 10s time period are displayed in gray and single step trajectories are given in black with additional markers for each time step

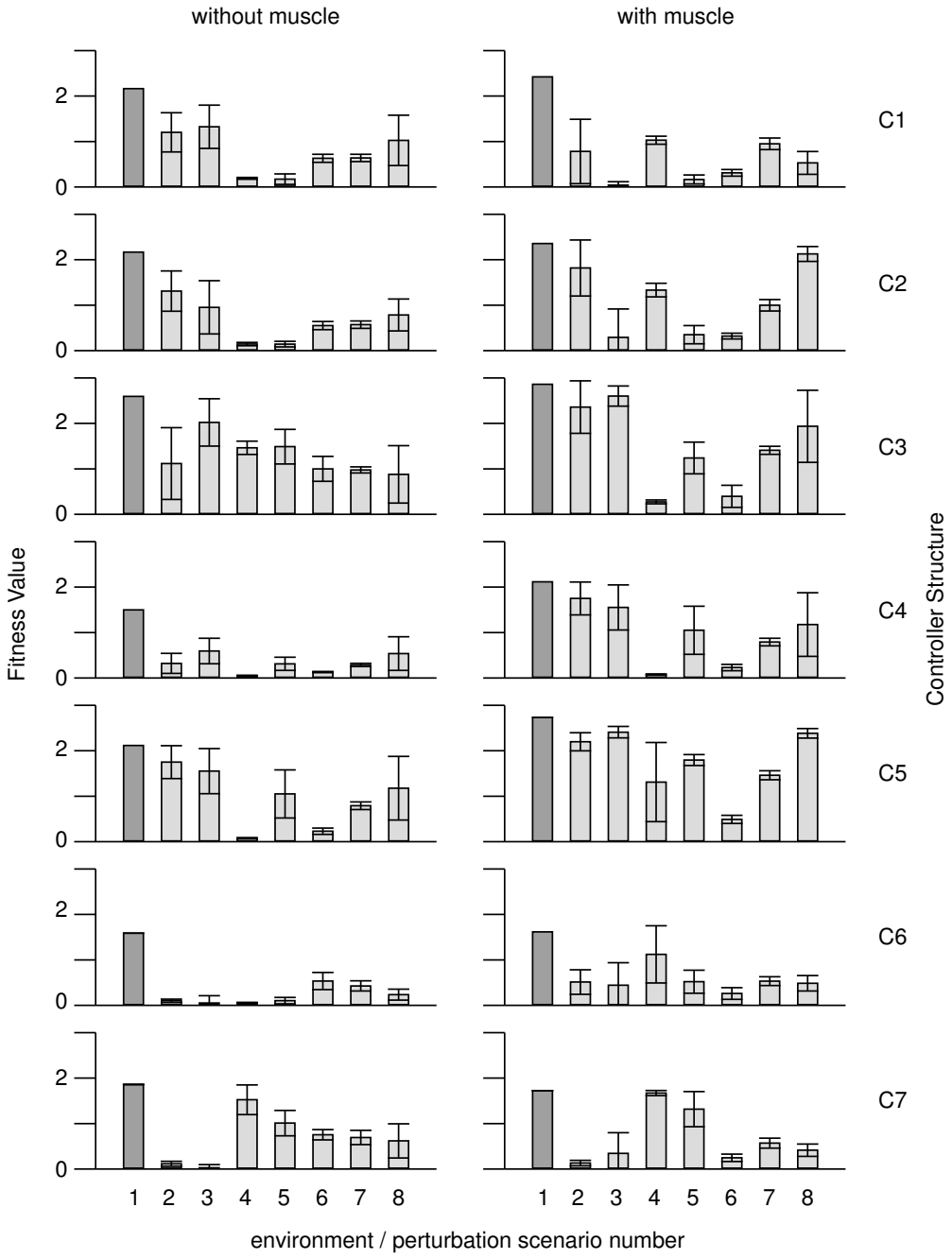

Figure 7.10.: Using the method depicted in Fig. 7.3, multiple controllers (C1-C7, cp. Fig. 7.2) were parameter-optimized for one standard environmental condition (E1), once with muscle model, once without. Evaluating the fitness of these optimized controllers under multiple perturbing conditions (E1-E8, cp. Fig. 4.9) shows an increased robustness when using the muscle model. Controllers were optimized for 150 generations with a population size of 40 and for 2000 time steps (20.0s). For each controller type the individual with the highest fitness during optimization was evaluated. For details see section 7.1

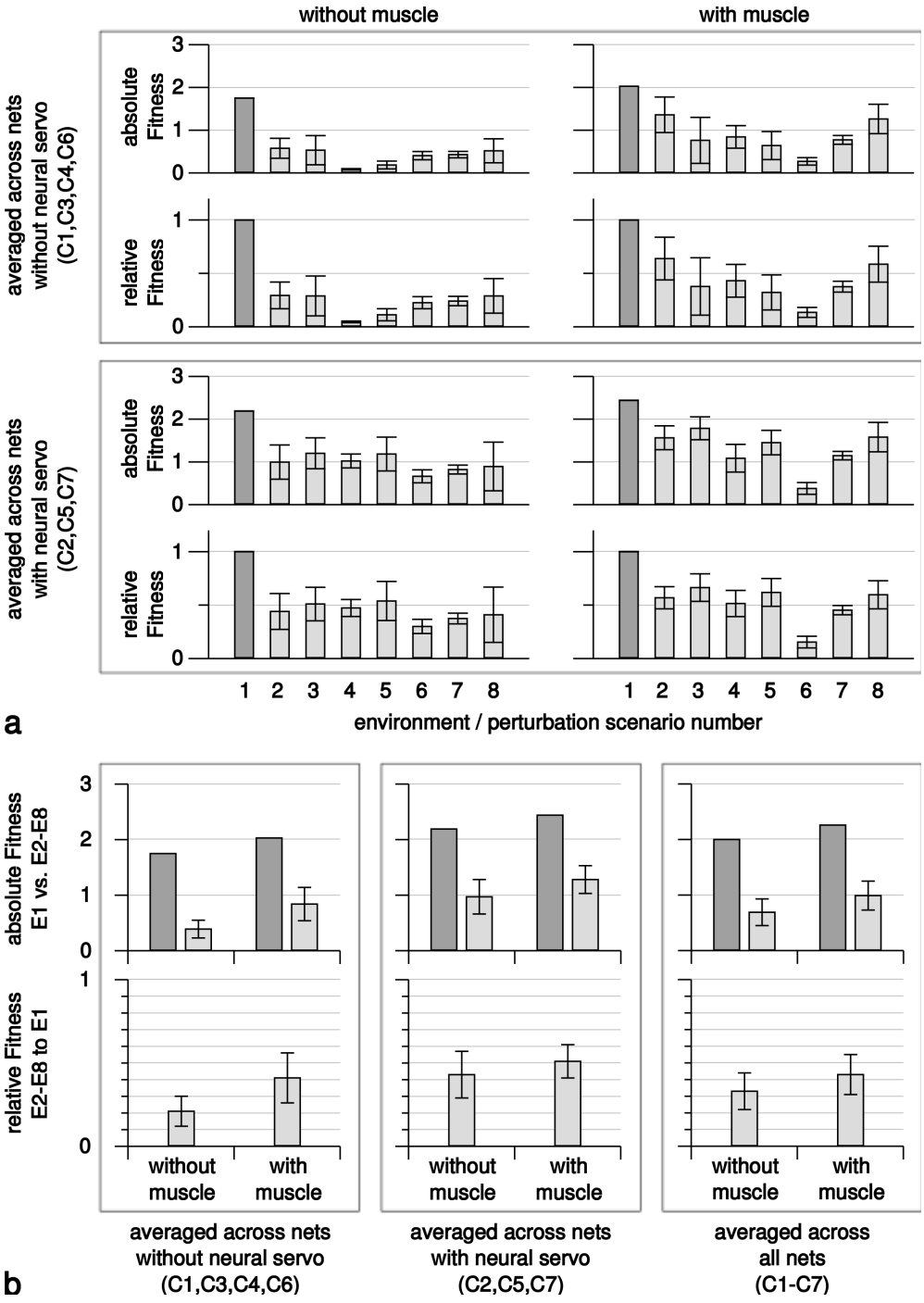

Figure 7.11.: The data from the previous Fig. 7.10 was averaged **a** across all networks without (top) and with (bottom) extra intra-joint feedback, realized as neural joint position servos, and **b** across all alternative environments and all networks without (left) and with (middle) additional intra-joint feedback and both combined (right)

respective standard deviations are given. Immediately visible is the performance dominance of at least one for the simple reflex oscillators (C3-C5) without muscle (C3) and with muscle (C5), followed by the neuro-biologically inspired controllers (C1-C2) and the CPG-controllers (C6-C7). On average the combinations with muscle models seem to perform better, with the exception of combinations with environment E7. Also a relative performance advantage of muscle model combinations vs. non-muscle combinations seemed to exist for controllers without additional intra-joint feedback, see especially C4 and C6.

To quantify the previous hypotheses, three controller groups were formed, namely all controllers, all controllers with and all controllers without additional intra-joint sensory feedback. For these groups the data was averaged, once for each perturbing condition separately (cp. 7.11 a) and then for all perturbing conditions together (cp. 7.11 b). This alternative visualization supports the above hypotheses: the overall performance with muscle model was slightly better, the relative performance advantage for combinations with muscle models was better for controllers without intra-joint sensory feedback than for those with intra-joint feedback and finally environment 6 generally resulted in a bad performance for combinations with muscles.

7.3. Stick Insect Model

All of the beneficial effects of the muscle model that were demonstrated on a single leg of the simulated robot Octavio also apply for the stick insect simulation. Instead of presenting the qualitatively comparable data on working range stabilization, noise robustness etc., novel aspects concerning the stick insect are presented hereafter. As controller only the extended neuro-biologically inspired controller is employed (cp. section 3.2.3).

7.3.1. Influence of the Torque-Velocity Characteristics

In contrast to the robotic model, the maximum muscle torque was not capped at the maximum torque at zero joint velocity and the muscle model update frequency was four times higher, i.e. 400Hz instead of 100Hz for the robotic model. Corresponding details are given in section 4.1.4. Therefore, a stronger effect of the muscle models torque-velocity characteristic on behavior was expected for the stick insect simulation. In Fig. 7.12 the influence of the force velocity characteristics on the walking performance in a single middle leg is depicted, focusing on the FTi joint. Foot trajectories as well as time-plots of joint sensors clearly show that the walking movement was more regular and smooth for the muscle model with torque-velocity characteristics. In detail this means e.g. that the working range of the joints were more restricted (they did not hit the mechanical joint limits), overshoots at AEP and PEP were less pronounced, leading to reduced negative torso velocities at AEP and the neural ThC and FTi velocity servos were more effective in producing nearly constant retraction and flexion velocities. The decreased AEP overshoot was due to a strong increase in flexor force shortly after AEP, despite of a similar or even weaker and shorter flexor motor neuron peak activity when

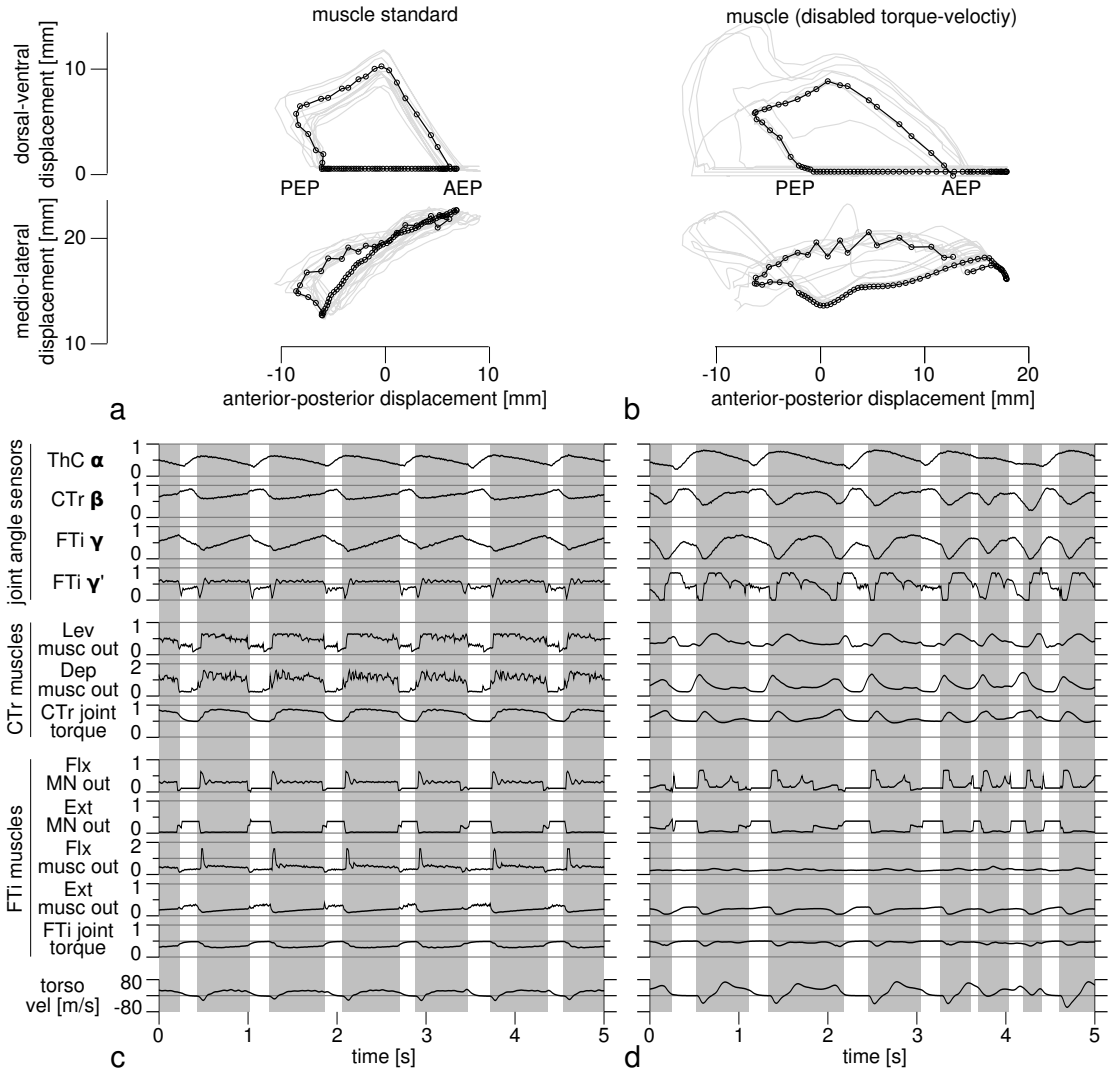

Figure 7.12.: Influence of the force-velocity characteristics of the muscle model. **a** and **b** depict the foot trajectories in lateral and dorsal view. 10s are given in gray and one complete step in black with individual markers for each time step. Trajectories for the **a** standard muscle model were regular and stable whereas those for the **b** muscle model without disabled torque-velocity influence were irregular and substantial "overshoots" at AEP (anterior directed movements after foot touchdown) occurred. **c** and **d** show the corresponding time-plots of important parameters like joint sensors and muscle activations. They demonstrate the regularization of movement due to the torque-velocity characteristics. Two examples are given: 1. The flexor torque peaks in **c** shortly after touchdown led to a sharper swing-stance transition and therefore to a reduced AEP "overshoot". 2. FTi joint velocity as well as torso velocity in **d** fluctuate much stronger despite the neural velocity servos employed in ThC and FTi when compared to **c**

compared to the muscle model with disabled torque-velocity properties. This again correlated with a strong negative FTi velocity at the beginning of stance.

7.3.2. Dealing With Time-Delays at Transitions

At the beginning of this chapter it was asked how short swing durations and stable swing-stance and stance-swing transition fit together with the extremely slow muscles of the stick insect? What kind of neural control is needed to achieve these fast transitions and short swing phases? To at least partially answer this question the extended neurobiologically inspired controller (cp. section 3.2.3) was tested, driving a single simulated stick insect leg, once with the full featured muscle model, once with a minimized delay (20ms) of the activation function (cp. Fig. 7.13 a). As depicted in Fig. 7.13 d, swing times were reduced from 300ms to 150ms when deactivating the low pass properties. Fig. 7.13 e additionally shows how the activation delay leads to overshoots at PEP and AEP. These overshoots are movements directly after transitions that take place in the opposite direction of the expected movement. Time-plots of the same movements are given in Fig. 7.14 a with a minimized activation delay and in Fig. 7.14 b with the standard activation function: although motor neuron activations displayed a similar timing and magnitude at swing-stance and stance swing transitions, resulting muscle torque changes were more rapid and pronounced for the minimized activation delay.

Subsequently two controller extensions were tested for their ability to achieve shorter swing times and sharper swing-stance and stance-swing transitions for all joints. In Fig. 7.13 b a controller that additionally used sensor information from CTr joint torque and its derivative to initiate stance-swing transitions in all joint is shown. It achieved a reduction of the retraction overshoots at PEP (cp. Fig. 7.13 e) by an advanced activation of the protractor (cp. Fig. 7.14 c). Note that the extensor was already activated prior to the protractor activation due to its standard biphasic movement during stance. In Fig. 7.13 c a controller that additionally employed "AEP-servos" in ThC and FTi joints, i.e. position servos that were only activated at the end of swing (cp. Fig. 7.14 d), led to reduced protraction overshoots at AEP despite the muscle activation dynamics leading to delayed torque buildup.

Figure 7.13. ***(facing page)***: **a** The low pass filter properties of the muscle model activation function, as derived from biological data, lead to considerable delays in muscle torque buildup after motor neuron activation. This in turn poses a considerable challenge regarding the timely co-ordination of joint torques at swing-stance (AEP) and stance-swing (PEP) transitions. **b** A controller extension using load and load derivative information to contribute to swing-stance transitions in all three major leg joints in addition to foot contact information. **c** A second controller extension using position servos in ThC and FTi joints at the end of swing phase. These "AEP-servos" are switched off during stance muscle activity (flexor or retractor) and during early swing phase, determined by joint angle and angular velocity information. **d**+**e** The performance of four different controller - muscle-model combinations, driving a single-leg on the rail structure, are shown. For time-plots of relevant sensor and muscle activations see Fig. 7.14. In **d** swing vs stance durations are plotted for all four combinations for all steps of a 40s time period. In **e** foot trajectories for all four combination are shown. A 10s period is shown in gray, one step is additionally shown in black with individual markers for each time step

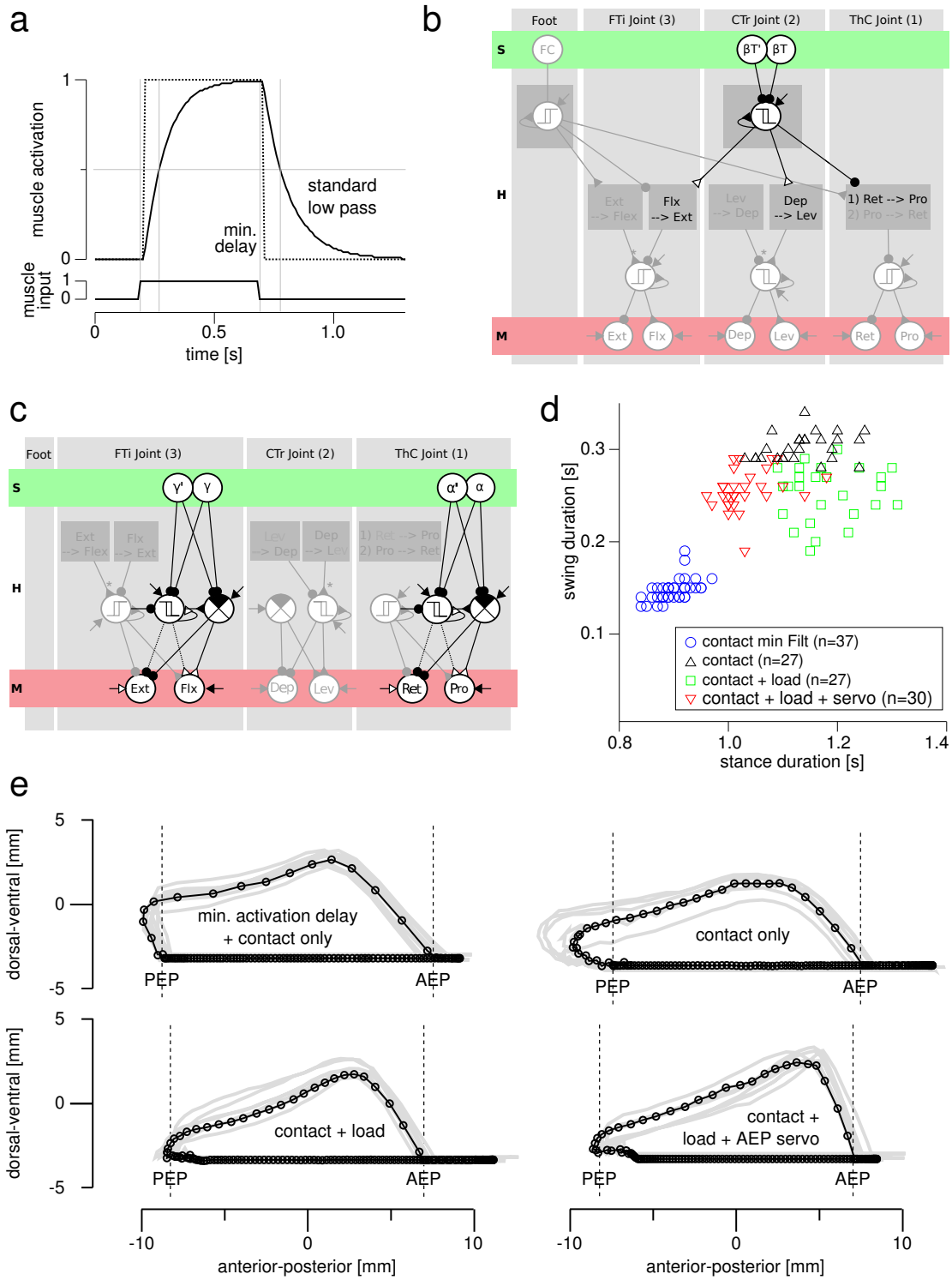
a
muscle activation
standard
low pass
min.
delay
muscle input
time [s]
b
Foot
FTi Joint (3)
CTr Joint (2)
ThC Joint (1)
S
H
M
FC
βT'
βT
Ext --> Flex
Flx --> Ext
Lev --> Dep
Dep --> Lev
1) Ret --> Pro
2) Pro --> Ret
Ext
Flx
Dep
Lev
Ret
Pro
c
γ'
γ
α'
α
d
swing duration [s]
stance duration [s]
contact min Filt (n=37)
contact (n=27)
contact + load (n=27)
contact + load + servo (n=30)
e
dorsal-ventral [mm]
min. activation delay
+ contact only
contact only
contact + load
contact +
load + AEP servo
PEP
AEP
anterior-posterior [mm]

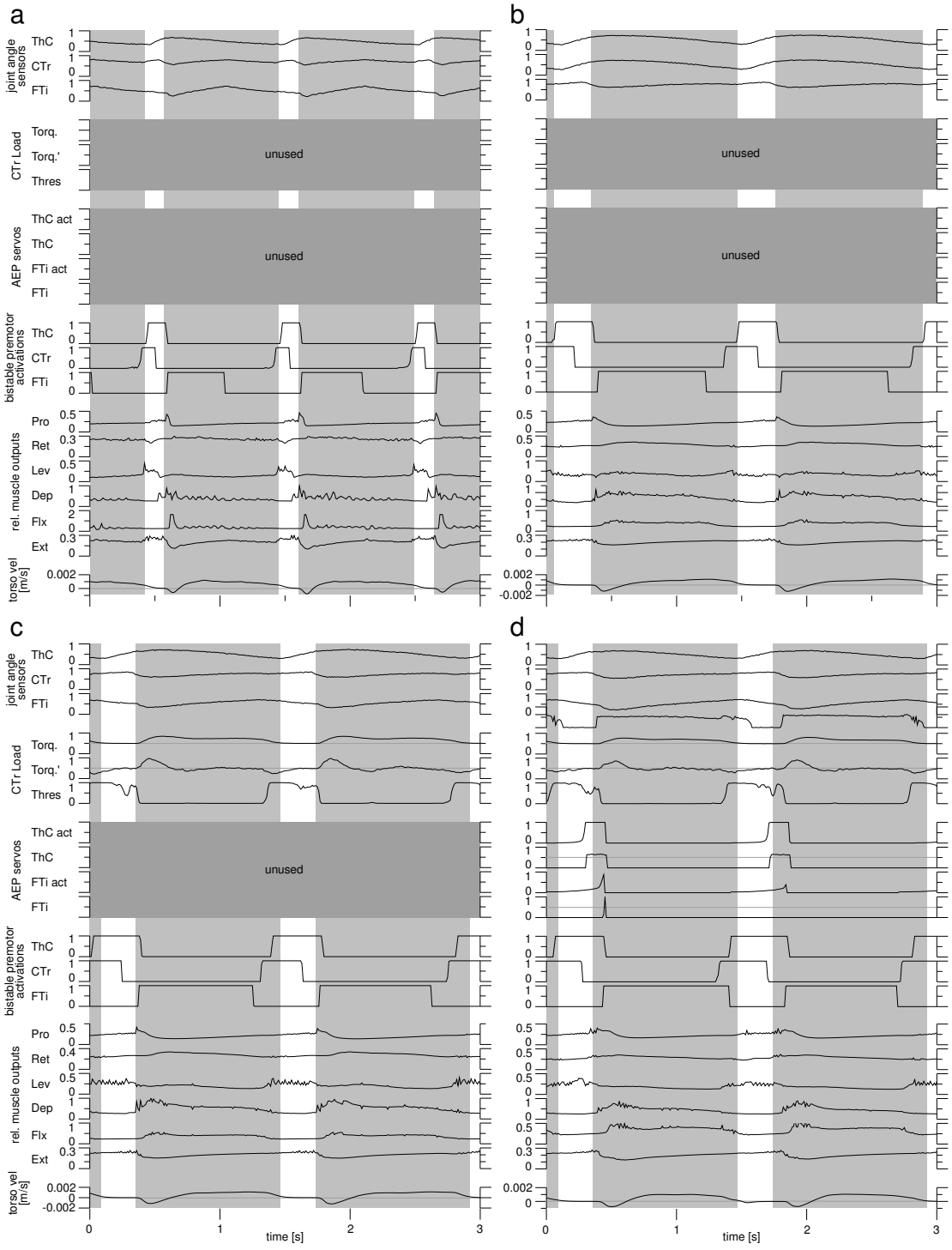

Figure 7.14.: Time-plots of neural and muscular activations of four different controller - muscle-model combinations during single leg stepping on a single-leg on the rail structure (cp. Fig. 7.13). Muscle models use either a minimum muscle model activation delay (**a**) or a muscle model activation delay as retrieved from stick insect data (**b-d**). Controllers use either foot contact information only for stance-swing and swing-stance transitions (**a**+**b**), additional load information (**c**) or additionally both load information and "AEP servos" (**d**)

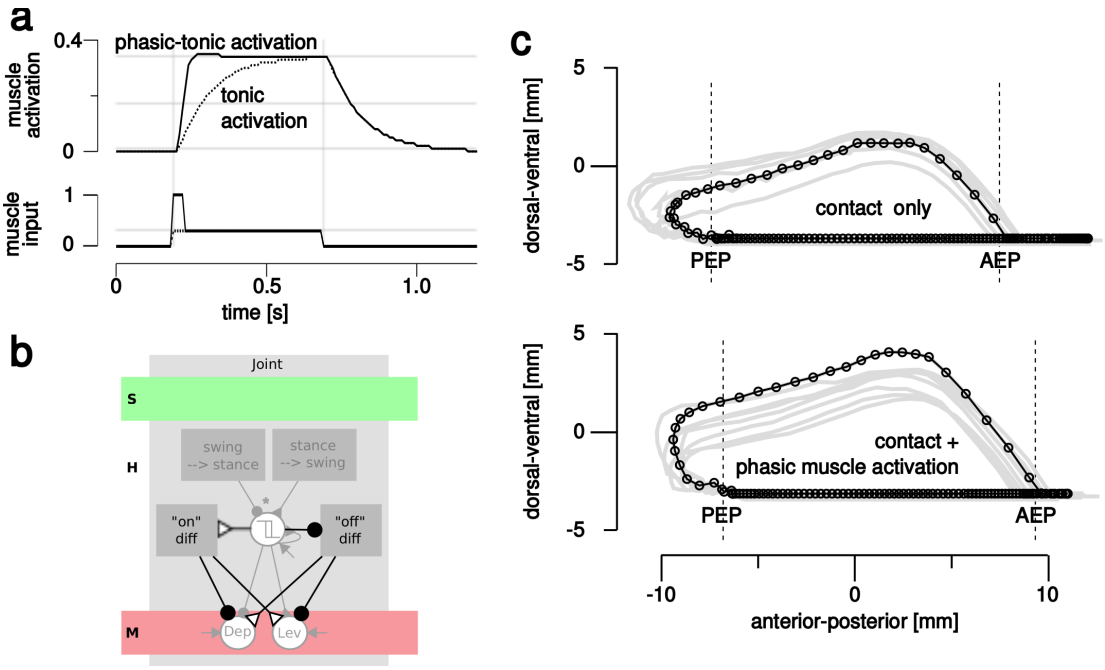

Figure 7.15.: **a** If sub-maximal muscle torques are desired the dynamic range of the muscle activation may be exploited via an additional phasic activation at transitions to effectively reduce time-delay effects. **b** A possible neural implementation of such an extra phasic activation: when the joints bistable premotor element switches its state, either a large positive or large negative impulse is added to the individual motor neurons. **c** The phasic motor neuron and muscle activation led to a reduced AEP overshoot

Finally a more general approach was tested (cp. Fig. 7.15) which made use of dynamic muscle activation range when a sub-maximal muscle torque was desired. An effective reduction of the muscle activation time-delay could be achieved by a phasic tonic motor neuron activation. Initial experiments succeeded in reducing AEP overshoots but not PEP overshoots. Additionally the swing height became more variable.

7.4. Discussion

Employing muscle(-model)s with properties as found in the stick insect extensor muscle (Blümel et al., 2011b; Guschlbauer et al., 2007) was demonstrated to have several advantages for neural locomotion control of simulated stick insects and robots: a stabilization of the joints working range while reducing the need for intra-joint position feedback, support for rather slow and large amplitude reflex-oscillations, an increased robustness against (neural) noise and other perturbing conditions without a prior optimization, an increased robustness for swing-stance transitions and an improved velocity control. Problems due to the low-pass filter properties, e.g. delayed movement reversals at stance-swing transitions, could be largely attenuated by various and rather simple neural control strategies. The constraints and opportunities offered by the mus-

cle properties have implications for robotics and stick insect neurobiology, which will be discussed hereafter.

7.4.1. Implications for Robotics

Despite its output power limiting effect outside of the optimal joint angle and joint angular velocity range (cp. section 4.1.4), the application of pairs of scaled stick insect extensor muscle models as a layer between neural control and DC-motors of the simulated robotic leg led to desirable system properties summarized above. This was especially true for minimal network structures with reduced intra-joint sensory feedback, where the systems with muscle models showed a superior performance under diverse perturbing conditions (cp. Fig. 7.11). To some extent this was expected, because the muscle models inherently supply an intra-joint feedback for at least position and velocity, comparable to technical servo controllers that use sensory information in addition to controller commands to generate motor commands. Furthermore, the regularization and noise tolerance of stepping movements with muscle models are in line with previous studies of more simplified muscle models on robotic systems (Rutter et al., 2007) and more theoretical studies (Buehrmann and Paolo, 2006). When adding intra-joint feedback to the control structures, the relative performance advantage of systems with muscle models almost decreased to the performance of the systems without muscle models. For the perturbing scenario with randomly increased joint friction (E6), the performance of systems without muscle models was on average superior (cp. Fig. 7.11), which could be ascribed to the reduced motor output power with muscle models at non-optimal joint angles due to the muscles torque-angle characteristics.

As demonstrated in chapter 5, neural hysteresis in reflex loops leads to delayed switching of movement directions and, therefore, to oscillation frequencies and amplitudes favorable for the walking task. This is analogous to the findings of increased amplitude and decreased frequency of stepping due to the low pass filter characteristics of the muscle's activation function presented in Fig. 7.6. Similar to e.g. the mechanical properties of a pendulum this leads to a modified bandwidth of oscillation frequencies (cp. e.g. Hatsopoulos, 1996; Neptune and Kautz, 2001; Schumacher, 2008). Since the muscle's activation function is not a pure time-delay, its dynamic bandwidth may be exploited to reduce effective time-delays, or alternative control strategies may be employed to reduce the effects of the activation function (cp. Fig. 7.15 and 7.13 and the corresponding discussion further below).

In contrast to a simulation study of aimed limb movements in locusts by Zakotnik et al. (2006) the role of the passive torque component of the muscle model was not found to have a prime importance. In Fig. 7.5 a slightly less regular stepping pattern is shown for a muscle model without the passive component and a neural controller without any sensory feedback. Because the torque-angle characteristics had a (far) greater influence on performance in all experiments, muscle model performance without torque-angle and without passive influence was otherwise shown together. The minor role of passive muscle forces shown here is probably due to their relatively small magnitude when compared to active forces in the stick insect extensor (Guschlbauer et al., 2007, cp.). In

non-locomotion task, such as posture control, their relative role was shown to be much higher (Hooper et al., 2009). Zakotnik et al. (2006) further found the passive damping properties to be of high importance for motor performance, whereas here this property was not ascribed to the muscles and, therefore, not systematically investigated as the other muscle model components. Future studies should address this issue.

For more complex control structures it has yet to be investigated whether systems without muscle models may offer a performance advantage because of their ability to produce more power throughout their whole working range. Also an application of different perturbing conditions, fitness functions or optimization methods may lead to different results. Due to the combinatorial complexity this cannot be excluded here. For the controller-environment combinations optimized here, the systems with muscle models showed a walking performance en par or better when compared with the systems without muscle models and they could even replace neural intra-joint feedback. The implementation of the muscle model as a simple modular neural network (cp. section 4.1.4) allows an efficient deployment on standard robot hardware with DC-motors, neither requiring costly and experimental artificial muscles (Bar-Cohen, 2004; Herr and Kornbluh, 2004; Pons, 2005; Siciliano and Khatib, 2008), as well as a computationally efficient use in evolutionary robotics experiments with e.g. hexapod robots (cp. following chapter 8).

The simulations of the single robotic legs with and without muscle models further demonstrated the roles of (mechanical) embodiment and situatedness: additional to the neural control system and the muscles, joint stops and constraints of the environment had stabilizing effects on walking movements. Neural controller without intra-joint feedback (cp. e.g. Figs. 7.4 and 7.5) could stabilize their walking movements without muscle models by using the joint stops as range limiters. Even without using any joint stop neural controllers without any direct intra-joint feedback could, without using muscle models, generate stable walking trajectories by employing a combination of inter-joint reflex loops and movement limiting effects of the environment, usually the foot contact (see Fig. 7.6 for an example).

7.4.2. Implications for Stick Insect Neurobiology

Contribution of velocity characteristics to robust stance-swing transitions The influence of torque-velocity part of the muscle model on the performance of the robotic model was limited: in Fig. 7.5 the movement amplitude is increased for a neural CPG controller without sensory feedback when the velocity influence is disabled. This was ascribed to the omission of the torque-velocity's damping influence. Similar in Figs. 7.7 and 7.9 movement amplitudes decreased less and became slightly more jittery during strong motor neuron noise applications with disabled torque-velocity properties. Possible explanations for the limited influence of the torque-velocity influence are: on the one hand, due to the constraints of the robots DC-motors, torques higher than the maximum torque at zero velocity could not be produced for negative velocities. On the other hand, the joints mechanics already produced non-negligible damping forces.

In contrast in the stick insect simulator, torques for negative velocities could reach 160% of those maximally reached at zero velocity. Fig. 7.12 demonstrated the high

negative impact of disabling the torque-velocity characteristics in the stick insect model: stepping patterns became irregular, AEP overshoots, i.e. protractions movements after touchdown, became much larger and velocity control much less effective, especially for slow velocities. Analysis of the AEP overshoots revealed that, despite comparable motor neuron activations, flexor torques with muscles with torque-velocity characteristics were much higher than without. Obviously the flexor muscle acts as a very strong brake, i.e. active damper, at touchdown (cp. Blickhan et al., 2007; Dickinson et al., 2000; Haeufle et al., 2010). Using the non-linear torque-velocity characteristics (cp. chapter 4.1.4), therefore, allows to reproduce behaviors of the real stick insect which could not be reproduced by previous studies: Ekeberg et al. (2004) were, probably due to a linear force-velocity relationship, not able to produce fast swing movements in their stick insect model whereas Rutter et al. (2007) had difficulties replicating robust swing-stance transitions in their robotic model of a stick insect leg. Relatively high touchdown forces at AEP correlate with biological data of stick insects (Cruse and Bartling, 1995).

Future studies will have to show how the muscle's torque-velocity property effects leg coordination (cp. also Schneider, 2006). As an analogy, multiple trains, with different engines and together pulling a load, will each contribute a force automatically adapted to the engines power due to their engine's force-velocity relationship.

Dealing With Delayed Muscle Activations at Swing-Stance and Stance-Swing Transitions Previous simulation studies of stick insect walking did not consider the low-pass filter characteristics of the muscle's activation function (Cruse et al., 2007; Ekeberg et al., 2004; Schilling et al., 2007) and therefore parts of the suggested controller mechanisms might not be able to reproduce the behavior of the real stick insect when acting on top of a realistic muscle model layer. Especially transitions between stance and swing and vice-versa are problematic: loading and contact signals at the beginning of stance are probably too late to account for flexor and retractor activation (Gruhn et al., 2006; Rosenbaum et al., 2010) and loss of contact signals are definitely too late for a timely extensor and protractor activation (Rosenbaum et al., 2010). For the latter transitions the use of unloading information rather than loss of contact signals was suggested (Rosenbaum et al., 2010), based on data by (Akay et al., 2001, 2004, 2007). For the transition from swing to stance only speculations are available:

> "[...] at present we can only speculate about whether only sensory signals from proximal campaniform sensillae play a role as in the locust or whether other information unrelated to a touchdown signals also contributes, as it seems to be the case in fast walking cockroaches (Tryba and Ritzmann, 2000a,b)."
>
> *(Gruhn et al., 2006, p. 205)*

For both transitions multiple alternative controller extensions were tested here.

First of all the unloading hypothesis for extensor and protractor activation was successfully tested, i.e. a rapid and smooth transition from stance to swing without overshoots could be produced with muscle activation sequences similar to biological data

(cp. Figs 7.13b,d+e and 7.14b+c). The unloading information was derived using a threshold combination of CTr torque and torque derivative (cp. Fig. 7.14c). The question remains if and how this unloading signal can be reliably derived in hexapod coupling or under perturbing conditions. During single leg walking, as investigated here, load is increasing at the beginning of stance, reaches is maximum around the middle of stance and then decreases steadily Duysens et al. (2000). In unconstrained stick insects walking on a flat surface a strong step-to-step variation of support forces was observed Cruse (1976). This step-to-step variation is not surprising if one considers the high variability in muscle activation patterns (Hooper et al., 2006) and the high impact of subtle phase shifts in inter-leg coordination on local leg load. Future studies employing torque perturbations will have to clarify if force or torque signals are sufficient or if a more complex sensor-integration is necessary to reliably trigger stance-swing transitions. Suitable technical load sensors in principle allow an application of the unloading signal for stance-swing transitions (Kaliyamoorthy et al., 2005).

Subsequently another hypothesis was tested with respect to appropriate swing-stance transitions: from behavioral observations it is known (Cruse, 1979; Dean and Wendler, 1983) that stick insect middle- and hind-legs may display a so-called "targeting" behavior whereby their touchdown position at the end of swing is close to the position of the anterior tarsus. No neuro-biological data for this behavior during locomotion exists to date, but see Brunn and Dean (1994) for neural data on targeting information transfer in standing and resting animals. In the WALKNET simulation (Cruse et al., 2007) information about the position of the anterior leg is translated into the legs local joint angle space and fed into position servos for ThC and FTi joints. Such a position servo mechanism, that was only active at the end of swing with a fixed reference input, was tested here (cp. Figs. 7.13c-e and 7.14d). Employing this controller extension, AEP overshoots could be reduced by reducing swing phase muscle activity and increasing stance phase muscle activity slightly before touchdown. Alternative mechanisms are feasible, e.g. upon activation of the depressor swing muscle activation could be decreased (cp. e.g. Figs. 5b and 6 in (Gabriel and Büschges, 2007) for a decrease in extensor activity during swing) and stance muscle activation increased. Experiments where the ground height is unexpectedly varied before touchdown could shed light on this question.

Finally a more general approach to compensate for muscle activation delays was tested, exploiting the low-pass properties of the muscle's activation function. If a sub-maximal muscle torque is desired a phasic-tonic activation of the muscle leads to a reduced delay in torque buildup yet the same final torque (cp. 7.15). Despite only using foot contact information for swing-stance transitions a controller extended by phasic activations of all muscles could reduce the AEP overshoot. At the same time swing height became more variable, suggesting that phasic muscle activations should be applied more selectively and graded in future studies. Biological data, e.g. Fig. 6 from Gabriel and Büschges (2007) (cp. also von Uckermann and Büschges, 2009), suggests that flexor-extensor transitions have a strong phasic component whereas extensor-flexor transitions are more gradual. Data from Rosenbaum et al. (2010) (cp. also Büschges et al., 1994) supports phasic-tonic protractor activations at the end of stance and also slightly phasic retractor activations at the beginning of stance. Additionally data from Fisch (2007)

shows phasic-tonic activities in sensor- and motor neurons and, therefore, it may be speculated that already sensor-neurons supply the phasic activity that lead to a compensation of muscle activation delays. Similar sensor-motor neuron correlations are known for the hysteresis effect in sensor neurons that counteracts muscle catch Zill and Jepson-Innes (1988). In a different context, changes in phasic muscle activations were found as a compensation for muscle fatigue effects Corcos et al. (2002).

An alternative mechanism to compensate for muscle activation delays is a co-contraction of antagonists because it allows to trigger large changes in joint torque by only small neural activation changes Zakotnik et al. (2006).

7.5. Conclusion

Taken together, it could be demonstrated that the constraints and opportunities imposed by the muscle model have an important influence on neural motor control, in line with previous studies (cp. e.g. Buehrmann and Paolo, 2006; Gerritsen et al., 1998; Haeufle et al., 2010; Hof, 2003). On the one hand, parts of controller structures, developed for stick insect or robotic simulators without muscle models (e.g. Cruse et al., 2007; Rosano and Webb, 2007), may be replaced by muscles (Schneider, 2006, s. above, cp.), which display stabilizing and reflex-like properties. On the other hand, additional controller structures might become necessary to cope with complicating effects of the muscles, such as time-delayed activations due to the muscle's low pass properties. In extreme cases, even control principles could differ between models with and without muscles. Because the muscle models major impact on behavior control, together with the possibility of a computationally efficient implementation as presented here, future simulation studies and bio-inspired robots should consider to use such muscle models. Hereby the comparability and transferability of (neural) controllers between, on the one hand, robotic and biological results and, on the other hand, functional and morphological approaches to stick insect locomotion could be improved. Furthermore, due to a potential improvement in search space for the neural controller (Buehrmann and Paolo, 2006), muscle models may prove advantageous during artificial evolution experiments.

8. Hexapod Neuro-Controllers

In this chapter the results from the previous chapters were merged: modular neural hexapod controllers, embedded into the sensori-motor loop of robotic and stick insect simulators, were developed either by modular evolution or by hand construction. It is demonstrated that the modular approach to hexapod controller development worked well for all simulation platforms presented in this thesis, with and without an intermediate muscle layer. The results from the artificial evolution experiments, where single-leg controllers and sensori-motor coupling structures were co-evolved, indicate, that inter-leg coordination may replace intra-leg coordination, further simplifying already minimalistic single-leg controllers. Finally, for the first time it is demonstrated that six neuro-biologically inspired controllers, as presented in chapter 6, are capable to robustly drive a realistically simulated stick insect hexapod, when coupled by the biologically inspired "Cruse"-coupling rules. Hereby, all joints of the hexapod were fully equipped with muscle models, as presented in chapter 7.

8.1. Simple Hexapod

Sets of three simple single leg controllers (cp. Fig. 5.3) were coupled by structure evolution (cp. section 3.3) to drive the hexapod robot AMOS-WD06 (cp. section 4.2.1). The single-leg controllers and the coupling structure were co-evolved (cp. section 3.3.3). To constrain the search space, a lateral symmetry (cp. section 3.3.3 and Beer and Gallagher (1992)) constraint was introduced, therefore parameters for only three single-leg networks and one (parameter halved) coupling network had to be evolved. During evolution, coupling was done by allowing synapses from sensor neurons (ThC angle and foot contact sensors were chosen due to their importance in the "Cruse-rules" (Cruse, 1990) for stick insect walking) to spread not only to local (in the sense of a single leg controller) neurons but also to neurons of other legs. The experiment was conducted for a six legged robot and its performance in even terrain and rough terrain was analyzed in form of a swing stance plot. The structure of the best performing controller is depicted in Fig. 8.1a. For the even terrain condition, the controller showed a typical tripod gait (see Fig. 8.1b) whereas rough terrain caused the coupling of the single leg movements to become more irregular (see Fig. 8.1c). It has to be noted that this modular structure consisting of extremely simple single leg controllers managed to navigate in a very rough environment showing its ability to cope with obstacles.

When looking at the resulting controller structure, it is striking to see how simple the complete controller (36 neurons and 36 synapses) is. The single-leg's controller complexity is even further reduced when compared with single-leg experiments in chapter 5. If the inter-leg influences are removed, neither all fore- (FTi), nor all middle-leg joints

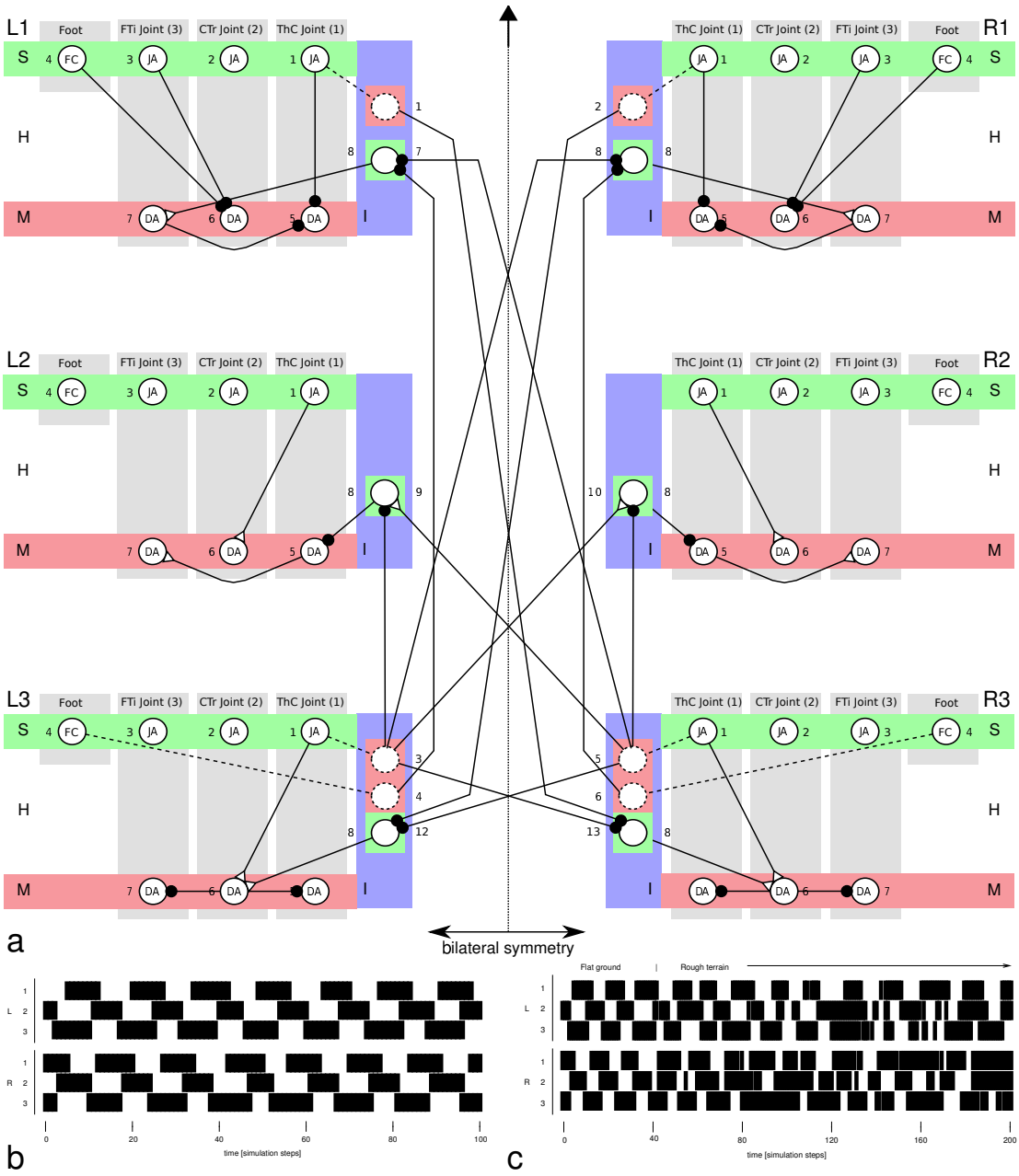

Figure 8.1.: **a** Hexapod controller derived by modular evolution of three single-leg controller (FL, ML and HL) and a coupling structure with a bilateral symmetry constraint. Furthermore, only couplings from sensor neurons to interface neurons were allowed. **b** Swing- and Stance Phases of all 6 legs walking on flat ground. The black boxes denote the feet having ground contact whereas the white spaces show the leg having no ground contact. The controller consisted of six single leg-controllers similar to the ones in the section above and of connections between these single-leg controllers. **c** Swing- and Stance Phases of all 6 legs in rough terrain. When comparing with plot **b** please note the different timescale

(ThC+FTi) receive synaptic input any more. Therefore, global inter-leg control has replaced local intra-leg control during the process of evolution. Furthermore, only using sensori-motor couplings and no central control structure is sufficient to generate robust walking.

8.2. Octavio

8.2.1. CPG Driven Hexapod

Similar to earlier approaches (Fischer et al., 2004; Manoonpong et al., 2005), a single central SO(2) (Pasemann et al., 2003) oscillator was employed to drive all 18 DOFs of the hexapod robot Octavio (see Fig. 8.2). The two outputs of the SO(2) oscillator, which are shifted by 90°, are "mixed" by parameter evolution for each motor neuron. Thereby, any phase may be expressed by any joint, depending on the parameter combination. A nice sinusoidal oscillation leads to small output amplitudes (Pasemann et al., 2003) and, therefore, two amplifier neurons are additionally used. Note that in order to achieve regular walking patterns, the standard motor equipment was not sufficient. Therefore, motor strengths were doubled during this experiment. The resulting movement was not very smooth, showing strong body velocity oscillations with a frequency twice the individual step frequency (corresponding to one period per each tripod touchdown) and nearly falling to zero in every period. Interestingly each leg shows a specialized behavior (cp. Fig. 8.2b), whereby the hind-legs do not use their ThC joint at all. This means that the hind-legs only perform pushing movements by using their CTr and FTi joints.

8.2.2. Mixed CPG- and Reflex-Driven 6x2DOF Hexapod Controller

In Fig. 8.3 an example of a simple hexapod controller for the simplified 2DOF leg version, i.e. with a fixated FTi joint, is shown that was successfully transferred to hardware without any parameter adaptations (von Twickel et al., 2012). The locomotor rhythm is generated by a combination of local reflexive elements and an inter-leg coupling structure: Each leg has a sensori-motor coupling from the foot sensor to the α (ThC) joint that simply switches to leg protraction upon foot contact and to retraction upon loss of ground contact. Two local neurons form a ring module that couples with two other legs to result in a 12-ring oscillator for the complete hexapod. In the configuration shown a wave gait pattern is produced. The ring module switched the β (CTr) joint state between levation and depression and, therefore, determined swing and stance phases. Together with the local reflex mechanism this resulted in stable wave-gait walking of Octavio (see Fig. 8.3 c for the simulation performance). Not the oscillating body velocity with a frequency twice that of the ring-oscillator and the drops to zero velocity.

8.2.3. Evolved Sensori-Motor Coupled 6x2DOF Hexapod Controller

In Fig. 8.4 an example of a hexapod controller with an evolved inter-leg coupling structure and its performance in simulation is shown. The controller shown was developed for

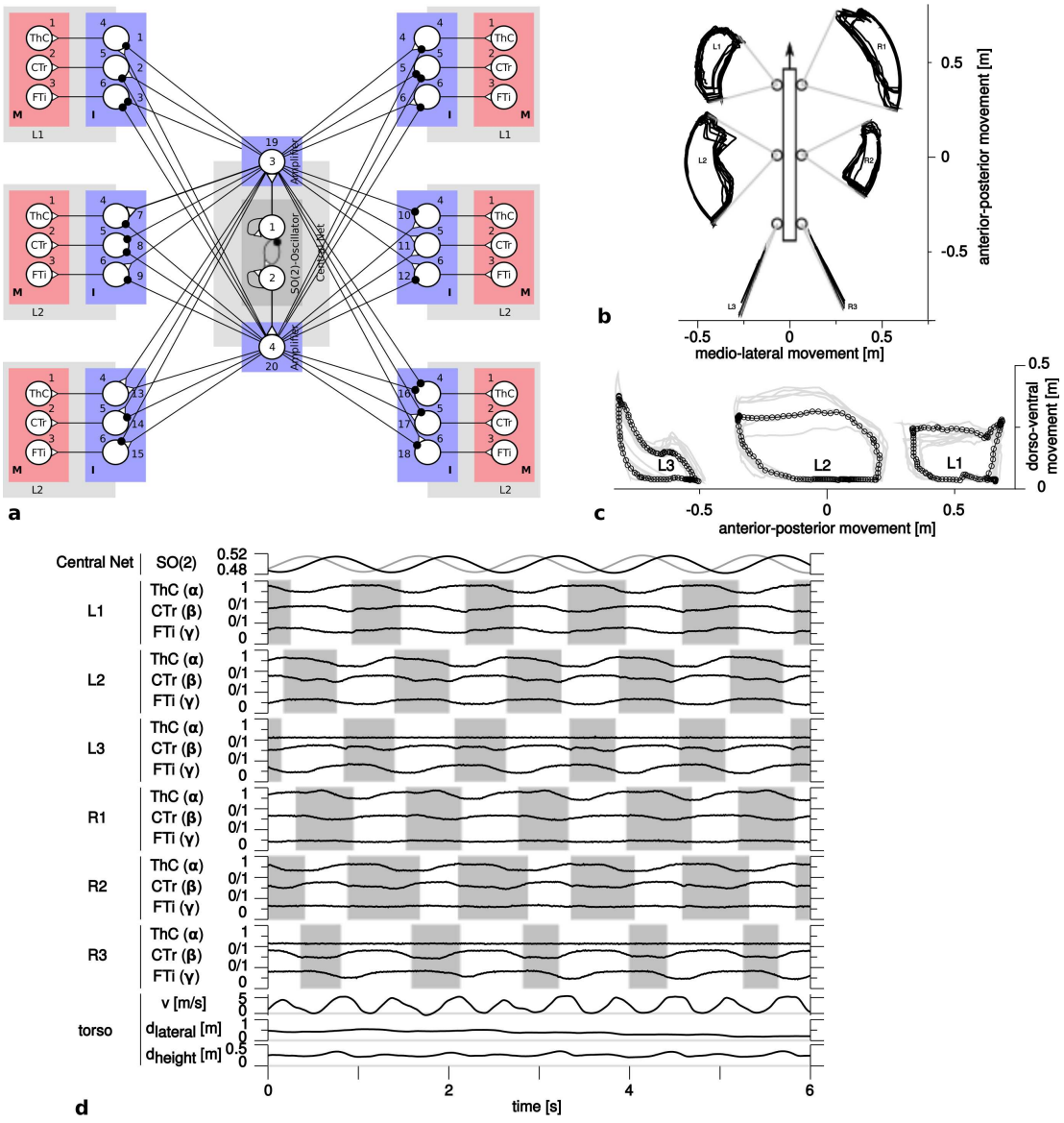

Figure 8.2.: **a** A simple central SO(2) oscillator provided a central rhythm of ≈1.2Hz with two 90 degree shifted outputs. A mixture of both signals was send as input to each servo-motor, whereby the individual synaptic weightings were determined by evolution. **b** Dorsal view of foot trajectories relative to the torso. Note the left-right asymmetry and the straight stepping trajectories of the hindlegs. **c** Lateral view of the foot trajectories of all left feet. **d** Timeplot of important neural activities and body movements. Note the oscillation of body velocity with twice the frequency of individual steps

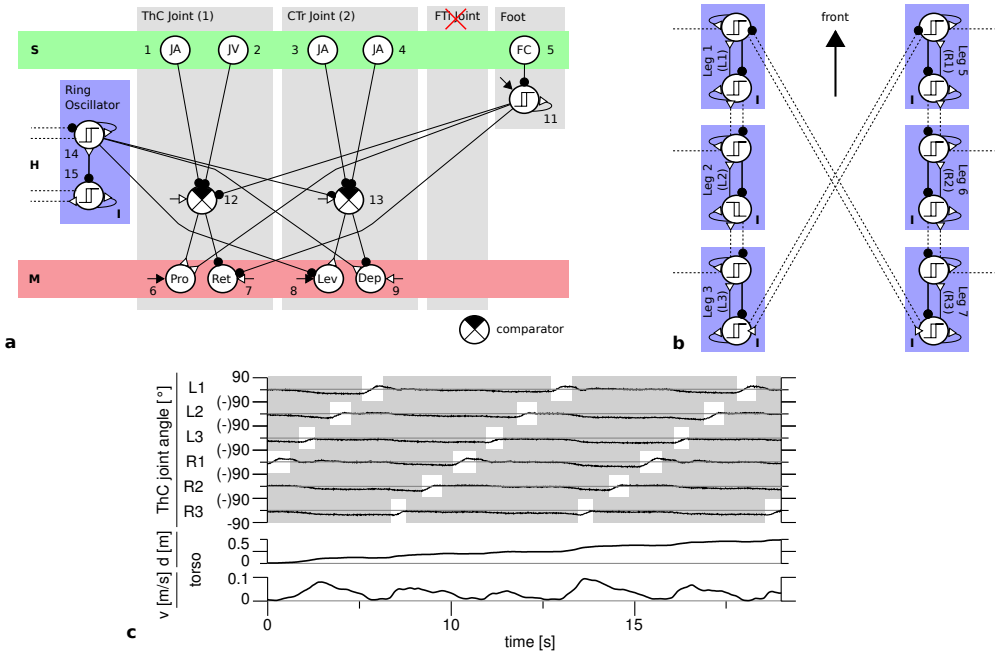

Figure 8.3.: Example of **a** a single-2DOF-leg neuro-controller (the FTi joint was fixated) and **b** its coupling with other legs. The network structure was hand designed and parameters optimized via evolution. The leg modules worked purely reflexive whereas the coupling structure between legs formed a 12-ring oscillator producing a wave-gait pattern. Single joints possessed a neural servo mechanism with a stabilizing joint angle velocity sensor (JV) input. This hexapod controller was successfully transfered to hardware without any parameter changes. **c** Performance of the controller in simulation. Foot contact phases are shown as gray boxes. For further explanations see Fig. 5.8 and text

the restricted leg with 2 active DOFs, the fixation angle of the γ joint was determined by evolution.

Single leg controllers were initialized (according to previous evolution experience) with neural servo controllers for each joint with a stabilizing joint velocity input and a sensorimotor coupling that produces reflex oscillations resulting in stable stepping patterns: The foot contact influences the α (ThC) joint premotor neuron (5-12-10) resulting in α changes (10-6, 10-7), the α angle sensor influences the β premotor neuron (1-13-11) which results in β changes (11-8, 11-9) and eventually in foot sensor changes. An interface neuron (14) projecting to the β premotor neuron 13 was added to receive inter-leg coupling influences. During evolution single leg controller structure and parameters were allowed to change including the fixation angle of the γ (FTi) joint and inter-leg connections from sensors onto the interface neurons of other legs allowed.

The coupling structure and leg controllers were only developed using the lateral symmetry constraint, i.e. only left body side controllers were developed but right body side controller mirrored and coupling synapses only developed with source neurons on the left body side but mirrored to those on the right body side. Despite initialization with functional single leg controllers, restriction to 2DOF legs and the lateral symme-

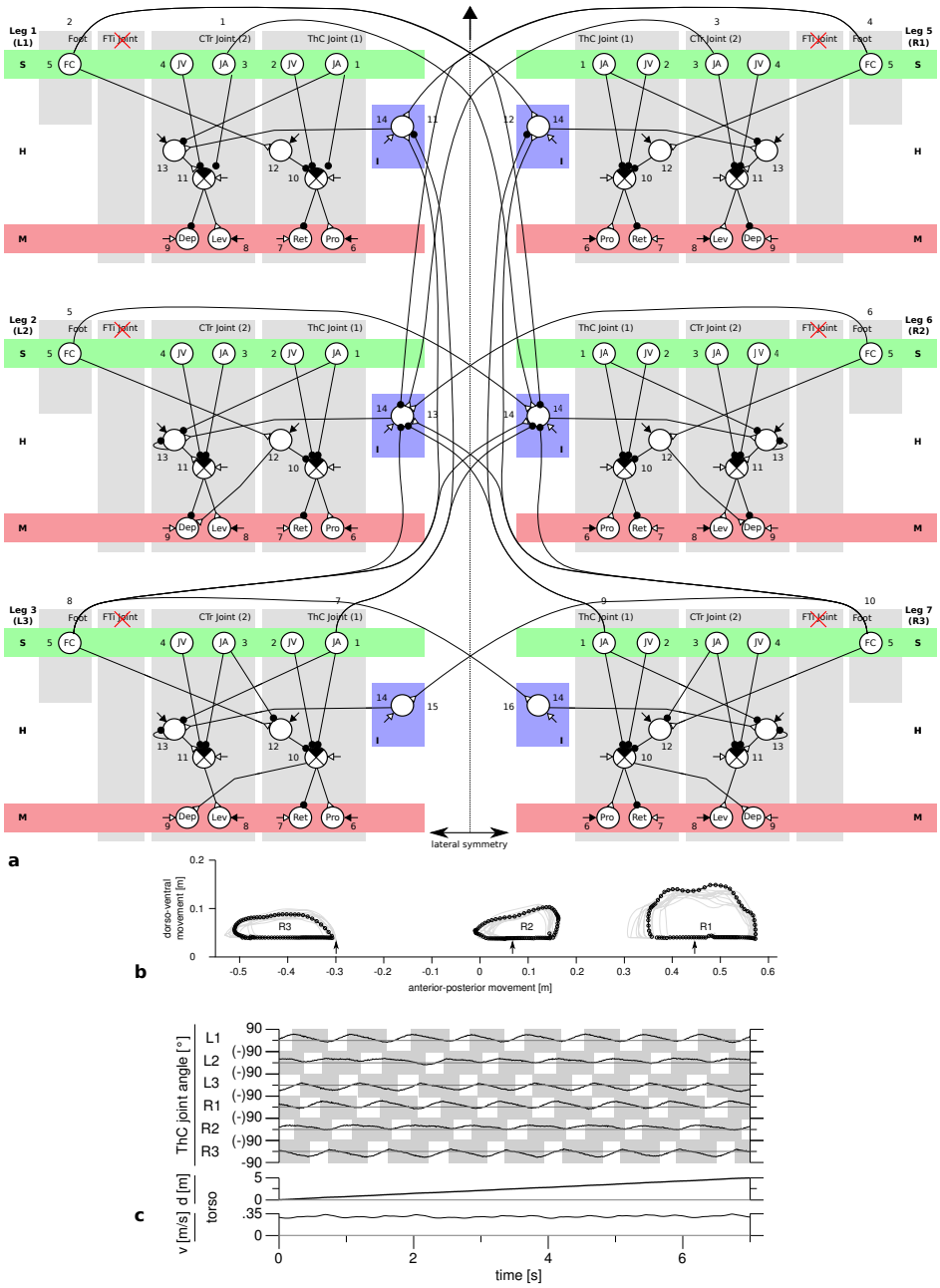

Figure 8.4.: Example of an hexapod controller with evolved coupling structure. **a** Controller structure: Purely reflexive leg modules for front-, middle- and hind-legs were co-evolved with a coupling structure where only connections from sensors of one leg to the interface neuron of another leg were allowed. Without any central pattern generator the network produces a stable tripod gait in the interaction with body and environment. **b** Foot trajectories on flat terrain (lateral view) with posterior-anterior movement relative to torso. In gray trajectories are shown for 10s, in black trajectories are shown for one step cycle with a marker for each time step. Arrows indicate anterior-posterior coxa attachment positions on the torso. **c** ThC joint angles of all six legs with ground contact phases marked as gray boxes in the background. A regular tripod step pattern can be observed. On the bottom the forward progress of the walking machine is shown. For further explanations see Fig. 5.8 and text

try constraint the task for evolution is non-trivial because many local minima exist, e.g. non-desirable locomotion patterns like "forward trembling" or middle legs being used as "carrying wheels". Therefore additional constraints have been employed: The environment was randomly equipped with small obstacles to enforce leg lift up and neighboring legs were not allowed to be without ground contact simultaneously. Finally costs for synapses were introduced to reduce the structure complexity while preserving the performance.

Co-evolution of single leg controllers and the coupling structure resulted in specialized front-, middle- and hind-leg-controllers (see Fig. 8.4 a and b): 1. front- and middle-legs operate in more anterior positions and hind-legs in more posterior positions. 2. Front-legs are further lifted up during swing phase to allow obstacles to be overcome and middle-legs have a smaller movement range acting as stabilizers. This can also be seen in the evolved fixation angles of the γ joint (front-leg: °, middle-leg: °, hind-leg: °) and the differentiated single leg controller structures.

Despite the lack of a central rhythm generating network the resulting controller shows a robust tripod walking pattern on the walking machine with smooth forward progression (see Fig. 8.4 c). Interestingly coupling between front-, middle- and hind-legs is non symmetrical: Front-legs project to contra-lateral front- and middle-legs, middle-legs only to contra-lateral middle-legs and hind-legs to contra-lateral hind- and middle-legs and ipsi-lateral middle- and front-legs. Partly the coupling structure explains the tripod pattern, e.g. the hind-leg foot-contact sensor excites the contra-lateral hind-leg to lift off, but its projections to middle- and front-legs seem to have the opposite effect. One has to take into account the combination of multiple inter-leg coupling influences as well as mechanical coupling influences not visible in the neural connectivity structure.

8.2.4. Evolved Sensori-Motor Coupled 6x3DOF Hexapod Controller

Taking the previous experiment a step further, the FTi joint was released and put under control of the neural network. Again, evolution was bootstrapped with functional front-, middle- and hind-leg controllers. It was found to be necessary to apply many strategies to constrain the search space (cp. section 3.3.3). In Fig. 8.5 an example of a resulting controller structure for a simulator version with servo motor interface is given. Compared to the controllers presented above this one is very complicated and cannot be analyzed in a simple manner. Therefore, only its performance is discussed (cp. Fig. 8.6): A tripod gait pattern is observed with an asymmetry between middle-legs on the one hand, and front- and hind-legs on the other hand. Because of their smaller anterior-posterior movement range, middle-legs act more like struts and front- and hind-legs provide the forward movement. The footfall patterns show that middle-legs additionally have a prolonged stance phase when compared to the front- and hindlegs, suggesting a stabilizing role. Body velocity oscillates with twice the step frequency, but velocities do not fall to zero.

Additional to the presented controller multiple other hexapod controllers were evolved, not only for the servo motor interface but also for the antagonist and muscle motor interfaces. Those controllers possessed an even more complicated structure and are

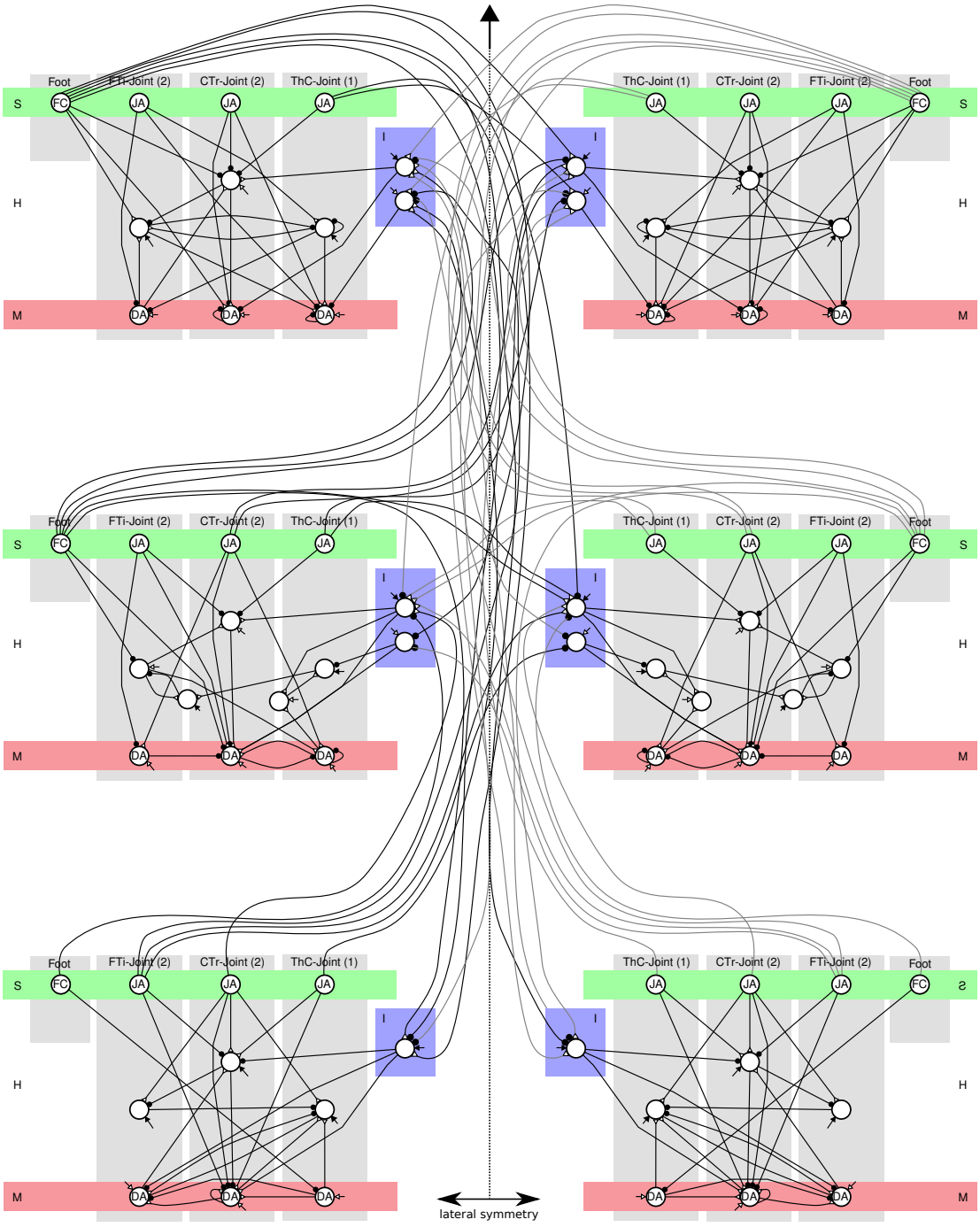

Figure 8.5.: Example of a more complex network structure controlling an unrestricted Octavio hexapod robot with a servo motor interface

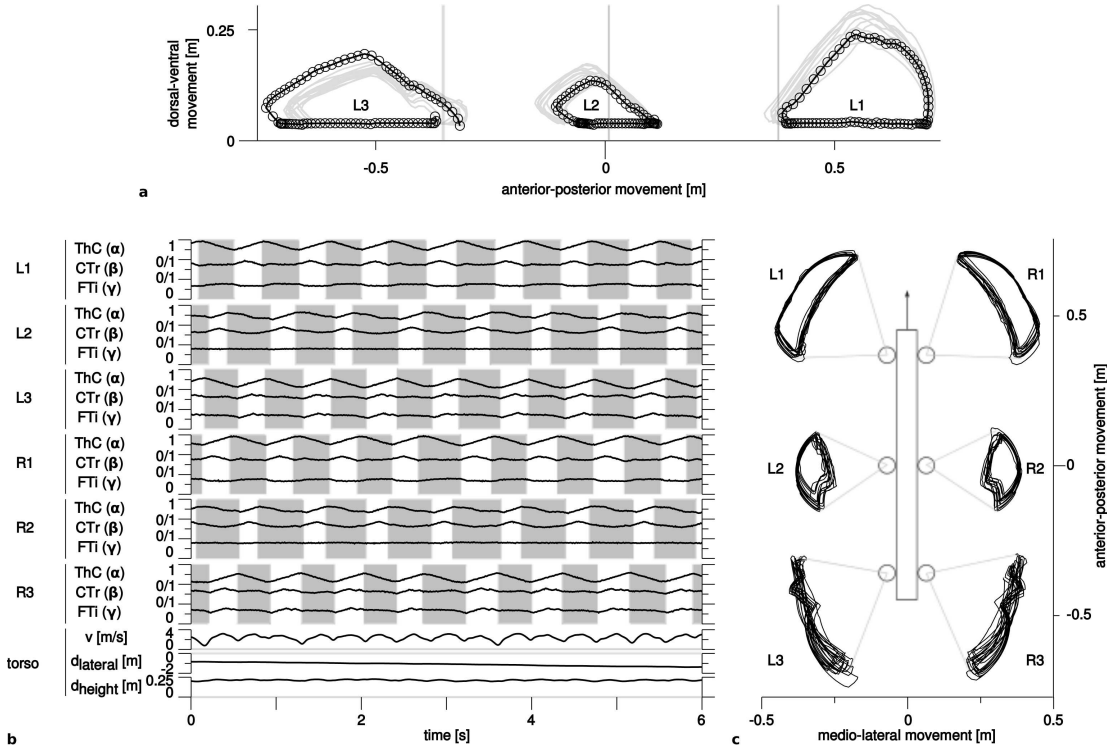

Figure 8.6.: Performance of the unrestricted hexapod controller depicted in Fig. 8.5

therefore not discussed here.

8.3. Stick Insect

The stick insect simulator (cp. section 4.2.3) was extended to six legs and initially six standard neuro-biologically inspired controllers were used (cp. Fig. 3.11) in experiment on a rail structure. First of all it was found that stick insect models using the muscle model were found to be controlled much easier. Without a detailed investigation this was assigned to an increased damping due to the torque-velocity curve (but cp. section 7 for alternative possibilities). Despite the inclusion of a muscle model it was found that this setup did not provide a simple means to control walking speed in a smooth way because interaction force between legs would rapidly change walking speeds due to an irregular stepping. Therefore the controller was extended by ThC and FTi velocity controllers (cp. Fig. 3.6), resulting in the extended neuro-biologically inspired controller (cp. section section 3.2.3). This setup allowed a sufficiently smooth velocity control. The next problem appeared when the rail structure was removed: it was extremely difficult to configure a controller that would result in stable postures. This was due to the caudal center of mass, which lies behind the hind-leg coxae (cp. table D.1). Stick insects use a tarsus attachment (cp. section 4.2.3) and their abdomen as extra stabilizing measures. Therefore, an attachable tarsus was implemented in simulation (cp. Fig. 4.8). The performance of the extended controller with muscle models and tarsus attachments via the retractor unguis (Run) motor neuron are given in Fig. 8.7a+b for a middle- and a hind-leg. As a next step the single-leg controller's parameters were tuned in such a way that the single leg would react with a good entrainment behavior (cp. Fig. 8.8)

8.3.1. Hexapod Performance

Subsequently the morphological single-leg approach was merged with the functional approach by adding the "Cruse-Coupling-Rules" (Cruse, 1990, cp. Fig. 3.13). See Fig. 8.9 for the resulting hexapod controller. Using lateral symmetry constraints parameters had then to be tuned for three leg controllers and the coupling influences. As a result stable hexapod walking was achieved. Resulting data is given in Figs. 8.10 (time plots) and 8.11 (foot trajectories).

8.4. Discussion

For all simulators used throughout this thesis (AMOS-WD06, Octavio and Stick Insect) as well as for simulators with and without muscle models, a modular approach to the development of hexapod controllers was successfully applied. Modular controller development either was done by hand-tuning (stick insect) or by evolutionary robotics. This approach promises to lead to insights about the neural organization of inter-leg coupling in stick insects. It may combine the morphological and functional approaches (Cruse et al., 2007) to stick insect locomotion control modeling with evolutionary robotics Beer and Gallagher (1992); Nolfi and Floreano (2000) to explore the coupling parameter space. Hereby the search space may be constrained by recent neuro-biological data on inter-leg coupling (Borgmann et al., 2007, 2009; Ludwar et al., 2005) on the one hand

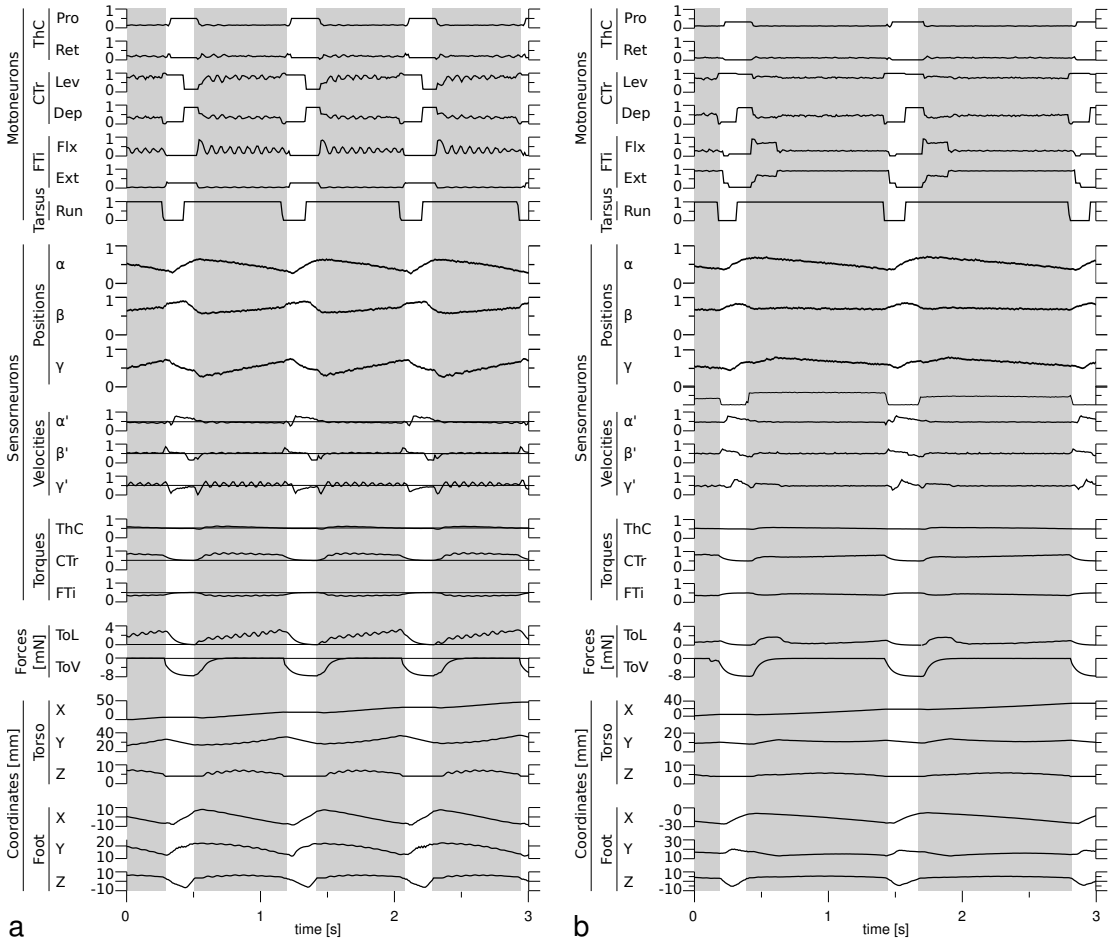

Figure 8.7.: Single leg performance with the extended neuro-biologically inspired controller, with tarsus attachment and muscle models for **a** middle- and **b** hind-leg

and desired behaviors on the other hand, such as those displayed by the WALKNET controller (Dürr et al., 2004).

In the context of artificial evolution of walking behaviors Bongard (2011); Filliat et al. (1999); Floreano et al. (2008); Gallagher et al. (1996); Lewis et al. (1992); Lipson et al. (2006); Mazzapioda and Nolfi (2006) most of the studies used legs with only 2 DOFs, and considered complete 4- or 6-legged robots, which often existed in simulations only. Furthermore, the structures of the evolved neural controllers were mostly designed by hand, like, e.g., coupled oscillators. Therefore, evolution was used only as an optimization technique. The approach presented here promises to lead to new insights about interesting hexapod control structures that may be analyzed to derive general control principles and that may be deployed on real robots.

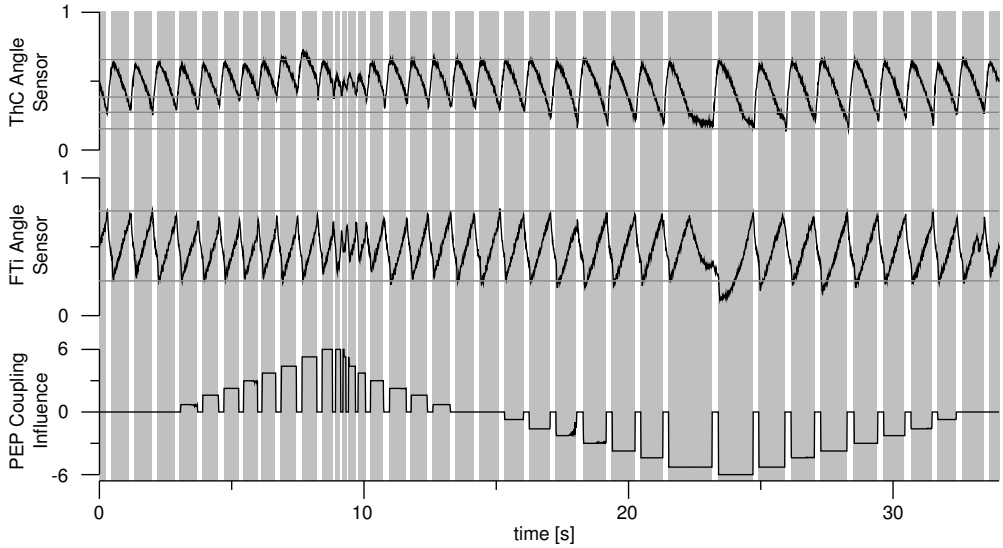

Figure 8.8.: Single-leg controller tuned to display a favorable behavioral reaction to inter-leg coupling influences. With increasing positive influence the PEP shifts anterior, the stance duration is shortened (gray bars indicate stance phase) and vice versa with increasing negative influence. At very high positive and negative coupling influences, the FTi movement range is affected and itself affects the ThC movement range, but stable step patterns persist. Note that coupling influences are muted during swing phases by foot contact information

Figure 8.9. ***(facing page)***: Merged functional and morphological controller for hexapod stick insect walking. Note that single-leg controller are simplified due to space constraints. Cp. Fig. 3.12 for the complete single leg controller

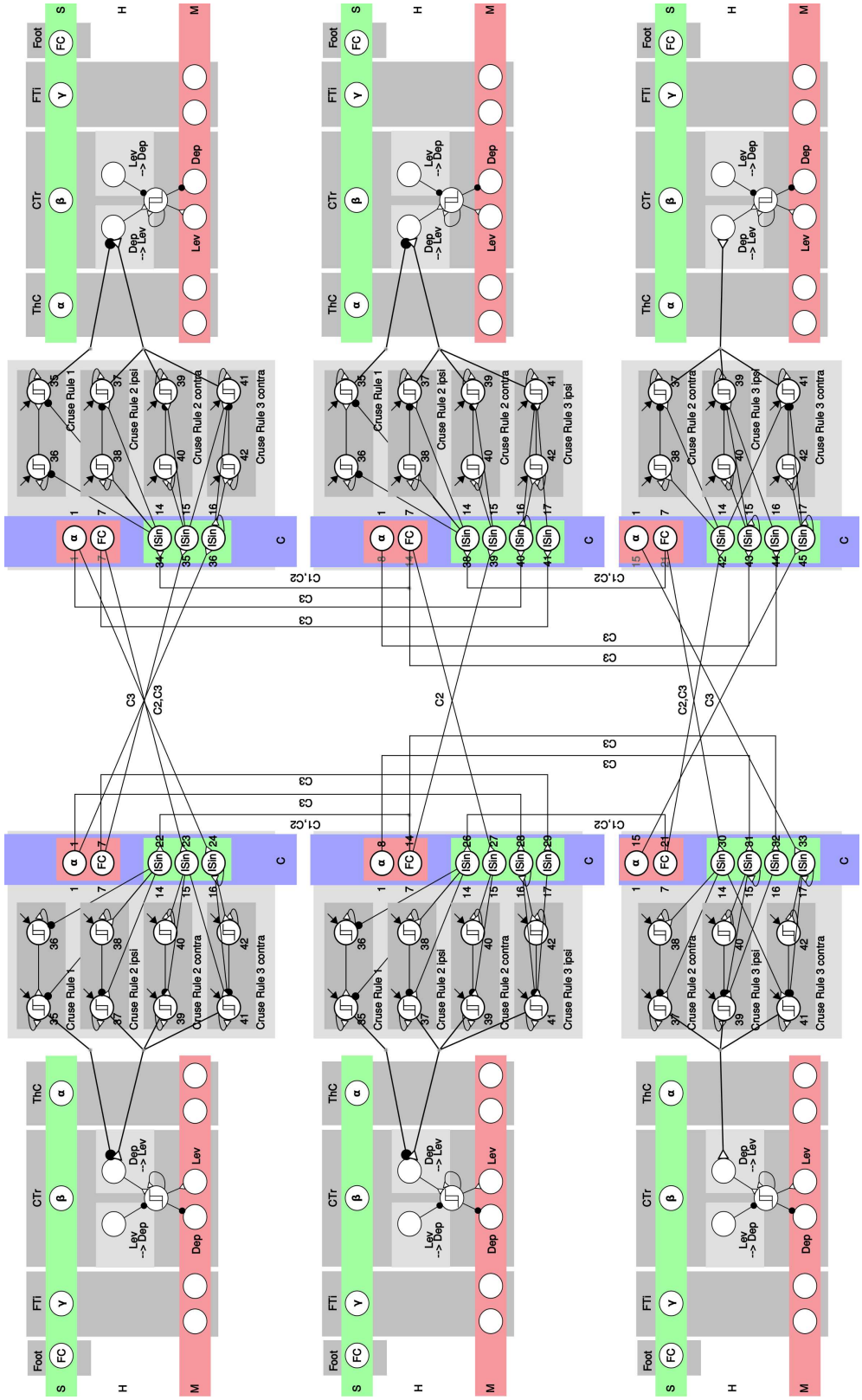
Foot
FC
FTi
γ
CTr
β
ThC
α
S
H
M
Dep
Lev
Lev --> Dep
Dep --> Lev
Cruse Rule 1
Cruse Rule 2 ipsi
Cruse Rule 2 contra
Cruse Rule 3 ipsi
Cruse Rule 3 contra
C
lSin
C1,C2
C2
C3
C2,C3

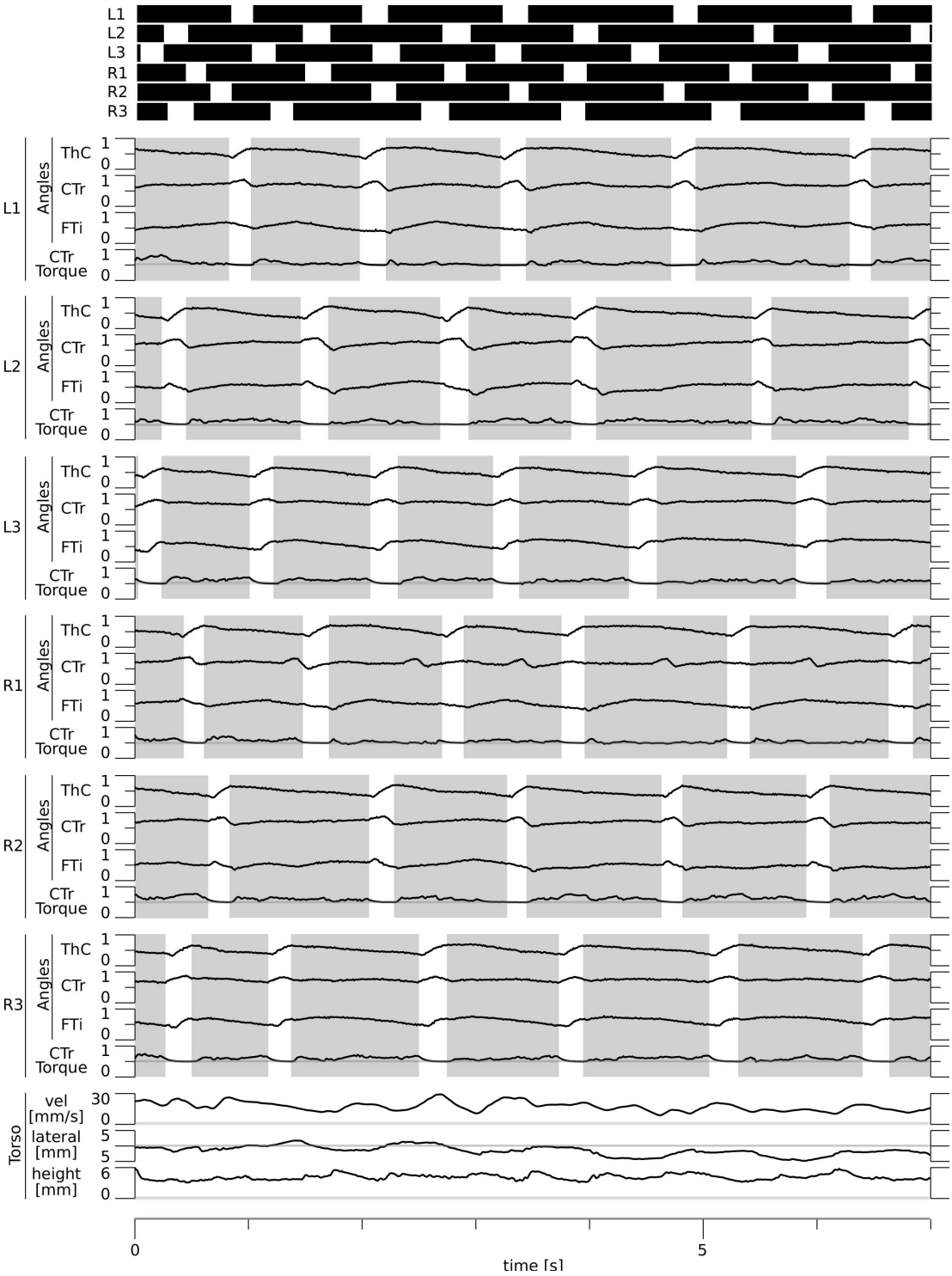

Figure 8.10.: Time plot of important parameters of all six legs during stick insect hexapod walking

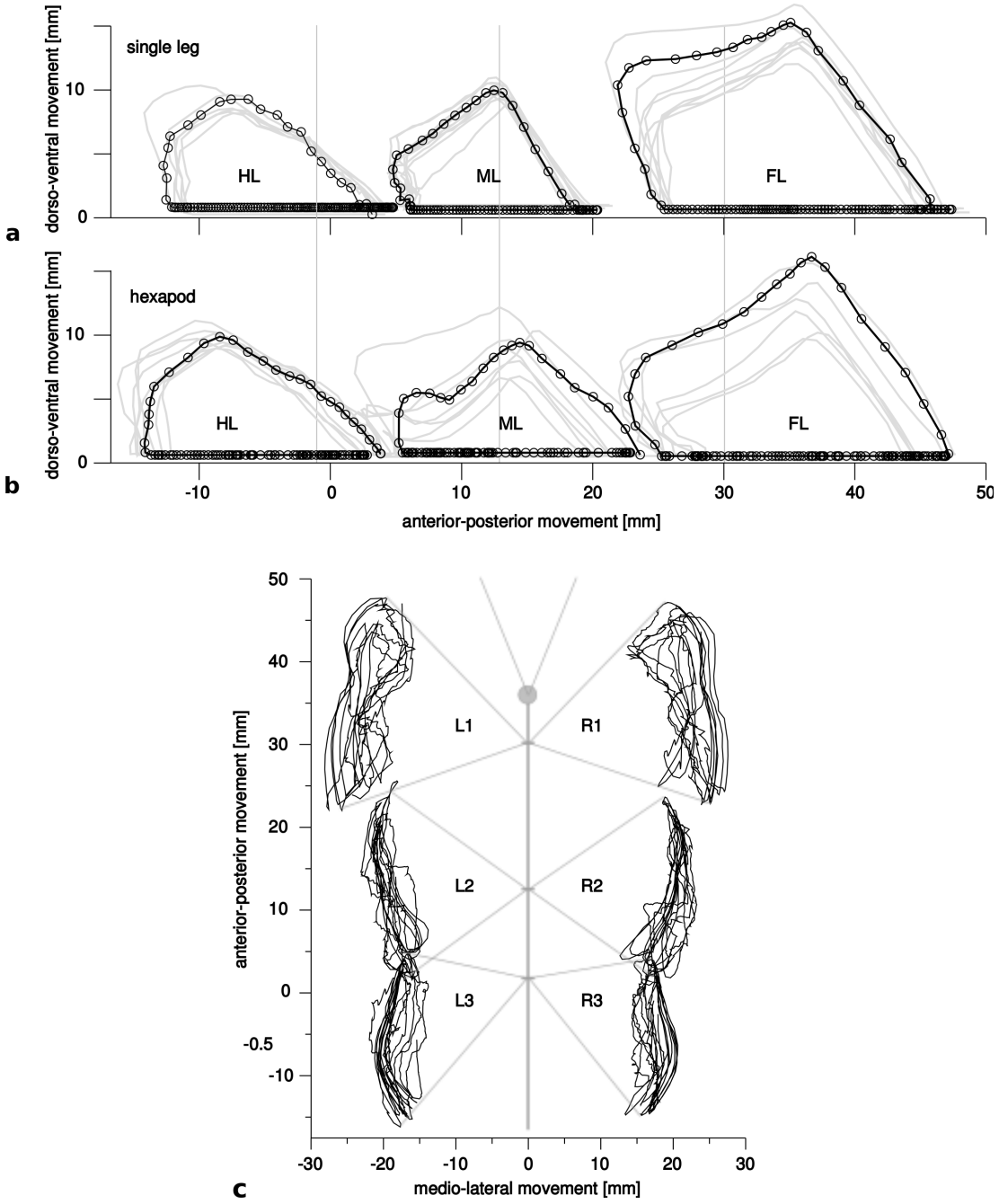

Figure 8.11.: Foot trajectories of all feet of the simulated stick insect: **a** lateral view for single leg walking, **b** lateral view for hexapod walking and **c** dorsal view for hexapod walking

9. General Conclusions

"Man darf daher mit Gewissheit erwarten, dass man, wenn man den Mechanismus des Gehens recht erkannt haben wird, daraus grossen Vortheil für die Erfindung neuer auf das Fortkommen berechneter Maschinen werde ziehen können, welche auch in unwegsamen Gegenden, wo das Fuhrwerk nicht zu gebrauchen ist, und wo sich der Mensch auf die Dienste der Kameele und andrer Thiere beschränken muss, ihren Zweck erfüllen werden."

(Wilhelm Weber and Eduard Weber: Mechanik der menschlichen Gehwerkzeuge, Weber and Weber (1836), p. 3)

"Happily, attention to biological detail has lead to a number of striking and unexpected similarities between neural and behavioral characteristics of the artificial insect and those of natural animals."

(Randall Beer: Intelligence as Adaptive Behavior, Beer (1990), p. 19)

9.1. Summary of Findings

Chapters 2–4: Approaches In chapter 2 the functional constraints and opportunities provided by the body and the environment, in robotics as well as in biology, were discussed in detail. This provided the basis for establishing transferability and comparability between natural and artificial systems.

Chapter 3 and 4 shaped the framework for integrative biological and robotic simulations of locomotion, by providing common sensor and motor interfaces to the neural controllers, including antagonistic motor interfaces with and without muscle models. Modular (neuro-)biologically inspired single-leg control structures and muscle models were implemented as neural networks. Finally, the method of modular evolution of hexapod controllers was introduced, together with a set of constraints, including perturbing scenarios, symmetry and structure cost functions.

Chapter 5: Evolved Single-Leg Neuro-Controllers By applying the evolutionary robotics approach to the control of walking in single robotic (AMOS-WD06) legs, extremely simple, yet very robust and effective, neuro-controllers were derived. As basic control mechanisms they exploited properties of body and environment by integrating multiple sensori-motor feedback (or reflex) loops and they made extensive use of hysteresis effects, i.e. bistability.

Chapter 6: Bio-Inspired Single-Leg Neuro-Controllers By applying multiple perturbation scenarios to the robotic model Octavio, the behavioral robustness of completely decentralized and modular neuro-biologically inspired single-leg controllers could be demonstrated. Furthermore the same controllers could easily be transferred to the stick insect simulator which differed tremendously in scale. Data from swing control, velocity control and support force experiments matched, to a large extent, biological data. The results suggested that the single leg controllers are well suited as modules of a hexapod controller. Therefore it was suggested, that the neuro-biologically inspired single-leg controller could serve as a bridge between morphological and functional approaches to stick insect locomotion control.

Chapter 7: Implications of Muscle-Model Properties for the Neural Control of Single-Leg Stepping Applying a muscle model derived from stick insect extensor data to robotic and stick insect models, advantages and constraints of the muscle model could be determined. On the one hand, an application of pairs of muscle models to all joints had the following advantages: muscle models could stabilize the joints working range, they supported slow and large amplitude step patterns, they showed an increased robustness under perturbing and noisy conditions and they could stabilize swing-stance transitions by their torque-velocity characteristics. On the other hand, several hypotheses were tested of how the nervous system could compensate for the slowness of stick insect muscle, including the usage of unloading information to trigger swing phase muscle activities, the usage of a servo mechanism that was active at the end of swing phase to stabilize swing-stance transitions and finally the general approach of phasic muscle activation to compensate for activation delays. All three hypotheses led to an improved behavioral performance.

Chapter 8: Hexapod Neuro-Controllers By combining the results on single-leg controllers of the previous chapters and by adding either bio-inspired or evolved sensorimotor coupling structures, robust hexapod controllers were developed. Hereby the feasibility of the modular approach, starting by the development of single-legs, was demonstrated for all simulated walkers presented in this thesis – from the stick insect-modeling point of view as well as from the evolutionary robotics point of view. For the first time it could be shown that the neuro-biologically inspired controller introduced by Ekeberg et al. (2004) is applicable to the control of a hexapod that is fully equipped with muscle models. Coupling was done by integrating it with the "Cruse" coupling rules derived from behavioral experiments (Cruse, 1990). Furthermore the role of leg specialization and examples of local vs. global co-ordination were shown.

9.2. Conclusion

Overall the four main objectives of this thesis were met: 1. General principles of sensorimotor couplings were discovered, 2. mechanisms of magnitude control of the neuro-biologically inspired controller (Ekeberg et al., 2004) were demonstrated in addition

to its suitability as a module in hexapod control, 3. the influence of a model of the stick insect extensor muscle on neural control of stepping was thoroughly characterized and 4. the introduced simulation framework was successfully used to develop hexapod controllers by evolution and by merging morphological and functional approaches of stick insect modeling.

The framework presented here offers an extensive approach to investigate neural and bio-mechanical control mechanisms of walking in stick insects and robots. It is seen as a step towards a more general integration of functional and morphological approaches to stick insect locomotion (Cruse et al., 2007). Since the "Cruse-rules" are only one possible coupling structure that produces the observed inter-leg co-ordination, it would be beneficial to develop alternative coupling schemes on top of the neuro-biologically inspired single-leg controllers. Hereby the evolutionary robotics approach will be employed, whereby recent data and modeling studies on neural inter-leg co-ordination (Borgmann et al., 2007, 2009; Daun-Gruhn, 2010; Ludwar et al., 2005) will be used to constrain the search space for the evolutionary algorithm.

Finally the standardized implementation of controllers and muscle models simplifies their transfer to hardware. Some evolved and bio-inspired single leg controllers, as well as simple hexapod controllers (cp. e.g. Fig. 8.3), have already been successfully transferred to the robot Octavio (Patel, 2008; von Twickel et al., 2012).

Literature by the Author

Journal Contributions

von Twickel A, Pasemann F (2007) Reflex-oscillations in evolved single leg neurocontrollers for walking machines. Natural Computing 6(3):311–337

von Twickel A, Büschges A, Pasemann F (2011) Deriving neural network controllers from neurobiological data – implementation of a single-leg stick insect controller. Biological Cybernetics 104(1–2):95–119

von Twickel A, Hild M, Siedel T, Patel V, Pasemann F (2012) Neural control of a modular multi-legged walking machine: Simulation and hardware. Robotics and Autonomous Systems 60(2):227 – 241

Conference Contributions

Hülse M, Wischmann S, Manoonpong P, von Twickel A, Pasemann F (2007) Dynamical systems in the sensorimotor loop – on the interrelation between internal and external mechanisms of evolved robot behavior. In: Lungarella M, et al (eds) 50 Years of Artificial Intelligence, Springer, LNAI, vol 4850, pp 186–195

von Twickel A, Pasemann F (2005) Evolved neural reflex-oscillators for walking machines. Lecture Notes in Computer Science 3561:376–385

von Twickel A, Pasemann F (2006) Adaptive behaviour of single legs with evolved neural control. In: Ijspeert AJ, Buchli J, Selverston A, Rabinovich M, Hasler M, Gerstner W, Billard A, Markram H, Floreano D (eds) Dynamical principles for neuroscience and intelligent biomimetic devices, EPFL, pp 137–138, iSBN 978-2-8399-0134-5

von Twickel A, Hild M, Siedel T, Pasemann F (2006) Octavio: Autonomous legs for a reconfigurable walking machine. In: Simonidis C (ed) HLR 2006, French-German Workshop on Humanoid and Legged Robots, Karlsruhe

von Twickel A, Blümel M, Pasemann F (2008a) Comparing neurocontrollers for walking evolved with and without muscle model. In: Proc. 4th Int. Symp. Adaptive Motion of Animals and Machines (AMAM 2008), Cleveland, OH, USA

von Twickel A, Blümel M, Pasemann F (2008b) Towards operational comparability of (neuro-)controllers in biology and robotics. In: Neuromechanics, Workshop at the Mathematical Bioscience Institute, Columbus, Ohio, USA

von Twickel A, Hellekes K, Pasemann F, Büschges A (2011) Interplay of local and global co-ordination in stick insect walking - an evolutionary robotics approach. In: 9th Göttingen Meeting of the German Neuroscience Society, pp T21–3B

Zahedi K, von Twickel A, Pasemann F (2008) Yars: A physical 3d simulator for evolving controllers for real robots. In: Carpin S, Noda I, Pagello E, Reggiani M, von Stryk O (eds) Simulation, Modeling and Programming for Autonomous Robots (SIMPAR 2008), Springer, LNAI, vol 5325, pp 75–86

Other Contributions

von Twickel A (2004) Obstacle perception by scorpions and robots – from biology to robotics via physical simulation and evolving neural networks. Diplomarbeit, Universität Bonn

Bibliography

Ahn AN, Full RJ (2002) A motor and a brake: two leg extensor muscles acting at the same joint manage energy differently in a running insect. Journal of Experimental Biology 205:379–389

Akay T, Bässler U, Gerharz P, Büschges A (2001) The role of sensory signals from the insect coxa-trochanteral joint in controlling motor activity of the femur-tibia joint. Journal of Neurophysiology 85:594–604

Akay T, Haehn S, Schmitz J, Büschges A (2004) Signals from load sensors underlie interjoint coordination during stepping movements of the stick insect leg. Journal of Neurophysiology 92:42–51

Akay T, Ludwar BC, Goritz ML, Schmitz J, Büschges A (2007) Segment specificity of load signal processing depends on walking direction in the stick insect leg muscle control system. The Journal of Neuroscience 27(12):3285–3294

Albu-Schäffer A, Ott C, Hirzinger G (2007) A unified passivity based control framework for position, torque and impedance control of flexible joint robots vol. 26, no. 1, 23-39, 2007 dlr science award 2007. Int Journal of Robotics Research 26(1):23–39

Alexander RM (1989) Optimization and gaits in the locomotion of vertebrates. Physiological Reviews 69:1199–1227

Alexander RM (1992) The work that muscles can do. Nature 357:360–361

Alexander RM (2002) Principles of Animal Locomotion. Princeton University Press

Anderson F, Arnold A, Pandy M, Goldberg S, Delp S (2006) Human Walking, Lippincott Williams & Williams, Inc., Philadelphia, chap Simulation of Walking

Aristotle (2007) On the Gait of Animals. eBooks@Adelaide, URL http://ebooks.adelaide.edu.au/a/aristotle/gait/

Audu ML, Davy DT (1985) The influence of muscle model complexity in musculoskeletal motion modeling. Journal of Biomechanical Engineering 107:147–157

Azevedo C, Espiau B, Amblard B, Assaiante C (2007) Bipedal locomotion: toward unified concepts in robotics and neuroscience. Biological Cybernetics 96:209–228

Azizi E, Brainerd EL, Roberts TJ (2008) Variable gearing in pennate muscles. PNAS 105(5):1745–1750

Bain A (1855) The senses and the intellect. J. W. Parker

Bar-Cohen Y (ed) (2004) Electroactive Polymer (EAP) Actuators as Artificial Muscles: Reality, Potential, and Challenges. Spie Press

Bartling C, Schmitz J (2000) Reaction to disturbances of a walking leg during stance. Journal of Experimental Biology 203:1211–1223

Bässler U (1983) Neural Basis of Elementary Behavior in Stick Insects. Springer Verlag

Bässler U (1988) Functional principles of pattern generation for walking movements of stick insect forelegs: The role of the femoral chordotonal organ afferences. The Journal of Experimental Biology 136:125–147

Bässler U (1993) The femur-tibia control system of stick insects — a model system for the study of the neural basis of joint control. Brain Research Reviews 18(2):207–226

Bässler U, Büschges A (1998) Pattern generation for stick insect walking movements – multisensory control of a locomotor program. Brain Research Reviews 27:65–88

Beer R, Gallagher J (1992) Evolving dynamical neural networks for adaptive behavior. Adaptive Behavior 1:91–122

Beer RD (1990) Intelligence as Adaptive Behavior. Academic Press

Beer RD (2003) The dynamics of active categorical perception in an evolved model agent. Adaptive Behavior 11(4):209–243

Beer RD (2009) Beyond control: The dynamics of brain-body-environment interaction in motor systems. In: Sternard D (ed) Progress in Motor Control V: A Multidisciplinary Perspective, Springer, Advances In Experimental Medicine And Biology, vol 629, pp 7–24

Beer RD, Williams PL (2009) Animals and animats: Why not both iguanas? Adaptive Behavior 17:296–302

Beer RD, Quinn RD, Chiel HJ, Ritzmann RE (1997) Biologically inspired approaches to robotics – what can we learn from insects? Communications of the ACM 40(3):31–38

Beer RD, Chiel HJ, Quinn RD, Ritzmann RE (1998) Biorobotic approaches to the study of motor systems. Current Opinion in Neurobiology 8:777–782

Bekey GA (2005) Autonomous Robots – From Biological Inspiration to Implementation and Control. MIT Press

Belanger JH (2005) Contrasting tactics in motor control by vertebrates and arthropods. Integr Comp Biol 45(4):672–678, DOI 10.1093/icb/45.4.672

Benner PF (2008) Phase relations of coupled oscillatory neural networks and applications in walking machines. Bachelor's thesis, University of Osnabrück

Bennet-Clark H (1995) Insect sound production: transduction mechanisms and impedance matching. Symp Soc Exp Biol 49:199–218

Bicchi A, Tonietti G (2002) Design, realization and control of soft robot arms for intrinsically safe interaction with humans. In: Proc. IARP/RAS Workshop on Technical Challenges for Dependable Robots in Human Environments, pp 79–87

Biewener AA (2003) Animal Locomotion. Oxford Univ Press

Biewener AA (2005) Biomechanical consequences of scaling. The Journal of Experimental Biology 208:1665–1676

Blaesing B, Cruse H (2004) Stick insect locomotion in a complex environment: climbing over large gaps. Journal of Experimental Biology 207:1273–1286

Blickhan R, Seyfarth A, Geyer H, Grimmer S, Wagner H, Günther M (2007) Intelligence by mechanics. Phil Trans R Soc A 365:199—-220

Blitz DM, Nusbaum MP (2007) Mechanosensory regulation of invertebrate motor systems. In: North G, Greenspan RJ (eds) Invertebrate Neurobiology, Cold Spring Harbor Laboratory, pp 185–208

Blümel M, Guschlbauer C, Gruhn S, Hooper SL, Büschges A (2011a) Hill-type muscle model parameters determined form experiments on single muscles show large animal-to-animal variation. (submitted to Biological Cybernetics)

Blümel M, Guschlbauer C, Hooper SL, Büschges A (2011b) Determining all parameters necessary to build hill-type muscle models from experiments on single muscles. (submitted to Biological Cybernetics)

Bobbert MF (2001) Dependence of human squat jump performance on the series elastic compliance of the triceps surae: A simulation study. The Journal of Experimental Biology 204:533–542

Bongard J (2011) Morphological change in machines accelerates the evolution of robust behavior. PNAS 108(4):1234–1239, DOI 10.1073/pnas.1015390108

Borgmann A, Scharstein H, Büschges A (2007) Intersegmental coordination: Influence of a single walking leg on the neighboring segments in the stick insect walking system. J Neurophysiol 98:1685–1696

Borgmann A, Hooper SL, Büschges A (2009) Sensory feedback induced by front-leg stepping entrains the activity of central pattern generators in caudal segments of the stick insect walking system. Journal of Neuroscience 29(9):2972—-2983

Brezina V, Weiss KR (2000) The neuromuscular transform constrains the production of functional rhythmic behaviors. J Neurophysiol 83:232–259

Brooks RA (1989) A robot that walks: Emergent behaviors from a carefully evolved network. Tech. Rep. AI MEMO 1091, MIT

Brooks RA (1991) Intelligence without representation. Artificial Intelligence (47):139–159

Brunn DE, Dean J (1994) Intersegmental and local interneurons in the metathorax of the stick insect carausius morosus that monitor middle leg position. Journal of Neurophysiology 72(3):1208–1219

Bucher D, Akay T, DiCaprio RA, Büschges A (2003) Interjoint coordination in the stick insect leg-control system: The role of positional signaling. Journal of Neurophysiology 89:1245–1255

Buddenbrock Wv (1921) Der Rhythmus der Schreitbewegungen der Stabheuschrecke Dyxippus. Biol Zentralblatt 41:41–48

Buehrmann T, Paolo ED (2006) Biological actuators are not just springs. In: SAB 2006

Burrows M (2010) Energy storage and synchronisation of hind leg movements during jumping in planthopper insects (hemiptera, issidae). Journal of Experimental Biology 213:469–478, DOI 10.1242/jeb.037861

Büschges A (2005) Sensory control and organization of neural networks mediating coordination of multisegmental organs for locomotion. Journal of Neurophysiology 93:1127–1135

Büschges A, Kittmann R, Schmitz J (1994) Identified nonspiking interneurons in leg reflexes and during walking in the stick insect. J Comp Physiol A 174:685–700

Büschges A, Schmitz J, Bässler U (1995) Rhythmic patterns in the thoracic nerve cord of the stick insect induced by pilocarpine. Journal of Experimental Biology 198:435–456

Büschges A, Akay T, Gabriel JP, Schmidt J (2008) Organizing network action for locomotion: Insights from studying insect walking. Brain Research Reviews 57:162–171

Calvitti A, Beer RD (2000) Analysis of a distributed model of leg coordination i. individual coordination mechanisms. Biol Cybern 82:197–206

Campolo D (2010) Motor selection via impedance-matching for driving nonlinearly damped, resonant loads. Mechatronics 20(5):566–573

Chakraborty A (2007) Neuro-controllers for single leg using torque driven motor system. Master thesis, Fachhochschule Bonn-Rhein-Sieg

Chiel H, Beer R (1997) The brain has a body: Adaptive behavior emerges from interactions of nervous system, body and environment. Trends in Neurosciences 20:553–557

Chiel HJ, Ting LH, Ekeberg O, Hartmann MJZ (2009) The brain in its body: Motor control and sensing in a biomechanical context. The Journal of Neuroscience 29(41):12,807–12,814

Chow CK, Jacobson DH (1971) Studies of human locomotion via optimal programming. Mathematical Biosciences 10(3-4):239–306

Clayton NS, Hen R (2005) Neural circuits and behaviour: developmental and evolutionary perspectives. Current Opinion in Neurobiology 15:683—-685

Collins S, Ruina A, Tedrake R, Wisse M (2005) Efficient bipedal robots based on passive-dynamic walkers. Science 307:1082–1085

Corcos D, Jiang HY, Wilding J, Gottlieb G (2002) Fatigue induced changes in phasic muscle activation patterns for fast elbow flexion movements. Experimental Brain Research 142:1–12

Cruse H (1976) The function of the legs in the free walking stick insect, carausius morosus. J comp Physiol 112:235–262

Cruse H (1979) The control of the anterior extreme position of the hindleg of a walking insect carausius morosus. Physiol Entomol 4:121–124

Cruse H (1980) A quantitative model of walking incorporating central and peripheral influences i. the control of the individual leg. Biol Cybern 37:131–136

Cruse H (1990) What mechanisms coordinate leg movement in walking arthropods? Trends in Neurosciences 13:15–21

Cruse H (2002) The functional sense of central oscillations in walking. Biological Cybernetics 86:271–280

Cruse H, Bartling C (1995) Movement of joint angles in the legs of a walking insect, carausius morosus. J Insect Physiol 41(9):761–771

Cruse H, Schmitz J, Braun U, Schweins A (1993) Control of body height in a stick insect walking on a treadwheel. Journal of Experimental Biology 181(1):141–155

Cruse H, Kühn S, Park S, Schmitz J (2004) Adaptive control for insect leg position: controller properties depend on substrate compliance. J Comp Physiol 190(12):983–991

Cruse H, Dürr V, Schmitz J (2007) Insect walking is based on a decentralized architecture revealing a simple and robust controller. Phil Trans R Soc A 365(1850):221–250

Dassow GV, Munro E (1999) Modularity in animal development and evolution: Elements of a conceptual framework for evodevo. Journal Of Experimental Zoology (Mol Dev Evol) 285:307–325

Daun-Gruhn S (2010) A mathematical modeling study of inter-segmental coordination during stick insect walking. Journal of Computational Neuroscience Online First:1–24, URL http://dx.doi.org/10.1007/s10827-010-0254-3

d'Avella A, Tresch M (2002) Modularity in the motor system: decomposition of muscle patterns as combinations of time-varying synergies. In: Dietterich T, Becker S, Ghahramani Z (eds) Advances in Neural Information Processing Systems 14, MIT Press

Dean J (1991) Effect of load on leg movement and step coordination of the stick insect carausius morosus. Journal of Experimental Biology 159:449–471

Dean J (1998) Animats and what they can tell us. Trends in Cognitive Science 2(2):60–67

Dean J, Wendler G (1983) Stick insect locomotion on a walking wheel: Interleg coordination of leg position. Journal of Experimental Biology 103:75–94

Dean J, Kindermann T, Schmitz J, Schumm M, Cruse H (1999) Control of walking in the stick insect: From behavior and physiology to modeling. Autonomous Robots 7:271–288

Debrodt B, Bässler U (1990) Responses of flexor motor neurons to stimulation of the femoral chordotonal organ of the phasmid extratosoma tiaratum. Zool Jb Physiol 94:101––119

Delcomyn F (1999) Walking robots and the central and peripheral control of locomotion in insects. Autonomous Robots 7:259–270

Dennis R, Herr H (2005) Engineered muscle actuators: cells and tissues. In: Cohen YB (ed) Biomimetics: biologically inspired technologies, CRC Press, New York

Dickinson MH, Farley CT, Full RJ, Koehl MAR, Kram R, Lehmann S (2000) How animals move: An integrative view. Science 288:100–106

Dillmann R, Albiez J, Gaßmann B, Kerscher T, Zöllner M (2007) Biologically inspired walking machines: design, control and perception. Phil Trans R Soc A 365(1850):133–151

Dirks JH, Federle W (2011) Mechanisms of fluid production in smooth adhesive pads of insects. Journal of The Royal Society Interface DOI 10.1098/rsif.2010.0575

Dirks JH, Clemente CJ, Federle W (2010) Insect tricks: two-phasic foot pad secretion prevents slipping. Journal of The Royal Society Interface 7(45):587–593

Drechsler P, Federle W (2006) Biomechanics of smooth adhesive pads in insects: influence of tarsal secretion on attachment performance. Journal of Comparative Physiology A: Neuroethology, Sensory, Neural, and Behavioral Physiology 192:1213–1222

Dudek DM, Full RJ (2006) Passive mechanical properties of legs from running insects. Journal of Experimental Biology 209:1502–1515, DOI 10.1242/jeb.02146

Dumont JPC, Robertson RM (1986) Neuronal circuits: An evolutionary perspective. Science 233:849–853

Dürr V (2001) Stereotypic leg searching movements in the stick insect: Kinematic analysis, behavioural context and simulation. Journal of Experimental Biology 204:1589–1604

Dürr V (2005) Context-dependent changes in strength and efficacy of leg coordination mechanisms. Journal of Experimental Biology 208:2253–2267

Dürr V, Schmitz J, Cruse H (2004) Behaviour-based modelling of hexapod locomotion: Linking biology and technical application. Arthropod Structure & Development 33:237–250

Duysens J, Clarac F, Cruse H (2000) Load-regulating mechanisms in gait and posture: comparative aspects. Physiological Reviews 80(1):83–133

Ekeberg O, Pearson KG (2005) Computer simulation of stepping in the hind legs of the cat: an examination of mechanisms regulating the stance-to-swing transition. Journal of Neurophysiology 94:4256–4268

Ekeberg O, Blümel M, Büschges A (2004) Dynamic simulation of insect walking. Arthropod Structure & Development 33:287–300

English C, Russell D (1999) Implementation of variable joint stiffness through antagonistic actuation using rolamite springs. Mechanism and Machine Theory 34(1):27–40

Espenschied KS, Quinn RD, Beer RD, Chiel HJ (1996) Biologically based distributed control and local reflexes improve rough terrain locomotion in a hexapod robot. Robotics and Autonomous Systems 18:59–64

Farahat WA, Herr HM (2010) Optimal workloop energetics of muscle-actuated systems: An impedance matching view. PLoS Comput Biol 6(6):e1000,795

Farley CT, Houdijk HHP, Strien CV, Louie M (1998) Mechanism of leg stiffness adjustment for hopping on surfaces of different stiffnesses. J Appl Physiol 85:1044–1055

Feng J (ed) (2004) Computational Neuroscience – A comprehensive Approach. Chapman & Hall/CRC

Ferrell C (1995) A comparison of three insect inspired locomotion controllers. Robotics and Autonomous Systems 16:135–159

Filliat D, Kodjabachian J, Meyer JA (1999) Evolution of neural controllers for locomotion and obstacle avoidance in a six-legged robot. Connection Science 11(3+4):225–242

Fisch K (2007) Untersuchungen zur rolle und funktion tarsaler sensorischer signale bei der laufmustergenerierung im mittelbein der stabheuschrecke carausius morosus. Master's thesis, Universität zu Köln

Fischer H, Schmidt J, Haas R, Büschges A (2001) Pattern generation for walking and searching movements of a stick insect leg. i. coordination of motor activity. Journal of Neurophysiology 85:341–353

Fischer I, Hennecke F, Bannes C, Zell A (2002) Javanns: Java neural network simulator, user manual, version 1.1. URL http://www.ra.cs.uni-tuebingen.de/software/JavaNNS/manual/JavaNNS-manual.html, last visited November 4th, 2009

Fischer J, Pasemann F, Manoonpong P (2004) Neuro-controllers for walking machines - an evolutionary approach to robust behavior. In: Proc. of the 7th int. Conference on Climbing and Walking Robots (CLAWAR)

Flash T, Hochner B (2005) Motor primitives in vertebrates and invertebrates. Current Opinion in Neurobiology 15:1–7

Floreano D, Husbands P, Nolfi S (2008) Evolutionary robotics. In: Siciliano B, Khatib O (eds) Handbook of Robotics, Springer, chap 61

Foth E, Graham D (1983) Influence of loading parallel to the body axis on the walking coordination of an insect – i. ipsilateral effects. Biological Cybernetics 47(1):17–23

Franklin RF (1985) The locomotion of hexapods on rough ground. In: Gewecke M, Wendler G (eds) Insect Locomotion, Paul Parey, pp 69–78

Frigon A, Rossignol S (2006) Experiments and models of sensorimotor interactions during locomotion. Biological Cybernetics 95(6):607–627

Full RJ, Blickhan R, Ting LH (1991) Leg design in hexapedal runners. Journal of Experimental Biology 158:369–390

Futakata Y, Iwasaki T (2008) Formal analysis of resonance entrainment by central pattern generator. J Math Biol

Gabriel JP, Büschges A (2007) Control of stepping velocity in a single insect leg during walking. Phil Trans R Soc A 365:251–271

Gabriel JP, Scharstein H, Schmidt J, Büschges A (2003) Control of flexor motoneuron activity during single leg walking of the stick insect on an electronically controlled treadwheel. Journal of Neurobiology 56:237–251

Gallagher JC, Beer RD, Espenscheid KS, Quinn RD (1996) Application of evolved locomotion controllers to a hexapod robot. Robotics and Autonomous Systems 19:95–103

Garcia M, Kuo A, Peattie A, Wang P, Full R (2000) Damping and size: Insights and biological inspiration. In: First International Symposium on Adaptive Motion of Animals and Machines, Montreal, Canada

Gerritsen KGM, van den Bogert AJ, Hulliger M, Zernicke RF (1998) Intrinsic muscle properties facilitate locomotor control – a computer simulation study. Motor Control 2:206–220

Ghatak A, Majumder A, Kumar R (2009) Hysteresis of soft joints embedded with fluid-filled microchannels. J R Soc Interface 6(31):203—-208

Ghazi-Zahedi KM (2008) Self-regulating neurons. A model for synaptic plasticity in artificial recurrent neural networks. PhD thesis, University of Osnabrück

Goldammer J, Mentel T, Büschges A (2007) A tracing study of leg motoneurons in carausius morosus. In: 100th Annual meeting of the Deutsche Zoologische Gesellschaft, Köln

Gorb SN, Beutel RG, Gorb EV, Jiao Y, Kastner V, Niederegger S, Popov VL, Scherge M, Schwarz U, Vötsch W (2002) Structural Design and Biomechanics of Friction-Based Releasable Attachment Devices in Insects. Integrative and Comparative Biology 42(6):1127–1139

Goslow GE, Reinking RM, Stuart DG (1973) The cat step cycle: Hind limb joint angles and muscle lengths during unrestrained locomotion. Journal of Morphology 141(1):1–41

Graham D (1972) A behavioural analysis of the temporal organization of walking movements in the 1st intar and adult stick insect *Carausius morosus*. J Comp Physiol 81:23–52

Graham D (1983) Insects are both impeded and propelled by their legs during walking. J Exp Biol 104:129–137

Graham D (1985) Pattern and control of walking in insects. Advances in Insect Physiology 18:31–140

Graham D, Cruse H (1981) Coordinated walking of stick insects on a mercury surface. J exp Biol 92:229–241

Grebenstein M, van der Smagt P (2008) Antagonism for a highly anthropomorphic hand–arm system. Advanced Robotics 22:39–55

Gribble P, Mullin L, Cothros N, Mattar A (2003) Role of cocontraction in arm movement accuracy. J Neurophysiol 89:2396–2405

Gribble PL, Ostry DJ (1999) Compensation for interaction torques during single- and multijoint limb movement. The Journal of Neurophysiology 82(5):2310–2326

Grillner S (1981) Control of locomotion in bipeds, tetrapods, and fish. In: Bethesda M (ed) Handbook of Physiology. The Nervous System. Motor Control. sect. 1, vol 2, Am. Physiol. Soc., pp 1179–1236

Grillner S (2006) Biological pattern generation: The cellular and computational logic of networks in motion. Neuron 52(5):751–766

Grillner S, Ekeberg O, Manira AE, Lansner A, Parker D, Tegner J, Wallen P (1998) Intrinsic function of a neuronal network - a vertebrate central pattern generator. Brain Res Rev 26(2–3):184–197

Gruhn M, Hoffmann O, Duebbert M, Scharstein H, Büschges A (2006) Tethered stick insect walking: A modified slippery surface setup with optomotor stimulation and electrical monitoring of tarsal contact. Journal of Neuroscience Methods 158:195–206

Gruhn M, von Uckermann G, Westmark S, Wosnitza A, Büschges A, Borgmann A (2009) Control of stepping velocity in the stick insect carausius morosus. J Neurophysiol 102:1180–1192

Guschlbauer C (2009) Characterisation of the biomechanical, passive, and active properties of femur-tibia joint leg muscles in the stick insect carausius morosus. PhD thesis, Universität zu Köln

Guschlbauer C, Scharstein H, Büschges A (2007) The extensor tibiae muscle of the stick insect: Biomechanical properties of an insect walking muscle. Journal of Experimental Biology 210:1092–1108

Haeufle DFB, Grimmer S, Seyfarth A (2010) The role of intrinsic muscle properties for stable hopping—stability is achieved by the force–velocity relation. Bioinspir Biomim 5:016,004

Halbertsma J (1983) The stride cycle of the cat: the modelling of locomotion by computerized analysis of automatic recordings. Acta Physiol Scand Suppl 521:1–75

Ham RV, Damme MV, Verrelst B, Vanderborght B, Lefeber D (2007) Maccepa, the mechanically adjustable compliance and controllable equilibrium position actuator: A 3dof joint with two independent compliances. International Applied Mechanics 43(4):467–474

Hatsopoulos NG (1996) Coupling the neural and physical dynamics in rhythmic movements. Neural Computation 8:567–581

Hatsopoulos NG, Burrows M, Laurent G (1995) Hysteresis reduction in proprioception using presynaptic shunting inhibition. Journal of Neurophysiology 73(3):1031–1042

Haykin S (1999) Neural Networks - A Comprehensive Foundation, 2nd edn. Prentice Hall International, New Jersey

He J, Deem MW (2010) Hierarchical evolution of animal body plans. Developmental Biology 337(1):157–161

Heinzel HG, Weimann JM, Marder E (1993) The behavioral repertoire of the gastric mill in the crab, *Cancer pagurus*: An in situ endoscopic and electrophysiological examination. Journal of Neuroscience 13(4):1793–1803

Heitler WJ (1974) The locust jump. Journal of Comparative Physiology A: Neuroethology, Sensory, Neural, and Behavioral Physiology 89(1):93–104

Herr HM, Kornbluh RD (2004) New horizons for orthotic and prosthetic technology: artificial muscle for ambulation. In: Bar-Cohen Y (ed) Smart Structures and Materials 2004: Electroactive Polymer Actuators and Devices (EAPAD), Proceedings of the SPIE, vol 5385, pp 1–9

Hess D, Büschges A (1997) Sensorimotor pathways involved in interjoint reflex action of an insect leg. Journal of Neurobiology 33(7):891–913

Hild M (2008) Neurodynamische Module zur Bewegungssteuerung Autonomer Mobiler Roboter. PhD thesis, Humboldt-Universität zu Berlin

Hill AV (1938) The heat of shortening and the dynamic constants of muscle. Proc R Soc Lond B 126:126–195

Hirose M, Ogawa K (2007) Honda humanoid robots development. Phil Trans R Soc A 365(1850):11–19

Hof A (2003) Muscle mechanics and neuromuscular control. Journal of Biomechanics 36:1031–1038

Hogan N (1985) Impedance control - an approach to manipulation. i - theory. ASME, Transactions, Journal of Dynamic Systems, Measurement, and Control 107:1–7

Hooper SL, Weaver AL (2000) Motor neuron activity is often insufficient to predict motor response. Current Opinion in Neurobiology 10:676–682

Hooper SL, Guschlbauer C, von Uckermann G, Büschges A (2006) Natural neural output that produces highly variable locomotory movements. J Neurophysiol 96:2072–2088

Hooper SL, Guschlbauer C, von Uckermann G, Büschges A (2007) Slow temporal filtering may largely explain the transformation of stick insect (carausius morosus) extensor motor neuron activity into muscle movement. J Neurophysiol 98:1718–1732

Hooper SL, Guschlbauer C, Blümel M, Rosenbaum P, Gruhn M, Akay T, Büschges A (2009) Neural control of unloaded leg posture and of leg swing in stick insect cockroach, and mouse differs from that in larger animals. The Journal of Neuroscience 29(13):4109–4119

Hülse M, Pasemann F (2006) Modular design of irreducible systems. In: Nolfi S (ed) From animals to Animats 9. 9th International Conference on Simulation of Adaptive Behavior, SAB 2006, Springer-Verlag, Berlin, no. 4095 in LNAI, pp 534–545

Hülse M, Wischmann S, Pasemann F (2004) Structure and function of evolved neuro-controllers for autonomous robots. Connection Science 16(4):249–266

Hülse M, Wischmann S, Manoonpong P, von Twickel A, Pasemann F (2007) Dynamical systems in the sensorimotor loop – on the interrelation between internal and external mechanisms of evolved robot behavior. In: Lungarella M, et al (eds) 50 Years of Artificial Intelligence, Springer, LNAI, vol 4850, pp 186–195

Iida F, Minekawa Y, Rummel J, Seyfarth A (2009) Toward a human-like biped robot with compliant legs. Robotics and Autonomous Systems 57(2):139–144

Ijspeert A, Crespi A, Ryczko D, Cabelguen JM (2007) From swimming to walking with a salamander robot driven by a spinal cord model. Science 315(5817):1416–1420

Iwasaki T, Zheng M (2006) Sensory feedback mechanism underlying entrainment of central pattern generator to mechanical resonance. Biol Cybern 94:245–261

Izhikevich EM (2007) Dynamical Systems in Neuroscience: The Geometry of Excitability and Bursting. The MIT Press

Izquierdo EJ, Lockery SR (2010) Evolution and analysis of minimal neural circuits for klinotaxis in caenorhabditis elegans. The Journal of Neuroscience 30(39):12,908–12,917, DOI 10.1523/JNEUROSCI.2606-10.2010

Jacob D, Polani D, Nehaniv CL (2005) Legs that can walk: Embodiment-based modular reinforcement learning applied. In: IEEE Computational Intelligence in Robotics & Automata (IEEE CIRA 2005), pp 365–372

Jander R (1975) Ecological aspects of spatial orientation. Annual Review of Ecology and Systematics 6:171–188

Jansen T, Niemeijer J (2007) The Great pretender: Works of art by Theo Jansen. Uitgeverij 010

Jindrich DL, Full RJ (2002) Dynamic stabilization of rapid hexapedal locomotion. Journal of Experimental Biology 205:2803–2823

Johansson J, Sherrill D, Riley P, Bonato P, Herr H (2005) A clinical comparison of variable-damping and mechanically passive prosthetic knee devices. Am J Phys Med Rehabil 84(8):563–575

Johnson K (2004) Closing in on the neural mechanisms of finger joint angle sense. focus on "quantitative analysis of dynamic strain sensitivity in human skin mechanoreceptors". J Neurophysiol 92:3167—-3168

Kaliyamoorthy S, Quinn RD, Zill SN (2005) Force sensors in hexapod locomotion. The International Journal of Robotics Research 24:563–574

Katz PS, Harris-Warrick RM (1999) The evolution of neuronal circuits underlying species-specific behavior. Current Opinion in Neurobiology 9:628—-633

Kavanau JL (1990) Conservative behavioural evolution, the neural substrate. Animal Behaviour 39:758–767

Kavounoudias A, Roll R, Roll JP (2001) Foot sole and ankle muscle inputs contribute jointly to human erect posture regulation. The Journal of Physiology 532:869–878

Kindermann T (2002) Behavior and adaptability of a six-legged walking system with highly distributed control. Adaptive Behavior 9(1):16–41

Klug S, Möhl B, von Stryk O, Barth O (2005) Design and application of a 3 dof bionic robot arm. In: Proc. 3rd Intl. Symposium on Adaptive Motion in Animals and Machines (AMAM)

Klute GK, Czerniecki JM, Hannaford B (2002) Artificial muscles: Actuators for biorobotic systems. The International Journal of Robotics Research 21(4):295–309

Koditschek DE, Full RJ, Buehler M (2004) Mechanical aspects of legged locomotion control. Arthropod Structure & Development 33:251–272

Komsuoglu H, Sohn K, Full RJ, Koditschek DE (2009) A physical model for dynamical arthropod running on level ground. In: Khatib O, Kumar V, Pappas GJ (eds) Experimental Robotics – The Eleventh International Symposium, Springer, pp 303–317

Kononenko NI, Dudek FE (2006) Persistent calcium current in rat suprachiasmatic nucleus neurons. Neuroscience 138:377–388

Kostyukov AI (1998) Muscle hysteresis and movement control: A theoretical study. Neuroscience 83(1):303–320

Kovac M, Schlegel M, Zufferey JC, Floreano D (2010) Steerable miniature jumping robot. Autonomous Robots 28(3):295–306

Kubow TM, Full RJ (1999) The role of the mechanical system in control: a hypothesis of self-stabilization in hexapedal runners. PhilTrans R Soc Lond B 354:849–861

Laffranchi M, NGTsagarakis, Cannella F, DGCaldwell (2009) Antagonistic and series elastic actuators: A comparative analysis on the energy consumption. In: The 2009 IEEE/RSJ International Conference on Intelligent Robots and Systems, St. Louis, USA

Lee DV, McGuigan MP, Yoo EH, Biewener AA (2008) Compliance, actuation, and work characteristics of the goat foreleg and hindleg during level, uphill, and downhill running. J Appl Physiol 104(1):130—-141

Lee PJ, Rogers EL, Granata KP (2006) Active trunk stiffness increases with co-contraction. J Electromyogr Kinesiol 16(1):51—-57

Lee RH, Heckman CJ (1998) Bistability in spinal motoneurons in vivo: Systematic variations in persistent inward currents. J Neurophysiol 80:583–593

Levine WS (ed) (1996) The Control Handbook. Crc Press

Lévy J, Cruse H (2008) Controlling a system with redundant degrees of freedom: II. solution of the force distribution problem without a body model. J Comp Physiol A 194(8):735–750

Lewinger WA, Rutter BL, Blümel M, Büschges A, Quinn RD (2006) Sensory coupled action switching modules (SCASM) generate robust, adaptive stepping in legged robots. In: Proceedings of the 9th International Conference on Climbing and Walking Robots (CLAWAR 2006), Brussels

Lewis M, Fagg AH, Solidumsp A (1992) Genetic programming approach to the construction of a neural network for control of a walking robot. In: IEEE International Conference on Robotics and Automation, pp 2618–2623

Lichtwark GA, Barclay CJ (2010) The influence of tendon compliance on muscle power output and efficiency during cyclic contractions. Journal of Experimental Biology 213:707–714

Linder CR (2005) Embodiment in two dimensions. In: Proceedings of the 7th International Conference on Climbing and Walking Robots 2004

Lindstedt SL, LaStayo PC, , Reich TE (2001) When active muscles lengthen: Properties and consequences of eccentric contractions. News Physiol Sci 16:256–261

Lipson H, Bongard J, Zykov V, Malone E (2006) Evolutionary robotics for legged machines: From simulation to physical reality. In: Proceedings of the 9th Int. Conference on Intelligent Autonomous Systems. (2006, pp 11–18

Loeb GE, Brown IE, Cheng EJ (1999) A hierarchical foundation for models of sensorimotor control. Experimental Brain Research 126(1):1–18

Ludwar BC, Göritz ML, Schmidt J (2005) Intersegmental coordination of walking movements in stick insects. Journal of Neurophysiology 93:1255–1265

Maas H, Sandercock TG (2010) Force transmission between synergistic skeletal muscles through connective tissue linkages. Journal of Biomedicine and Biotechnology pp 1–9, DOI 10.1155/2010/575672, article ID 575672

Manoonpong P, Pasemann F, Fischer J, Roth H (2005) Neural processing of auditory signals and modular neural control for sound tropism of walking machines. International Journal of Advanced Robotic Systems 2:223–235

Manoonpong P, Pasemann F, Wörgötter F (2008) Sensor-driven neural control for omnidirectional locomotion and versatile reactive behaviors of walking machines. Robotics and Autonomous Systems 56(3):265–288

Markelic I, Zahedi K (2007) An evolved neural network for fast quadrupedal locomotion. In: Proceedings of the 10th International Conference on Climbing and Walking Robots (CLAWAR)

Marques H, Jäntsch M, Wittmeier S, Alessandro C, Holland O, Alessandro C, Diamond A, Lungarella M, Knight R (2010) Ecce1: the first of a series of anthropomimetic musculoskelal upper torsos. In: Proceedings of Humanoids 2010

Martinez-Villalpando EC, Herr H (2009) Agonist-antagonist active knee prosthesis: A preliminary study in level-ground walking. Journal of Rehabilitation Research & Development 46(3):361—-374

Maturana H, Varela F (1992) The tree of knowledge: the biological roots of human understanding. Shambhala

Maufroy C, Kimura H, Takase K (2008) Towards a general neural controller for quadrupedal locomotion. Neural Networks 21:667–681

Mazzapioda M, Nolfi S (2006) Synchronization and gait adaptation in evolving hexapod robots. Springer, pp 113–125

McGeer T (1990a) Passive dynamic walking. International Journal of Robotics Research 9:62–82

McGeer T (1990b) Passive walking with knees. In: Proc. IEEE Robotics & Automation Conference, Cincinnati, OH, pp 1640–1645

McGowan CP, Neptune RR, Clark DJ, Kautz SA (2010) Modular control of human walking: Adaptations to altered mechanical demands. Journal of Biomechanics 43:412—-419

McMahon TA (1984) Muscles, Reflexes, and Locomotion. Princeton University Press

Mei ZQ, Yang RQ, Liang C, Li GB (2004) The study of backlash compensation and its application in the robot checking the filter. The International Journal of Advanced Manufacturing Technology 25(3–4):396–401

Mentel T, Weiler V, Büschges A, Pflüger HJ (2008) Activity of neuromodulatory neurones during stepping of a single insect leg. Journal of Insect Physiology 54:51–61

Meyer JA (1995) The animat approach to cognitive science. In: Roitblat H, Meyer JA (eds) Comparative Approaches to Cognitive Science, MIT Press / Bradford Books

Missenard O, Mottet D, Perrey S (2008) The role of cocontraction in the impairment of movement accuracy with fatigue. Exp Brain Res 185:151—-156

Morris LG, Thuma JB, Hooper SL (2000) Muscles express motor patterns of non-innervating neural networks by filtering broad-band input. Nature Neuroscience 3:245–250

Muybridge E (1967) Animals in Motion. Dover Pubn Inc

Nakanishi Y, Namiki Y, Urata J, Mizuuchi I, Inaba M (2007) Design of tendon driven humanoid's lower body equipped with redundant and high-powered actuators. In: Proceedings of the 2007 IEEE/RSJ International Conference on Intelligent Robots and Systems, San Diego, CA, USA

Nef T, Lum P (2009) Improving backdrivability in geared rehabilitation robots. Medical and Biological Engineering and Computing 47(4):441–447

Negrello M, Hülse M, Pasemann F (2008) Adaptive neurodynamics. In: Yang A, Shan Y (eds) Applications of Complex Adaptive Systems, Idea Group: Hershey, PA. USA, pp 85 – 111

Neptune RR, Kautz SA (2001) Muscle activation and deactivation dynamics: The governing properties in fast cyclical human movement performance? Exerc Sports Sci Rev 29(2):76–81

Newcomb JM, Katz PS (2009) Different functions for homologous serotonergic interneurons and serotonin in species-specific rhythmic behaviours. Proceedings of the Royal Society B 276:99–108

Nishikawa K, Biewener AA, Aerts P, Ahn AN, Chiel HJ, Daley MA, Daniela TL, Full RJ, Hale ME, Hedricka TL, Lappin AK, Nichols TR, Quinn RD, Satterlie RA, Szymik B (2007) Neuromechanics: an integrative approach for understanding motor control. Integr Comp Biol 47(1):16–54

Nolfi S, Floreano D (2000) Evolutionary Robotics: The Biology, Intelligence, and Technology of Self-Organizing Machines. MIT Press, Cambridge, MA

Orlovsky G, Deliagina T, Grillner S (1999) Neuronal Control of Locomotion. Oxford University Press

Pasemann F (1993) Dynamics of a single model neuron. International Journal of Bifurcation and Chaos 2:271–278

Pasemann F (1995) Characterization of periodic attractors in neural ring networks. Neural Networks 8:421–429

Pasemann F (2002) Complex dynamics and the structure of small neural networks. Network: Computation in neural systems 13:195–216

Pasemann F, Steinmetz U, Hülse M, Lara B (2001) Robot control and the evolution of modular neurodynamics. Theory in Biosciences 120:311–326

Pasemann F, Hild M, Zahedi K (2003) SO(2)-networks as neural oscillators. In: Mira J, Alvarez J (eds) Computational Methods in Neural Modeling, IWANN, Springer, Berlin, pp 144–151

Patel V (2008) Neuro-control in the sensorimotor loop: Multi-modal motor control for a modular walking machine. Master's thesis, Fachhochschule Bonn-Rhein-Sieg

Paul C (2006) Morphological computation: A basis for the analysis of morphology and control requirements. Robotics and Autonomous Systems 54(8):619 – 630

Pearson K, Iles J (1973) Nervous mechanisms underlying intersegmental co-ordination of leg movements during walking in the cockroach. J Exp Biol 58:725–744

Pearson K, Ekeberg O, Büschges A (2006) Assessing sensory function in locomotor systems using neuromechanical simulations ¨. Trends Neurosci 29(11):625–631

Pearson KG, Franklin R (1984) Characteristics of leg movements and patterns of coordination in locusts walking on rough terrain. International Journal of Robotics Research 3(2):101–112

Peterka RJ (2002) Sensorimotor integration in human postural control. The Journal of Neurophysiology 88(3):1097–1118

Pfeifer R, Bongard J (2006) How the Body Shapes the Way We Think – A New View of Intelligence. MIT Press

Pfeifer R, Gómez G (2009) Morphological computation – connecting brain, body, and environment. In: Sendhoff B, Körner E, Sporns O, Ritter H, Doya K (eds) Creating Brain-Like Intelligence, Lecture Notes in Computer Science, vol 5436, Springer, Berlin Heidelberg, pp 66–83

Pfeiffer F (2007) The tum walking machines. Phil Trans R Soc A 365(1850):109–131

Pons JL (2005) Emerging Actuator Technologies: A Micromechatronic Approach. John Wiley & Sons, Ltd

Pratt GA (2002) Low impedance walking robots. Integr Comp Biol 42(1):174–181

Pratt J, Krupp B (2004) Series elastic actuators for legged robots. In: Proceedings of SPIE-The International Society for Optical Engineering

Pratt J, Pratt G (1999) Exploiting natural dynamics in the control of a 3d bipedal walking simulation. In: Proceedings of the International Conference on Climbing and Walking Robots (CLAWAR99), Portsmouth, UK

Prochazka A, Gillard D, Bennett DJ (1997) Implications of positive feedback in the control of movement. Journal of Neurophysiology 77(6):3237–3251

Psujek S, Ames J, Beer R (2006) Connection and coordination: The interplay between architecture and dynamics in evolved model pattern generators. Neural Computation 18:729–747

Quinn RD, Nelson GM, Bachmann RJ, Kingsley DA, Offi JT, Allen TJ, Ritzmann RE (2003) Parallel complementary strategies for implementing biological principles into mobile robots. International Journal of Robotics Research 22(3):169–186

Radnikow G, Bässler U (1991) Function of a muscle whose apodeme travels through a joint moved by other muscles: Why the retractor unguis muscle in stick insects is tripartite and has no antagonist. Journal of Experimental Biology 157:87–99

Raibert M, Blankespoor K, Nelson G, Playter R, the BigDog Team (2008) Bigdog, the rough-terrain quadruped robot. In: Proceedings of the 17th World CongressThe International Federation of Automatic Control, Seoul, Korea

Rapoport S, Mizrahi J, Kimmel E, Verbitsky O, Isakov E (2003) Constant and variable stiffness and damping of the leg joints in human hopping. Journal of Biomechanical Engineering 125:507–514

Rassier DE, MacIntosh BR, Herzog W (1999) Length dependence of active force production in skeletal muscle. J Appl Physiol 86:1445–1457

Rathmayer W (2001) Motorische Steuerung bei Invertebraten. In: Neurowissenschaft – Vom Molekül zur Kognition, Springer

Redies C, Puelles L (2001) Modularity in vertebrate brain development and evolution. BioEssays 23(12):1100–1111

Rempis C, von Twickel A, Pasemann F (2008) Octavio: Evolution of modular neural control for legged locomotion. In: Workshop on Force and Load Feedback, Cologne, Germany

Revzen S, Koditschek DE, Full RJ (2009) Towards testable neuromechanical control architectures for running. In: Sternad D (ed) Progress In Motor Control – A Multidisciplinary Perspective, Springer, Advances In Experimental Medicine And Biology, vol 629, pp 25–56

Ritzmann RE, Büschges A (2007) Insect walking: From reduced preparations to natural terrain. In: North G, Greenspan RJ (eds) Invertebrate Neurobiology, Cold Spring Harbor Laboratory, pp 229–250

Ritzmann RE, Quinn RD, Watson JT, Zill SN (2000) Insect walking and biorobotics: A relationship with mutual benefits. BioScience 50(1):23–33

Ritzmann RE, Quinn RD, Fischer MS (2004) Convergent evolution and locomotion through complex terrain by insects, vertebrates and robots. Arthropod Structure & Development 33(3):361–379

Roberts TJ, Azizi E (2010) The series-elastic shock absorber: tendons attenuate muscle power during eccentric actions. J Appl Physiol 109:396–404

Rosano H, Webb B (2007) A dynamic model of thoracic differentiation for the control of turning in the stick insect. Biol Cybern 97:229–246

Rose GJ (2004) Insights into neural mechanisms and evolution of behaviour from electric fish. Nature Reviews Neuroscience 5:943–951

Rosenbaum P, Wosnitza A, Buschges A, Gruhn M (2010) Activity patterns and timing of muscle activity in the forward walking and backward walking stick insect Carausius morosus. Journal of Neurophysiology 104(3):1681–1695

Rutter BL, Lewinger WA, Blümel M, Büschges A, Quinn RD (2007) Simple muscle models regularize motion in a robotic leg with neurally-based step generation. In: 2007 IEEE International Conference on Robotics and Automation, Roma, pp 630–635

Sangbae Kim JEC, Cutkosky MR (2004) isprawl : Autonomy, and the effects of power transmission. In: Proceedings CLAWAR 2004

Scheint M, Sobotka M, Buss M (2008) Compliance in gait synthesis: Effects on energy and gait. In: 8th IEEE-RAS International Conference on Humanoids, pp 259–264

Schilling M, Cruse H, Arena P (2007) Hexapod walking: an expansion to walknet dealing with leg amputations and force oscillations. Biological Cybernetics 96(3):323–340

Schmitz J, Bartling C, Brunn D, Cruse H, Dean J, Kindermann T, Schumm M, Wagner H (1995) Adaptive properties of 'hard-wired' neuronal systems. Verh Dt Zool Ges 88:165—179

Schmitz J, Dean J, Kindermann T, Schumm M, Cruse H (2001) A biologically inspired controller for hexapod walking: Simple solutions by exploiting physical properties. Biol Bull 200:195–200

Schneider A (2006) Local positive velocity feedback for the movement control of elastic joints in closed kinematic chains: A modelling and simulation study of a 2dof arm and a 3dof insect leg. PhD thesis, Universität Bielefeld

Schneider A, Cruse H, Schmitz J (2006) Decentralized control of elastic limbs in closed kinematic chains. The International Journal of Robotics Research 25:913–930

Scholz I, Baumgartner W, Federle W (2008) Micromechanics of smooth adhesive organs in stick insects: pads are mechanically anisotropic and softer towards the adhesive surface. Journal of Comparative Physiology A: Neuroethology, Sensory, Neural, and Behavioral Physiology 194:373–384

Schumacher J (2008) Reflex oscillation in the sensorimotor loop of walking machines. Bachelor's thesis, University of Osnabrück

Schumm M, Cruse H (2006) Control of swing movement: influences of differently shaped substrate. Journal of Comparative Physiology A: Neuroethology, Sensory, Neural, and Behavioral Physiology 192(10):1147–1164

Scrivens J, DeWeerth S, Ting L (2008) A robotic device for understanding neuromechanical interactions during standing balance control. Bioinspir Biomim 3:026,002

Selverston AI, Panchin YV, Arshavsky YI, Orlovsky GN (1999) Shared features of invertebrate central pattern generators. In: Stein PS, Grillner S, Selverston AI, Stuart DG (eds) Neurons, Networks, and Motor Behavior, MIT Press, Cambridge, MA, pp 105–117

Serhan H, Nasr C, Henaff P (2010) Muscle emulation with dc motor and neural networks for biped robots. Int J Neural Syst 20(4):341–353

Seyfarth A, Kalveram KT, Geyer H (2007) Simulating muscle-reflex dynamics in a simple hopping robot. In: Brauer W, Berns K, Luksch T (eds) Autonome Mobile Systeme 2007, Informatik aktuell, Springer Berlin Heidelberg, pp 294–300

Seyfarth A, Iida F, Tausch R, Stelzer M, von Stryk O, Karguth A (2009) Towards bipedal jogging as a natural result of optimizing walking speed for passively compliant three-segmented legs. The International Journal of Robotics Research 28(2):257–265

Siciliano B, Khatib O (eds) (2008) Handbook of Robotics. Springer

Smith R (2009) Open dynamics engine. URL http://www.ode.org, (last visited: 18/11/2009)

Spenneberg D, Kirchner F (2007) Climbing & Walking Robots, Towards New Applications, Itech Education and Publishing, Vienna, Austria, chap The Bio-Inspired SCORPION Robot: Design, Control & Lessons Learned, pp 197–218

de Spinoza B (1994) A Spinoza Reader: The Ethics and Other Works. Princeton University Press

Sponberg S, Full RJ (2008) Neuromechanical response of musculo-skeletal structures in cockroaches during rapid running on rough terrain. Journal of Experimental Biology 211:433–446

Storrer J (1976) Systemanalytische untersuchungen am ʻkniesehnenreflexʻ der stabheuschrecke carausius morosus br. (orthoptera). PhD thesis, Universität Kaiserslautern

Suzuki M (2007) Complex and flexible robot motions by strand-muscle actuators. In: Zhang H (ed) Climbing and Walking Robots, Towards New Applications, Itech Education and Publishing, Vienna, Austria

Suzuki M, Ichikawa A (2004) Toward springy robot walk using strand-muscle actuators. In: Proc. 7th Int. Conference on Climbing and Walking Robots, pp 467–474

Taga G (1995) A model of the neuro-musculo-skeletal system for human locomotion i. emergence of basic gait. Biol Cybern 73:97–111

Thorson I, Svinin M, Hosoe S, Asano F, Taji K (2007) Design considerations for a variable stiffness series elastic actuator in a robot that walks and runs. In: ROBOMEC, Akita, Japan

Tierney A (1996) Evolutionary implications of neural circuit structure and function. Behavioural Processes 35:173–182

Toth TI, Hughes SW, Crunelli V (1998) Analysis and biophysical interpretation of bistable behaviour in thalamocortical neurons. Neuroscience 87(2):519–523

Trivedi D, Rahn CD, Kierb WM, Walker ID (2008) Soft robotics: Biological inspiration, state of the art, and future research. Applied Bionics and Biomechanics 5(3):99–117

Tryba A, Ritzmann R (2000a) Multi-joint coordination during walking and foothold searching in the Blaberus cockroach. I. Kinematics and electromyograms. Journal of Neurophysiology 83(6):3323

Tryba A, Ritzmann R (2000b) Multi-joint coordination during walking and foothold searching in the Blaberus cockroach. II. Extensor motor neuron pattern. Journal of Neurophysiology 83(6):3337

Turvey MT, Fonseca S (2009) Nature of motor control: Perspectives and issues. In: Sternad D (ed) Progress in Motor Control, Springer Science Business Media

von Twickel A, Pasemann F (2007) Reflex-oscillations in evolved single leg neurocontrollers for walking machines. Natural Computing 6(3):311–337

von Twickel A, Hild M, Siedel T, Pasemann F (2006) Octavio: Autonomous legs for a reconfigurable walking machine. In: Simonidis C (ed) HLR 2006, French-German Workshop on Humanoid and Legged Robots, Karlsruhe

von Twickel A, Büschges A, Pasemann F (2011) Deriving neural network controllers from neurobiological data – implementation of a single-leg stick insect controller. Biological Cybernetics 104(1–2):95–119

von Twickel A, Hild M, Siedel T, Patel V, Pasemann F (2012) Neural control of a modular multi-legged walking machine: Simulation and hardware. Robotics and Autonomous Systems 60(2):227 – 241

von Uckermann G, Büschges A (2009) Premotor interneurons in the local control of stepping motor output for the stick insect single middle leg. J Neurophysiol 102:1956–1975

Vanderborght B (2011) Dynamic Stabilisation of the Biped Lucy Powered by Actuators with Controllable Stiffness, Springer Tracts in Advanced Robotics, vol 63

Vanderborght B, Ham RV, Lefeber D, Sugar TG, Hollander KW (2009) Comparison of mechanical design and energy consumption of adaptable, passive-compliant actuators. The International Journal of Robotics Research 28(1):90–103

Verdaasdonk B, Koopman H, der Helm FV (2007) Resonance tuning in a neuro-musculo-skeletal model of the forearm. Biol Cybern 96(2):165–180

Wakeling JM, Liphardt AM, Nigg BM (2003) Muscle activity reduces soft-tissue resonance at heel-strike during walking. Journal of Biomechanics 36:1761—-1769

Watson J, Ritzmann R (1998) Leg kinematics and muscle activity during treadmill running in the cockroach, blaberus discoidalis. i. slow running. J Comp Physiol A Neuroethol Sens Neural Behav Physiol 182:11—-22

Webb B (2002) Robots in invertebrate neuroscience. Nature (417):359–363

Webb B (2009) Animals versus animats: Or why not model the real iguana? Adaptive Behavior 17(4):269–286

Weber WE, Weber EFW (1836) Mechanik der menschlichen Gehwerkzeuge – Eine anatomisch-physiologische Untersuchung. Göttingen, in der Dieterichschen Buchhandlung

Wendler G (1964) Laufen und Stehen der Stabheuschrecke Carausius Morosus: Sinnesborstenfelder in den Beingelenken als Glieder von Regelkreisen. Zeitschrift für vergleichende Physiologie 48:198–250

Wendler G (1966) The co-ordination of walking movements in arthropods. Symp Soc exp Biol 20:229–249

Williams CA, DeWeerth SP (2007) A comparison of resonance tuning with positive versus negative sensory feedback. Biological Cybernetics 96(6):603–614

Winter DA (2009) Biomechanics and Motor Control of Human Movement. John Wiley & Sons

Wischmann S (2008) Neural dynamics of social behavior – an evolutionary and mechanistic perspective on communication, cooperation, and competition among situated agents. PhD thesis, Universität Bonn

Wischmann S, Hülse M, Pasemann F (2005) (co)evolution of (de)centralized neural control for a gravitationally driven machine. In: et al C (ed) ECAL 2005, Springer, no. 3630 in LNAI, pp 179–188

Wisse M (2004) Essentials of dynamic walking analysis and design of two-legged robots. PhD thesis, Technische Universiteit Delft

Wolf H, Büschges A (1995) Nonspiking local interneurons in insect leg motor control. ii. role of nonspiking local interneurons in the control of leg swing during walking. J Neurophysiol 73:1861–1875

Wood R (2007) Design, fabrication, and analysis of a 3dof, 3cm flapping-wing mav. In: Proceedings of the 2007 IEEE/RSJ International Conference on Intelligent Robots and Systems, San Diego, CA, USA

Wu GC, Wright JC, Whitaker DL, Ahn AN (2010) Kinematic evidence for superfast locomotory muscle in two species of teneriffiid mites. Journal of Experimental Biology 213:2551–2556

Xiong G, Zhang J, Hong Y, Guan Y, Guan H (2008) Motor unit number estimation of the tibialis anterior muscle in spinal cord injury. Spinal Cord 46(10):696–702

Yakovenko S, Gritsenko V, Prochazka A (2004) Contribution of stretch reflexes to locomotor control: a modeling study. Biol Cybern 90(2):146–155

Yakovenko S, McCrea D, Stecina K, Prochazka A (2005) Control of locomotor cycle durations. J Neurophysiol 94:1057–1065

Yeadon M, King M, Forrester S, Caldwell G, Pain M (2010) The need for muscle co-contraction prior to a landing. Journal of Biomechanics 43(2):364–369

Yox D, DiCaprio R, Fourtner C (1982) Resting tension and posture in arthropods. J Exp Biol 96:421—-425

Zack TI, Claverie T, Patek SN (2009) Elastic energy storage in the mantis shrimp's fast predatory strike. Journal of Experimental Biology 212:4002–4009

Zahedi K, von Twickel A, Pasemann F (2008) Yars: A physical 3d simulator for evolving controllers for real robots. In: Carpin S, Noda I, Pagello E, Reggiani M, von Stryk O (eds) Simulation, Modeling and Programming for Autonomous Robots (SIMPAR 2008), Springer, LNAI, vol 5325, pp 75–86

Zajac FE (1993) Muscle coordination of movement: A perspective. J Biomechanics 26(Suppl. 1):109–124

Zakotnik J, Matheson T, Dürr V (2006) Co-contraction and passive forces facilitate load compensation of aimed limb movements. The Journal of Neuroscience 26(19):4995–5007

Zill S, Schmitz J, Büschges A (2004) Load sensing and control of posture and locomotion. Arthropod Structure & Development 33(3):273–286

Zill SN, Jepson-Innes K (1988) Evolutionary adaptation of a reflex system: sensory hysteresis counters muscle 'catch' tension. J Comp Physiol A 164:43–48

Appendix

A List of Figures

B List of Tables

C Abbreviations

AEP	Anterior Extreme Position
CPG	Central Pattern Generator
CTr	Coxa-Trochanter
DOF	Degree Of Freedom
fCO	femoral chordotonal organ
FL	Fore-Leg
FTi	Femur-Tibia
HL	Hind-Leg
ML	Middle-Leg
PEP	Posterior Extreme Position
PID	proportional-integral-derivative
ThC	Thorax-Coxa

D Technical Data of Robot Octavio and Stick Insect

Table D.1 on the following page gives detailed technical data of the simulated robot Octavio together with corresponding data from the stick insect (where available). Unless otherwise noted single leg data is only shown for middle-legs. Remarks for superscript indices: [1] Note that the modular robot Octavio has detachable legs which include the part corresponding to the thorax parts of the stick insect where the coxae attach, including the motor (muscles). For better comparison this part is here added to the thorax and not to the legs. [2] ThC joint setup in stick insects and Octavio differ, see text for details. In brackets angle ranges for *in vivo* walking on flat terrain are given. v is joint rotational velocity in rad/s. Joint friction in stick insects is more difficult to express in numbers due to complex muscle properties. Details are given in the cited literature.

Table D.1.: Technical data of stick insect and robotic model Octavio. See text for details

Quantity	Stick Insect	Data Source	Octavio	Ratio
Body length [mm]	75.0	Cruse (1976); Guschlbauer et al. (2007)	850.0	11.33
FL-HL coxae [mm]	28.4	Cruse (1976)	740.0	26.06
Total body mass [g]	0.9	Cruse (1976); Guschlbauer et al. (2007)	21970.0	24411.11
Distance head to [mm]				
Fl coxae	7.1	Cruse (1976)	55.0	7.75
Ml coxae	24.6	Cruse (1976)	495.0	20.12
Hl coxae	35.5	Cruse (1976)	795.0	22.39
COM	35.8	Cruse (1976)	447.0	12.49
Segment length [mm]				
a) ML	23.6	Cruse (1976)	562.5	23.83
Coxa	1.5	Cruse (1976)	51.0	34.00
Trochanterofemur	11.4	Cruse (1976)	232.5	20.39
Tibia+Tarsus	10.7	Cruse (1976)	279.0	26.07
Segment mass [g][1]				
Head-thorax-abdomen	0.77	Ekeberg et al. (2004)	5890.0	7649.35
a) ML	0.0108	Ekeberg et al. (2004)	2680.0	$2.48 * 10^5$
Coxa	0.0010	Ekeberg et al. (2004)	1200.0	$1.20*10^6$
Trochanterofemur	0.0081	Ekeberg et al. (2004)	1210.0	$1.49*10^5$
Tibia+Tarsus	0.0017	Ekeberg et al. (2004)	270.0	$1.58*10^5$
Joint Max Torques [mNm]				
a) ML				
ThC Pro	NA		9310.00	NA
ThC Ret	NA		9310.00	NA
CTr Lev	NA		9310.00	NA
CTr Dep	NA		9310.00	NA
FTi Flx	0.234	Guschlbauer (2009)	9310.00	39786.32
FTi Ext	0.043	Guschlbauer (2009)	9310.00	$2.17 * 10^5$
Joint Max Velocities [°/s]				
a) ML				
ThC Pro	NA		151.00	NA
ThC Ret	NA		151.00	NA
CTr Lev	NA		151.00	NA
CTr Dep	NA		151.00	NA
FTi Flx	616.0	Guschlbauer (2009)	151.00	0.25
FTi Ext	895.0	Guschlbauer (2009)	151.00	0.17
Joint Max Angles [°][2 3]				
a) ML				
ThC Min	NA(-48.0)	(Cruse and Bartling (1995))	-90.0	NA
ThC Max	NA(33.0)	(Cruse and Bartling (1995))	90.0	NA
CTr Min	-80.0(-8.0)	Cruse (1976)(Cruse and Bartling (1995))	-90.0	1.12
CTr Max	80.0(29.0)	Cruse (1976)(Cruse and Bartling (1995))	90.0	1.12
FTi Min	NA(42.0)	(Cruse and Bartling (1995))	-15.0	NA
FTi Max	NA(99.0)	(Cruse and Bartling (1995))	165.0	NA
Joint Friction [mNm][4]				
a) ML				
ThC static	[5]	Guschlbauer (2009)	1200	[5]
ThC dynamic	[5]	Guschlbauer (2009)	[2]	[5]
CTr static	[5]	Guschlbauer (2009)	1200	[5]
CTr dynamic	[5]	Guschlbauer (2009)	[2]	[5]
FTi static	[5]	Guschlbauer (2009); Hooper et al. (2009)	1200	[5]
FTi dynamic	[5]	Guschlbauer (2009); Hooper et al. (2009)	[2]	[5]

E Neural Network Parameters

Non listed parameters are assumed to have the value 0.0. Parameters are given first for the robotic model Octavio and then differing parameters for the stick insect model are listed.

Middle-Leg Sidewards

Synapse Strengths Octavio 1 14: - 4.0, 2 14: - 1.0, 3 22: - 4.0, 3 23: 4.0, 3 24: - 4.2, 5 19: 32.0, 5 21: - 32.0, 5 22: 4.0, 5 23: - 4.0, 5 25: 32.0, 5 28: - 32.0, 7 26: - 20.0, 7 29: 20.0, 14 8: 32.0, 14 9: - 32.0, 15 10: 8.0, 15 11: - 2.0, 15 15: 16.0, 16 12: 32.0, 16 13: - 32.0, 16 16: 16.0, 19 19: 5.0, 19 20: 32.0, 20 15: 32.0, 21 15: - 24.0, 21 21: 5.0, 22 24: 23.4, 23 24: 23.4, 24 10: 20.0, 24 11: - 20.0, 25 25: 5.0, 25 27: 32.0, 26 26: 5.0, 26 27: 32.0, 27 16: - 24.0, 28 28: 5.0, 28 30: 20.0, 29 29: 5.0, 29 30: 20.0, 30 16: 32.0

Bias Strengths 8: - 16.0, 9: 16.0, 10: - 14.0, 11: 11.0, 12: - 16.0, 13: 16.0, 14: 2.5, 15: - 8.0, 16: - 8.0, 17: - 17.5, 18: 0.0, 19: - 20.63, 20: - 26.0, 21: 15.81, 22: 0.18, 23: 0.82, 24: - 25.56, 25: - 20.63, 26: 12.5, 27: - 26.0, 28: 22.03, 29: - 17.5, 30: - 32.0

Differing Synapse Strengths Stick Insect 14 8: 8.0, 14 9: - 8.0, 15 10: 2.0, 16 12: 2.0, 16 13: - 2.0, 21 15: - 24.0, 24 10: 5.0, 24 11: - 5.0, 27 16: - 24.0

Differing Bias Strengths Stick Insect 8: - 4.0, 9: 4.0, 10: - 3.5, 11: 3.5, 12: - 1.0, 13: 1.0, 22: 0.336, 23: 0.664, 24: - 25.397

Middle-Leg Forward (Standard)

Synapse Strengths 1 18: - 32.0, 3 22: - 4.0, 3 23: 4.0, 3 24: - 4.2, 5 19: 32.0, 5 21: - 32.0, 5 22: 4.0, 5 23: - 4.0, 5 25: 32.0, 5 28: - 32.0, 7 17: 20.0, 7 26: - 20.0, 7 29: 20.0, 14 8: 4.0, 14 9: - 4.0, 14 14: 4.0, 15 10: 8.0, 15 11: - 2.0, 15 15: 16.0, 16 12: 32.0, 16 13: - 32.0, 16 16: 16.0, 17 14: - 1.0, 17 17: 5.0, 18 18: 5.0, 18 20: 32.0, 19 19: 5.0, 19 20: 32.0, 20 15: 32.0, 21 15: - 24.0, 21 21: 5.0, 22 24: 23.4, 23 24: 23.4, 24 10: 20.0, 24 11: - 20.0, 25 25: 5.0, 25 27: 32.0, 26 26: 5.0, 26 27: 32.0, 27 16: - 24.0, 28 28: 5.0, 28 30: 20.0, 29 29: 5.0, 29 30: 20.0, 30 16: 32.0

Bias Strengths 8: - 2.0, 9: 1.8, 10: - 14.0, 11: 11.0, 12: - 16.0, 13: 16.0, 14: - 1.65, 15: - 8.0, 16: - 8.0, 17: - 17.5, 18: 12.26, 19: - 23.3, 20: - 26.0, 21: 15.81, 22: 0.18, 23: 0.82, 24: - 25.56, 25: - 20.63, 26: 12.5, 27: - 26.0, 28: 22.03, 29: - 17.5, 30: - 32.0

Differing Synapse Strengths Stick Insect 14 8: 3.0, 14 9: - 8.0, 15 10: 2.0, 16 12: 2.5, 16 13: - 2.0

Differing Bias Strengths Stick Insect 8: - 4.0, 9: 1.0, 10: - 3.5, 11: 3.5, 12: - 1.0, 13: 0.0, 22: 0.336, 23: 0.664, 24: - 25.397

Middle-Leg Forward (Plus ThC Servo)

Synapse Strengths 1 14: - 4.0, 1 18: - 32.0, 2 14: - 2.0, 3 22: - 4.0, 3 23: 4.0, 3 24: - 4.2, 5 19: 32.0, 5 21: - 32.0, 5 22: 4.0, 5 23: - 4.0, 5 25: 32.0, 5 28: - 32.0, 7 17: 20.0, 7 26: - 20.0, 7 29: 20.0, 14 8: 32.0, 14 9: - 32.0, 15 10: 16.0, 15 11: - 2.0, 15 15: 16.0, 16 12: 32.0, 16 13: - 2.0, 16 16: 16.0, 17 14: - 2.0, 17 17: 5.0, 18 18: 5.0, 18 20: 32.0, 19 19: 5.0, 19 20: 32.0, 20 15: 32.0, 21 15: - 24.0, 21 21: 5.0, 22 24: 23.4, 23 24: 23.4, 24 10: 10.0, 24 11: - 10.0, 25 25: 5.0, 25 27: 32.0, 26 26: 5.0, 26 27: 32.0, 27 16: - 24.0, 28 28: 5.0, 28 30: 20.0, 29 29: 5.0, 29 30: 20.0, 30 16: 32.0

Bias Strengths 8: - 16.0, 9: 16.0, 10: - 18.0, 11: 6.0, 12: - 16.0, 13: 1.0, 14: 3.25, 15: - 8.0, 16: - 8.0, 17: - 17.5, 18: 12.26, 19: - 23.3, 20: - 26.0, 21: 15.81, 22: 0.18, 23: 0.82, 24: - 25.56, 25: - 20.63, 26: 12.5, 27: - 26.0, 28: 22.03, 29: - 17.5, 30: - 32.0

Differing Synapse Strengths Stick Insect 14 8: 8.0, 14 9: - 8.0, 15 10: 2.0, 16 12: 2.0, 24 10: 5.0, 24 11: - 5.0

Differing Bias Strengths Stick Insect 8: - 4.0, 9: 4.0, 10: - 3.5, 11: 3.5, 12: - 1.0, 13: 0.25, 22: 0.336, 23: 0.664, 24: - 25.397

Velocity Control Parameters Average stance locomotion speed is given with corresponding retractor (neuron 9) and flexor (neuron 12) bias values in the format *speed (neuron 9 bias, neuron 12 bias)*:

0,26 m/s (5.3, -31.3), 0,38 m/s (5.3, -31.0), 0,46 m/s (5.5, -30.5), 0,51 m/s (6.0, -30.0), 0,52 m/s (6.0, -29.5), 0,57 m/s (7.0, -28.5), 0,59 m/s (8.0, -27.5), 0,60 m/s (9.0, -26.0), 0,62 m/s (11.0, -24.0), 0,66 m/s (13.0, -20.0), 0,75 m/s (16.0, -16.0)

Front-Leg Forward (Plus ThC Servo)

Synapse Strengths 1 14: - 4.0, 1 18: - 32.0, 2 14: - 0.5, 3 22: - 4.0, 3 23: 4.0, 3 24: - 4.2, 5 19: 32.0, 5 21: - 32.0, 5 22: 4.0, 5 23: - 4.0, 5 25: 32.0, 5 28: - 32.0, 7 17: 20.0, 7 26: - 20.0, 7 29: 20.0, 14 8: 32.0, 14 9: - 32.0, 15 10: 8.0, 15 11: - 8.0, 15 15: 16.0, 16 12: 32.0, 16 13: - 4.0, 16 16: 16.0, 17 14: - 4.0, 17 17: 5.0, 18 18: 5.0, 18 20: 32.0, 19 19: 5.0, 19 20: 32.0, 20 15: 32.0, 21 15: - 24.0, 21 21: 5.0, 22 24: 23.4, 23 24: 23.4, 24 10: 20.0, 24 11: - 20.0, 25 25: 5.0, 25 27: 32.0, 26 26: 5.0, 26 27: 32.0, 27 16: - 24.0, 28 28: 5.0, 28 30: 20.0, 29 29: 5.0, 29 30: 20.0, 30 16: 32.0

Bias Strengths 8: - 16.0, 9: 16.0, 10: - 14.0, 11: 11.0, 12: - 16.0, 13: 2.0, 14: 3.7, 15: - 8.0, 16: - 8.0, 17: - 17.5, 18: 18.48, 19: - 19.48 20: - 26.0, 21: 15.81, 22: 0.18, 23: 0.82, 24: - 25.56, 25: - 18.86, 26: 12.5, 27: - 26.0, 28: 20.26, 29: - 17.5, 30: - 32.0

Differing Synapse Strengths Stick Insect 14 8: 8.0, 14 9: - 8.0, 15 10: 2.0, 15 11: - 2.0, 16 12: 2.0, 16 13: - 2.0, 24 10: 5.0, 24 11: - 5.0

Differing Bias Strengths Stick Insect 8: - 4.0, 9: 4.0, 10: - 3.5, 11: 3.5, 12: - 1.0, 13: 1.0, 22: 0.269, 23: 0.731, 24: - 25.467

Hind-Leg Forward (Plus ThC Servo)

Synapse Strengths 1 14: - 4.0, 1 18: - 32.0, 1 21: 32.0, 2 14: - 0.5, 3 24: - 4.0, 3 25: 4.0, 3 26: - 4.2, 5 19: - 32.0, 5 22: 32.0, 5 24: 4.0, 5 25: - 4.0, 7 17: 20.0, 7 27: 20.0, 14 8: 32.0, 14 9: - 32.0, 15 10: 8.0, 15 11: - 16.0, 15 15: 16.0, 16 12: 32.0, 16 13: - 16.0, 16 16: 16.0, 17 14: - 2.0, 17 17: 5.0, 18 18: 5.0, 18 20: 32.0, 19 19: 5.0, 19 20: 32.0, 20 15: 24.0, 21 21: 5.0, 21 23: 32.0, 22 22: 5.0, 22 23: 32.0, 23 15: - 32.0, 24 26: 23.4, 25 26: 23.4, 26 10: 20.0, 26 11: - 20.0, 27 16: - 32.0, 27 27: 5.0

Bias Strengths 8: - 16.0, 9: 16.0, 10: - 14.0, 11: 18.0, 12: - 16.0, 13: 8.0, 14: 2.45, 15: - 8.0, 16: 8.0, 17: - 17.5, 18: 8.7, 19: 13.15 20: - 26.0, 21: - 16.19, 22: - 17.96, 23: - 26.00, 24: 0.18, 25: 0.82, 26: - 25.56 27: - 12.5

Differing Synapse Strengths Stick Insect 14 8: 8.0, 14 9: - 8.0, 15 10: 5.0, 15 11: - 2.0, 16 12: 10.0, 16 13: - 4.0, 26 10: 3.0, 26 11: - 3.0

Differing Bias Strengths Stick Insect 8: - 4.0, 9: 4.0, 10: - 3.5, 11: 2.5, 12: - 3.0, 13: 0.0, 14: 3.25, 24: 0.158, 25: 0.842, 26: - 25.54 27: - 12.5

Hind-Leg Forward (Plus ThC Servo Plus FTi Middle-Leg Structure)

Synapse Strengths 1 14: - 4.0, 1 18: - 32.0, 1 21: 32.0, 2 14: - 0.5, 3 24: - 4.0, 3 25: 4.0, 3 26: - 4.2, 5 19: - 32.0, 5 22: 32.0, 5 24: 4.0, 5 25: - 4.0, 5 27: 32.0, 5 30: - 32.0, 7 17: 20.0, 7 28: 20.0, 7 31: - 20.0, 14 8: 32.0, 14 9: - 32.0, 15 10: 8.0, 15 11: - 16.0, 15 15: 16.0, 16 12: 32.0, 16 13: - 16.0, 16 16: 16.0, 17 14: - 2.0, 17 17: 5.0, 18 18: 5.0, 18 20: 32.0, 19 19: 5.0, 19 20: 32.0, 20 15: 24.0, 21 21: 5.0, 21 23: 32.0, 22 22: 5.0, 22 23: 32.0, 23 15: - 32.0, 24 26: 23.4, 25 26: 23.4, 26 10: 20.0, 26 11: - 20.0, 27 27: 5.0, 27 29: 32.0, 28 28: 5.0, 28 29: 32.0, 29 16: - 24.0, 30 30: 5.0, 30 32: 20.0, 31 31: 5.0, 31 32: 20.0, 32 16: 32.0

Bias Strengths 8: - 16.0, 9: 16.0, 10: - 14.0, 11: 18.0, 12: - 16.0, 13: 8.0, 14: 2.45, 15: - 8.0, 16: - 8.0, 17: - 17.5, 18: 8.7, 19: 13.15 20: - 26.0, 21: - 16.19, 22: - 17.96, 23: - 26.00, 24: 0.18, 25: 0.82, 26: - 25.56, 27: - 20.63, 28: - 12.5, 29: - 26.0, 30: - 22.03, 31: 7.5, 32: - 32.0

Differing Synapse Strengths Stick Insect 14 8: 16.0, 14 9: - 8.0, 15 10: 4.0, 15 11: - 2.0, 16 12: 10.0, 16 13: - 4.0, 26 10: 3.0, 26 11: - 3.0

Differing Bias Strengths Stick Insect 8: - 8.0, 9: 4.0, 10: - 3.5, 11: 2.5, 12: - 2.0, 13: 0.0, 14: 3.25, 16: 8.0, 24: 0.158, 25: 0.842, 26: - 25.54

F Acknowledgements

First of all I am grateful to Prof. Dr. Ansgar Büschges and Prof. Dr. Frank Pasemann for supervising and supporting my work from the two different, yet complimentary perspectives of a neurobiologist and a theoretical physicist. The resulting interdisciplinary atmosphere has been an inexhaustible source of motivation for me.

Especially I would like to thank Dr. Silvia Gruhn for agreeing to review this thesis in such a short period of time.

The excellent atmosphere created by my supervisors was of course also supported by their respective research groups and, therefore, I would like to thank everyone from the former INDY team at the Fraunhofer IAIS, Sankt Augustin, from the neurocybernetics department in Osnabrück and from the animal physiology lab in Cologne. Faced by the danger of forgetting someone, I forbear from listing the individual names here.

Co-operations with the neurobotics lab in Berlin and a three month fellowship at the Institute for Advanced Study, Berlin, have been extremely inspiring.

Special thanks go to people that provided feedback on parts of my manuscripts or program code of simulations, amongst others these were: Dr. Manfred Hild, Torsten Siedel, Marcus Blümel, Christian Rempis, Dr. Keyan Zahedi, Katja Hellekes, Vishal Patel, Prof. Dr. Holk Cruse, Prof. Dr. Volker Dürr, Dr. Sergiy Yakovenko, Prof. Dr. Harald Wolf, Dr. Niko Kladt, Prof. Dr. Hans-Georg Heinzel, Prof. Dr. Wolfgang Alt and multiple anonymous reviewers.

Throughout my thesis, the pmi team has provided me with excellent music.

Finally, I do not really know how to thank my wife Teresa. She has endured my frequent (mental) absences, my night-shifts in front of the computer and much more. Still she has always been a source of support to me – thank you!

G Declaration

Ich versichere, dass ich die von mir vorgelegte Dissertation selbstständig angefertigt, die benutzten Quellen und Hilfsmittel vollständig angegeben und die Stellen der Arbeit – einschließlich Tabellen, Karten und Abbildungen –, die anderen Werken im Wortlaut und Sinn nach entnommen sind, in jedem Einzelfall als Entlehnung kenntlich gemacht habe; dass diese Dissertation noch keiner anderen Fakultät oder Universität zur Prüfung vorgelegen hat; dass sie – abgesehen von oben angegebenen Teilpublikationen – noch nicht veröffentlicht worden ist sowie, dass ich eine solche Veröffentlichung vor Abschluss des Promotionsverfahrens nicht vornehmen werde. Die Bestimmungen dieser Promotionsordnung sind mir bekannt. Die von mir vorgelegte Dissertation ist von Prof. Dr. Ansgar Büschges betreut worden.

Köln, den 01.03.2011